UNIVERSIDADE FEDERAL DO RIO GRANDE DO SUL
CENTRO DE ESTUDOS E PESQUISAS EM SENSORIAMENTO REMOTO E METEOROLOGIA
PROGRAMA DE PÓS-GRADUAÇÃO EM SENSORIAMENTO REMOTO

TESE DE DOUTORADO

DESENVOLVIMENTO DE METODOLOGIA ANALÍTICA E DE SENSORIAMENTO REMOTO VISANDO ANALISAR OS NÍVEIS DE HPA´S EM PARTÍCULAS ATMOSFÉRICAS ULTRAFINAS NA REGIÃO METROPOLITANA DE PORTO ALEGRE

Orientador: Prof. Dra. Elba Calesso Teixeira
Aluna de Doutorado: Dayana Milena Agudelo Castañeda

Porto Alegre
2014

UNIVERSIDADE FEDERAL DO RIO GRANDE DO SUL
CENTRO ESTADUAL DE PESQUISAS EM SENSORIAMENTO REMOTO E METEOROLOGIA
PROGRAMA DE PÓS-GRADUAÇÃO EM SENSORIAMENTO REMOTO

DESENVOLVIMENTO DE METODOLOGIA ANALÍTICA E DE SENSORIAMENTO REMOTO VISANDO ANALISAR OS NÍVEIS DE HPA´S EM PARTÍCULAS ATMOSFÉRICAS ULTRAFINAS NA REGIÃO METROPOLITANA DE PORTO ALEGRE

DAYANA MILENA AGUDELO CASTAÑEDA

Tese de Doutorado submetida ao Programa de Pós-Graduação em Sensoriamento Remoto da Universidade Federal do Rio Grande do Sul como requisito parcial para obtenção do título de Doutor em Sensoriamento Remoto.

Orientadora:
Dra. Elba Calesso Teixeira**.**

Coorientadora:
Dra. Silvia Beatriz Alves Rolim

Banca Examinadora:
Dr. Jorge Ricardo Ducati
Dra. Adalgiza Fornaro
Dr. Luis Felipe Silva Oliveira

Porto Alegre
2014

Aprovada pela Banca Examinadora em cumprimento ao requisito exigido para obtenção do Título de Doutor(a) em Sensoriamento Remoto

_____
Dra. Elba Calesso Teixeira (UFRGS/FEPAM)
Orientadora

_____
Dra. Silvia Beatriz Alves Rolim
Coorientadora

_____
Dr. Jorge Ricardo Ducati

_____
Dra. Adalgiza Fornaro

_____
Dr. Luis Felipe Silva Oliveira

Aluna: Dayana Milena Agudelo Castañeda

Porto Alegre
2014

Agudelo Castañeda, Dayana Milena
Desenvolvimento de metodologia analítica e de sensoriamento remoto visando analisar os níveis de HPA´s em partículas atmosféricas ultrafinas na região metropolitana de Porto Alegre./ Dayana Milena Agudelo Castañeda. - Porto Alegre: IGEO/UFRGS, 2014.
[146 f.] il.

Tese (Doutorado). - Universidade Federal do Rio Grande do Sul.Programa de Pós-Graduação em Sensoriamento Remoto. Instituto de Geociências. Porto Alegre, RS - BR,2014.

Orientador(es):Elba Calesso Teixeira
Coorientador(es):Silvia Beatriz Alves Rolim

1.Qualidade do ar.2.Espectrometria de infravermelho.3.Hidrocarbonetos policíclicos. 4.I. Título. **CDU 55**

Catalogação na Publicação
Biblioteca Instituto de Geociências – UFRGS
Alexandre Ribas Semeler CRB 10/1900

Universidade Federal do Rio Grande do Sul - Campus do Vale Av. Bento Gonçalves, 9500 - Porto Alegre - RS - Brasil
CEP: 91501-970 / Caixa Postal: 15001.
Fone: +55 51 3308-6329 Fax: +55 51 3308-6337
E-mail: bibgeo@ufrgs.br

DEDICATÓRIA

À Deus, meu esposo Fabrício e minha mãe Luz Nelly por seu apoio e compreensão por todas as horas investidas neste projeto de vida.

AGRADECIMENTOS

À minha orientadora, Professora Dra. Elba Calesso Teixeira, meus agradecimentos pela ajuda, apoio, confiança, dedicação e paciência.

Ao Conselho Nacional de Desenvolvimento Científico e Tecnológico – CNPq pela bolsa de doutorado concedida.

À Universidade Federal do Rio Grande do Sul (UFRGS) e ao Centro Estadual de Pesquisa em Sensoriamento Remoto e Meteorologia pelo ensino, pela qualidade e pela estrutura disponibilizada.

À Professora Naira por seus ensinamentos sobre infravermelho e por permitir realizar as medições das curvas espectrais no DRIFTS, dados sem os quais a pesquisa não poderia ter sido concluída.

Aos professores pelos ensinamentos para meu crescimento intelectual.

A Fundação Estadual de Proteção Ambiental Henrique Luis Roessler (FEPAM-RS) por disponibilizar a oportunidade do desenvolvimento da pesquisa, concedendo a estrutura física para realizar as amostragens e as análises.

Aos funcionários da FEPAM que colaboraram na pesquisa: Felipe Norte, Flávio Wiegand, e funcionários do PROAR, sem a sua ajuda não seria possível o término deste trabalho.

Aos Bolsistas de Iniciação Científica Mauricio, Amália, Camila, Luciana, Marianni, Yourrei, Greice, pelo grande apoio e colaboração na pesquisa.

A toda mi familia que desde Colombia me dio su apoyo emocional y espiritual durante todo este proceso, siempre me entendieron y brindaron su amor incondicional, principalmente a mi mamá, mi hermano y mis tíos Sandra y Norberto.

Ao meu esposo Fabrício, por seu amor, apoio, luta e paciência.

À todos los amigos que conocí durante esta travesía y que me apoyaron en todo momento. Me refiro a Adri, Leandro, Fausto, Lila, Grethel, Victoria, Maria Cristina, Ester. También a aquellos que a pesar de la distancia no me dejaron desistir: Johe, Wendy, Anya, Zhyla, Sheila, Vane, Ilse, Rox, Diana.

Aos meus colegas da FEPAM e da Pós que me ajudaram durante a pesquisa, me apoiaram e agora são meus grandes amigos: Raquel, Maria, Paulo, Ismael, Helenise, Priscila, Karine, Yourrei.

“Por vezes sentimos que aquilo que fazemos não é senão uma gota de água no mar. Mas o mar seria menor se lhe faltasse uma gota.”

Madre Teresa de Calcuta (1910-1997)

RESUMO

Nos últimos anos, a deterioração da qualidade do ar urbano devido ao material particulado atmosférico está recebendo atenção significativa e continuamente ameaça a qualidade de vida dos habitantes das áreas urbanas. A poluição do ar pelas partículas atmosféricas nas zonas urbanas é causada principalmente pelas emissões de fontes antropogênicas em sua maioria veiculares. Além disso, a poluição causada por partículas atmosféricas não está apenas relacionada com a sua concentração, mas também com a distribuição dos seus diferentes diâmetros. As partículas na fração estudada, < 1 μm, apresentam maior risco porque podem penetrar nos pulmões, afetam a função alveolar e ocasionam efeitos nocivos na saúde humana. Contudo, as partículas atmosféricas podem carregar diferentes compostos que são tóxicos e/ou cancerígenos, produzindo riscos para a saúde, como os Hidrocarbonetos policíclicos aromáticos – HPAs. Os HPAs são um grupo de diversos compostos orgânicos complexos, constituídos por carbono e hidrogênio junto com dois ou mais anéis benzênicos condensados. Portanto, foi desenvolvido um procedimento científico apto para estudar material particulado atmosférico < 1 μm (MP_1) com a finalidade de analisar quantitativa e qualitativamente os HPAs associados a esta fração, a concentração em número das partículas e a distribuição de tamanho de partículas na Região Metropolitana de Porto Alegre usando técnicas analíticas e de sensoriamento remoto. As amostras foram coletadas em filtros de PTFE nos municípios de Sapucaia do Sul e Canoas, pertencentes à Região Metropolitana de Porto Alegre, usando o amostrador sequencial automático PM162M da Environnement S.A. As amostras foram extraídas utilizando o método EPA TO-13A para analisar 16 HPAs, utilizando um cromatógrafo gasoso acoplado a um espectrômetro de massa (CG-EM). A distribuição do tamanho de partícula nas frações PR1 (0.3-1.0 μm), PR2.5 (1.0-2.5 μm) e PR10 (2.5-10 μm) foi obtida utilizando o analisador de partículas CPM em Sapucaia do Sul. Os dados das concentrações de poluentes atmosféricos relacionados com MP_{10}, óxidos de nitrogênio (NO, NO_x, NO_2) e ozônio (O_3) foram obtidos utilizando os analisadores MP101M, AC32M e O342M da Environnement, respectivamente. Dados das variáveis meteorológicas como velocidade do vento, direção do vento, umidade relativa, radiação solar e temperatura ambiente foram medidos simultaneamente de modo concomitante. Os espectros de emissividade e transmitância, através da espectroscopia no infravermelho, foram obtidos utilizando espectrômetro FTIR D&P e o BOMEM MB-series FTIR-Hartmann & Braun Michelson, respectivamente. A determinação dos resultados usando cromatografia mostraram que no inverno as concentrações de HPAs foram significativamente maiores do que no verão, mostrando assim uma variação sazonal. A

identificação das fontes de emissão, aplicando razões diagnóstico, confirmou que os HPAs na área de estudo são originários de fontes móveis, especialmente, das emissões de diesel e da gasolina. A análise por modelo receptor PMF também mostrou a contribuição dessas duas fontes principais, seguido pela combustão de carvão, combustão incompleta/petróleo não queimado e da combustão de madeira. Os fatores tóxicos equivalentes foram calculados para caracterizar o risco de câncer por exposição ao HPA em amostras de $MP_{1,}$ e benzo[*a*]pireno e dibenzo[*ah*] antraceno que dominaram os níveis de BaPeq. Com exceção do O_3, a análise de tendência do NO, NO_2 e NO_x mostrou um aumento da concentração destes compostos no inverno. Também a correlação destes poluentes com os parâmetros meteorológicos permitiu evidenciar a influência das fontes móveis na área de estudo. Os resultados das assinaturas espectrais no infravermelho das amostras de MP_1 comparando com os padrões e com outros trabalhos mostraram que o maior número de bandas de fortes intensidades ocorreu na região espectral de 680-900 cm^{-1}, devido às deformações angulares CC fora do plano e deformações angulares CH fora do plano dos HPAs. Bandas de média intensidade na região de 2900-3050 cm^{-1}, também foram observadas devido ao estiramento CH, característico de compostos aromáticos. A presente pesquisa foi o ponto de partida para obter um banco de dados das concentrações de HPAs associados à fração MP_1 e dos poluentes $NO_x/NO_2/NO/MP_{10}/O_3$; caracterizar a distribuição de tamanho de partículas atmosféricas, que são de grande importância e preocupação atual; avaliar a sua variação sazonal e sua relação com as condições meteorológicas usando técnicas estatísticas; e aprofundar o conhecimento do comportamento espectral dos HPAs, poluentes cancerígenos e mutagênicos, presentes no material particulado atmosférico na fração fina e ultrafina.

Palavras chave: qualidade do ar, hidrocarbonetos policíclicos aromáticos, material particulado atmosférico, distribuição de tamanho de partícula, PMF, espectrometria de infravermelho.

ABSTRACT

In recent years, the urban air quality deterioration due to atmospheric particulate matter is receiving significant attention; also, it continually threatens the life quality of urban residents. Air pollution by atmospheric particles in urban areas is mainly caused by emissions from anthropogenic sources, mostly vehicular sources. Moreover, the pollution caused by atmospheric particles is not only related to its concentration, but also with the size distribution. The particles studied in the fraction <1μm have a greater risk because they can penetrate into the lungs, affect cellular function and cause adverse effects on human health. However, atmospheric particles can carry different compounds that are toxic and/or carcinogenic, producing health risks, such as polycyclic aromatic hydrocarbons - PAH. PAHs are a group of several complex organic compounds consisting of carbon and hydrogen along with two or more fused benzene rings. Consequently, a scientific procedure was developed to study the atmospheric particulate matter < 1 μm (PM_1) in order to analyze qualitatively and quantitatively the PAHs associated with this fraction, also the particle number concentration and particle size distribution in the Metropolitan Region of Porto Alegre using remote sensing techniques. PM_1 samples were collected in PTFE filters in Sapucaia South and Canoas sites, in the Metropolitan Region of Porto Alegre using the automatic sequential sampler PM162M of Environnement S.A. The samples were extracted using the EPA Method TO-13A and 16 PAHs were analyzed using a gas chromatograph coupled to a mass spectrometer (GC-MS). The particle size distribution of fractions PR1 (0.3 - 1.0 μm), PR2.5 (1.0 - 2.5 μm) and PR10 (2.5 – 10 μm) was obtained using the particulate analyzer CPM. The data of related air pollutants concentrations such as PM_{10}, nitrogen oxides (NO, NO_x, NO_2), ozone (O_3) were obtained using the analyzers MP101M, AC32M, O342M of Environnement, respectively. Data from meteorological variables, wind speed, wind direction, relative humidity, solar radiation and ambient temperature were continuously measured and simultaneously. The emissivity and transmittance spectra through infrared spectroscopy were obtained using FTIR spectrometer D&P and the Bomem MB-series FTIR-Hartmann & Braun Michelson, respectively. The results showed that in winter, the concentrations of PAHs were significantly higher than in summer, thus showing their seasonal variation. The identification of emission sources, applying diagnostic ratios confirmed that PAHs in the study area originate from mobile sources, especially diesel and gasoline emissions. The analysis by PMF receptor model also showed the contribution of these two sources, followed by coal combustion, incomplete combustion/unburned petroleum and wood combustion. The toxic equivalent factors were calculated to characterize the risk of cancer

from PAH exposure to $PM_{1.0}$ samples, and benzo[*a*]pyrene and dibenz[*ah*]pyrene dominated BaPeq levels. The trend analysis of O_3, NO, NO_2, NO_x showed a trend of increased concentration at winter, except O_3. Also the correlation of these pollutants with meteorological parameters has demonstrated the influence of mobile sources in the study area. The results of the IR spectral signatures of the PM_1 samples compared to the standards and other studies showed that the greatest number of strong bands occurred in the spectral region of 680-900 cm^{-1} due to the CC out-of-plane angular deformation and CH out-of-plane angular deformation of PAHs. Bands of medium intensity in the 2900-3050 cm^{-1} region were also observed due to the CH stretch, characteristic of aromatic compounds. This research was the starting point for a concentrations database of PAHs associated fraction PM_1 and pollutants $NO_x/NO_2/NO/PM_{10}/O_3$, characterize the size distribution of atmospheric particles that are of great importance and current concern. Furthermore, to assess their seasonal variation and its relationship with meteorological conditions, using statistical techniques. Also to deepen the knowledge of the spectral behavior of PAHs that are carcinogenic and mutagenic pollutants present in atmospheric particulate matter in the fine and ultrafine fraction.

Key words: air quality, polycyclic aromatic hydrocarbons, particulate matter, particle size distribution, PMF.

APRESENTAÇÃO DA ESTRUTURA DA TESE

Esta Tese de Doutorado, intitulada "**DESENVOLVIMENTO DE METODOLOGIA ANÁLITICA E DE SENSORIAMENTO REMOTO VISANDO ANALISAR OS NÍVEIS DE HPA´S EM PARTÍCULAS ATMOSFÉRICAS ULTRAFINAS NA REGIÃO METROPOLITANA DE PORTO ALEGRE"**, foi desenvolvida entre Junho de 2010 e Agosto de 2014 no Centro Estadual de Pesquisas em Sensoriamento Remoto e Meteorologia da Universidade Federal do Rio Grande do Sul (UFRGS) em colaboração com a Fundação Estadual de Proteção Ambiental do Rio Grande do Sul Henrique Luiz Roessler - RS (FEPAM-RS).

A Tese é composta das seguintes partes:

- **Capítulo I: Aspectos introdutórios**
  Trata sobre os aspectos introdutórios, objetivos, revisão bibliográfica, metodologia.

- **Capítulo II, III, IV, V, VI: Resultados na forma de artigos científicos publicados, submetidos ou à serem submetidos para publicação.**
  Capítulo II. Artigo publicado intitulado "Measurement of particle number and related pollutant concentrations in an urban area in South Brazil", autores: AGUDELO-CASTAÑEDA, D. M.; Teixeira, E.C.; Rolim, S.B.A.; Pereira, F.N.; Wiegand, F. Publicado na Atmospheric Environment 70, 254-262, 2013.

  Capítulo III. Artigo publicado intitulado "Seasonal changes, identification and source apportionment of PAH in $PM_{1.0}$", autores: AGUDELO-CASTAÑEDA, D. M.; Teixeira, E.C. Publicado na Atmospheric Environment 96, 186-200, 2014.

  Capítulo IV. Artigo publicado intitulado "Time–series analysis of surface ozone and nitrogen oxides concentrations in an urban area at Brazil", autores: AGUDELO-CASTAÑEDA, D. M.; Teixeira, E.C.; Pereira, F.N. Publicado em Atmospheric Pollution Research 5, 411-420, 2014.

  Capítulo V. Artigo intitulado "Infrared spectra of emissivity, transmittance and reflectance of PAHs and comparison with samples of atmospheric particulates (< 1μm)", autores: AGUDELO-CASTAÑEDA, D. M.; Teixeira; Schneider, I.; Rolim, S.; Balzaretti, N. A ser submetido.

  Capítulo VI. Artigo intitulado "Evaluation of particle number-mass concentration distribution and gaseous pollutants in urban area", autores: AGUDELO-CASTAÑEDA, D. M.; Teixeira, E.C.; Schneider, I.; Pereira, F.N.; Silva, L.F.O. A ser submetido.

- **CAPITULO VII: Considerações finais**
  Apresenta as conclusões, considerações finais e recomendações de futuras pesquisas.

- **ANEXO A:** Resumos dos trabalhos publicados como co-autor

SUMÁRIO

LISTA DE ABREVIATURAS E SIGLAS

O_3: ozônio troposferico ($\mu g \cdot m^{-3}$)
NO: óxido nítrico ($\mu g \cdot m^{-3}$)
NO_x: óxidos de nitrogênio ($\mu g \cdot m^{-3}$)
NO_2: dióxido de nitrogênio ($\mu g \cdot m^{-3}$)
CO: monóxido de carbono (ppm)
OX: soma da concentração de NO_2 e O_3 ($\mu g \cdot m^{-3}$)
PR1: número de partículas atmosféricas na faixa 0,3 – 1 µm ($N° \cdot L^{-1}$)
PR2.5: número de partículas atmosféricas na faixa 1 - 2,5 µm ($N° \cdot L^{-1}$)
PR10: número de partículas atmosféricas na faixa 2,5 – 10 µm ($N° \cdot L^{-1}$)
MP_{10}: material particulado atmosférico < 10 µm ($\mu g \cdot m^{-3}$)
$MP_{2,5}$: material particulado atmosférico < 2,5 µm ($\mu g \cdot m^{-3}$)
MP_1: material particulado atmosférico < 1 µm ($\mu g \cdot m^{-3}$)
PMF: Positive Matrix Factorization
HPA: Hidrocarbonetos policíclicos aromáticos ($ng \cdot m^{-3}$)
FTIR: espectroscopia de infravermelho termal com transformada de Fourier
DRIFTS: espectroscopia por refletância difusa no infravermelho com transformada de Fourier
TEF: fator de equivalência tóxica
BaPeq :fator de equivalência tóxica baseado em Benzo[*a*]pireno

CAPITULO I

Aspectos Introdutórios: Introdução, Objetivos, Revisão Bibliográfica, Metodologia

CAPITULO I -

INTRODUÇÃO

Nas regiões ou áreas metropolitanas a poluição do ar é um grave problema que continuamente ameaça a qualidade de vida dos habitantes. O material particulado é de grande interesse por ser um dos poluentes que podem afetar negativamente a saúde humana. Dos diversos fatores geradores da poluição do ar, destacam-se a emissão de poluentes de veículos automotores (Colvile *et al.*, 2001), que são a principal fonte de material particulado, e NO (óxido de nitrogênio) nas áreas urbanas (Bathmanabhan e Saragur, 2010). As partículas atmosféricas < 1 µm apresentam maior risco pelo fato de que podem se depositar no trato respiratório (Slezakova *et al.*, 2007) e, por possuirem maior área especifica, podem carregar maiores concentrações de compostos tóxicos e/ou cancerígenos, o que dá a importância do seu estudo. Entre os compostos de importância encontram-se os dos hidrocarbonetos policíclicos aromáticos (HPAs) por fazer parte do grupo dos mais fortes agentes cancerígenos ou mutagênicos conhecidos. Devido à natureza ubíqua dos HPAs na atmosfera e seus altos níveis de concentração no ambiente urbano, o risco de exposição humana é elevado para os habitantes das cidades (Sienra et. al, 2005). A maioria dos prováveis HPAs cancerígenos encontram-se associados com o material particulado, especialmente com as partículas finas ou ultrafinas no ambiente (Bi et. al, 2003).

Estudos realizados em vários paises (Tsapakis *et al.*, 2002; Guo *et al.*, 2003; Manoli *et al.*, 2004; Fang *et al.*, 2004; Ravindra *et al.*, 2006; Ströher *et al.*, 2007) mostraram que as principais fontes de HPAs em áreas urbanas são as emissões veiculares, especialmente o tráfego intenso de veículos e as emissões de motores de combustão a diesel. No entanto, estudos de partículas atmosféricas < 1 µm são mundialmente escassos (Krumal *et al.*, 2013; Klejnowski *et al.*, 2010; Ladji *et al.*, 2009) e no Brasil inexistentes, o que evidencia a importância deste estudo. No Brasil, a análise do perfil de concentrações de HPAs somente tem sido realizada com partículas de diâmetro < 10 e < 2,5 µm, entre os quais podemos citar: Barra *et al.* (2007); Bourotte *et al.* (2005); Dallarosa *et al.* (2005a, 2005b); Dallarosa *et al.* (2008); De Martinis *et al.* (2002); Fernandes *et al.* (2002); Netto *et al.* (2002); Teixeira *et al.* (2012); Teixeira *et al.* (2013); Vasconcellos *et al.* (2011). Nos diversos estudos mencionados, as altas concentrações de HPAs podem ser explicadas pelo

alto tráfego de veículos e o transporte dos compostos desde as áreas industrializadas localizadas em regiões suburbanas, junto com uma concentração elevada do material particulado (Barra *et al*., 2007).

A análise das características químicas do material particulado é uma tarefa difícil pelo fato de que existem centenas de compostos orgânicos presentes na atmosfera, como os HPAs. Além de utilizar técnicas analíticas de cromatografia, podem ser usadas técnicas de sensoriamento remoto como a espectrorradiometria de infravermelho (FTIR) (Bauschlicher *et al.*, 1997; Mastalerz *et al.*, 1998; Hudgins and Sanford, 1998; Kubicki, 2001; Coury and Dillner, 2008; Basire *et al.*, 2011). A técnica de FTIR pode ser usada para identificar um composto ou investigar a composição química de uma amostra, em virtude de que o espectro de um composto químico na região do infravermelho é considerado uma de suas propriedades físico-químicas mais características, principalmente nos compostos orgânicos. As características do espectro dependem do tipo de estrutura interna dos constituintes, do tamanho dos seus raios iônicos, das forças de ligação e das impurezas contidas no material (Meneses, 2001).

Para partículas de aerossóis, a espectroscopia pode analisar o comportamento espectral (Allen and Palen, 1989). Entre outras vantagens, pode-se citar a sua capacidade de detectar os compostos em pequenas quantidades, sem extração ou derivatização (técnica não destrutiva); a instrumentação pode estar no local de amostragem, o que elimina as perdas ou transformações durante o transporte, congelamento e armazenamento (Allen *et al.*,1994; Marshall *et al.*,1994; Coury and Dillner, 2008; Navarta *et al.*, 2008); e realizar medições praticamente em tempo real. Outro motivo é que podem ser usadas amostras de diversos tamanhos e não é necessária uma preparação da amostra. Com está técnica podem ser escolhidas várias amostras para posteriormente fazer a análise quantitativa por GC/MS, o que traz benefícios por diminuir os custos.

Finalmente, entre as razões da importância do estudo das partículas atmosféricas MP_1, dos HPAs associados e da distribuição de tamanho de partículas encontram-se:

- Em ambientes urbanos, mais de 90% da concentração de número das partículas atmosféricas emitidas por fontes móveis pertence à fração < 1 μm.
- Hoje em dia, os padrões de qualidade do ar existentes estão restritos a $MP_{2.5}$ e MP_{10} frações geradas por processos mecânicos e eles são incapazes de controlar eficazmente partículas sub micrométricas emitidos a partir de fontes de combustão, tais como os veículos.

- As medições da maioria das redes de monitoramento da qualidade do ar não estão imediatamente disponíveis, como é o caso do número de partículas atmosféricas. Também essas medidas fornecem pouca informação sobre a distribuição de partículas para diferentes diâmetros e sua variação em tempo real. A concentração do número de partículas atmosféricas precisa ser controlada por várias razões, tais como a capacidade das partículas ultrafinas penetrar nos pulmões, afetando a função celular e causar efeitos nocivos na saúde humana (Slezakova *et al.*, 2007). A determinação da concentração da massa de partículas finas por métodos tradicionais é demorada e causando muito trabalho, porque as massas envolvidas são baixas. Também pelos métodos tradicionais, há problemas de artefatos como a de condensação de gases voláteis em filtros ou a evaporação a partir do material particulado nos filtros.
- MP_1 pode ser um bom indicador de fontes veiculares em locais com tráfico pesado, áreas urbanas e rodovias. Vários autores têm relatado que as emissões provenientes de fontes móveis são os maiores contribuintes de HPAs em áreas urbanas (Sienra *et al.*, 2005; Ravindra *et al.*, 2008). Portanto, maiores concentrações de HPAs estarão na fração MP_1 e poderão causar maiores efeitos na saúde. MP_1 apresenta maior risco porque se pode depositar no trato respiratório, aumentando os efeitos negativos para a saúde e pode transportar poluentes, como os hidrocarbonetos aromáticos policíclicos (HPAs).
- Há uma preocupação considerável sobre a relação entre a exposição ao HPA no ar e o potencial de contribuir para a incidência de câncer nas pessoas. O Parlamento Europeu e o Conselho da União Europeia estabeleceram as diretrizes de qualidade do ar ambiente para HPAs (1,0 ng m^{-3} de BaP na fração MP_{10}). Este limite e a publicação científica Air Pollution and Cancer (IARC, 2013) demonstram a importância de seu estudo e exigem sua máxima redução.
- A técnica do FTIR detecta compostos em pequenas quantidades, sem extração ou derivatização (técnica não destrutiva), e ajuda a diminuir os custos do monitoramento da qualidade do ar.

OBJETIVOS

Objetivo geral

Desenvolver um procedimento multi-analítico para analisar quantitativa e qualitativamente os HPAs associados às partículas atmosféricas < 1 µm (MP_1), usando técnicas analiticas (CG-MS) e de sensoriamento remoto, respectivamente, e os modos de distribuição de tamanho de partículas na Região Metropolitana de Porto Alegre.

Objetivos específicos

i. Quantificar a concentração dos HPAs associados às partículas atmosféricas ultrafinas durante o período de tempo escolhido para esta pesquisa.
ii. Analisar os valores de concentração dos HPAs comparando com os dados meteorológicos da área de estudo
iii. Identificar a variação sazonal das concentrações dos HPAs associados às partículas atmosféricas ultrafinas durante o período da pesquisa.
iv. Analisar as emissões de HPAs associados a MP_1 através da aplicação do método estatístico (razões diagnósticas) e modelo receptor (PMF- Positive Matrix Factorization)
v. Analisar os modos de distribuição das partículas atmosféricas
vi. Realizar medidas de emissividade em HPAs associados às partículas atmosféricas ultrafinas com espectroradiometro de IRT.
vii. Associar a relação dos HPAs e número de partículas com poluentes relacionados: óxidos de nitrogênio e ozônio troposférico.

REVISÃO BIBLIOGRÁFICA

Partículas atmosféricas e poluentes associados

As partículas atmosféricas estão constituídas por uma mistura de partículas sólidas, gotas de líquidos, e componentes líquidos contidos nas partículas sólidas que variam de alguns nanômetros a cerca de 100 micrômetros (Seinfeld e Pandis, 2006), sendo que a massa de uma partícula de 10 micrômetros de diâmetro é equivalente à massa de um bilião de partículas de 10 nanômetros. A concentração, bem como as suas características físico-químicas e morfológicas, são variáveis. O material particulado (MP) é uma mistura complexa de vários compostos químicos provenientes de uma variedade de fontes e das diversas reações que ocorrem na atmosfera. As partículas podem ser emitidas diretamente para a atmosfera (partículas primárias) ou podem ser formadas na atmosfera pela conversão de gás a partícula (partículas secundárias). As partículas primárias são principalmente de origem natural, enquanto que partículas secundárias provêm de reações químicas dos precursores gasosos como o dióxido de enxofre, óxidos de nitrogênio e compostos orgânicos voláteis. Porém, as partículas emitidas diretamente das fontes de combustão também são consideradas primárias. As fontes naturais de geração das partículas estão associadas com a ação do vento no solo (resuspensão) e no mar (spray marinho), emissão biogênica, vulcões e queimadas naturais. As partículas atmosféricas estão principalmente constituídas por sulfatos, nitratos, amônio, sais marinhos, metais, material carbonáceo. Materiais carbonáceos representam um conjunto de espécies orgânicas semi-voláteis (SVOC), carbono orgânico (OC), *Black Carbon* (BC) também conhecido como carbono elementar (CE). O BC ou o CE é definido como absorvedor de luz (black) ou carbono térmico refratário (elementar). BC ou CE são também chamados de fuligem, termo que muitas vezes inclui o revestimento orgânico, que geralmente está associada a estas partículas e se origina em vários tipos de combustão. Além das partículas primárias de carbono, existe uma quantidade substancial de partículas orgânicas secundárias. Uma vez formadas, estas partículas orgânicas estão sujeitas a modificações químicas na atmosfera por reações fotoquímicas e reações com outros radicais OH. Partículas ricas em conteúdo orgânico podem ser formadas por condensação

de gases orgânicos em partículas pré-existentes, que podem ser tão pequenas como as nanopartículas formadas na nucleação.

As partículas geradas na combustão, como as das emissões de fontes movéis e queima de madeira, podem ter diâmetros que variam de 10 nm (muito pequenas) a 1 µm (grandes). Poeira, pólen, fragmentos de plantas e sais marinhos podem ter diâmetros maiores de 1 µm. Também as partículas secundárias produzidas pelos processos fotoquímicos são principalmente < 1 µm. O tamanho destas partículas afeta seu tempo de vida na atmosfera e suas propriedades físico-químicas. As partículas em ambientes urbanos são uma mistura de emissões primárias e partículas secundárias. A distribuição do número de partículas está dominada por partículas menores que 0,1 µm, ou nanopartículas, enquanto que na distribuição em massa a concentração está dominada pelas partículas grossas (< 10 µm). A Figura 1 apresenta a distribuição de tamanho de partículas atmosféricas. A distribuição por número apresenta três modos principais: nucleação, Aitken e de acumulação. As partículas do modo nucleação, Aitken e acumulação são menores que 10 nm, entre 10 e 100 nm de diâmetro, e entre 100 e 1000 nm de diâmetro, respectivamente. As partículas no modo nucleação são formadas no processo de nucleação, podendo crescer em diâmetro pelo processo de condensação e formar as partículas no modo Aitken. A condensação afeta o tamanho mas não a distribuição por número. As partículas podem sofrer o processo de coagulação, do qual afeta a distribuição por número e por massa, diminuindo as concentrações do número e da massa (Figura 1). Por exemplo, as partículas no modo acumulação podem ser formadas pela coagulação de partículas menores ou a condensação de vapores (Figura 1). A distribuição também varia em função da distância, sendo que concentrações elevadas de partículas finas (< 2,5 µm) são encontradas cerca das fontes de emissão (rodovias e industrias), porém sua concentração diminue rapidamente em função da distância da fonte. As partículas atmosféricas < 1 µm, objeto deste estudo, são formadas por partículas primárias provenientes da combustão (Zhao *et al.*, 2008; Wingfors *et al.*, 2011) e partículas secundárias. Esta fração de tamanho de partículas é constituída dos modos núcleo (partículas de combustão dos veículos a motor), Aitken e acumulação (partículas da combustão e smog fotoquímico) (Bathmanabhan and Saragur, 2010).

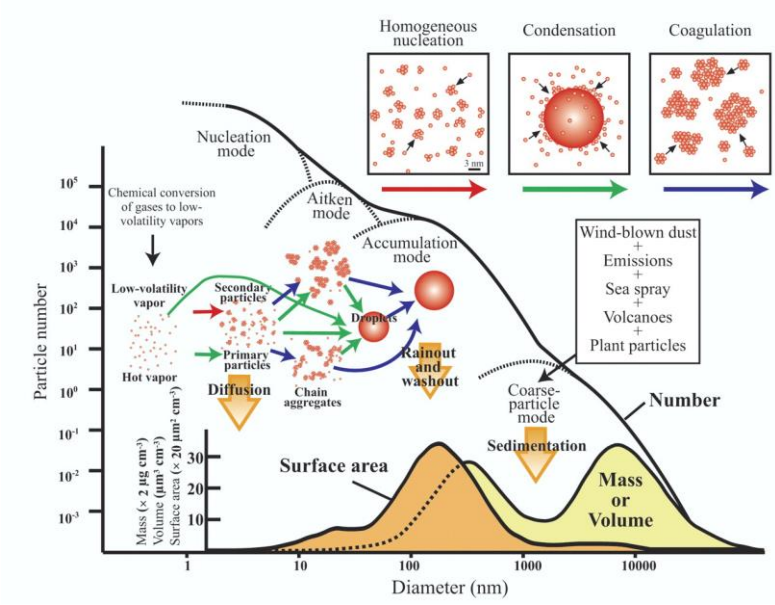

Figura 1. Distribuição de tamanho de partículas atmosféricas em função do número, massa e volume
Fonte: [http://www. elements.geoscienceworld.org]

Dos diversos fatores geradores de poluição do ar, destacam-se a emissão de poluentes de veículos automotores (Colvile *et al.*, 2001), que é a principal fonte de material particulado nas áreas urbanas. O tamanho das partículas depende da multiplicidade de fontes e processos que conduzem à sua formação e, por conseguinte, sobre o material a partir do qual foram formadas as partículas (Morawska *et al.*, 2008). O número e a distribuição de tamanho de partículas podem alterar-se rapidamente, devido à influência de processos de transformação, tais como a coagulação e condensação, e da turbulência que melhora a mistura e diluição (Kumar *et al.* 2011). A distribuição de tamanho da partícula é um parâmetro crucial para determinar a dinâmica dos aerossóis na atmosfera, seu transporte, deposição e tempo de residência (Colbeck and Lazaridis, 2010). As partículas grossas são facilmente retidas pelas vias respiratórias, enquanto que as finas podem entrar no sistema cardiorrespiratório. Portanto, é de grande importância a análise da distribuição granulométrica do material particulado e a sua concentração.

Das partículas atmosféricas emitidas pelas fontes móveis, mais de 90% da concentração em número pertence à fração < 1 µm (Bond *et al.*, 2004; Morawaska *et al.*, 2008), daí a importância do estudo desta fração. Esta fração pode afetar a saúde e, por sua vez, pode ser um bom indicador de fontes veiculares em locais perto das vias ou estradas (Lee *et al.*, 2006). Contudo, a emissão das partículas depende da temperatura, com maiores concentrações a temperaturas baixas (Olivares *et al.*, 2007), e maior teor de

enxofre do combustível (Wålhin, 2009), como por exemplo no combustível diesel. No entanto, no Brasil a adição de biodiesel no diesel contribui na redução da emissão de partículas, em razão que há uma menor formação de partículas de sulfato durante a combustão (Dwivedi *et al.*, 2006). Também as emissões veiculares são uma das principais fontes de emissão de óxidos de nitrogênio, especialmente na forma de NO (Gaffney e Marley, 2009), o que leva a emissão quase direta na camada limite planetária. Os motores diesel produzem cinco vezes a quantidade de NO_x por massa de combustível queimado quando comparado aos veículos a gasolina (Kirchstetter *et al.*, 1998). Somado a isso, a adição de biodiesel no diesel pode incrementar levemente as emissões de NO_x (Coronado *et al.*, 2009). Os poluentes secundários como NO_2 e O_3 troposférico, embora não tenham fontes de emissão naturais ou antropogênicas significativas (PORG, 2007**)**, podem ser formados por diversas reações no ar de poluentes primários (Finlayson-Pitts e Pitts, 2000). As principais reações de conversão entre NO e NO_2 são (Jenkin e Clemitshaw, 2000):

$$2NO + O_2 \rightarrow 2NO_2. \quad (1)$$

Porém, na maioria das condições troposféricas, a reação (1) é insignificante, e a via predominante pela qual o NO é convertido em NO_2 é através da reação com O_3:

$$NO + O_3 \rightarrow NO_2 + O_2. \quad (2)$$

Durante o dia, com a influência da luz solar, o NO_2 sofre fotólise e é novamente convertido a NO de acordo com a reação abaixo:

$$NO_2 + h\nu\ (\lambda<420\ nm) \rightarrow NO + O(^3P), \quad (3)$$

$$O(^3P) + O_2(+M) \rightarrow O_3 + M, \quad (4a)$$

onde M é um terceiro composto (geralmente N_2 ou O_2) que absorve a energia vibracional em excesso e, assim, estabiliza a molécula formada de O_3; *hv* representa a energia de um fóton; e O (^{3}P) é o oxigénio mono-atómico ativo (Han *et al.*, 2011). A fotólise de NO_2 é a uma fonte de geração de O_3 de grande significância (Zielinska, 2005). O NO_x tem um

tempo de vida químico curto e os seus maiores efeitos no O_3 estão limitados a sua proximidade das fontes de emissão (Uherek *et al.*, 2010).

Outros processos químicos na presença da luz solar geralmente envolvem radicais livres. De particular importância são os radicais hidroperoxilos (HO_2) e os peróxidos orgânicos (RO_2), que são produzidos principalmente na troposfera como intermediários na oxidação fotoquímica de monóxido de carbono (CO) e de compostos orgânicos voláteis (COVs). A luz solar inicia o processo fornecendo radiação ultravioleta que dissocia certas moléculas estáveis, conduzindo à formação de radicais livres de hidrogênio (HO_x) (PORG, 1997). Os compostos orgânicos estão envolvidos na produção de ozônio porque os RO_2 reagem com NO, convertendo-o em NO_2. Também os HO_2 fornecem uma rota adicional de conversão, segundo as reações (4b) e (4c)

$$HO_2 + NO \rightarrow OH + NO_2, \quad (4b)$$

$$RO_2 + NO \rightarrow RO + NO_2. \quad (4c)$$

Os peróxidos orgânicos (RO_2) e radicais hidroperoxilos (HO_2) são produtos que irão reagir com NO, convertendo NO para NO_2, o qual será fotolisado e formará posteriormente O_3 (Atkinson, 2000). Na ausência de COVs, o O_3 é formado a partir da fotólise do NO_2 pelas reações (3) e (4).

No entanto, uma vez que a conversão do NO em NO_2 como resultado destas reações não consome O_3, a subsequente fotólise de NO_2 (reação 3), seguido pela reação (4a), representa uma fonte de O_3. Há também fontes adicionais de consumo de O_3 troposférico, em ambientes marcados por concentrações baixas de NO. O O_3 é fotolisado formando o O (^3P) (reação 4a) e reage com vapor de água para formar os radicais OH nas reações (4d) e (4e):

$$OH + O_3 \rightarrow HO_2 + O_2, \quad (4d)$$

$$HO_2 + O_3 \rightarrow OH + 2O_2. \quad (4e)$$

Consequentemente, a produção de O_3 é sensível à concentração do COVs em relação à concentração de NO_x ($NO + NO_2$).

Equilibrio fotoestacionário: As reações (2) e (3) constituem um ciclo e na ausência de outras reações concorrentes de interconversão, atingem o equilíbrio em poucos

minutos e alcançam o chamado estado fotoestacionário, estabelecido por Leighton (1961):

$$[NO]\cdot[O_3]/[NO_2]=J_1/k_4, \quad (5)$$

onde J_1 é a taxa de fotólise do NO_2, e varia ao longo do dia dependendo do zênite solar e a transmissão da radiação solar através da atmosfera (Kewley and Post, 1978); k_4 é o coeficiente de taxa da reação de NO com O_3, em função da temperatura (Jenkin and Clemitshaw, 2000; Notario *et al.*, 2012), de tal forma que podem ser encontrados diversos valores experimentais, dependendo do intervalo de temperatura em que foram realizadas as medições. O valor de k_4 na reação (5) foi calculado usando a equação de Seinfeld and Pandis (2006): k_4 ($ppm^{-1}\cdot min^{-1}$) = 3.23×103 exp[-1430/T]. Porém, as reações (4b) e (4c) também podem perturbar o estado fotoestacionário.

Hidrocarbonetos Policíclicos Aromáticos (HPAs)

As partículas atmosféricas < 1 μm (MP_1) apresentam maior risco pelo fato que podem se depositar no trato respiratório, aumentando os efeitos negativos à saúde (Slezakova *et al.*, 2007), e podem carregar poluentes como os hidrocarbonetos policíclicos aromáticos (HPAs). Os HPAs são um grupo de diversos compostos orgânicos complexos, constituídos por carbono e hidrogênio junto com dois ou mais anéis benzênicos condensados (Ravindra *et al.*, 2008). Os HPAs podem ser encontrados na fase gasosa ou sólida (associado ao material particulado) dependendo do seu peso molecular ou volatilidade. Existem mais de 100 HPAs identificados no ar urbano, desde espécies com dois anéis (de baixo peso molecular) e que apresentam uma maior concentração na fase gasosa, até espécies de sete ou mais anéis (de alto peso molecular) que estão frequentemente associados com o material particulado (Bi *et al.*, 2003). As concentrações podem variar desde poucos $ng\cdot m^{-3}$ até 100 $ng\cdot m^{-3}$. HPAs de alto peso molecular estão principalmente na fração fina porque requerem muito mais tempo para sua partição às partículas grossas do que HPAs de baixo peso molecular (Duan *et al.*, 2007). Além disso, as partículas finas < 1 μm apresentam maior conteúdo de carbono orgânico e maior área de superfície específica, portanto as partículas finas podem ter maior adsorção de HPAs que as partículas grossas (Sheu *et al.*, 1997). Consequentemente, as maiores

concentrações de HPAs apresentam-se na fração fina. As características dos HPAs estudados encontram-se descritos na Tabela 1. Os compostos de alto peso molecular são considerados aqueles com 5 ou 6 anéis e encontram-se principalmente na fase sólida, associados ao material particulado; HPAs de 4 anéis podem estar tanto na fase gasosa como sólida.

Tabela 1. Propriedades dos HPAs estudados

HPAs	Peso Molecular	Número de anéis
Naftaleno	128,1	2
Acenaftaleno	152,1	3
Acenafteno	154,2	3
Fluoreno	166,2	3
Fenantreno	178,1	3
Antraceno	178,2	3
Fluoranteno	202,1	4
Pireno	202,1	4
Benzo[*a*]Antraceno	228,1	4
Criseno	228,1	4
Benzo[*b*+*k*]Fluoranteno	252,1	5
Benzo[*a*]Pireno	252,1	5
Indeno[*1*,*2*,*3*-cd]Pireno	276,3	6
Dibenzo[*a*,*h*]Antraceno	276,3	5
Benzo[*ghi*]perileno	276,1	6

O carbono orgânico é um componente principal nas partículas finas, constituindo, por exemplo, ~ 45,7% de MP_1 em ambientes perto de estradas, onde as emissões veiculares são uma fonte importante (Lee *et al.*, 2006). No processo de formação das partículas orgânicas formadas na combustão, os HPAs são considerados os principais intermediários moleculares para a formação e crescimento da fuligem. Os núcleos de fuligem crescem através de várias reações químicas, atingindo diâmetros maiores que 10 nm, momento em que eles começam os processos de coagulação e, consequentemente, crescem rapidamente em virtude das reações de superfície (Seinfeld and Pandis, 2006).

As fontes de emissão de HPAs podem ser processos de combustão ou pirólise de matéria orgânica (Li *et al.*, 2005). Entre as fontes de combustão se encontram combustão de carvão e queima de madeira; refino de etanol, petróleo e gás; motores de veículos e queima a céu aberto. As fontes móveis (veículos), junto com o aquecimento doméstico e a queima a céu aberto não controlada, são fontes susceptíveis de fornecer a maior parte da exposição humana aos HPAs na atmosfera, uma vez que os humanos se reúnem em ambientes urbanos caracterizados por essas fontes (Howsan e Jones, 2010). Zhang e Tao (2009) mostraram que as principais fontes de emissões atmosféricas antropogênicas de

HPAs incluem queima de biomassa e carvão, combustão de petróleo e coque, e produção de metal. As principais fontes de HPAs nas regiões urbanas são as fontes móveis, especialmente pelos motores de combustão diesel (Devos, 2006). Isto porque as partículas de fuligem do diesel têm uma grande relação superfície/volume e superfícies reativas, e por isso atraem materiais condensáveis, como os HPAs, logo após a emissão para o ar ambiente (Watson *et al.*, 2005). Além disso, os HPAs são mais propensos a acumular-se ao longo do tempo no óleo lubrificante dos veículos durante o processo de combustão no motor, porém a fonte dominante de HPAs nas emissões veiculares é dependente do combustível utilizado e de tecnologias empregadas nos catalizadores (Kleeman *et al.*, 2008; Russel, 2013). As concentrações de HPAs mostram maiores concentrações no inverno, uma tendência sazonal possivelmente causada pelo aumento da adsorção destas substâncias em menores temperaturas. A redução da concentração dos HPAs associados ao MP_1 está relacionada com os mecanismos de redução de partículas, como a deposição seca e úmida. A deposição úmida refere-se à remoção pela chuva ou neve e à deposição seca refere-se à sedimentação e a impactação inercial. Porém, os HPAs podem se decompor pela fotodegradação, reações químicas com poluentes no ambiente urbano ou pela partição gás-partícula. A fotodegradação é o principal mecanismo de decomposição química para HPAs associados ao material particulado de 4 a 6 anéis (Finlayson-Pitts e Pitts, 2000). O particionamento gás-partícula é também um fenômeno importante para a perda de HPAs de 2 a 4 anéis associados às partículas atmosféricas. Os principais compostos da fotólise e das oxidações de HPAs são peróxidos, dionas, fenóis e quinonas (Neilson, 2010).

Os HPAs podem reagir na atmosfera com NO_2 ou com o radical NO_3 (à noite) e dar origem aos nitro-HPAs (NHPAs). Ainda durante o dia, podem sofrer fotólise ou reagir com ozônio ou radicais OH. A fotólise dos HPAs depende da intensidade da luz solar, da temperatura, da umidade relativa e também da natureza da superfície da partícula sólida, incluindo a presença de uma camada orgânica que "protege" à partícula. O material carbonáceo pode proteger o HPA da fotólise ou da degradação.

Identificar as fontes de emissão de HPAs é muito importante para poder reduzir a concentração de tais componentes no ar. A identificação pode ser realizada mediante o uso de razões diagnósticos ou modelos receptores. O método da razão diagnósticos para identificação das fontes de HPAs envolve a comparação destas razões com valores encontrados na literatura ou estudos de emissão (Ravindra *et al.*, 2008). Porém, este

método deve ser usado com precaução porque é muitas vezes difícil de distinguir entre algumas fontes (Ravindra *et al.*, 2006) e igualmente, porque as concentrações de HPAs das fontes de emissão podem ser alteradas devido à reatividade dos HPAs com espécies atmosféricas (ozônio, óxidos de nitrogênio) e variáveis ambientais, como temperatura, radiação solar, umidade, direção do vento, velocidade do vento, radiação solar e precipitação, que podem afetar a deposição seca e a fotólise que são provavelmente os processos de perda mais importantes dos HPAs (Neilson 2010).

O princípio fundamental nos modelos receptores das relações fonte/receptor é que uma conservação da massa considerada e uma análise de balanço de massa pode ser utilizada para identificar e conhecer a contribuição das fontes de emissão de material particulado (Hopke, 2003). Além de serem constituintes ubíquos no ar urbano, são de grande preocupação da saúde, principalmente devido às suas conhecidas propriedades carcinogênicas e mutagênicas (Panther *et al.,* 1999). Os isômeros conhecidos como carcinogênicos estão associados principalmente ao material particulado e às concentrações mais elevadas, encontrando-se geralmente na fração respirável de < 5 µm (Sienra *et al.*, 2005). Segundo a *International Agency for Research on Cancer* (IARC, 2010), o benzo[*a*]pireno foi classificado como carcinogênico para humanos, dibenzo[*a,h*]antraceno como provável cancerígeno para os seres humanos e indeno[1,2,3-*cd*]pireno como possível cancerígeno para os seres humanos. Apesar disso, destaca-se que criseno, benzo(b)fluoranteno, benzo(k)fluoranteno, benzo[*a*]pireno, dibenzo[*a,h*]antraceno e antraceno foram encontrados como cancerígenos em animais experimentais após a inalação ou ingestão intratraqueal, aumentando a preocupação com os níveis destas substâncias cancerígenas no ar (IARC, 2013). O Parlamento Europeu e o Conselho da União Europeia estabeleceram as diretrizes de qualidade do ar para HPAs (1,0 $ng \cdot m^{-3}$ de BaP na fração MP_{10}). Este limite e a publicação científica *Air Pollution and Cancer* (IARC, 2013) demonstram a importância da máxima redução e estudo destes poluentes.

Espectrorradiometria no infravermelho

Desde o surgimento do sensoriamento remoto orbital há mais de 40 anos, a espectrorradiometria óptica é uma importante técnica para estudos sobre a estrutura e

composição de alvos, como minerais, rochas, solos, água, vegetação, gases, etc. Mais recentemente, tais estudos se estenderam para a região do infravermelho termal, fomentando pesquisas com a caracterização de materiais geológicos, alvos urbanos, atmosfera (poluentes, aerossóis, nuvens), água, entre outras A espectrorradiometria é definida como a medida da distribuição da energia radiante (Meneses, 2001). A radiação infravermelha corresponde à parte do espectro eletromagnético entre as regiões do visível e das micro-ondas. A porção de maior utilidade para a análise e identificação de compostos orgânicos está situada entre 4000 e 400 cm^{-1}. As radiações da banda infravermelha são geradas em grande quantidade pelo Sol, em razão da sua temperatura elevada; entretanto podem também ser produzidas por objetos aquecidos (como filamentos de lâmpadas). Muitos gases são fortes absorvedores nesta porção do espectro, especialmente vapor de água, dióxido de carbono, o óxido nitroso e o metano. Portanto, ambientes secos são preferíveis para medidas utilizando esta técnica, devido a que o vapor de água é um contribuinte principal de ruído.

Nesta região, a radiação infravermelha faz com que os átomos vibrem com maior rapidez. Quando a ligação absorve energia, ela sofre alterações e, ao retornar ao estado original, libera essa energia, que então é detectada pelo espectrômetro. A espectroscopia no infravermelho fornece evidências da presença de vários grupos funcionais na estrutura orgânica em virtude da interação das moléculas ou átomos com a radiação eletromagnética em um processo de vibração molecular (Silvestain e Webster, 2005). Existem dois tipos de vibrações moleculares: estiramentos e deformações angulares. Os estiramentos podem ser simétricos ou assimétricos e são caracterizados pelas deformações que ocorrem ao longo do eixo de ligação, que resultam em um contínuo alogamento e encurtamento da distância interatômica da ligação (Figura 1). As vibrações de deformação angular correspondem ao movimento de um grupo de átomos em relação ao resto da molécula, sem que as posições relativas dos átomos do grupo se alterem. Essas deformações recebem a denominação de deformação angular simétrica e assimétrica no plano e deformação angular simétrica e assimétrica fora do plano (Figura 2 e 3).

Figura 2 a,b. Estiramento Simétrico (a), Estiramento Assimétrico (b).

(a) **(b)**

Figura 3 a,b. Deformação Angular Simétrica no Plano (a); Deformação Angular Asimétrica no Plano (b).

As ligações covalentes que constituem as moléculas orgânicas estão em constantes movimentos axiais e angulares. A incidência de radiação infravermelha em uma molécula faz com que átomos e grupos de átomos dessa molécula vibrem com amplitude aumentada ao redor das ligações covalentes que as ligam (Brown *et al.*, 1998). O processo é quantizado, ou seja, as ligações químicas de uma molécula possuem frequências vibracionais especificas. Assim, se a frequência da radiação incidida sobre a molécula coincidir com a sua frequência vibracional, a radiação será absorvida, causando uma mudança na amplitude da vibração molecular.

Na região do infravermelho, qualquer objeto com temperatura >0 K emite radiação termal. O material que absorve toda a energia incidente, e emite toda ela, é chamado de corpo negro. O fluxo radiante emitido é função da temperatura do objeto, de modo que quanto maior a temperatura, maior o fluxo. O fluxo radiante por unidade de área ($W \cdot m^{-2}$) e por unidade de comprimento de onda (ou frequência) é chamado de excitância espectral ou emitância. Planck desenvolveu uma teoria que explicava teoricamente a emissão termal pela seguinte fórmula para a excitância espectral de um corpo negro:

$$E_\lambda = \frac{C_1}{(\lambda^5\,[exp(C_2/\lambda T)-1]\,)} \qquad (6)$$

onde,

Eλ é a excitância espectral do corpo negro ($W \cdot m^{-3}$),

λ comprimento de onda (m),

T temperatura absoluta (K),

C_1 primeira constante de radiação = 3.74151 x 10-16 ($W.m^2$),

C_2 segunda constante de radiação = 0.0143879 (m.K).

Esta equação, conhecida como a distribuição de Planck, está plotada na Figura 3 para determinadas temperaturas.

A Figura 3 apresenta a distribuição espectral de energia para corpos negros a várias temperaturas e onde se pode notar o deslocamento máximo de emissão em função da temperatura. Nesta figura pode ser observado que a distribuição espectral tem a máxima emissão dependendo da temperatura e do comprimento de onda. O comprimento de onda no qual ocorre a máxima excitância pode ser obtido utilizando a lei de deslocamento de Wien:

$$\lambda_{max} T = C_3 , \qquad (7)$$

onde,

$C_3 = 2.898 \times 10^{-3}$ m·K.

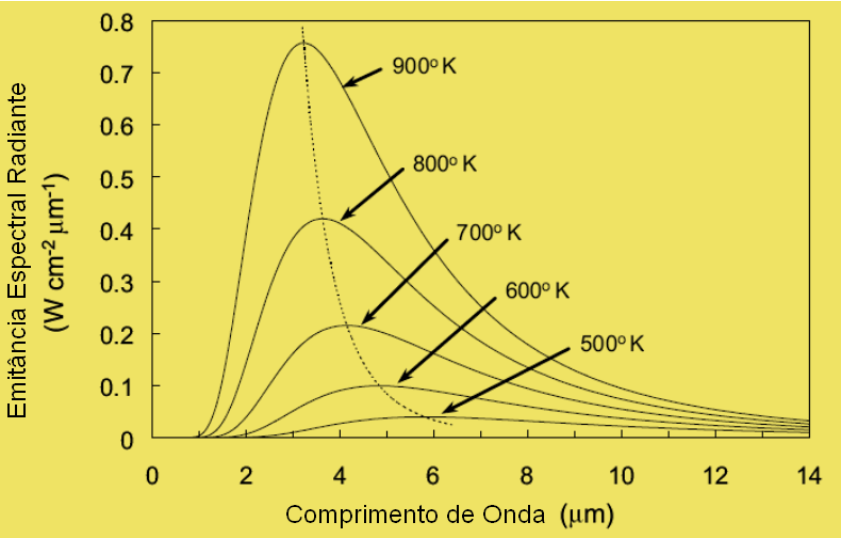

Figura 4. Curvas de excitância espectral de corpo negro às diferentes temperaturas na região do infravermelho.

Fonte: ELACHI E VAN ZYL (2006)

Porém, as superfícies reais não são ideais como os corpos negros e, consequentemente, devemos usar o corpo negro como uma referência para descrever a emissão de uma superfície real. A propriedade radiativa de superfície, conhecida como emissividade, pode ser definida como a razão entre a radiação emitida (exitância) pela superfície e a de um corpo negro na mesma temperatura:

$$\varepsilon_\lambda = L_{\lambda s} / L_{\lambda b}, \quad (8)$$

onde,

$0 < \varepsilon < 1$.

Os HPAs têm estruturas complexas e, por causa da sua larga variabilidade na formação de isômeros, vários tipos diferentes de HPAs podem existir. Por exemplo, para HPAs contendo seis anéis aromáticos, são possíveis a formação de 82 configurações isoméricas. Como a toxicidade, a carcinogenicidade e mutagenicidade de diferentes isômeros podem ser diferentes, a habilidade de distinguir esses isômeros para avaliação ambiental e subsequente remediação é importante. Em geral, os espectros dos HPAs consistem em pelo menos uma banda na região espectral de 900-680 cm^{-1} em razão da deformação angular CH fora do plano. Uma banda de forte/média intensidade na região espectral de 3100-3000 cm^{-1} é característica de estiramentos das ligações CH aromáticos. A região espectral de 1300-1000 cm^{-1} contém vários picos fracos devida às deformações angulares CH no plano. Por sua vez, a região de 1600-1300 cm^{-1} também apresenta picos de fraca intensidade em virtude dos diversos estiramentos das ligações C-C e C=C aromáticas (Semmler, 1991).

METODOLOGIA

Área de estudo

Os equipamentos foram instalados em dois locais de amostragem, nos municípios de Sapucaia do Sul e Canoas, localizados na área de estudo: a Região Metropolitana de Porto Alegre (RMPA). A área de estudo situa-se na parte centro-leste do Rio Grande do Sul, delimitada pelos paralelos 28°S e 31°S e longitudes 50°W e 54°W. A área compreende atualmente 9.652,54 km^2 e, de acordo com estimativas da Fundação Estadual de Planejamento Metropolitano e Regional (METROPLAN), tem 4,1 milhões de habitantes (METROPLAN, 2012).

Os locais foram selecionados devido à sua influência veicular, embora haja algumas diferenças entre os sítios. Sapucaia do Sul tem uma influência veicular maior: frota leve e pesada, congestionamentos e velocidades lentas. Este local também tem influência industrial baixa (refinaria de petróleo e siderúrgicas que não utilizam coque) a montante dos ventos dominantes. Canoas está sob uma forte influência de veículos, congestionamentos diários, a base aérea de Canoas (Quinto Comando Aéreo Regional da Força Aérea – *V COMAR*), e industrias (refinaria de petróleo) a montante dos ventos dominantes, que têm uma influência média neste local de amostragem.

A região constitui o eixo mais urbanizado do estado, é caracterizada por diferentes tipologias industriais, incluindo diversas fontes estacionárias como a Refinaria Alberto Pasqualini, indústrias siderúrgicas (Siderúrgica Riograndense e Aços Finos Piratini), o Complexo Industrial do III Pólo Petroquímico e usinas termelétricas movidas a carvão (Termelétrica de Charqueadas - TERMOCHAR e a Usina Termelétrica de São Jerônimo - USTJ). Além das diferentes tipologias industriais encontradas na RMPA, estima-se que a contribuição mais significativa sejam as fontes móveis em virtude do grande número de veículos em circulação na região, que representam 20% do total de carros da frota total no estado (Dallarosa *et al.*, 2008). Esta região possui um grande número de veículos em circulação, cerca de 2,06 milhões de veículos (DETRAN, 2013), dos quais cerca de 84,98% da frota é movida a gasolina, 6,67% a diesel, 6,58% a álcool, 1,03% a gás natural e 0,74% com tecnologia flex (Teixeira *et al.*, 2008). O local de estudo está próximo do eixo inferior da BR-116, onde o fluxo é de aproximadamente 150 mil veículos/dia (MT, 2012). Atualmente, os veículos a gasolina utilizam uma mistura de gasolina+etanol, já com adição de 20% de etanol na própria gasolina (PETROBRAS, 2012). O diesel

metropolitano usado na região contém um nível de enxofre de 500 ppm e é aditivado com 5% de biodiesel (Mattiuzi *et al.*, 2012). Mesmo que a frota a diesel na Região seja somente 6,67%, o impacto ambiental no ar é elevado. O estudo dos autores Teixeira *et al.* (2008) mostra que das emissões totais de fontes móveis de poluentes na RMPA, os veículos a diesel contribuem com mais material particulado e NO_x do que os veículos movidos a gasolina ou álcool.

Devido a sua localização, a área de estudo apresenta estações definidas, além de um clima fortemente influenciado pelas massas de ar frio que migram das regiões polares. A média histórica da precipitação é de 1300-1400 $mm \cdot ano^{-1}$ (INPE – CPTEC, 2003). A direção do vento apresenta variações sazonais marcantes: durante o verão e a primavera, a direção preponderante é este - sudeste; já durante o outono e inverno, além dos ventos de origem este–sudeste, ocorrem ventos vindo de oeste e noroeste (EMBRAPA, 2003). A Figura 5 apresenta a localização das estações de monitoramento, na quais se encontram os equipamentos.

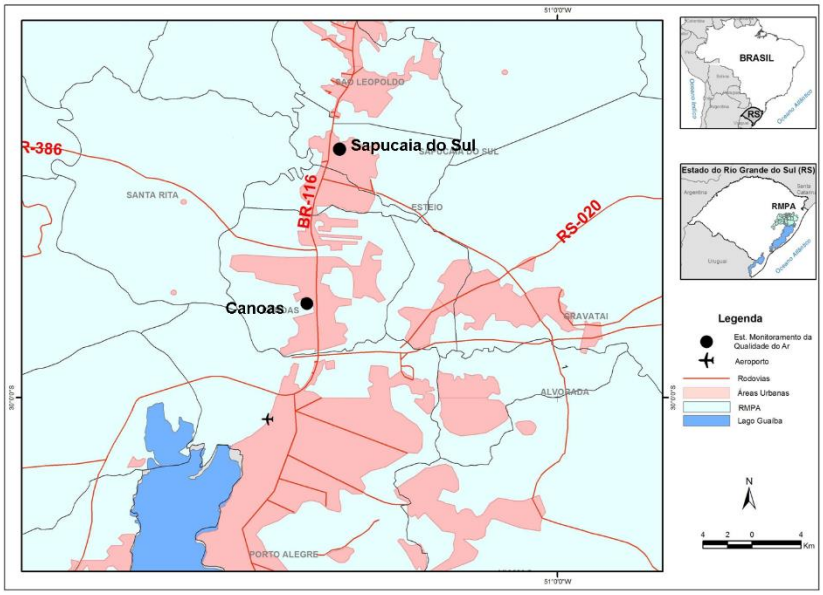

Figura 5. Localização dos pontos de amostragem em Sapucaia do Sul e Canoas na Região Metropolitana de Porto Alegre, RS.

Materiais e métodos

Equipamentos

Os amostradores automáticos, o medidor contínuo de granulometria e os analisadores de NO, NO_2 e NO_x, e O_3 foram instalados junto à rede da FEPAM em função dos motivos seguintes: software, avarias e roubo. O número de partículas atmosféricas foi medido usando o analisador de partículas. NO, NO_2 e NO_x foram medidos usando o analisador AC32M e O_3 usando o O342M.

A *distribuição granulométrica das partículas* foi medida usando o analisador de partículas suspensas no ar da Environnement S.A. O analisador de partículas é do tipo óptico, que utiliza um feixe de laser para medir a intensidade do espalhamento causado pelas partículas atmosféricas presentes na amostra de ar, aplicando o princípio do espalhamento Mie (ENVIRONNEMENT, 2010). Seu princípio consiste em um laser (635 nm) que incide sobre a amostra, sendo espalhado em várias direções. Um fotodiodo, situado em torno de 15º do laser incidente, mede a intensidade da radiação espalhada. Neste ângulo, a intensidade da luz dispersa independe da natureza das partículas, sendo função do seu tamanho (Renard *et al.*, 2010). O analisador mede essa intensidade e classifica o material particulado em três faixas de tamanho de diâmetro de partícula: PR1 (número de partículas atmosféricas com diâmetro entre 0,3-1,0 µm), PR2.5 (1-2,5 µm) e PR10 (2,5-10 µm).

Óxidos de nitrogênio (NO, NO_2 e NO_x) em baixas concentrações no ar foram medidos usando o AC32M. O AC32M é um analisador por quimiluminescência que opera sob o princípio que o NO emitirá luz (quimiluminescência) na presença de moléculas de O_3 altamente oxidantes. O NO será oxidado pela presença de O_3 formando moléculas de NO_2 excitado, o qual emitirá radiação luminosa nos comprimentos de onda de 600-1200 nm do espectro. A leitura da radiação é realizada em um fotomultiplicador. Para a medição de NO_2, ele deve ser transformado a NO no forno de molibdênio. A medição é realizada, então, em três etapas: ciclo de referência, ciclo de NO e ciclo de NO_x. O cálculo da quantidade de NO_2 é realizado pela diferença entre as concentrações de NO e NO_x.

Ozônio troposférico foi medido usando o O342M, um analisador que usa o princípio de absorção de radiação UV pelas moléculas de O_3. A concentração de O_3 é determinada pela diferença entre a absorção de radiação UV da amostra de ar e da amostra sem O_3

após filtragem no conversor catalítico. Uma média das medidas instantâneas é realizada pelo aparelho.

A amostragem de *partículas atmosféricas < 1.0 µm* ($MP_{1.0}$) presentes no ar seguiu os critérios estabelecidos pela USEPA (1994), através do amostrador automático sequencial de partículas modelo PM162M construído pela Environnement S.A. O amostrador de partículas inclui um jogo de dois recipientes (holders) que funcionam como suporte para os filtros. O equipamento usa o método EN 12341 (LECES, n° RC/L 9826) e trabalha por impacto com vazão volumétrica de 1,0 $m^3 \cdot h^{-1}$. Possui sensores de temperatura e pressão atmosférica localizados no ponto de amostragem, que regulam a temperatura da linha. Este tubo de amostragem regulado foi desenhado para evitar artefatos no filtro, tais como a condensação ou a perda de compostos semi-voláteis. As amostras de partículas atmosféricas foram coletadas em filtros de PTFE de 47 mm de diâmetro durante um período contínuo de 72 horas, desde agosto de 2011 até junho de 2014. Os filtros foram embalados em papel alumínio e transportados sob refrigeração até o laboratório para em seguida ser congelados em freezer para posterior análise. O procedimento de preparação dos filtros é descrito em trabalhos anteriores (Teixeira *et al.* 2011).

Os *dados meteorológicos* como temperatura do ar, umidade relativa, radiação, velocidade e direção do vento foram obtidos da estação meteorológica em Esteio pertencente à REFAP, situado a uma distância próxima aos equipamentos de amostragem.

O espectrorradiômetro portátil de campo utilizado para obtenção de *espectros de emissividade* foi o modelo 102F da Design and Prototypes de infravermelho termal com transformada de Fourier (FTIR). As análises foram realizadas no Centro Estadual de Pesquisa em Sensoriamento Remoto e Meteorologia (CEPSRM) da Universidade Federal do Rio Grande do Sul (UFRGS). O FTIR consiste em um módulo óptico/eletrônico, o interferômetro Michelson e os detectores de infravermelho. O espectrômetro possui dois detectores, um de Insb (Indio-antimônio) e outro de MCT (Mercurio-câdmio-telurio) cobrindo as faixas espectrais de 3330-2000 cm^{-1} e 2000-700 cm^{-1}, respectivamente, resfriados por nitrogênio líquido (Salisbury, 1998). Também conta com um jogo de corpos negros que podem ser regulados para diferentes temperaturas entre 5°C e 60°C durante a calibragem do instrumento. A faixa espectral é 3330 até 700 cm^{-1} e foi operado com uma resolução espectral de 4 cm^{-1} e precisão espectral de + / - 1 cm^{-1}. Entretanto, os resultados analisados foram na faixa de 700 até 1660 cm^{-1} devido a que este equipamento apresenta uma baixa relação sinal/ruído na faixa de 1660 até 3330 cm^{-1} (Korb *et al.*,

1996). Também nesta faixa (1660 até 3330 cm^{-1}) há pouca transmitância fora da janela atmosférica pela existência de fortes bandas de metano, CO_2 e vapor de água (Korb *et al.*, 1996). Os dados foram obtidos usando uma média de 100 varreduras, ou seja, 100 interferogramas coadicionados (100 co-added interferograms). As medições foram realizadas a uma distância menor a 1 metro (50 cm) para minimizar a atenuação da atmosfera (Korb *et al.*, 2006). Além disso, todas as medições de emissividade foram realizadas em campo sob condições de céu aberto sem nuvens e umidade relativa de baixa a moderada (< 60%). Foi utilizado o telescópio de 2,54 cm de diâmetro e uma distância menor de 50 cm para garantir que o tamanho do campo de visão (FOV) fosse menor que o da amostra, que possuía um diâmetro de 47 mm.

Os *espectros de transmitância* foram obtidos em um aparelho BOMEM MB-series FTIR-Hartmann & Braun Michelson (DRIFTS) equipado com um detector DTGS. Os espectros de transmitância foram medidos com uma resolução de 4 cm^{-1} e 50 varreduras foram tomadas para obter uma relação sinal/ruído apropriada. A faixa espectral medida foi de 400 até 4000 cm^{-1}. Os espectros de transmitância do material particulado MP_1 foram coletados de cada amostra e são apresentados em unidades arbitrárias (u.a.). Os espectros foram calculados usando um filtro branco, sem amostra, como background. Os padrões sólidos foram preparados em pastilhas de KBr sólidas para obter espectros de transmitância por DRIFTS. Para a obtenção de espectros de emissividade dos padrões sólidos por FTIR, os padrões foram colocados sem nenhuma preparação em pratos de 50 mm de diâmetro. Padrões sólidos Sigma-Aldrich de 99% de pureza de HPAs foram utilizados. Foram obtidos espectros dos padrões fluoranteno, pireno, benzo[*a*]pireno e benzo[*a*]antraceno.

Análise de HPAs

Os extratos dos filtros foram analisados de acordo com o método USEPA TO 13A (USEPA, 1999) para a determinação dos 16 HPAs (Hidrocarbonetos Policíclicos Aromáticos) prioritários: Naftaleno, Acenaftaleno, Acenafteno, Antraceno, Benzo[*a*]antraceno, Benzo[*a*]pireno, Benzo[*b*]fluoranteno, Benzo[*k*]fluoranteno, Benzo[*ghi*]perileno, Criseno, Dibenzo[*a,h*]antraceno, Fenantreno, Fluoranteno, Fluoreno, Indeno[*1,2,3-cd*]pireno, Pireno. As concentrações de Benzo[*b*]fluoranteno e Benzo[*k*]fluoranteno foram somadas por ter tempos de retenção iguais e denotados como Benzo[b+*k*]fluoranteno. A análise de HPAs foi realizada no Laboratório de Química da

Fundação Estadual de Proteção Ambiental Henrique Luiz Roessler (FEPAM) do Rio Grande do Sul.

Filtros com MP_1 foram extraídos em Soxhlet com 125 mL de diclorometano (CH_2Cl_2) durante 18 horas (USEPA, 1999). Após este procedimento os extratos foram separados/pré-concentrados através do procedimento de *clean up*, utilizando uma coluna de sílica gel (ativada com 5% de H_2O destilada) para eliminar possíveis interferências (Teixeira *et al.*, 2011; Dallarosa *et al.*, 2005a; 2005b; 2008) e usando quatro frações de solventes com diferentes polaridades: a primeira fração de 20 mL de hexano (alifáticos); a segunda fracção, 10 mL de hexano e 10 mL de diclorometano (HPA); a terceira fração, 15 ml de hexano e 5 mL de diclorometano (HPA); e quarta fracção, 20 ml de diclorometano (nitro-HPA). O volume das frações 2 e 3 foi reduzida até à secura usando um evaporador rotativo, seguido por um fluxo de gás de nitrogênio puro. Finalmente, é adicionado 1 mL de diclorometano com micropipeta electrónica para análise subsequente.

HPAs foram identificados por cromatografia gasosa acoplada a um detector de espectrometria de massa (Shimadzu, modelo GCMS-QP5050A), através de monitoramento seletivo dos íons (SIM). O cromatógrafo foi equipado com uma coluna capilar de sílica fundida de 30 m, DB-5 (0,2 mm ID, 0,25 mm de espessura) com hélio como gás de transporte (1,5 ml/min, de fluxo constante). O programa de temperatura da coluna trabalhou de 60 ºC a 300 °C, com aumento gradativo de 6 °C/min. A temperatura da coluna foi mantida isotérmica a 300 ºC durante 20 min. Todas as amostras foram injetadas no modo de splitless. Os dados para análise qualitativa foram adquiridos por meio do processo de ionização de elétrons (EI) (70 eV). Os detalhes da técnica de detecção de HPAs encontram-se descritos em Dallarosa *et al.* (2005a; 2005b) e Teixeira *et al.* (2013).

Análises de três amostras de SRM-1649b (Standard Urban Dust Reference Material) do National Institute of Standards and Technology (NIST) foram usadas para validar o método analítico. O SRM-1649b foi extraído conforme a metodologia descrita anteriormente. A Tabela 2 apresenta os resultados com os respectivos valores de recuperação. As análises foram realizadas através de replicatas (n=3). As recuperações do SRM-1649b (NIST, Washington, DC) variaram entre 80,4% (Indeno(1,2,3-cd) Pireno) e 124,4% (Fluoreno) com uma média de recuperação de 96,9%, de 0,02 g de SRM-1649b. A precisão foi representada pelo desvio padrão relativo (RSD), que foi <13%.

Tabela 2. As concentrações de HPAs obtidas no SRM-1649b e este estudo ($mg \cdot kg^{-1}$).

Nome	Material certificado SRM 1649b	Valor medido	Recuperação (%)	RSD (%)
Fenantreno	3.941±0.047	4.39±0.19	111.3%	4%
Antraceno	0.509±0.002	0.50±0.05	97.7%	10%
Fluoranteno	6.14±0.12	5.14±0.24	83.7%	5%
Pireno	4.784±0.029	4.44±0.34	92.8%	8%
Benzo[*a*]antraceno	2.092±0.048	2.23±0.05	106.7%	2%
Criseno	3.008±0.044	3.12±0.39	103.8%	12%
Benzo[*b+k*]fluoranteno	7.738±0.283	6.63±0.31	85.7%	5%
Benzo[*a*]pireno	2.47±0.17	2.35±0.07	95.1%	3%
Indeno[1,2,3-*cd*]pireno	2.96±0.17	2.38±0.30	80.4%	13%
Dibenzo[*a,h*]antraceno	0.29±0.004	0.26±0.03	88.8%	12%
Benzo[*ghi*]perileno	3.937±0.052	3.62±0.06	92.0%	2%

Análise de dados

Banco de dados: O banco de dados do distribuidor de tamanho de partículas, o analisador de óxido de nitrogênio e analisador de ozônio foram gerados a partir dos dados brutos registrados no aparelho. Para todos os casos (partículas, óxidos de nitrogênio e ozônio), as medições foram realizadas a cada 15 minutos de forma contínua. O banco de dados foi gerado a partir dos dados brutos registrados (a cada 15 min) e, posteriormente, calculadas as médias horárias e diárias. Os dados foram analisados usando o programa STATISTICA 7©. Com as médias de 15 minutos dos dados, foram calculadas as concentrações médias horárias para $NO/NO_x/NO_2/O_3$ para cada uma das quatro estações do ano. Além disso, a variação média diária de poluentes estudados foi calculada. Análises de correlação entre as concentrações médias horárias de $O_3/NO/NO_x/OX/MP_{10}/CO$ e parâmetros meteorológicos foram realizados. Um gráfico de dispersão da variação da média diária de $[NO_2]/[OX]$ em função de NO_x foi usado para fornecer uma melhor visão e interpretação das relações entre NOx e os poluentes $NO_2/NO_x/O_3$.

Modelo Receptor PMF: Os dados de HPAs foram utilizados para identificar as fontes de emissão usando o modelo receptor Positive Matrix Factorization (PMF). PMF é uma ferramenta de análise fatorial multivariada que decompõe a matriz de dados em duas matrizes, contribuições de cada fator e perfis (Paatero e Tapper, 1994; Paatero, 1997), com uma matriz residual (Vestenius *et al.*, 2011). O princípio fundamental das relações

fonte/receptor de modelos receptores é que a conservação de massa pode ser assumida e que uma análise de balanço de massa pode ser usada para identificar fontes de material particulado atmosférico (Hopke, 2003). O modelo receptor utilizado neste estudo foi o EPA PMF v3.0, desenvolvido por U.S. EPA (USEPA, 2008), para identificar o perfil de origem e de sua contribuição. O modelo receptor PMF é descrito resumidamente abaixo e em outro estudo recentemente publicado (Teixeira *et al.*, 2013). O modelo matemático em forma matricial é (Equação 9):

$$X = GF + E, \quad (9)$$

onde X é a matriz conhecida de concentração das m espécies químicas em n amostras; G é a matriz nxp das contribuições de cada fonte para cada amostra; F é a matriz caracterizando cada fonte (perfil) e é definida como uma matriz residual. O objetivo do PMF é encontrar valores para G e F que melhor reproduzirem os dados medidos (X). Estes valores são ajustados até um valor mínimo de Q encontrado (Reff *et al.*, 2007). Q é um parâmetro de benevolência de ajuste, e é definido pela equação 10 abaixo:

$$Q = \sum^{m} \sum^{n} \left[\frac{E}{U}\right]^2, \quad (10)$$

onde E é a diferença entre o conjunto de dados originais (X) e a saída de PMF (GF), U é a incerteza dos dados medidos, m é o número de espécies e n é o número de amostras (Wang *et al.*, 2009; Reff *et al.*, 2007). Se a análise é devidamente ponderada, o valor Q deve ser aproximadamente igual ao valor Q teórico, o qual pode ser estimado pela seguinte equação 11 (USEPA, 2008):

$$Q_t = m*n - p(m+n), \quad (11)$$

onde p é o número de fatores selecionados no modelo.

Os valores de incertezas (U) foram calculados para dois casos: quando a concentração da espécie (X) é inferior ou igual ao limite de detecção Método - MDL (Equação 12) e quando a concentração da espécie é maior do que o MDL (Equação 13) (Reff *et al.*, 2007):

$$U = {}^{5}/_{6} \times MDL, \quad (12)$$

$$U = (0{,}05 \times X) + MDL. \quad (13)$$

A qualidade dos dados para cada uma das espécies (HPAs) foi baseado no sinal-ruído (S/N) e a percentagem de amostras anteriores ao MDL. Naftaleno, acenaftileno e acenafteno foram classificados como espécies ruins. Fluoreno e benzo [*gh*i] perileno foram classificados como fracas. Espécies fracas têm a sua incerteza multiplicada por um fator de 3; espécies ruins são excluídas do processo de modelagem.
O modelo foi realizado várias vezes com número variável de elementos (que variam de 3 a 7), utilizando o modo de semente aleatória. A solução de seis fatores foi a que apresentou melhores resultados em termos de interpretações físicas significativas.

Avaliação de risco carcinogênico: O risco de câncer pela exposição a determinados HPAs é expressa em termos de BaP, como o fator de equivalência tóxica (TEF), porque os humanos são expostos a misturas complexas de HPAs (Cristale *et al.*, 2012). As concentrações no ambiente de 12 HPAs, começando a partir de fluoreno e seu fator de equivalência tóxica (TEF), foram usados no cálculo. A soma dos produtos de cada uma das concentrações de HPA e seu respectivo TEF é chamado valor BaPeq. O BaPeq foi calculado para amostras de MP_1 de Sapucaia do Sul e Canoas usando a Equação (14),

$$BaP_{eq} = \sum PAH_{conc} * PAH_{TEF} \ , \tag{14}$$

onde BaP_{eq} é o fator de equivalência tóxica baseado em BaP, PAH_{conc} é a concentração individual de cada HPA e PAH_{TEF} é o fator equivalente tóxico de cada HPA individual usando os fatores propostos por Nisbet e Lagoy (1992). Neste trabalho foi utilizada uma TEF de 1 em vez de 5 para DahA, como proposto por Nisbet e Lagoy (1992).

Filtro Kolmogorov-Zurbenko (KZ): O tratamento com filtro KZ foi aplicado aos dados das médias de 15 min de O_3 para analisar as séries temporais para o período de 2006-2009. Este filtro foi proposto por Kolmogorov e formalmente definido por Zurbenko (1986). Ele pode ser escrito como:

$$KZ_{m,p}[X(t)] = \sum_{S=-p(m-1)/2}^{p(m-1)/2} \frac{a_s}{m^p} X(t+S), \tag{15}$$

onde $X(t)$ corresponde para a série temporal, t é uma posição da série temporal e a_s corresponde aos coeficientes do polinômio $(1 + \mathrm{z} + \mathrm{z}^2 + \cdots + \mathrm{z}^{\mathrm{m}-1})^{\mathrm{p}}$.

O filtro KZ também pode ser definido como as *p* vezes das iterações de uma média móvel (Eq. 16) com o tamanho *m* da janela,

$$MA = \sum_{S=-(m-1)/2}^{(m-1)/2} \frac{X(t+S)}{m} \tag{16}$$

O filtro KZ é um filtro passa-baixa, eliminando variações de alta frequência da série temporal. A largura efetiva (P) deste filtro depende do número de iterações (*p*) e o tamanho da janela (*m*), estimado como $\sqrt[m]{p} \leq P$ (Milanchus *et al.*, 1998).

O filtro KZ é capaz de separar a tendência e as variações de curto prazo na série temporal, e também a componente sazonal. O componente de curto prazo é atribuível a tempo e flutuações de curto prazo nas emissões de precursores; o componente sazonal é resultado de mudanças no ângulo solar; e tendência é os resultados de mudanças nas emissões totais, transporte de poluentes, clima, política, e/ou economia (Rao and Zurbenko, 1994; Wise and Comrie, 2005). O componente sazonal reflete variações "normais" que se repetem todos os anos, na mesma medida (OECD, 2007). Ele também é conhecido como a sazonalidade de uma série temporal.

O filtro KZ baseia-se na declaração de Rao e Zurbenko (1994) que uma série temporal de poluentes atmosféricos pode ser representado por:

$$A(t) = e(t) + S(t) + W(t), \tag{17}$$

onde $A(t)$, $e(t)$, $S(t)$ e $W(t)$ são as séries temporais originais, a tendência, a variação sazonal e o componente de curto prazo, respectivamente. A soma da tendência e a variação sazonal corresponde ao componente da linha base.

Neste trabalho, utilizou-se um valor de *p* de 5 e um valor *m* de 15 dias para o início do estudo (Rao *et al.*, 1997). Para obter o componente de tendência, foi utilizado um valor de KZ ($_{m,p}$) igual a KZ ($_{365,3}$), usado no Wise and Comrie (2005) para o ozônio

troposférico. Subtraindo-se o valor de $e(t)$ da linha base, o componente sazonal $S(t)$ foi obtido.

O filtro KZ tem várias vantagens, uma vez que pode ser aplicado diretamente para os conjuntos de dados que têm valores em falta, sem a necessidade de um tratamento especial para as lacunas. No presente estudo, a quantidade de dados que faltaram correspondeu a 7,4% do banco de dados. Vários autores como Kang *et al.* (2013), Papanastasiou *et al.* (2012), Sebald *et al.* (2000), Wise e Comrie (2005) utilizaram este tipo de filtro.

REFERÊNCIAS

ALLEN, D.T., PALEN, E. J. 1989. Recent advances in aerosol analysis by infrared spectroscopy. Journal Aerosol Science 20, No. 4, 441-455.

ALLEN, D.T., PALEN, E.J. HAIMOV, M.I., HERING, S.V., YOUNG, J.R. 1994. Fourier Transform Infrared Spectroscopy of Aerosol Collected in a Low Pressure Impactor (LPI/FTIR): Method Development and Field Calibration, Aerosol Science and Technology 21:4, 325-342

ATKINSON, R. 2000.Atmospheric chemistry of VOCs and NO. Atmospheric Environment 34. 2063-2101.

BARRA, R., CASTILLO, C., MACHADO, J.P. 2007. Polycyclic Aromatic Hydrocarbons in the South American Environment. Reviews Environmental Contamination Toxicology 191. 1–22.

BASIRE, M., P. PARNEIX, T. PINO, P. BRÉCHIGNAC, AND F. CALVO, 2011. Modeling the anharmonic infrared Emission Spectra of PAHs: Application to the Pyrene Cation. EAS Publications Series 46, 95–101

BATHMANABHAN, S., SARAGUR, S.N., 2010.Analysis and interpretation of particulate matter - PM10, PM2,5 and PM1 emissions from the heterogeneous traffic near an urban roadway. Atmospheric Pollution Research 1, 184-194,

BAUSCHLICHER, C.H., LANGHOFF, S.R., SANDFORD, S.A., HUDGINS, D.M. 1997. Infrared Spectra of Perdeuterated Naphthalene, Phenanthrene, Chrysene, and Pyrene . The Journal of Physical Chemistry A 101, 2414-2422

BI, X., SHENG, G., PENG, P., CHEN, Y., ZHANG, Z., FU, J., 2003. Distribution of particulate- and vapor-phase nalkanes and polycyclic aromatic hydrocarbons in urban atmosphere of Guangzhou, China. Atmospheric Environment 37, p. 289– 298.

BOND, T.C., 2004. A technology-based global inventory of black and organic carbon emissions from combustion. Journal of Geophysical Research 109, 1–43.

BOUROTTE, C.; FORTI, M.C.; TANIGUCHI, S.; BÍCEGO, M.C.; LOTUFO, P.A. 2005. A wintertime study of PAHs in fi ne and coarse aerosols in São Paulo city, Brazil. Atmospheric Environment. vol. 39., p. 3799–3811.

BROWN, D. W., FLOYD, A. J., SAINSBURY, M., 1998. Organic Spectroscopy. Hoboken, NJ, U.S.A.: John Wiley & Sons, Inc.

COLBECK, H., LAZARIDIS, M. 2010. Aerosols and environmental pollution: Review. Naturwissenschaften 97, 117–131

COLVILE, R. N.; HUTCHINSON, E. J.; MINDELL, J. S.; WARREN, R. F., 2001.The transport sector as a source of air pollution. Atmospheric Environment 35, 1537–1565.

CORONADO C.R., CARVALHO JR J.A., SILVEIRA J.L., 2009. Biodiesel CO_2 emissions: A comparison with the main fuels in the Brazilian market. Fuel Process Technology 90, 204-211.

COURY, C., AND A. M. DILLNER, 2008. ATR-FTIR characterization of organic functional groups and inorganic ions in ambient aerosols at a rural site. Atmospheric Environment, 43, 940–948.

CRISTALE, J., SILVA, F.S., ZOCOLO, G.J., MARCHI, M.R.R., 2012. Influence of sugarcane burning on indoor/outdoor PAH air pollution in Brazil. Environmental Pollution 169, 210–6.

DALLAROSA, J.B.; MÔNEGO, G.J.; TEIXEIRA, E.C.; STEPHENS, J.L.; WIEGAND, F. 2005a . Polycyclic aromatic hydrocarbons in atmospheric particles in the metropolitan area of Porto Alegre, Brazil. Atmospheric Environment 39, 1609-1625.

DALLAROSA, J.B.; TEIXEIRA, E.C.; PIRES , M.; FACHEL, J. 2005b. Study of the profile of polycyclic aromatic hydrocarbons in atmospheric particles (PM10) using multivariate methods. Atmospheric Environment 39, 6587-6596.

DALLAROSA, J.B.; TEIXEIRA, E.C.; MEIRA, L.; WIEGAND, F. 2008. Study of the chemical elements and polycyclic aromatic hydrocarbons in atmospheric particles of PM_{10} and $PM_{2.5}$ in the urban and rural areas of South Brazil. Atmospheric Environment. v. 89. p. 76-92

DE MARTINIS, B.S., OKAMOTO, R.A., KADO, N.Y., GUNDEL, L.A., CARVALHO, L.R.F., 2002, Polycyclic aromatic hydrocarbons in a bioassay-fractionated extract of PM10 collected in São Paulo, Brazil. Atmospheric Environment. vol.36, p. 307–314.

DETRAN, 2013. Departamento Estadual de Trânsito - DETRAN/RS. Disponível em: http://www.detran.rs.gov.br/index.php?action=estatistica&codItem=99. Acessado em: Maio de 2013.

DEVOS, O., COMBET, E., TASSEL, P., PATUREL, L. 2006.Exhaust emissions of PAHs of passenger cars. Polycyclic Aromatic Compounds, 26: 1, 69 — 78.

DUAN, J., BI, X., TAN, J., SHENG, G., FU, J., 2007. Seasonal variation on size distribution and concentration of PAHs in Guangzhou city, China.Chemosphere 67, 614–22.

DWIVEDI D., AGARWAL A.K., SHARMA M., 2006. Particulate emission characterization of a biodiesel vs. diesel-fuelled compression ignition transport engine: A comparative study. Atmospheric Environment 40, 5586-5595.

ELACHI, C., VAN ZYL, J.J. 2006. Introduction to the Physics and Techniques of Remote Sensing. John Wiley & Sons, Inc. New Jersey.

EMBRAPA. Empresa Brasileira de Pesquisa Agropecuária. 2003. Clima do Rio Grande do Sul. Secção de Geografia. Secretaria da Agricultura. Porto Alegre Disponível em <http://www. cnpt.embrapa.br/agromet/cli_pf8.html.>

ENVIRONNEMENT. MP101M. Suspended particulate beta gauge monitor. Technical Manual. 2010.

FANG, G.C., WU, Y.S., CHEN, M.H., HO, T.T., HUANG, S.H., RAU, J.Y. Polycyclic aromatic hydrocarbons study in Taichung, Taiwan, during 2002–2003. Atmospheric Environment 38, 3385–3391. 2004.

FERNANDES, M.B.; BRICKUS, L.; MOREIRA, J.C.; CARDOSO, J.N. 2002. Atmospheric BTX and polyaromatic hydrocarbons in Rio de Janeiro, Brazil. Atmospheric Environment. v. 47. p. 417-425.

FINLAYSON-PITTS, B.J., PITTS, J.N. JR., 2000. Chemistry of the Upper and Lower Atmosphere: Theory, Experiments, and Applications, ed. Wiley, New York.

GAFFNEY, J. S.; MARLEY, N.A. 2009. The impacts of combustion emissions on air quality and climate – From coal to biofuels and beyond. Atmospheric Environment 43, 23–36

GUO, H., LEE, S.C., HO, K.F., WANG, X.M., ZOU, S.C., Particle-associated polycyclic aromatic hydrocarbons in urban air of Hong Kong. Atmospheric Environment 37, 5307–5317. 2003.

HAN, S., BIAN, H., FENG, Y., LIU, A., LI, X., ZENG, F., ZHANG. X. 2011. Analysis of the Relationship between O_3, NO and NO_2 in Tianjin, China. Aerosol and Air Quality Research 11, 128–139.

HOPKE, P.K., 2003. A Guide to Positive Matrix Factorization.Available in: http://www.epa.gov/ttnamti1/files/ambient/pm25/workshop/laymen.pdf, Accessed in November of 2013.

HOWSAN, M. ,JONES, C., 2010. Sources of PAHs in the environment. In: Neilson, A.H., 2010. PAHs and related compounds.The handbook of Environmental Chemistry:v.3. Springer-VerlagBerlin Heidelberg. Germany.

HUDGINS, D. M., AND S. A. SANDFORD, 1998: Infrared Spectroscopy of Matrix Isolated Polycyclic Aromatic Hydrocarbons . 3 . Fluoranthene and the Benzofluoranthenes. Society, 5639, 353–360.

JENKIN, M.E., CLEMITSHAW, K.C., 2000. Ozone and other secondary photochemical pollutants: chemical processes governing their formation in the planetary boundary layer. Atmospheric Environment 34, 2499-2527.

IARC, International Agency for Research on Cancer, 2013.Air pollution and cancer, Straif,K., Cohen,A., Samet J.(Eds.) (IARC Scientific Publications; 161).

INPE – CPTEC, Instituto Nacional de Pesquisas Espaciais - Centro de Previsão de Tempo e Estudos Climáticos, 2003. http://www.cptec.br/clima.

KANG, D., HOGREFE, C., FOLEY, K.L., NAPELENOK, S.L., MATHUR, R., TRIVIKRAMA RAO, S., 2013. Application of the Kolmogorov–Zurbenko filter and the decoupled direct 3D method for the dynamic evaluation of a regional air quality model. Atmospheric Environment 80, 58–69.

KEWLEY, D.J., POST, K., 1978. Photochemical ozone formation in the Sydney airshed, Atmospheric Environment 12, 2179-2184

KIRCHSTETTER, W.T., MIGUEL, H.A., HARLEY, A.R., On-road comparison of exhaust emissions from gasoline and diesel engines. In: CRC On-road Vehicle Emissions Workshop 8. Apr. 1998. San Diego, CA

KLEEMAN, M.J., RIDDLE, S.G., ROBERT, M. A., JAKOBER, C. A., 2008. Lubricating oil and fuel contributions to particulate matter emissions from light-duty gasoline and heavy-duty diesel vehicles. Environmental Science & Technology 42, 235–42.

KLEJNOWSKI, K., KOZIELSKA, B., KRASA, A., ROGULA-KOZ1OWSKA, W., 2010.Polycyclic aromatic hydrocarbons in PM1, PM2.5, PM10 and TSP in the upper Silesian agglomeration, Poland. Archives of Environmental Protection 36, 65-72

KORB, A.R; DYBWAD, P.; WADSWORTH, W.; SALISBURY, J.W. 1996. Portable Fourier transform infrared spectroradiometer for field measurements of radiance and emissivity. Applied Optics, Vol. 35, Issue 10, pp. 1679-1692

KŘŮMAL, K., MIKUŠKA, P., VEČEŘA, Z., 2013. Polycyclic aromatic hydrocarbons and hopanes in PM1 aerosols in urban areas. Atmospheric Environment 67, 27–37.

KUBICKI, 2001. Interpretation of Vibrational Spectra Using Molecular Orbital Theory Calculations. Reviews in Mineralogy & Geochemistry 42(1), 459-483.

KUMAR, P., M. KETZEL, S. VARDOULAKIS, L. PIRJOLA, AND R. BRITTER, 2011. Dynamics and dispersion modelling of nanoparticles from road traffic in the urban atmospheric environment – a review. Journal of Aerosol Science, 42, 580–603.

LADJI, R., YASSAA, N., BALDUCCI, C., CECINATO, A., MEKLATI, B.Y., 2009. Distribution of the solvent-extractable organic compounds in fine (PM1) and coarse (PM1-10) particles in urban, industrial and forest atmospheres of Northern Algeria. The Science of the Total Environment 408, 415–24.

LEE, S. C., CHENG, Y. HO, K. F., CAO, J. J., LOUIE,P. K.-K. , CHOW,J. C., 2006. $PM_{1.0}$ and $PM_{2.5}$ Characteristics in the Roadside Environment of Hong Kong. Aerosol Science and Technology 40, 157–165

LEIGHTON, P.A., 1961. Photochemistry of Air Pollution, ed. Academic Press, New York.

MANOLI, A. KOURAS, K. SAMARA. Profile Analysis of Ambient and Source Emitted Particle-bound Polycyclic Aromatic Hydrocarbons from Three Sites in Northern Greece, Chemosphere 56, 867-878, 2004.

MARSHALL, T. L.; CHAFFIN, C. T.; HAMMAKER, R. M.; FATELEY, W. G. 1994. An introduction to open-path FT-IR. Atmospheric monitoring. Environmental Science & Technology *28*, 224A-232A

MASTALERZ, M.; GLIKSON, M.; SIMPSON, R.W.; 1998. Analysis of atmospheric particulate matter; application of optical and selected geochemical techniques. International Journal of Coal Geology. v. 37. p. 143-153.

MATTIUZI, C.D.P., PALAGI, A.C., TEIXEIRA, E.C., WIEGAND, F. Poluição Atmosférica do Biodiesel – Estado da Arte. In: Teixera, E.C. (Coord), Wiegand, F., Tedesco, M. Biodiesel: Impacto Ambiental Agronômico e Atmosférico. Cadernos de Planejamento e Gestão Ambiental N°6. Porto Alegre: FEPAM, 2012. Cap 2. p. 43-67.

MENESES, P. R. Fundamentos de Radiometria Óptica Espectral. 2001. In: MENESES, P. R.; NETTO, J. S. M. (Orgs.) Sensoriamento Remoto: Reflectância dos alvos naturais. Brasília, DF: UnB; Planaltina: Embrapa Cerrados. 26p.

METROPLAN. Fundação Estadual de Planejamento Metropolitano e Regional. 2012. Evolução da população na RMPA. Disponível em <http://www.metroplan.rs.gov.br/mapas_estatisticas/ au_rmpa.htm>.

MILANCHUS, M.L., RAO, S.T. , ZURBENKO, I.G., 1998. Evaluating the Effectiveness of Ozone Management Efforts in the Presence of Meteorological Variability. *Journal of Air and Waste Management Association* 48, 201-215

MORAWSKA, L., Z. RISTOVSKI, E. JAYARATNE, D. KEOGH, AND X. LING, 2008: Ambient nano and ultrafine particles from motor vehicle emissions: Characteristics, ambient processing and implications on human exposure. Atmospheric Environment, 42, 8113–8138,

MT, 2012 MT. Ministério dos Transportes, Brasil, 2012. Available at http://www.transportes.gov.br/obra/conteudo/id/36986. Accessed in May 2012.

NAVARTA, M. D. F., C. B. OJEDA, AND F. S. ROJAS, 2008: Aplicación de la Espectroscopia del Infrarrojo Medio en Química Analítica de Procesos. 2, 93–103.

NEILSON, A.H., 2010. The Handbook of Environmental Chemistry: PAHs and Related Compounds, vol. 3 Part 1. Springer, New York, NY, pp. 347-385.

NETTO, A.D.; BARRETO, R.P.; MOREIRA, J.C.; ARBILLA, G. 2002. Polycyclic Aromatic Hydrocarbons in Total Suspended Particulate of Niterói, RJ, Brazil: A Comparison of Summer and Winter Samples. Bulletin Environmental Contamination Toxicology. New York. v. 69. p. 173–180.

NISBET, C., LAGOY, P., 1992. Toxic Equivalency Factors (TEFs) for polycyclic aromatic hydrocarbons (PAHs). Regulatory Toxicology and Pharmacology 16, 290–300.

NOTARIO, A., BRAVO, I., ADAME, J. A., DÍAZ-DE-MERA, Y., ARANDA, A., RODRÍGUEZ, A., RODRÍGUEZ, D., 2012. Analysis of NO, NO_2, NO_x, O_3 and oxidant ($OX=O_3+NO_2$) levels measured in a metropolitan area in the southwest of Iberian Peninsula. Atmospheric Research 104, 217–226.

OECD (Organization for Economic Co-operation and Development), 2007. Guidelines for the reporting of different forms of data, in: Data and Metadata Reporting and Presentation Handbook, OECD, Paris, 59-72.

OLIVARES, G., JOHANSSON, C., STROM, J., HANSSON, H.-C. 2007. The role of ambient temperature for particle number concentrations in a street canyon. Atmospheric Environment, 41, 2145–2155.

PAATERO, P., TAPPER, U. 1994. Positive matrix factorization: a non-negative factor model with optimal utilization of error estimates of data values. Environmental Metrics 5, 11-126

PAATERO, P. 1997. Least squares formulation of robust non–negative factor analysis. Chemometrics and Intelligent Laboratory Systems 37, 23–35.

PANTHER, B. C., HOOPER, M. A., TAPPER, N. J. 1999. A comparison of air particulate matter and associated polycyclic aromatic hydrocarbons in some tropical and temperate urban environments.. Atmospheric Environment, v. 33, I. 24-25, p. 4087-4099

PAPANASTASIOU, D. K., MELAS, D., BARTZANAS, T., KITTAS, C., 2012. Estimation of Ozone Trend in Central Greece, Based on Meteorologically Adjusted Time Series. Environmental Modeling Assessment 17, 353–361.

PETROBRAS, 2012. Disponível em: http://www.petrobras.com.br/pt/produtos/para-voce/nas-ruas/. Acessada em Maio de 2012.

PORG, 1997. Ozone in the United Kingdom. Fourth Report of theUKPhotochemical Oxidants Review Group, Department of the Environment, Transport and the Regions, London.

RAO, S. T. , ZURBENKO, I. G., 1994. Detecting and Tracking Changes in Ozone Air Quality. Journal of Air and Waste Management Association 44, 1089–1092,

RAO, S. T., ZURBENKO, I.G., NEAGU, R., PORTER, P.S., KU, J.Y., HENRY, R.F., 1997. Space and Time Scales in Ambient Ozone Data. *Bulletin American Meteorology Society* 78, 2153-2166,

RAVINDRA, K. BENCS, L., WAUTERS, E., DE HOOG, J.,DEUTSCH, F., ROEKENS, E., BLEUX, N., BERGHMANS, P., VAN GRIEKEN, R. 2006. Seasonal and site-specific variation in vapour and aerosol phase PAHs over Flanders (Belgium) and their relation with anthropogenic activities. Atmospheric Environment, 40, 771–785.

RAVINDRA, K., SOKHIA R., VAN GRIEKENET R. 2008. Atmospheric polycyclic aromatic hydrocarbons: Source attribution, emission factors and regulation. Atmospheric Environment, v. 42, I. 13, p. 2895-2921

REFF, A., EBERLY, S.I., BHAVE, P. V, 2007. Receptor modeling of ambient particulate matter data using positive matrix factorization: review of existing methods. Journal of Air & Waste Management Association 57, 146–54.

RUSSEL A., 2013. Combustion emissions. In: Air pollution and cancer, Straif,K., Cohen,A., Samet J. (Eds.) Chap 4. (IARC Scientific Publications; 161).

SALISBURY, 1998. Spectral Measurements Field Guide. Report No. ADA362372. Defense Technology Information Center. Earth Satellite Corporation. 88p.

SEBALD, L., TRE, R., REIMER, E., HIES, T., 2000. Spectral analysis of air pollutants. Part 2: ozone time series, *Atmospheric Environment* 34, 3503–3509.

SEINFEID, J.H., PANDIS, S.N., 2006. Atmospheric Chemistry and Physics: from Air Pollution to Climate Change. *Wiley*, New York.

SEMMLER, J., YANG, P. W., CRAWFORD, G. E. 1991. Gas chromatography/Fourier transform infrared studies of gas-phase polynuclear aromatic hydrocarbons, Vibrational Spectroscopy 2 (4), 189–203.

SIENRA, M.; ROSAZZA, N.; PRÉNDEZ, M. 2005. Polycyclic aromatic hydrocarbons and their molecular diagnostic ratios in urban atmospheric respirable particulate matter. Atmospheric Research. v. 75. p. 267-281.

SILVERSTAIN, R.M., WEBSTER, F.X., 2005. Spectrometric Identification of Organic Compounds, 7th Edition. Hoboken, NJ, U.S.A.: John Wiley & Sons, Inc.

SHEU, H.L., LEE, W.J., LIN, S.J., FANG, G.C., CHANG, H.C., YOU, W.C., 1997. Particle bound PAH content in ambient air. Environmental Pollution 96, 369–82.

SLEZAKOVA, K., PEREIRA, M.C., REIS, M.A., ALVIM-FERRAZ, M.C., 2007. Influence of traffic emissions on the composition of atmospheric particles of different sizes - Part 1: Concentrations and elemental characterization. Journal of Atmospheric Chemistry 58, 55-68.

STRÖHER, G.L., POPPI, N.R., RAPOSO JR., J.L., DE SOUZA, J.B.G., Determination of polycyclic aromatic hydrocarbons by gas chromatography–ion trap tandem mass spectrometry and source identifications by methods of diagnostic ratio in the ambient air of Campo Grande, Brazil. Microchemical Journal 86, 112–118.2007.

TEIXEIRA, E.C., FELTES, S., SANTANA, E.R., 2008, Estudo das emissões de fontes móveis na Região Metropolotana de Porto Alegre, Rio Grande do Sul. Química Nova 31, No. 2, 244-248.

TEIXEIRA, E.C., OLIVEIRA, K., MEINCKE, L., ALAM, K., 2011. Study of nitro-polycyclic aromatic hydrocarbons in fine and coarse atmospheric particles. Atmospheric Research 101, 631–639.

TEIXEIRA, E. C., MATTIUZI, C.D.P, FELTES, S., WIEGAND, F., SANTANA E.R.R., 2012. Estimated atmospheric emissions from biodiesel and characterization of pollutants in the metropolitan area of Porto Alegre-RS.Anais da Academia Brasileira de Ciências 84 (3), 245-261.

TEIXEIRA, E. C., MATTIUZI, C.D.P, AGUDELO-CASTAÑEDA, D.M., OLIVEIRA, K., WIEGAND, F., 2013. Polycyclic aromatic hydrocarbons study in atmospheric fine and coarse particles using diagnostic ratios and receptor model in urban/industrial region. Environmental monitoring and assessment185, 9587-9602.

TSAPAKIS, M., LAGOUDAKI, E., STEPHANOU, E.G., KAVOURAS, I.G., KOUTRAKIS, P., OYOLA, P., VON BAER, D. The composition and sources of HV PM10-2.5 organic aerosol in two urban areas of Chile. Atmospheric Environment 36, 3851–3863, 2002.

UHEREK, E., HALENKA, T., BORKEN-KLEEFELD, J., BALKANSKI, Y., BERNTSEN, T., BORREGO, C., GAUSS, M., HOOR, P., JUDA-REZLER, K., LELIEVELD, J., MELAS, D., RYPDAL, K., SCHMID, S. 2010: Transport impacts on atmosphere and climate: Land transport. Atmospheric Environment 44, 4772–4816

USEPA. U.S. Environmental protection agency, 1994. Environmental Protection Agency Quality Assurance Handbook for Air Pollution Measurement Systems: vol. II: Ambient Air Specific Methods, Section 2,11, EPA/600/R-94/038a, US Environmental Protection Agency, US Government Printing Office Washington, DC, April.

USEPA. U.S. Environmental protection agency. 1999. Determination of Polycyclic Aromatic Hydrocarbons (PAHs) in Ambient Air Using Gas Chromatography/Mass Spectrometry (GC/MS). Compendium Method TO-13A. Compendium of Methods for the Determination of Toxic Organic Compounds in Ambient Air. 2th Edition. Center for Environmental Research Information. Office of Research and Development. U.S. Environmental Protection Agency. Cincinnati, OH.

USEPA. 2008. EPA Positive Matrix Factorization (PMF) 3.0 Fundamentals and User Guide, USEPA Office of Research and Development.

VASCONCELLOS, P. C. , ZACARIAS, D. , MAGALHÃES, DULCE , ROCHA, G. 2011. Seasonal variation of n-alkanes and Polycyclic Aromatic Hydrocarbons

concentrations in PM10 samples collected at urban sites of São Paulo State, Brazil. Water, Air and Soil Pollution 222, 325-366.

VESTENIUS, M., LEPPÄNEN, S., ANTTILA, P., KYLLÖNEN, K., HATAKKA, J., HELLÉN, H., HYVÄRINEN, A.-P., HAKOLA, H., 2011.Background concentrations and source apportionment of polycyclic aromatic hydrocarbons in south-eastern Finland.Atmospheric Environment 45, 3391–3399.

WÅHLIN, P. 2009.Measured reduction of kerbside ultrafine particle number concentrations in Copenhagen.Atmospheric Environment 43, 3645–3647.

WANG, D., TIAN, F., YANG, M., LIU, C., LI, Y.-F., 2009.Application of positive matrix factorization to identify potential sources of PAHs in soil of Dalian, China. Environmental Pollution, 157, 1559–1564.

WANG, F., COSTABILE, F. , LI, H. , FANG, D. , ALLIGRINI, I. 2010. Measurements of ultrafine particle size distribution near Rome. Atmospheric Research 98, 69–77.

WINGFORS, H., HÄGGLUND, L., MAGNUSSON, R. 2011. Characterization of the size-distribution of aerosols and particle-bound content of oxygenated PAHs, PAHs, and n-alkanes in urban environments in Afghanistan, Atmospheric Environment 45, 4360-4369

WISE, E. K., COMRIE, A. C., 2005. Extending the Kolmogorov-Zurbenko filter: application to ozone, particulate matter, and meteorological trends. Journal of Air Waste Management 55, 1208–16.

ZHANG, Y., TAO, S., 2009. Global atmospheric emission inventory of polycyclic aromatic hydrocarbons (PAHs) for 2004. Atmospheric Environment 43, 812–819.

ZHAO, Y., WANG, S., DUAN, L., LEI, Y., CAO, P., HAO, J. 2008. Primary air pollutant emissions of coal-fired power plants in China: Current status and future prediction. Atmospheric Environment 42, 8442-8452

ZURBENKO, I., 1986. The Spectral Analysis of Time Series, North-Holland, New York, pp. 248.

ZIELINSKA, B., 2005. Atmospheric transformation of diesel emissions. Experimental and Toxicologic Pathology, 57, 31–42.

CAPITULO II

Measurement of particle number and related pollutant concentrations in an urban area in South Brazil

AGUDELO-CASTAÑEDA, D. M.; Teixeira, E.C.; Rolim, S.B.A.; Pereira, F.N.; Wiegand, F.

Atmospheric Environment 70, 254-262, 2013.

Atmospheric Environment 70 (2013) 254–262

Contents lists available at SciVerse ScienceDirect

Atmospheric Environment

journal homepage: www.elsevier.com/locate/atmosenv

Measurement of particle number and related pollutant concentrations in an urban area in South Brazil

D.M. Agudelo-Castañeda [a], E.C. Teixeira [a,b,*], S.B.A. Rolim [a], F.N. Pereira [b], F. Wiegand [b]

[a] Postgraduate Program in Remote Sensing and Meteorology, Geosciences Institute, Universidade Federal do Rio Grande do Sul (UFRGS), Av. Bento Gonçalves, 9500, 91501-970 Porto Alegre, Brazil
[b] Research Department, Fundação Estadual de Proteção Ambiental Henrique Luís Roessler, RS. Rua Carlos Chagas, 55, 90030-020 Porto Alegre, Brazil

HIGHLIGHTS

- Particle number and its association with NO, NO_2, NO_x, O_3 was analyzed.
- Results showed a higher number concentration of the PR2.5 and PR1.0 size ranges.
- Particle number concentration was influenced by emissions from motor vehicles.
- Correlation analysis suggest similar emission sources for NO, NO_x and particle number.
- Results indicate influence of meteorological conditions on particle number.

ARTICLE INFO

Article history:
Received 22 August 2012
Received in revised form
6 December 2012
Accepted 14 January 2013

Keywords:
Air quality
Particle number
Nitrogen oxides
Ozone

ABSTRACT

The purpose of the present study was to analyze atmospheric particle number concentration at Sapucaia do Sul, in the Metropolitan Area of Porto Alegre, and associate it with the pollutants NO, NO_2, and O_3. Measurements were performed in two periods: August to October, in 2010 and 2011. We used the following equipment: the continuous particulate monitor (CPM), the chemiluminescent nitrogen oxide analyzer (AC32M), and the UV photometric ozone analyzer (O342M). Daily and hourly particle number concentrations in fractions PR1.0 (0.3–1.0 μm), PR2.5 (1.0–2.5 μm), and PR10 (2.5–10 μm), and concentrations of pollutants NO, NO_2, NO_x, and O_3 were measured. These data were correlated with meteorological parameters such as wind speed, temperature, relative humidity, and solar radiation. The daily variation of OX ($NO_2 + O_3$) and its relation with NO_2 were also established. The results obtained for daily particle number concentration (particles L^{-1}) showed that the area of study had higher particle number of PR2.5 and PR1.0 size ranges, with values of 19.5 and 28.51 particles L^{-1}, respectively. Differences in particle number concentrations in PR1 and PR2.5 size ranges were found between weekdays and weekends. The daily variation per hour of concentrations of particle number, NO, and NO_x showed peaks during increased traffic flow in the morning and in the evening. NO_2 showed peaks at different times, with the first peak (morning) 2 h after the peak of NO, and a second peak in the evening (19:00). This is due to the oxidation of NO and to the photolysis of NO_3 formed overnight. Correlation analysis suggests that there may be a relationship between the fine and ultrafine particles and NO, probably indicating that they have similar sources, such as vehicular emissions. In addition, a possible relationship of solar radiation with fine particle number concentrations, as well as with O_3 was also observed. The results, too, show an inverse relationship between particle number concentration and relative humidity.

1. Introduction

Among many factors that generate air pollution, emission of pollutants from motor vehicles (Colvile et al., 2001) is a major source of particulate matter (Bathmanabhan and Saragur, 2010) and NO (Gaffney and Marley, 2009) in urban areas. With regard to particles emitted by mobile sources, over 90% of the particle

* Corresponding author. Research Department, Fundação Estadual de Proteção Ambiental Henrique Luís Roessler, RS. Rua Carlos Chagas, 55, 90030-020 Porto Alegre, Brazil. Tel.: +55 51 32889408. .
E-mail addresses: gerpro.pesquisa@fepam.rs.gov.br, elbact.ez@terra.com.br (E.C. Teixeira).

1352-2310/$ – see front matter © 2013 Elsevier Ltd. All rights reserved.
http://dx.doi.org/10.1016/j.atmosenv.2013.01.029

number concentration belong to the <1 μm fraction (Morawska et al., 2008). However, particle emission depends on temperature, with higher concentrations at low temperatures (Olivares et al., 2007), and higher sulfur content in fuel, e.g. in diesel (Wåhlin, 2009). Moreover, the addition of biodiesel to diesel contributes to a decrease in particle emission due to a lower formation of sulfate particles during combustion (Dwivedi et al., 2006).

Although automotive vehicles are the main source of fine particles in urban areas, the number and size distribution of particles can change rapidly due to the influence of transformation processes, such as coagulation and condensation, and to turbulence, which improves mixing and dilution (Kumar et al., 2011). Moreover, vehicle emissions are a major source of nitrogen oxides emissions, especially in the form of NO (Gaffney and Marley, 2009), causing an almost direct emission in the boundary layer. Diesel engines produce five times the amount of NO_x by mass of burnt fuel compared to gasoline vehicles. Furthermore, the addition of biodiesel to diesel can slightly increase NO_x emissions (Coronado et al., 2009).

Although not having significant natural or anthropogenic emission sources (PORG, 1997), secondary pollutants such as NO_2 and tropospheric O_3 may be formed by different reactions of primary pollutants in the air (Finlayson-Pitts and Pitts, 2000). According to Jenkin and Clemitshaw (2000), the main conversion reactions between NO and NO_2 are reactions (1), (2), (3), and (4):

$$2\,NO + O_2 \rightarrow 2\,NO_2 \quad (1)$$

However, under most tropospheric conditions, reaction (1) is not significant, and the major way by which NO is converted to NO_2 is by reaction (2) with O_3:

$$NO + O_3 \rightarrow NO_2 + O_2 \quad (2)$$

Under the influence of solar radiation during the day, NO_2 undergoes photolysis and reconverts to NO by reactions (3) and (4) below:

$$NO_2 + h\nu(\lambda < 420\ nm)) \rightarrow NO + O\left(^3P\right) \quad (3)$$

$$O\left(^3P\right) + O_2(+M) \rightarrow O_3 + M \quad (4)$$

where M is a third compound (typically N_2 or O_2), which absorbs the vibrational energy in excess and thereby stabilizes the O_3 molecule formed, $h\nu$ is the energy of one photon ($\lambda < 424$ nm), and O (^{3}P) is active monatomic oxygen (Han et al., 2011). Photolysis of NO_2 is an important source of O_3 generation (Zielinska, 2005). NO_x has a short chemical lifetime and its major effects on O_3 are limited to its proximity to emission sources (Uherek et al., 2010).

Tropospheric O_3 is formed by several complex photochemical reactions between nitrogen oxides (NO and NO_2) and volatile organic compounds (VOCs) in the presence of sunlight. However, in urban areas, concentrations of O_3 are usually lower than in rural areas due to its reaction with NO (from vehicle emissions) to produce NO_2. Sunlight starts the process by supplying UV radiation that dissociates certain stable molecules, leading to the formation of hydrogen free radicals (HO_x). In the presence of NO_x, these free radicals catalyze the oxidation of VOCs to form CO_2 and H_2O. Partially oxidized organic species are generated as intermediate oxidation products, such as O_3 formed as a byproduct. O_3 can be formed from the photolysis of NO_2 by reactions (3) and (4). In the presence of NO, the degradation reactions of VOCs lead to the formation of intermediate RO_2 and HO_2 radicals. These radicals react with NO converting it to NO_2 (Atkinson, 2000).

Within minutes, reactions (2) and (3) reach a balance and a so-called photostationary state, determined by Leighton (1961):

$$[NO]\cdot[O_3]/[NO_2] = J_1/k_4 \quad (5)$$

Where J_1 is the rate of NO_2 photolysis, which varies during the day according to the solar zenith and radiation transmission through the atmosphere (Kewley and Post, 1978), and k_4 is the reaction rate coefficient of NO with O_3, as a function of temperature (Jenkin and Clemitshaw, 2000; Notario et al., 2012) so that various experimental values may be found, depending on the temperature range in which the measurements were taken. The value of k_4 in reaction (5) was calculated using the equation of Seinfeld and Pandis (2006): $k_4\ (ppm^{-1}\ min^{-1}) = 3.23 \times 103\ \exp[-1430/T]$.

There are few studies on the atmospheric chemistry in the area of study and Brazil, specifically analyzing particle number concentrations in PR1 (0.3–1.0 μm), PR2.5 (2.5–1.0 μm), and PR10 (10–2.5 μm) size ranges, which are now being measured for the first time. This work is part of an attempt to investigate the particle size distribution of PR1, PR2.5, and PR10 size ranges and its relationship with gaseous pollutants (O_3, NO, NO_2, and NO_x) and weather conditions. This is important because the study of particle size distribution allows a more accurate assessment of the source of the particulate matter formed in the area of study, as well as of NO, NO_2, and O_3. We also examined the variation of OX ($NO_2 + O_3$) and the rate of NO_2 photolysis, besides the differences in weekend and weekday concentrations.

2. Materials and methods

2.1. Area of study

The sampling site Sapucaia do Sul (Fig. 1) is located in the area of study: the Metropolitan Area of Porto Alegre (MAPA). The area of study is located in central-eastern part of the Brazilian state of Rio Grande do Sul. It is delimited by parallels 28°S and 31°S and longitudes 50°W and 54°W. The area currently comprises 9652.54 km^2 and, according to estimates by METROPLAN (the State Foundation for Metropolitan and Regional Planning), has 4,101,032 inhabitants (METROPLAN, 2012).

The region is the most urbanized area of the state and is characterized by different industries, including several stationary sources such as the Alberto Pasqualini Refinery, steel mills that do not use coke (Siderurgica Rio-grandense and Aços Finos Piratini), the III Petrochemical Industrial Complex, and coal-fired power plants (Termelétrica de Charqueadas – TERMOCHAR, and the Usina Termelétrica de São Jerônimo – USTJ). However, this site has low industrial influence upstream of the prevailing winds. It is estimated that the most significant contribution are mobile sources due to the great number of vehicles in the region, which represent 20% of the total cars of the state's fleet (Dallarosa et al., 2008). This region has a high vehicles traffic, approximately 1,840,703 vehicles (DETRAN, 2012), of which circa 84.98% is fueled by gasoline, 6.67% by diesel, 6.58% by ethanol, 1.03% by natural gas, and 0.74% has flex technology (Teixeira et al., 2008). The sampling site is also near the lower axis of the BR-116 highway, where the daily flow is approximately 150,000 vehicles (MT, 2012), and traffic jams and slow speeds are frequent. Currently, gasoline-fueled vehicles use a mixture of gasoline and 20% of ethanol (PETROBRAS, 2012). The diesel used in the MAPA has a level of 500 ppm of sulfur and it is added of 5% of biodiesel (Mattiuzi et al., 2012). A study by Teixeira et al. (2012) shows that from the total emissions originating from mobile sources within the MAPA, diesel vehicles are responsible for most emissions of particulate matter and NO_x.

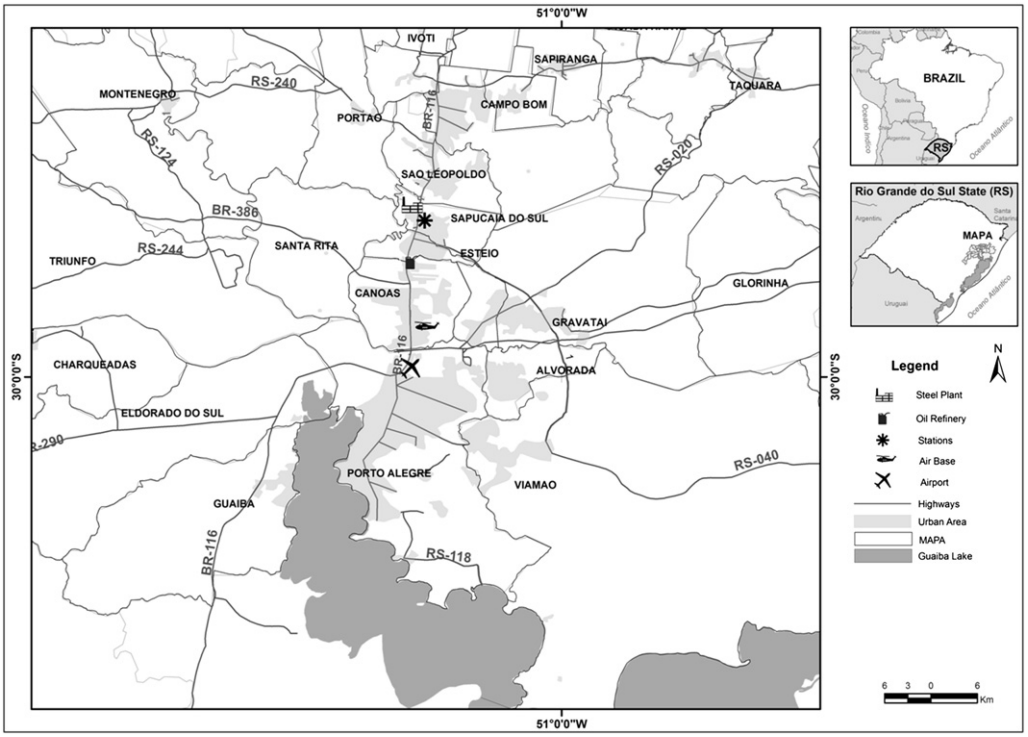

Fig. 1. Sampling site location, Sapucaia do Sul, in the Metropolitan Área of Porto Alegre, Rio Grande do Sul State – Brazil.

2.2. Equipment

Particle number concentration in PR1, PR2.5, and PR10 size ranges was measured using the continuous particulate monitor (CPM). NO, NO_2, and NO_x concentrations were measured with a chemiluminescent analyzer AC32M, while an analyzer O342M which uses the principle of UV radiation absorption by O_3 molecules was used for measuring O_3. The equipments used in the present work were located at the sampling site Sapucaia do Sul (Fig. 1).

The particle analyzer CPM is an optical analyzer, which uses a laser beam to measure the scattering intensity caused by atmospheric particles present in the air sample by applying the Mie scattering theory (ENVIRONNEMENT, 2010). This analyzer presents a new optical design for a solid aerosols counter that detects particulates and classifies them by size ranges (from 0.3 to 35 μm). A temperature regulated sampling line was used for obtaining representative samples of the atmospheric dust to be analyzed. A sampling head PM10 US-EPA was also used. The particulate that crosses the laser beam (635 nm) scatters the light into different directions. A photodiode located approximately 15° from the incident laser measures the intensity of the scattered radiation. At this angle, the intensity of the scattered light does not depend on the nature of the particles, but it is a function of their size (Renard et al., 2010). The analyzer measures the intensity and ranks the particulate matter in the three classes of particle diameter: PR1, PR2.5, and PR10.

2.3. Period of study and analysis of data

Concentrations of particle number in fractions PR1, PR2.5, and PR10, and of NO, NO_x, and NO_2 were measured during August (18th–31st), September (1st–30th), and October (1st–31st) 2010 and 2011. O_3 concentrations were measured from August 2011 on. Measurements were made every 15 min, continuously. The database was drawn up from the raw data recorded every 15 min, and then the hourly and daily means were calculated. Data were analyzed by using STATISTICA 7© software. Meteorological data such as air temperature, relative humidity, and wind speed were obtained from the meteorological station at Esteio, which belongs to the Alberto Pasqualini Refinery (REFAP). Radiation and precipitation data were obtained from the station at Porto Alegre, which belongs to the INMET. Both stations are located near the sampling site.

2.4. Meteorological conditions

Due to its location, the area of study shows well-defined seasons and a climate strongly influenced by cold air masses migrating from the polar regions. The historical average rainfall is 1300–1400 mm yr^{-1} (INPE – CPTEC, 2012). Prevailing winds are from SE (first preferred direction) and NE (second preferred direction) (EMBRAPA, 2003). The area of study is located in a subtropical, temperate climate with four well-defined seasons: summer (January–March), autumn (April–June), winter (July–September), and spring (October–December). The wind direction shows marked seasonal variations. During summer and spring, the prevailing direction is E–SE, while in fall and winter, besides E–SE winds, winds from W and NW also occur. Weather conditions in the area of study during the sampling period were as follows: average temperature was 18.10 °C, varying between 8.76 and 26.00 °C; relative humidity was 80.01%, varying between 59.32 and 99.90%; average radiation was 186.31 W m^2, varying between 16.31 and 372.57 W m^2, average rainfall was 9.2 mm day^{-1}, and accumulated rainfall was 367 mm. The maximum and average wind speeds were 5.6 m s^{-1} and 2.7 m s^{-1}, respectively. The prevailing wind direction was E–SE (resultant vector of 133°).

3. Results and discussion

3.1. Daily atmospheric particle number concentrations by size

Table 1 shows the descriptive statistics of mean particle number concentration for PR1, PR2.5, and PR10 size ranges during the period of study. Mean particle concentrations for fractions PR1, PR2.5, and

Table 1
Descriptive statistics of 24 h mean particle number concentration for PR1, PR10 and PR2.5 size classes (Particles L^{-1}).

	PR1 (<1.0 μm)	PR2.5 (1–2.5 μm)	PR10 (2.5–10 μm)
Arithmetic mean	19.15	28.51	7.04
Standard deviation	9.95	13.04	3.25
Minimum	3.86	8.49	2.27
Maximum	55.58	60.65	17.80
Median	16.62	25.48	6.52

PR10 were 19.15, 28.51, and 7.04 particles L^{-1}, respectively. These results, expressed in particles L^{-1}, were similar to those of the study of Renard et al. (2010), who used the same spectral ranges. PR1 and PR2.5 are the fractions that showed the highest particle number concentrations. These concentrations may be due to the presence of fine particles in urban environments, which usually originate from vehicular sources (Chen et al., 2010). Ultrafine particles (nucleation mode), formed during combustion in car engines, are present at high concentrations in the near wake of the car. Particles recently formed during combustion may be diluted with background air and then spread out, to be later transported by advection to far-off regions. Moreover, particles in nucleation mode can increase in size by condensation. In addition, there may be the coagulation of many of these particles and the dilution or turbulent mixing, thus altering the particle size distribution (Zhu et al., 2002). Furthermore, particles in the accumulation mode have a longer residence time than ultrafine particles because removal by diffusion is negligible (Junker et al., 2000). However, growth rates decrease with an increasing distance either from emission sources or from the highway (Kumar et al., 2011). Other authors also showed that the atmospheric particle number concentration might decrease as the distance from emission sources such as highways and streets increases (Morawska et al., 2008; Buonanno et al., 2009). The concentration is also influenced by other parameters such as vehicle speed, air temperature, and chemical factors (Yli-Tuomi et al., 2005). For example, lower vehicular speeds produce lower number of particles, as well as larger particles.

Table 2 shows the mean particle number concentration in the PR1, PR2.5, and PR10 size ranges (particles L^{-1}) for each day of the week. The data reveal that there was a change in PR1 and PR2.5 probably due to primary emissions from motor vehicles, which are characterized by their smaller diameter (fine particles) (Morawska et al., 2008). Higher particle number concentrations were observed on weekdays and lower concentrations on Sundays, except for the PR2.5 size range, which had its lowest concentration on Mondays. This is probably due to lower concentrations in the PR1 size range on Sundays, leading to a lower formation of these particles (PR2.5) on the following day.

3.2. Daily variation of atmospheric particle number, O_3, NO, NO_2, NO_x, and OX

Fig. 2 shows the mean daily variation of particle number concentration in the PR1, PR2.5 and PR10 size ranges, and of the gaseous pollutants NO, NO_2, NO_x, O_3, and OX. NO_2 and O_3 can be observed together as OX (OX = $NO_2 + O_3$), i.e., the total amount of photochemical oxidants (Han et al., 2011). In fact, OX is less sensitive to emissions and to their uncertainties and it is not influenced by the rapid photo-stationary equilibrium between NO, NO_2, and O_3 (Monteiro et al., 2005).

Table 2
Mean particle number concentration PR1, PR10 and PR2.5 size classes (Particles L^{-1}) for each day of the week.

	PR1	PR2.5	PR10
Monday	17.24	26.19	6.46
Tuesday	22.05	29.24	9.17
Wednesday	20.56	30.99	7.75
Thursday	19.22	30.48	6.17
Friday	18.42	26.35	6.74
Saturday	20.10	29.32	7.66
Sunday	16.64	27.11	5.52

Particle number in the PR1, PR2.5 and PR10 size ranges showed two concentration peaks, the first in the morning, with values of 21.05 and 29.61 particles L^{-1} at 08:00 for PR1 and PR2.5, respectively, and 7.09 particles L^{-1} at 09:00 for PR10. These peaks can be attributed to the beginning of the traffic flow and to an undeveloped boundary mixed layer, so that all emissions are accumulated (Wang et al., 2010). Moreover, low particle concentrations present in the beginning of the day favor the formation of new particles as well as their growth to larger diameters (Kulmala et al., 2004). In the late afternoon, emissions are diluted due to the increase of the mixing layer height and to higher wind speeds (Charron and Harrison, 2003). At this moment, the high concentrations of particles present promote the condensation of semi-volatile vapors from vehicular exhaust gases onto the particles and, therefore, they do not favor the formation of new particles (Kerminen et al., 2001).

The second concentration peak occurs in the late afternoon, at approximately 19:00 for PR1 and PR2.5 (25.50 and 38.37 particles L^{-1}, respectively), and 18:00 for PR10 (10.22 particles L^{-1}). During the second rush hour, after 18:00, particle number concentrations are higher. These results imply an influence of the decrease in the mixing layer height (lower temperature) during the night, of the lower turbulence and, consequently, the lower dispersion of particles. NO and NO_x also showed two peaks; however, their highest concentrations occurred in the morning. These data are consistent with several studies (Hagler et al., 2009; Park et al., 2008; Chen et al., 2010; Carslaw et al., 2011), which report the influence of vehicle emissions on the increase of NO concentrations and particle number.

NO concentration reached its peak at 08:00 (56.56 μg m^{-3}) and NO_2 increased too in the early hours of the day, reaching a concentration of 33.16 μg m^{-3} at 10:00. In the area of study, after sunrise (06:00), vehicular traffic increases (first rush hour), and an increase in NO and NO_2 concentrations in the atmosphere can be observed. At this time, NO_2 is produced by the oxidation of NO and by the photolysis of NO_3 formed during the night, as well as by the reaction of NO_3 with NO (Jenkin and Clemitshaw, 2000). At the end of the day, the highest concentration of NO was reported at 22:00 (38.88 μg m^{-3}) and of NO_2 at 19:00 (41.12 μg m^{-3}). With regard to O_3, the maximum concentration occurred at 15:00 (10.58 μg m^{-3}) and of OX at 19:00 (43.84 μg m^{-3}).

NO_x also showed a bimodal distribution (statistical curve), with maximum concentrations at 08:00 (79.99 μg m^{-3}) and 20:00 (72.02 μg m^{-3}). This pattern (Fig. 2), i.e., high concentrations of NO in relation to NO_2, is similar to that observed in the work of Notario et al. (2012) for urban sites influenced primarily by vehicular traffic. In the morning, NO_2 and O_3 peaks appear two and 7 h after the peak of NO, respectively, and O_3 peak occurs 5 h after the peak of NO_2. These results are similar to those obtained in other studies, e.g. Matsumoto et al. (2006) and Han et al. (2011). At night, NO_2 concentrations show a second peak, although slightly higher than that observed in the morning, probably due to a greater availability of O_3 to react with NO to form NO_2 and a nocturnal atmospheric stability (Wang et al., 2010). This pattern of hourly variation of these pollutants (NO, NO_2, NO_x, and O_3) can be found in many urban environments around the world (Dallarosa et al., 2007; Sanchez et al., 2007; Han et al., 2011; Teixeira et al., 2009).

Analyzing OX concentrations (Fig. 2), it may be seen that they follow NO_2 concentrations until the first hours in the afternoon, when O_3 concentrations begin to increase due to the influence of

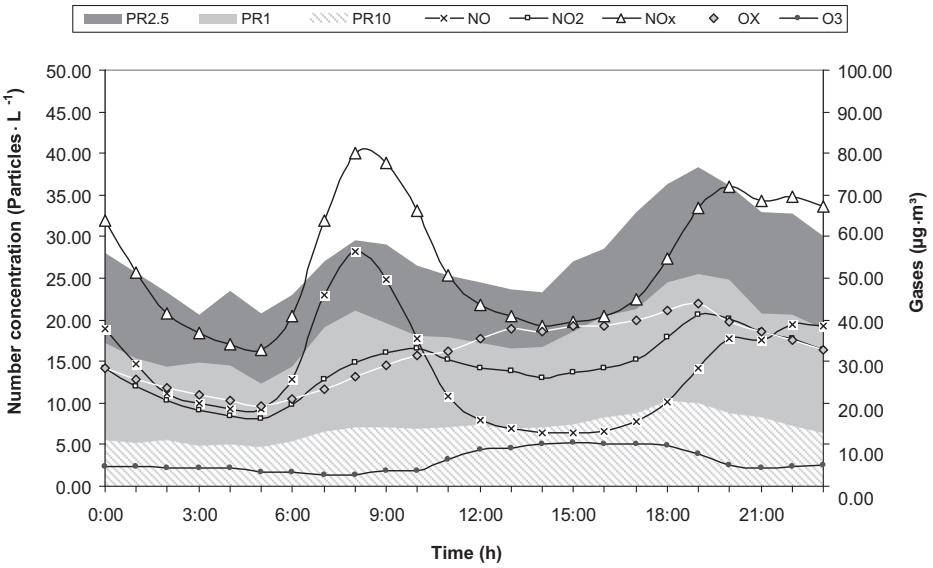

Fig. 2. Mean daily variation of particle number concentration in the PR1, PR2.5 and PR10 size ranges, and of gaseous pollutants NO, NO_2, NO_x, O_3 and OX, for the sampling period.

solar radiation. It is also observed that OX peaks are controlled by the variation of NO_2. The highest concentrations of OX occurred in the afternoon because the photochemical activity is strengthened (Notario et al., 2012) showing that there is an influence of photochemical processes (Han et al., 2011). At night, there is a decrease in NO_2 and O_3 concentrations until the beginning of the following day. This decrease is due to the absence of solar radiation, which impairs the formation of NO_2 and O_3 by photolytic reactions, as well as the reactions of NO_2 with NO_3, and of NO_2 with O_3 (Jenkin and Clemitshaw, 2000). Fig. 3 shows the variation in mean daily concentration of O_3 and solar radiation. Maximum O_3 concentration occurred 2 h after the maximum solar radiation value, mainly due to photo-oxidation of precursor gases in the presence of sufficient amounts of NO_x (Elminir, 2005). This may explain the similar behavior of the increase of O_3 and decrease of NO (Fig. 3) possibly evidencing a dependence of oxidation reactions from solar radiation.

3.3. Hourly particle number concentrations per weekday and weekends/holidays

The data were divided into two groups: weekdays and weekends/holidays. Then, hourly means were calculated for each group. Figs. 4 and 5 show the weekdays and weekends/holidays mean

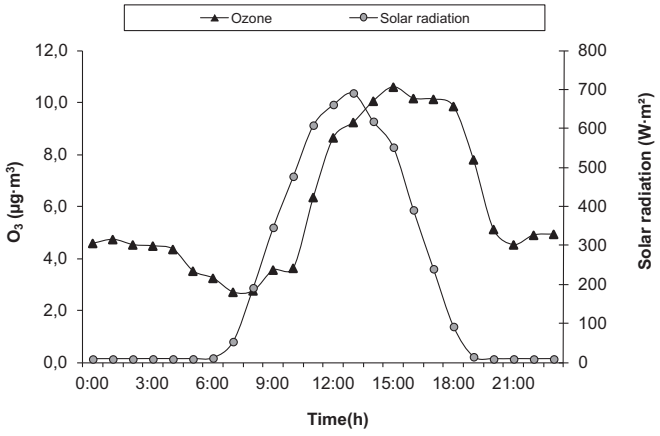

Fig. 3. Mean daily concentration of O_3 concentration and solar radiation, for the sampling period.

daily variation for particle number in the PR1, PR2.5, and PR10 size ranges, and gaseous pollutants (NO, NO_2, NO_x), in which the *X*-axis denotes the hours and the *Y*-axis the concentrations of particle number or gases.

Fig. 4 shows mean daily variation of particle number in the PR1, PR2.5, and PR10 size ranges, and of NO, NO_2, and NO_x during weekdays. Variations show similar results to those explained in the previous item: curves with two peaks, one in the morning and one in the evening. The high vehicular traffic and traffic congestion during rush hours can play a significant role in the peak concentrations observed (Seakins et al., 2002). Times at which the maximum concentrations in the morning and in the evening were reported show what was already expected: peaks at the same hours of high vehicular traffic, because particles in the PR2.5 and PR1 size ranges and NO are produced by local emissions from vehicle exhaust in urban areas. Moreover, traffic congestion may also play a significant role in these emission peaks (Seakins et al., 2002; Yli-Tuomi et al., 2005). After the rush hours, it was observed that the concentration of fine particles decreased. These findings were also reported by other authors, such as Hagler et al. (2009).

Fig. 5 shows weekends/holidays mean daily variation of particle number concentration in the PR1, PR2.5 and PR10 size ranges, and of NO, NO_2, and NO_x. The results show monomodal curves (statistical curve) for particle number for the PR1, PR2.5, and PR10 size ranges, and for NO_2. NO and NO_x curves showed two peaks, with the night peak slightly higher than the morning peak. Concentrations of particle number, NO, NO_2, and NO_x are lower compared to weekdays, as previously reported.

Statistical analysis was applied by using Student's *t*-test of means to compare daily mean concentrations (24 h) on weekdays and weekends. Table 3 shows Student's *t*-test results for particle number concentration and gaseous pollutants for weekdays and weekends. The daily mean particles concentrations in the PR1, PR2.5, and PR10 size ranges during weekdays were 19.09, 28.46 and 7.04 particles L^{-1}, respectively, while the values of hourly means for weekends and holidays were 16.66, 25.06 and 6.62 particles L^{-1}, respectively. Weekday means for particles in the PR1 (P value = 0.000602) and PR2.5 (P value = 0.000435) size ranges were significantly higher than for weekends, at a confidence level of 99.94% and 99.96%, respectively. As for particles in the PR10 fraction (P value = 0.102793), the test did not show any significant difference at a confidence level of 95%. This is consistent with other

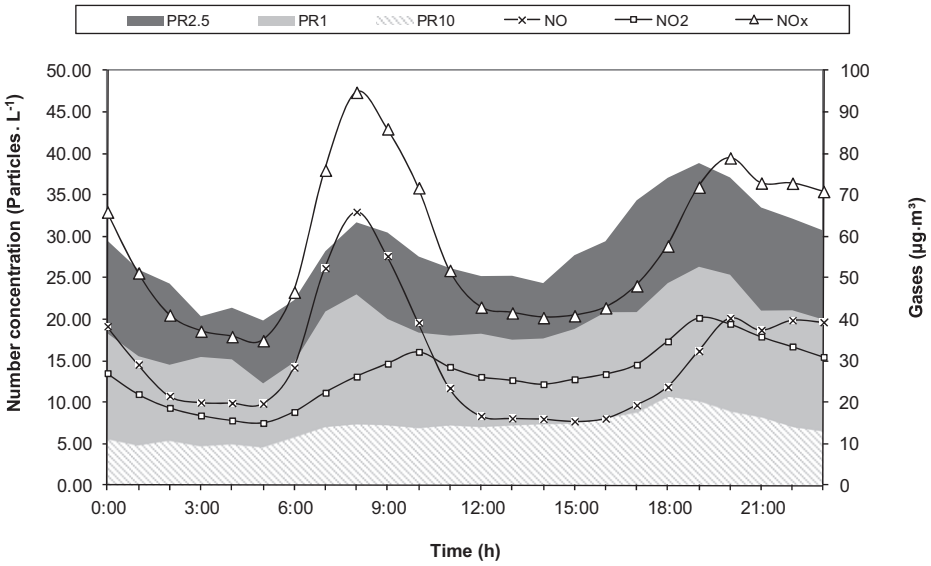

Fig. 4. Weekdays mean daily variation for particle number concentration in the fractions PR1, PR2.5 and PR10, and gaseous pollutants NO, NO_2, NO_x, for the sampling period.

studies, e.g. Morawska et al. (2002), Wang et al. (2010), Lonati et al. (2011), among others, who found lower concentrations in the fine and ultrafine particles during the weekends.

When comparing NO concentrations, it may be seen that its mean concentrations show slightly higher levels on weekdays (30.36 μg m^{-3}) than on weekends (28.96 μg m^{-3}). NO_2 mean concentrations for weekdays and weekends were similar, with values of 26.88 μg m^{-3} and 28.96 μg m^{-3}, mainly because NO_2 has a longer lifetime than the reactive NO (Han et al., 2011) and, consequently, less variation. As for the pollutants NO, NO_2, and NO_x, the test did not show any significant difference at a confidence level of 95%. However, when analyzing Figs. 4 and 5, it may be observed that the concentration peak of NO in the morning is higher on weekdays (65.98 μg m^{-3}) than on weekends (40.59 μg m^{-3}).

3.4. Variations in the relationships among NO, NO_2, and O_3

Based on the values of NO, NO_2, and O_3 measured in 2011, we calculated J_1 values (NO_2 photolysis rate) and k_4 coefficients of the reaction of NO with O_3 in order to obtain the variation of J_1/k_4 using reaction (5). J_1/k_4 values ranged between 0.014 and 0.048 ppm, and J_1 values remained between 0.35 and 1.10 min^{-1}. As expected, k_4 varied similarly to ambient temperature (Matsumoto et al., 2006).

Fig. 6a, b shows the daily variation of hourly means of NO, NO_2, and NO_x, as well as the ratios NO/NO_2 and NO_2/OX. Most of the time, the ratio NO/NO_2 (Fig. 6a) is controlled mainly by the concentration of NO and varies similarly to NO concentrations. Values of NO/NO_2 remain higher than one (1) in the evening and in the morning, between 22:00–10:00, indicating that during this time NO concentrations are higher than NO_2 concentrations. The conversion of NO to NO_2 probably takes place during the remaining time, thus increasing NO_2 concentrations and decreasing the NO/NO_2 ratio, which may indicate the formation of O_3. With regard to the NO_2/OX ratio (Fig. 6b), its variation is related to the rate of chemical processes or the time available for them to occur (Han et al., 2011). The lowest values were observed in the afternoon, around noon, when O_3 shows high concentration. The highest $NO_2/$

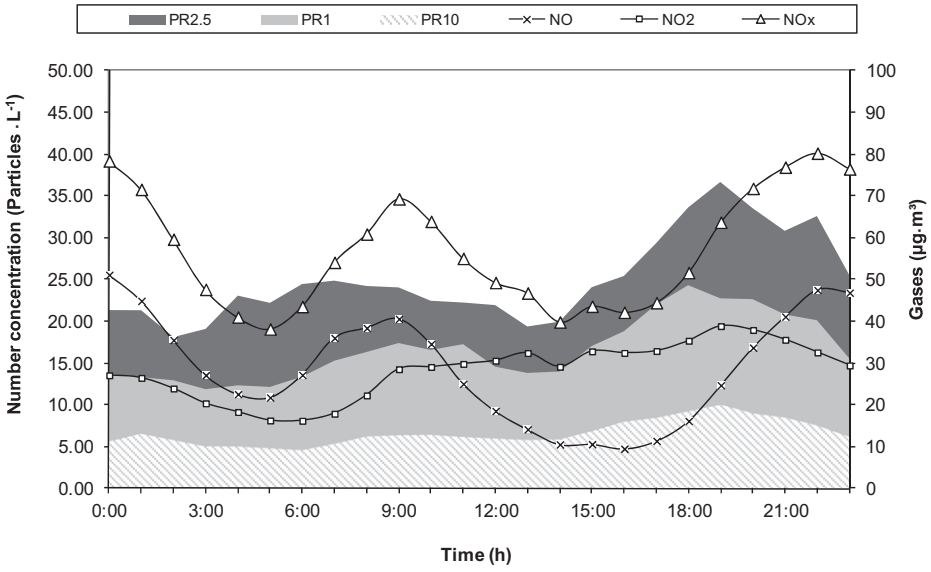

Fig. 5. Weekends mean daily variation for particle number concentration in the PR1, PR2.5 and PR10 size ranges, and gaseous pollutants NO, NO_2, NO_x, for the sampling period.

Table 3
Student's *t*-test results for particle number concentration and gaseous pollutants (μg m^{-3}) for weekdays and weekends.

	Mean		*t*-Value	*P* value
	Weekdays	Weekends		
PR1	19.09 ± 14.75	16.66 ± 13.56	3.44	0.000602
PR2.5	28.46 ± 19.52	25.06 ± 19.98	3.52	0.000435
PR10	7.04 ± 5.24	6.62 ± 4.88	1.63	0.102793
NO	30.36 ± 38.43	28.96 ± 33.39	0.72	0.469431
NO_2	26.88 ± 14.94	28.96 ± 16.23	−1.68	0.092455
NO_x	57.36 ± 45.60	57.34 ± 41.82	0.01	0.991639

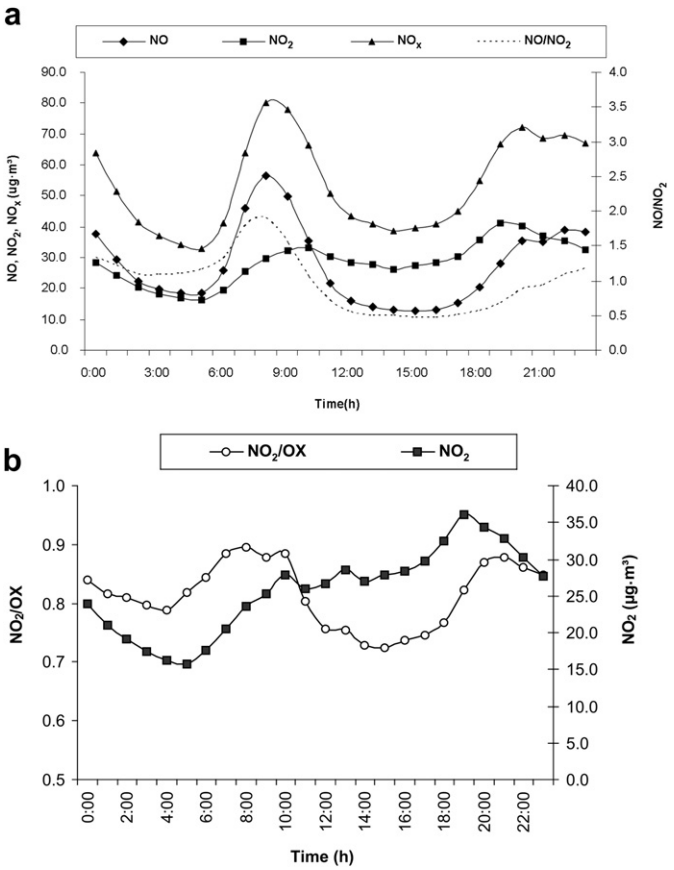

Fig. 6. a,b. Daily variation of hourly means of NO, NO_2, NO_x, NO/NO_2 and NO_2/OX.

OX values were reported in the morning until noon, at which time NO_2 is increasing and O_3 formation is only beginning.

3.5. Correlation of polluting particles and gases with meteorological parameters

Daily mean concentrations of different particle sizes were analyzed together with the gaseous pollutants and meteorological parameters. Table 4 shows Pearson's correlation coefficients between particle number concentration in the PR1, PR2.5 and PR10 size ranges and the gaseous pollutants NO, NO_2, and NO_x with meteorological parameters (wind speed, temperature, relative humidity, and solar radiation). The results show that PR1 and PR2.5 size classes have a positive correlation with NO and NO_x, indicating it may, in part, have similar sources to vehicular traffic emissions (Wang et al., 2010).

The wind speed had a low negative correlation with the particles, which shows that the higher the wind speed, the lower the particle number concentration, particularly those of accumulation modes (fine particles) because there is a greater horizontal dispersion of the pollutants (Shi et al., 2007). The wind speed can also influence the dispersion of pollutants such as NO, NO_2, and NO_x. These data show agreement with other studies, e.g. Guerra and Miranda (2011) and Jones et al. (2010). However, NO showed no significant correlation since it is more reactive and is more influenced by local emissions than by emissions transported from surrounding areas (Costabile and Allegrini, 2007). O_3, too, did not show any significant correlation with wind speed. NO, NO_2 and NO_x showed a low, although not significant, negative correlation with relative humidity. NO_2 in the presence of solar radiation may react with the OH radical to form HNO_3, which is a route of NO_2 consumption (Jenkin and Clemitshaw, 2000). Similar results were observed by Elminir (2005). O_3 also shows a negative correlation with relative humidity. In the presence of sunlight and water vapor, O_3 can form the radical OH, thereby favoring the consumption of O_3 (Uherek et al., 2010; Costabile and Allegrini, 2007). Variations in temperature also did not significantly affect concentrations of NO, NO_2, and NO_x. These data are in agreement with studies from other authors (Yli-Tuomi et al., 2005), which found low correlation between NO_x with temperature and relative humidity. As an indicator of photo-oxidation process, tropospheric O_3 showed a typical behavior, i.e., a clear trend to increase with temperature (Elminir, 2005). The correlation coefficients (Table 4) show that NO_2 is associated with solar radiation, since during day light hours this pollutant may be converted back to NO, as a result of photolysis. For this period, the sufficient availability of solar radiation might favor this photochemical process (Jenkin and Clemitshaw, 2000; Elminir, 2005). The correlation between O_3 and solar radiation is significant (Table 4) since, as explained above, the diurnal variation in O_3 is directly influenced by solar radiation (Fig. 3).

An inverse correlation between the number of particles (PR1, PR2.5, and PR10), relative humidity and rainfall was observed. This might be attributed to the fact that particles can be removed by their dissolution in water droplets (Baird, 2004) or by the coagulation of droplets on the particles and, thus, be easily removed by below-cloud or in-cloud processes (Wiegand et al., 2011).

As explained previously, the positive correlation between particle number (PR1, PR2.5, and PR10), temperature and solar radiation might be associated with days with low wind speeds and absence of rainfall, which explains the negative correlation with the

Table 4
Pearson correlation coefficients between particle number concentration and gaseous pollutants (μg m^{-3}) with meteorological parameters.

Variables	NO	NO_2	NO_x	Wind velocity (m s^{-1})	Ambient temperature (°C)	Relative humidity (%)	Solar radiation (W m^2)	Rainfall (mm)
PR_1	**0.36**	0.20	**0.32**	−0.22	0.08	**−0.59**	**0.48**	**−0.35**
$PR_{2.5}$	**0.32**	**0.26**	**0.32**	−0.21	0.16	**−0.53**	**0.32**	**−0.31**
PR_{10}	0.18	0.22	0.21	−0.09	**0.30**	**−0.66**	**0.40**	**−0.27**
NO		**0.57**	**0.97**	−0.20	−0.18	−0.09	−0.04	0.08
NO_2	**0.57**		**0.76**	**−0.24**	−0.11	−0.03	**−0.26**	−0.07
NO_x	**0.97**	**0.76**		**−0.23**	−0.17	−0.07	−0.13	−0.08
O_3	**−0.55**	**−0.71**	**−0.63**	0.05	0.25	−0.28	**0.36**	−0.07

The marked correlations in bold are significant for *P*-value <0.05.

latter two. A small contribution of photochemical activity might also be possible, leading to an increase in the concentration of fine and ultrafine particles (Park et al., 2008).

4. Conclusions

The mean daily variation of particle number concentration in the PR1, PR2.5, and PR10 size ranges, and of the gaseous pollutants NO, NO_2, and NO_x showed peaks during the periods of higher vehicle flow, with higher concentrations at night probably due to the influence of a stable boundary layer. The mean daily particle number concentrations in the area of study showed a greater number of fine and ultrafine particles (PR2.5 and PR1 size ranges) during the study period. The results also showed differences between the fine and ultrafine particle number concentrations during weekdays and weekends/holidays, with lower concentrations on weekends/holidays. These results, along with the increase in NO concentration in the morning rush hours, suggest that particle number concentration was affected by emissions from motor vehicles.

For the study period, analysis of the correlation between the number of fine and ultrafine particles and NO and NO_x suggests that there might be similar emission sources, e.g. vehicular sources.

The results indicate that there may be an influence of temperature, relative humidity, wind speed, and solar radiation on particle number concentration. The results also show that the concentration of O_3 might be directly influenced by solar radiation.

Acknowledgments

The authors are grateful to FAPERGS, FINEP, and CNPq for their financial support.

References

Atkinson, R., 2000. Atmospheric chemistry of VOCs and NO. Atmospheric Environment 34, 2063–2101.

Baird, C., 2004. Environmental Chemistry, second ed. W.H. Freeman and Company, New York. USA, 652 pp.

Bathmanabhan, S., Saragur, S.N., 2010. Analysis and interpretation of particulate matter – PM10, PM2,5 and PM1 emissions from the heterogeneous traffic near an urban roadway. Atmospheric Pollution Research 1, 184–194.

Buonanno, G., Lall, A.A., Stabile, L., 2009. Temporal size distribution and concentration of particles near a major highway. Atmospheric Environment 43, 1100–1105.

Carslaw, D.C., Beevers, S.D., Westmoreland, E., Williams, M., Tate, J., Murrells, T., Stedman, J., Li, Y., Grice, S., Kent, A., Tsagatakis, I., 2011. Trends in NO_x and NO_2 Emissions and Ambient Measurements in the UK. Version: 3rd March 2011. Draft for Comment.

Charron, A., Harrison, R.M., 2003. Primary particle formation from vehicle emissions during exhaust dilution in the roadside atmosphere. Atmospheric Environment 37, 4109–4119.

Chen, S.-C., Tsai, C.-J., Chou, C.-K., Roam, G.-D., Cheng, S.-S., Wang, Y.-N., 2010. Ultrafine particles at three different sampling locations in Taiwan. Atmospheric Environment 44, 533–540.

Colvile, R.N., Hutchinson, E.J., Mindell, J.S., Warren, R.A., 2001. The transport sector as a source of air pollution. Atmospheric Environment 35, 1537–1565.

Coronado, C.R., Carvalho Jr., J.A., Silveira, J.L., 2009. Biodiesel CO_2 emissions: a comparison with the main fuels in the Brazilian market. Fuel Process Technology 90, 204–211.

Costabile, F., Allegrini, I., 2007. Measurements and analysis of nitrogen oxides and ozone in the yard and on the roof of a street-canyon in Suzhou. Atmospheric Environment 41, 6637–6647.

Dallarosa, J., Teixeira, E.C., Alves, R.M., 2007. Application of numerical models in the formation of ozone and its precursors in areas of influence of coal-fired power station – Brazil. Water Air Soil Pollution 178, 385–399.

Dallarosa, J., Teixeira, E.C., Meira, L., Wiegand, F., 2008. Study of the chemical elements and polycyclic aromatic hydrocarbons in atmospheric particles of PM_{10} and $PM_{2.5}$ in the urban and rural areas of South Brazil. Atmospheric Research 89, 76–92.

DETRAN, 2012. Departamento Estadual de Trânsito – DETRAN/RSZ. Available at: http://www.detran.rs.gov.br/index.php?action=estatistica&codItem=99 (accessed in May 2012).

Dwivedi, D., Agarwal, A.K., Sharma, M., 2006. Particulate emission characterization of a biodiesel vs. diesel-fuelled compression ignition transport engine: a comparative study. Atmospheric Environment 40, 5586–5595.

Elminir, H.K., 2005. Dependence of urban air pollutants on meteorology. Science of the Total Environment 350 (1–3), 225–237.

EMBRAPA, 2003. Empresa Brasileira de Pesquisa Agropecuária. In: Clima do Rio Grande do Sul. Secção de Geografia. Secretaria da Agricultura, Porto Alegre. Available at: http://www. cnpt.embrapa.br/agromet/cli_pf8.html (accessed in May 2012).

ENVIRONNEMENT, 2010. CPM. Continuous Particulate Measurement, Technical Manual. pp. 1–44.

Finlayson-Pitts, B.J., Pitts Jr., J.N., 2000. Chemistry of the Upper and Lower Atmosphere: Theory, Experiments, and Applications. Academic press, San Diego, CA, USA.

Gaffney, J.S., Marley, N.A., 2009. The impacts of combustion emissions on air quality and climate – from coal to biofuels and beyond. Atmospheric Environment 43, 23–36.

Guerra, F.P., Miranda, R.M., 2011. Influência da meteorologia na concentração do poluente atmosférico $PM_{2.5}$ na RMRJ e na RMSP. In: Anais II Congresso Brasileiro de Gestão Ambiental. IBEAS, Paraná, Brasil.

Hagler, G.S.W., Baldauf, R.W., Thomas, E.D., Long, T.R., Snow, R.F., Kinsey, J.S., Oudejans, L., Gullet, B.K., 2009. Ultrafine particles near a major roadway in Raleigh, North Carolina: downwind attenuation and correlation with traffic-related pollutants. Atmospheric Environment 43, 1229–1234.

Han, S., Bian, H., Feng, Y., Liu, A., Li, X., Zeng, F., Zhang, X., 2011. Analysis of the Relationship between O_3, NO and NO_2 in Tianjin, China. Aerosol and Air Quality Research 11, 128–139.

INPE-CPTEC, 2012. Instituto Nacional de Pesquisas Espaciais. Centro de Previsão de Tempo e Estudos Climáticos. Available at: http://www.cptec.br/clima (Accessed in May 2012).

Jenkin, M.E., Clemitshaw, K.C., 2000. Ozone and other secondary photochemical pollutants: chemical processes governing their formation in the planetary boundary layer. Atmospheric Environment 34, 2499–2527.

Jones, A.M., Harrison, R.M., Baker, J., 2010. The wind speed dependence of the concentrations of airborne particulate matter and NO_x. Atmospheric Environment 44, 1682–1690.

Junker, M., Kasper, M., Ro, M., Camenzind, M., Ku, N., Monn, C., Theis, G., Braun-Fahrländer, C., 2000. Airborne particle number profiles, particle mass distributions and particle-bound PAH concentrations within the city environment of Basel: an assessment as part of the BRISKA Project. Atmospheric Environment 34, 3171–3181.

Kerminen, V.-M., Pirjola, L., Kulmala, M., 2001. How significantly does coagulational scavenging limit atmospheric particle production? Journal of Geophysical Research 106, 24119–24125.

Kewley, D.J., Post, K., 1978. Photochemical ozone formation in the Sydney airshed. Atmospheric Environment 12, 2179–2184.

Kulmala, M., Vehkamaki, H., Petaja, T., Dal Maso, M., Lauri, A., Kerminen, V., Birmilli, W., McMurry, P., 2004. Formation and growth rates of ultrafine atmospheric particles: a review of observations. Journal of Aerosol Science 35, 143–176.

Kumar, P., Ketzel, M., Vardoulakis, S., Pirjola, L., Britter, R., 2011. Dynamics and dispersion modelling of nanoparticles from road traffic in the urban atmospheric environment – a review. Journal of Aerosol Science 42, 580–603.

Leighton, P.A., 1961. Photochemistry of air pollution. Academic Press, New York.

Lonati, G., Crippa, M., Gianelle, V., Van Dingenen, R., 2011. Daily patterns of the multi-modal structure of the particle number size distribution in Milan, Italy. Atmospheric Environment 45, 2434–2442.

Matsumoto, J., Kosugi, N., Nishiyama, A., Isozaki, R., Sadanaga, Y., Kato, S., Bandow, H., Kajii, Y., 2006. Examination on photostationary state of NO_x in the urban atmosphere in Japan. Atmospheric Environment 40, 3230–3239.

Mattiuzi, C.D.P., Palagi, A.C., Teixeira, E.C., Wiegand, F., 2012. Poluição Atmosférica do Biodiesel – Estado da Arte. In: Teixera, E.C., Wiegand, F., Tedesco, M. (Eds.), Biodiesel: Impacto Ambiental Agronômico e Atmosférico. Cadernos de Planejamento e Gestão Ambiental N°6. FEPAM, Porto Alegre. Brazil, pp. 43–67. Chap. 2.

METROPLAN, 2012. Fundação Estadual de Planejamento Metropolitano e Regional. In: Evolução da população na RMPA. Available at: http://www.metroplan.rs.gov.br/mapas_estatisticas/au_rmpa.htm (accessed in May 2012).

Monteiro, A., Vautard, R., Borrego, C., Miranda, A.I., 2005. Long-term simulations of photo oxidant pollution over Portugal using the CHIMERE model. Atmospheric Environment 39, 3089–3101.

Morawska, L., Jayaratne, E.R., Mengersen, K., Jamriska, M., Thomas, S., 2002. Differences in airborne particle and gaseous concentrations in urban air between weekdays and weekends. Atmospheric Environment 36, 4375–4383.

Morawska, L., Ristovski, Z., Jayaratne, E.R., Keogh, D.U., Ling, X., 2008. Ambient nano and ultrafine particles from motor vehicle emissions: characteristics, ambient processing and implications on human exposure. Atmospheric Environment 42, 8113–8138.

MT, 2012. Ministério dos Transportes, Brasil. Available at: http://www.transportes.gov.br/obra/conteudo/id/36986 (accessed in May 2012).

Notario, A., Bravo, I., Adame, J.A., Díaz-de-Mera, Y., Aranda, A., Rodríguez, A., Rodríguez, D., 2012. Analysis of NO, NO_2, NO_x, O_3 and oxidant ($OX = O_3 + NO_2$) levels measured in a metropolitan area in the southwest of Iberian Peninsula. Atmospheric Research 104–105, 217–226.

Olivares, G., Johansson, C., Strom, J., Hansson, H.-C., 2007. The role of ambient temperature for particle number concentrations in a street canyon. Atmospheric Environment 41, 2145–2155.

Park, K., Park, J.Y., Kwak, J.-H., Cho, G.N., Kim, J.-S., 2008. Seasonal and diurnal variations of ultrafine particle concentration in urban Gwangju, Korea: observation of ultrafine particle events. Atmospheric Environment 42, 788–799.

PETROBRAS, 2012. Available at: http://www.petrobras.com.br/pt/produtos/para-voce/nas-ruas/ (accessed in May 2012).

PORG, 1997. Ozone in the United Kingdom. Fourth Report of the UK Photochemical Oxidants Review Group. Department of the Environment, Transport and the Regions, London.

Renard, J.-B., Thaury, C., Mineau, J.-L., Gaubicher, B., 2010. Small-angle light scattering by airborne particulates: Environnement S.A. continuous particulate monitor. Measurement Science and Technology 21, 1–10.

Sanchez, M.L., Torre, B.D., Garcia, M.A., Péreza, I., 2007. Ground-level ozone and ozone vertical profile measurements close to the foothills of the Guadarrama mountain range (Spain). Atmospheric Environment 32, 1615–1622.

Seakins, P.W., Lansley, D.L., Hodgson, A., Huntley, N., Pope, F., 2002. New directions: mobile laboratory reveals new issues in urban air quality. Atmospheric Environment 36 (7), 1247–1248.

Seinfeld, J.H., Pandis, S.N., 2006. Atmospheric Chemistry and Physics: From Air Pollution to Climate Change. John Wiley and Sons, Inc., New Jersey.

Shi, Z., He, K., Yu, X., Yao, Z., Yang, F., Ma, Y., Ma, R., Jia, Y., Zhang, J., 2007. Diurnal variation of number concentration and size distribution of ultrafine particles in the urban atmosphere of Beijing in winter. Journal of Environmental Sciences 19, 933–938.

Teixeira, E.C., Feltes, S., Santana, E.R., 2008. Estudo das emissões de fontes móveis na Região Metropolotana de Porto Alegre, Rio Grande do Sul. Química Nova 31 (2), 244–248.

Teixeira, E.C., Santana, E.R., Wiegand, F., Fachel, J., 2009. Measurement of surface ozone and its precursors in an urban area in South Brazil. Atmospheric Environment 43, 2213–2220.

Teixeira, E.C., Mattiuzi, C.D.P., Feltes, S., Wiegand, F., Santana, E.R.R., 2012. Estimated atmospheric emissions from biodiesel and characterization of pollutants in the metropolitan area of Porto Alegre-RS. Anais da Academia Brasileira de Ciências 84 (3), 245–261.

Uherek, E., Halenka, T., Borken-Kleefeld, J., Balkanski, Y., Berntsen, T., Borrego, C., Gauss, M., Hoor, P., Juda-Rezler, K., Lelieveld, J., Melas, D., Rypdal, K., Schmid, S., 2010. Transport impacts on atmosphere and climate: land transport. Atmospheric Environment 44, 4772–4816.

Wåhlin, P., 2009. Measured reduction of kerbside ultrafine particle number concentrations in Copenhagen. Atmospheric Environment 43, 3645–3647.

Wang, F., Costabile, F., Li, H., Fang, D., Alligrini, I., 2010. Measurements of ultrafine particle size distribution near Rome. Atmospheric Research 98, 69–77.

Wiegand, F., Pereira, F.N., Teixeira, E.C., 2011. Study on wet scavenging of atmospheric pollutants in south Brazil. Atmospheric Environment 45, 4770–4776.

Yli-Tuomi, T., Aarnioa, P., Pirjolab, L., Makela, T., Hillamo, R., Jantunen, M., 2005. Emissions of fine particles, NO_x, and CO from on-road vehicles in Finland. In: Atmospheric Environment 39, 6696–6706.

Zhu, Y., Hinds, W.C., Kim, S., Shen, S., 2002. Study of ultrafine particles near a major highway with heavy-duty diesel traffic. Atmospheric Environment 36, 4323–4335.

Zielinska, B., 2005. Atmospheric transformation of diesel emissions. Experimental and Toxicologic Pathology 57, 31–42.

CAPITULO III

Seasonal changes, identification and source apportionment of PAH in $PM_{1.0}$

AGUDELO-CASTAÑEDA, D. M; , Teixeira, E.C.

Atmospheric Environment 96, 186-200, 2014

Atmospheric Environment 96 (2014) 186–200

Contents lists available at ScienceDirect

Atmospheric Environment

journal homepage: www.elsevier.com/locate/atmosenv

Seasonal changes, identification and source apportionment of PAH in $PM_{1.0}$

Dayana Milena Agudelo-Castañeda [b], Elba Calesso Teixeira [a, b, *]

[a] Research Department, Fundação Estadual de Proteção Ambiental Henrique Luis Roessler, Rua Borges de Medeiros 261/9 Andar, 90020-021, Porto Alegre, RS, Brazil
[b] Postgraduate Program in Remote Sensing and Meteorology, Geosciences Institute, Universidade Federal do Rio Grande do Sul, Av. Bento Gonçalves, 9500, 91501-970, Porto Alegre, RS, Brazil

HIGHLIGHTS

- Quantification of concentrations of PAHs in $PM_{1.0}$.
- Mean PAHs and $PM_{1.0}$ concentrations were higher in winter, particularly HMW.
- Diagnostic ratios and PMF analysis confirmed influence of vehicular emissions.
- Correlation of PAHs with meteorological parameters.
- BaP and DahA dominated BaPeq levels in the study area, varying with the season.

ARTICLE INFO

Article history:
Received 27 January 2014
Received in revised form
9 July 2014
Accepted 12 July 2014
Available online 14 July 2014

Keywords:
PAHs
$PM_{1.0}$
PMF
Seasonal variation
Diagnostic ratios
Mobile sources
BaPeq

ABSTRACT

The objective of this research was to evaluate the seasonal variation of PAHs in $PM_{1.0}$, as well as to identify and quantify the contributions of each source profile using the PMF receptor model. $PM_{1.0}$ samples were collected on PTFE filters from August 2011 to July 2013 in the Metropolitan Area of Porto Alegre, Rio Grande do Sul, Brazil. The samples were extracted using the EPA method TO-13A and 16 Polycyclic Aromatic Hydrocarbons (PAHs) were analyzed using a gaseous chromatograph coupled with a mass spectrometer (GC–MS). Also, the data discussed in this study were analyzed to identify the relations of the PAHs concentrations with NO_x, NO, O_3 and meteorological parameters (temperature, solar radiation, wind speed, relative humidity). The results showed that in winter, concentrations of total PAHs were significantly higher than in summer, thus showing their seasonal variation. The identification of emission sources by applying diagnostic ratios confirmed that PAHs in the study area originate from mobile sources, especially, from diesel and gasoline emissions. The analysis by PMF receptor model showed the contribution of these two main sources of emissions, too, followed by coal combustion, incomplete combustion/unburned petroleum and wood combustion. The toxic equivalent factors were calculated to characterize the risk of cancer from PAH exposure to $PM_{1.0}$ samples, and BaP and DahA dominated BaPeq levels.

1. Introduction

Polycyclic aromatic hydrocarbons (PAHs), also known as polynuclear aromatic hydrocarbons or polyarenes, constitute a large class of organic compounds (Dabestani and Ivanov, 1999). The PAHs released into the atmosphere are normally present in the gaseous phase or sorbed to particulates. Low Molecular Weight (LMW) PAHs have a higher concentration in the gas phase, whereas High Molecular Weight (HMW) PAHs are often associated with atmospheric particulate matter (Bi et al., 2003). HMW PAHs are expected to require much longer time to partition to coarse particles than LMW PAHs (Duan et al., 2007).

PAHs are generated from the incomplete combustion or pyrolysis of organic material (Li et al., 2005). Amongst the PAHs sources are: combustion processes: coal and wood burning, oil and gas burning, vehicles engines and open burning. Mobile sources or

* Corresponding author. Research Department, Fundação Estadual de Proteção Ambiental Henrique Luis Roessler, Rua Borges de Medeiros 261/9 Andar, 90020-021, Porto Alegre, RS, Brazil.
E-mail addresses: elbact.ez@terra.com.br, gerpro.pesquisa@fepam.rs.gov.br (E.C. Teixeira).

http://dx.doi.org/10.1016/j.atmosenv.2014.07.030
1352-2310/

open/uncontrolled burning, together with domestic combustion processes, are likely to provide the majority of the human exposure to atmospheric PAH, since humans congregate in urban environments characterized by these sources (Howsan and Jones, 2010). Zhang and Tao (2009) showed, also, that the major anthropogenic atmospheric emission sources of PAHs include biomass burning, coal and petroleum combustion, and coke and metal production.

Atmospheric particles <1 μm are formed by primary particles resulting from combustion (Zhao et al., 2008; Wingfors et al., 2011). This particle size fraction consists of nucleation mode (from particles combustion engine vehicles) and accumulation mode (photochemical smog particles and combustion) (Bathmanabhan and Madanayak, 2010). In urban environments, the atmospheric particles emitted by mobile sources, over 90% of the number concentration, belongs to the fraction <1 μm (Bond, 2004; Morawska et al., 2008.). This fraction can affect health and, in the other hand, can be a good indicator of vehicular sources in roadside sites (Lee et al., 2006). Given that, becomes important to study the $PM_{1.0}$ particles in heavy traffic areas.

PAHs are ubiquitous in urban air and are a major health concern, mainly because of its known carcinogenic and mutagenic properties (Panther et al., 1999). The known carcinogens isomers are primarily associated with particulate material and, usually, the highest concentrations are in the respirable fraction <5 μm (Sienra et al., 2005). The $PM_{1.0}$ particles present a higher risk because they can deposit in the respiratory tract, increasing the negative health effects (Slezakova et al., 2007) and can carry pollutants such as PAHs. Thus, there is considerable concern about the relationship between PAH exposure in the ambient air and the potential to contribute to human cancer incidence (Dybing et al., 2013). Nowadays, existing ambient air quality standards are restricted to $PM_{2.5}$ and PM_{10} fractions generated by mechanical processes and they are unable to effectively control submicron particles emitted from combustion sources such as motor vehicles (Morawska et al., 2008).

The emission sources identification of total PAHs concentration in ambient air can be accomplished through the use of diagnostic ratios or receptor models. The use of diagnostic ratios for PAH source identification involves comparing ratios of pairs of frequently found PAH emissions (Ravindra et al., 2008), however should be use with caution because the PAHs concentrations of emission sources can change due to the reactivity of PAHs with atmospheric species (ozone, nitrogen oxides) and environmental variables. In the present study, we used the positive matrix factorization method (PMF) because is considered a reliable receptor modeling, a powerful and widely used multivariate method that can resolve the dominant positive factors without prior knowledge of sources (Paatero and Tapper, 1994; Gu et al., 2011). In the work of Teixeira et al. (2013), the PMF model was used for apportionment of total PAHs in $PM_{2.5}$ and PM_{10} samples source.

Studies conducted in various locations around the world showed that the main sources of PAHs in urban areas are vehicular emissions, especially intense traffic and diesel vehicles, among which we cite some authors: Tsapakis et al. (2002), Guo et al. (2003), Manoli et al. (2004), Fang et al. (2004), Ravindra et al. (2006), Stroher et al. (2007). In Brazil, the analysis of the profile of PAHs concentrations was performed with particles of <10 and <2.5 μm, among which we mention: Barra et al. (2007), Bourotte et al. (2005), Dallarosa et al. (2005a, 2005b, 2008), De Martinis et al. (2002), Fernandes et al. (2002), Netto et al. (2002), Teixeira et al. (2012, 2013), Vasconcellos et al. (2011). However, studies of atmospheric particles <1 μm are scarce: Krumal et al. (2013), Klejnowski et al. (2010), Ladji et al. (2009), among others.

Atmospheric particles in the fraction <1 μm bear a large surface area for adsorption of PAHs, therefore the fine and ultrafine particles are richer in PAHs than coarse ones (Da Limu et al., 2013; Fang et al., 2006). Thus, the study of the concentration and behavior of PAHs in the fraction <1 μm is important to subsidize the knowledge of the probably negative impact on human health.

Consequently, ambient $PM_{1.0}$ samples were collected during two years for PAH quantification in the study area. The objectives of this study were (i) to evaluate the seasonality of PAHs associated with airborne particulate matter <1 μm ($PM_{1.0}$), (ii) identify and quantify the contributions of each source profile using the PMF receptor model.

2. Experimental

2.1. Study area

The region is the most urbanized area of the state, is characterized by different types of industries, including some stationary sources such as the Alberto Pasqualini Refinery, steel mills – which do not uses coke- (Siderúrgica Riograndense e Aços Finos Piratini), III Petrochemical Industrial Complex, and coal-fired power plants (Termelétrica de Charqueadas e TERMOCHAR, and the Usina Termelétrica of São Jerônimo and the USTJ). Besides, it is estimated that the most significant contribution are mobile sources due to the large number of vehicles in circulation in the region (Teixeira et al., 2008, 2010; Agudelo-Castaneda et al., 2014). In the study by Teixeira et al. (2008) were found that of the total fleet in the study area, about 84.98% is fueled by gasoline, 6.67% diesel, 6.58% alcohol, 1.3% natural gas and 0.74% with flex technology. Currently, gasoline- fueled vehicles use a mixture of gasoline and 20% of ethanol (PETROBRAS, 2012). The diesel used in the Metropolitan Region of Porto Alegre (MAPA) has a level of 500 ppm of sulfur and it is added 5% of biodiesel (Mattiuzi et al., 2012). Even if the diesel fleet in the region is only 6.67%, the environmental impact caused by this source in the air is elevated. A study by Teixeira et al. (2012) shows that from the total emissions originating from mobile sources within the MAPA, diesel vehicles are responsible for most emissions of particulate matter and NO_x.

The sampling sites location (Sapucaia do Sul and Canoas) in the MAPA is shown in Fig. 1. The locations were selected due to their vehicular influence, although there are some differences between the two sites. Sapucaia do Sul site has a greater vehicular influence vehicle: light and heavy fleet, traffic congestions and slow speeds. This site also has low industrial influence (oil refinery, steel mills that do not use coke) upstream of prevailing winds. Canoas is under a strong vehicular influence, daily traffic congestions, Canoas air base and industries (oil refinery) upstream of the prevailing winds that have a medium influence in this sampling site.

The meteorological conditions were described in previous works (Teixeira et al., 2012), consequently here we are just including a brief explanation. Due to its location, the area of study presents well-defined seasons and a climate strongly influenced by cold air masses migrating from the polar regions. The study area is located in a subtropical, temperate climate with four well-defined seasons: summer (January–March), autumn (April–June), winter (July–September) and spring (October–December). The wind direction shows marked seasonal variations. During summer and spring, the prevailing direction is E–SE, while in fall and winter, besides E–SE winds, winds from W and NW also occur. The historical mean precipitation is 1.300–1.400 mm $year^{-1}$ (INPE-CPTEC, 2012). The weather conditions in the study area during the sampling period (August 2011–July 2013) were : average temperature 18.79 °C, ranging between −1.40 and 37.20 °C, mean relative humidity 79.92%, ranging between 16.80 and 100.00%, and mean solar radiation 224.18 W m^2. The maximum wind speed was 8.33 m s^{-1} and the mean wind speed was 2.03 m s^{-1}, with resultant wind direction vector southeast (113°).

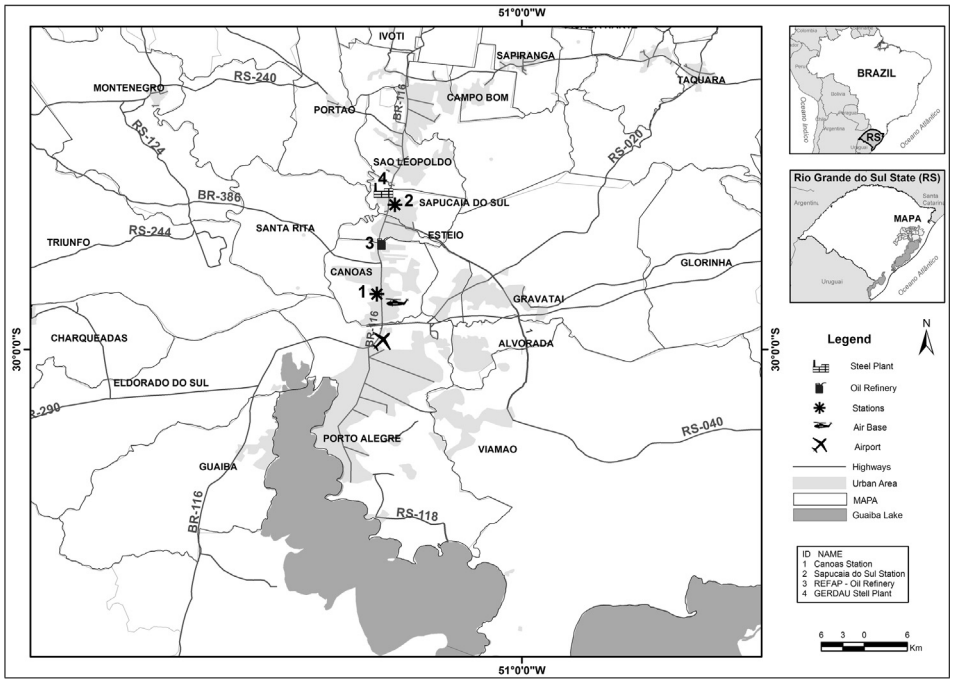

Fig. 1. Sampling sites location, Sapucaia do Sul and Canoas, in the Metropolitan Area of Porto Alegre.

2.2. Sampling

The sampling of atmospheric particulate matter <1.0 μm ($PM_{1.0}$) followed the criteria established by the USEPA (1994), using a sequential automatic particle sampler model PM162M of the Environnement S.A. The particulate matter sampler includes a set of two holders that act as support for the filters. The equipment uses the EN 12341 method (LECES, n° RC/L 9826). Samples of $PM_{1.0}$ were collected on PTFE filters of 47 mm diameter for a continuous period of 72 h from August 2011 to July 2013, with a flow rate of 1.0 $m^3\ h^{-1}$. The filters were wrapped in aluminum foil and transported under refrigeration to the laboratory and preserved in a freezer for later analysis. The procedure for the preparation of the filters is described elsewhere (Teixeira et al., 2011).

2.3. PAH analysis

The filters extracts were analyzed according to the USEPA method TO 13A (USEPA, 1999) for the determination of PAHs. The priority PAHs associated with $PM_{1.0}$, in the study area, considered in this study, were: naphthalene (Nap), acenaphthylene (Acy), acenaphthene (Ace), fluorene (Flu), phenanthrene (Phe), anthracene (Ant), fluoranthene (Flt), pyrene (Pyr), benzo[*a*]anthracene (BaA), chrysene (Chry), benzo[*b* + *k*]fluoranthene (BbkF), benzo[*a*]pyrene (BaP), indeno[1,2,3-*cd*]pyrene (Ind), dibenz[*a*,*h*]anthracene (DahA), benzo[*ghi*]perylene (BghiP). The benzo[*b*]fluoranthene and the benzo[*k*]fluoranthene were added for having the same retention times, so the results shows the concentration of benzo[*b* + *k*]fluoranthene. $PM_{1.0}$ filters were extracted in soxhlet with 125 mL of dichloromethane (CH_2Cl_2) for 18 h (USEPA, 1999). After this procedure the extracts were separated/preconcentrated through the clean up procedure using a silica gel column (activated with 5% of distilled H_2O) to eliminate possible interferences (Teixeira et al., 2011; Dallarosa et al., 2005a, 2005b, 2008). The clean up was performed through a columnation of the sample with four solvent fractions with different polarities:first fraction: 20 mL of hexane (aliphatic); second fraction: 10 mL of hexane, 10 mL of dichloromethane (PAHs); third fraction: 15 mL of hexane, 5 mL of dichloromethane (PAHs); and fourth fraction: 20 mL of dichloromethane (nitro-PAHs). The volume of fractions 2 and 3 was reduced to dryness using a rotary evaporator followed by a stream of pure nitrogen gas. Finally, it is added 1 mL of dichloromethane with electronic micropipette for subsequent analysis.

PAHs were identified by gas chromatograph coupled to a mass spectrometry detector (Shimadzu, model GCMS-QP5050A), using single ion monitoring (SIM). The chromatograph was equipped with a 30 m fused silica capillary column, DB-5 (0.2 mm ID, 0.25 m film thickness) with helium as carrier gas (1.5 ml/min, constant flow). The column temperature program started at 60 °C, and increased to 300 °C at 6 °C/min. It was held isothermal at 300 °C for 20 min. All samples were injected in the splitless mode. Data for qualitative analysis was acquired in the electron impact (EI) mode (70 eV). The details of the technique for the detection and quantification of PAH are described in Dallarosa et al. (2005a, 2005b) and Teixeira et al. (2013).

2.4. Quality control and assurance

Detection (DL) and quantification (QL) limits were calculated as explained in theTO13Amethod of USEPA (1999) and in Teixeira et al. (2013). DL is defined as 3.3 times the mean of the standard deviation of the replicates of the lowest point of the curve (5 μg L^{-1}) divided by the slope of the regression eq., and QL as ten times the DL. The concentration showed mean values between 3.97 and 5.85 μg L^{-1} and standard deviations between 0.24 and 1.02 μg L^{-1} among replicates of the lowest point of the curve of the standard solution (5 μg L^{-1}). DL and QL were in the range of 0.001–0.056 and 0.009–0.558 μg L^{-1}, respectively, for all PAHs studied. The accuracy of 98.0% was determined by the error obtained between the mean values of replicates of the standard solution (5 μg L^{-1}) taken as reference. The precision of 5% was calculated by means of percent relative standard deviation (%RSD).

To assess the trueness was used SRM-1649b, the Standard Urban Dust Reference Material of the National Institute of Standards and

Technology (NIST). The SRM-1649b was extracted in replicates ($n = 3$) according to methodology described above. Table 1 shows the results of the Standard Reference Material (SRM-1649b) with their recovery values. As can be seen in Table 1, the recoveries of SRM-1649b (NIST, Washington, DC) varied between 80.4% (indeno [1,2,3-*cd*]pyrene) and 111.3% (phenanthrene) with a mean recovery of 96.4%, of 0.02 g of urban dust.

2.5. NO_x,O_3 and meteorological data

NO, NO_2, and NO_x (NO_2 + NO) concentrations were measured with a chemiluminescent analyzer AC32M, while an analyzer O342M which uses the principle of UV radiation absorption by O_3 molecules was used for measuring O_3. All the equipments were made by Environnement S.A. These pollutants were measured during the same period of atmospheric particles: from August 2011 to July 2013. Meteorological data such as air temperature, relative humidity, radiation and wind speed were obtained from the meteorological station at Esteio, which belongs to the Alberto Pasqualini Refinery (REFAP). Precipitation data were obtained from the station at Porto Alegre, which belongs to the INMET. Both stations are located near the sampling site.

2.6. Receptor model: positive matrix factorization

Positive matrix factorization (PMF) is a multivariate factor analysis tool that decomposes the data matrix into two matrices: factor contributions and factor profiles (Paatero and Tapper, 1994; Paatero, 1997) with a residual matrix (Vestenius et al., 2011). The fundamental principle of source/receptor relationships in receptor models is that mass conservation can be assumed and a mass balance analysis can be used to identify and apportion sources of airborne particulate matter in the atmosphere (Hopke, 2003). The receptor model used in this study was the EPA PMF v3.0, developed by U.S. EPA (USEPA, 2008), to identify the source profile and their contribution. The PMF receptor model is described, briefly, below and in another recently published study (Teixeira et al., 2013). The mathematical model in matrix form is (Equation (1)):

$$X = GF + E \tag{1}$$

Where X is the known $n \times m$ concentration matrix of the m measured chemical species in n samples, G is an $n \times p$ matrix of source contributions to the samples, F is a $p \times m$ matrix characterizing each source (source profiles), and E is defined as a residual matrix. The objective of PMF is to find values for G and F that best reproduce the measured data (X). These values are adjusted until a minimum value of Q is found (Reff et al., 2007). Q is a goodness-of-fit parameter, and is defined as (Equation (2)):

$$Q = \Sigma^m \Sigma^n \left[\frac{E}{U}\right]^2 \tag{2}$$

Where E is the difference between the original dataset (X) and the PMF output (GF), U is the uncertainty of the measured data, m is the number of species and n is the number of samples (Wang et al., 2009; Reff et al., 2007). If the analysis is properly weighted, the Q value should be approximately equal to the theoretical Q value, which can be estimated by the following Equation (3) (USEPA, 2008):

$$Q_t = m*n - p(m+n) \tag{3}$$

Where p is the number of factors selected on the model.

The uncertainties values (U) were estimated for two cases: when the concentration of the specie (X) is less or equal to the Method Detection Limit – MDL (Equation (4)); and when the concentration of the specie is greater than the MDL (Equation (5)) (Reff et al., 2007):

$$U = 5/6 \times \text{MDL} \tag{4}$$

$$U = (0,05 \times X) + \text{MDL} \tag{5}$$

The quality of the data for each of the species (PAHs) was based on the signal-to-noise (S/N) and the percentage of samples above the MDL. Naphthalene, acenaphthylene and acenaphthene were classified as bad species. Fluorene and benzo[*ghi*]perylene were classified as weak. Weak species have their uncertainty multiplied by a factor of 3; bad species are excluded from the modeling process.

The model was run several times with varying number of factors (ranging from 3 to 7) using random seed mode. The six factor solution provided the better results in term of meaningful physical interpretations.

2.7. Carcinogenic risk assessment

The risk of cancer from exposure to particular PAH is expressed in terms of BaP, as the toxic equivalence factor (TEF), because humans are exposed to complex PAH mixtures (Cristale et al., 2012). The ambient concentrations of 12 PAHs, beginning from fluorene, and their toxic equivalence factor (TEF) were used in the calculation. The sum of the products of each PAH concentration and its respective TEF is called BaPeq value. The BaPeq was calculated for $PM_{1.0}$ samples of Sapucaia do Sul and Canoas using Equation (6).

$$\text{BaP}_{eq} = \sum \text{PAH}_{conc} * \text{PAH}_{TEF} \tag{6}$$

Where BaP_{eq} is the BaP-based toxic equivalency factor, PAH_{conc} is the concentration of individual PAH and PAH_{TEF} is the toxic equivalent factor of individual PAH using the factors proposed by Nisbet and LaGoy factors (1992). In this work was used a TEF of 1 instead of 5 for DahA, as proposed by Malcolm and Dobson (2004).

Table 1
Concentrations of PAH obtained in SRM1649a urban dust and this study (mg kg^{-1}).

Name	Certified SRM 1649b	Measured value	Recovery (%)	RSD (%)
Phenanthrene	3.941 ± 0.047	4.39 ± 0.19	111.3%	4%
Anthracene	0.509 ± 0.002	0.50 ± 0.05	97.7%	10%
Fluoranthene	6.14 ± 0.12	5.14 ± 0.24	83.7%	5%
Pyrene	4.784 ± 0.029	4.44 ± 0.34	92.8%	8%
Benzo[*a*]anthracene	2.092 ± 0.048	2.23 ± 0.05	106.7%	2%
Chrysene	3.008 ± 0.044	3.12 ± 0.39	103.8%	12%
Benzo[*b* + *k*]fluoranthene	7.738 ± 0.283	6.63 ± 0.31	85.7%	5%
Benzo[*a*]pyrene	2.47 ± 0.17	2.35 ± 0.07	95.1%	3%
Indeno[1,2,3-*cd*]pyrene	2.96 ± 0.17	2.38 ± 0.30	80.4%	13%
Dibenz[*a*,*h*]anthracene	0.29 ± 0.004	0.26 ± 0.03	88.8%	12%
Benzo[*ghi*]perylene	3.937 ± 0.052	3.62 ± 0.06	92.0%	2%

3. Results and discussion

3.1. $PM_{1.0}$ and polycyclic aromatic hydrocarbons concentrations

The mean concentrations of total PAHs and $PM_{1.0}$ were 1.99 ng m^{-3} and 14.81 μg m^{-3}, respectively, for Sapucaia do Sul and 1.52 ng m^{-3} and 9.58 μg m^{-3} for Canoas. The mean concentration of total PAHs and $PM_{1.0}$ in Sapucaia do Sul were higher than Canoas. Higher PAH concentrations in Sapucaia do Sul had been reported in

other studies for $PM_{2.5}$ (Teixeira et al., 2012, 2013), confirming the influence by mobile sources, especially heavy-duty vehicles (diesel engines). Table 2 shows the comparison of concentrations of $PM_{1.0}$ and ∑PAHs, analyzed for winter and summer during the study period in the sampling sites. Can be observed that total PAHs and $PM_{1.0}$ mean concentrations were higher in winter, for both sites. Particulate phase PAHs dominate in winter has been reported in several studies (Barrado et al., 2013; Callén et al., 2013; Li et al., 2006; Duan et al., 2007; Ma et al., 2010; Okuda et al., 2010; Pengchai et al., 2009; Teixeira et al., 2013), being the latter study conducted in the same study area.

Student's *t*-test for equal means was applied to compare $PM_{1.0}$ and total PAHs concentrations in winter and summer. For $PM_{1.0}$, the test showed significance difference between winter and summer means. $PM_{1.0}$ mean concentration in winter was significantly higher at a confidence level of 98.76% for Sapucaia do Sul (Sapucaia: P value = 0.00063) and 99.04% for Canoas (P value = 0.00961). PAHs mean concentration in winter for Sapucaia do Sul was significantly higher at a confidence level of 99.94% (P value = 0.01244) and 96.60% (P value = 0.03398) for Canoas. This shows that mean concentrations of $PM_{1.0}$ and PAHs in winter were significantly higher for both sites. The total PAHs concentration in winter was 1.94 times higher in Sapucaia do Sul and 1:53 times higher in Canoas. The $PM_{1.0}$ concentrations was 1.30 times higher in Sapucaia do Sul and 1:35 times higher in Canoas. This reveals, in part, the influence of seasonality of PAHs associated with $PM_{1.0}$ in the study area. In winter the primary emissions and stable atmospheric conditions affects the particle concentrations (Di Filippo et al., 2010). In relation to PAH concentrations, the possible reasons are that emissions increase (more traffic), dispersion of pollutants decreases due to adverse meteorological conditions, and photochemical degradation of PAHs due to ozone and NO_x reactions is reduced (Chirico et al., 2007), also higher condensation/adsorption of PAHs in suspended particles in the air at lower temperatures (Ravindra et al., 2006). At summer, there is a great vehicular traffic reduction near the study area due to the holiday period.

These results were also compared with the $PM_{1.0}$ and ΣPAHs concentrations obtained in different areas reported around the world (Table 2). It can be seen that the mean concentration of $PM_{1.0}$ in winter in Sapucaia do Sul and Canoas was, practically, lower than those reported in winter in Table 2, as well as the mean concentrations of ΣPAHs. The $PM_{1.0}$ concentrations in summer showed almost similar values with other studies (Table 2), except China, a location that had the highest concentrations in winter and summer. The main contributor in this location (Hong Kong) is vehicle exhaust (~38%), followed by secondary aerosols (~22%) and others (Cheng et al., 2011). The ΣPAH concentrations in summer were closer between Sapucaia do Sul and Czech Republic (2010).

In Fig. 2a,b the mean concentrations of each PAH in winter and summer can be observed. As shown in Fig. 2a,b, the winter PAHs concentrations were higher for mostly all PAHs, especially for higher molecular weight PAHs. The Low molecular Weight (LMW) PAHs are released in a vapor phase into the environment, while High Molecular Weight (HMW) PAHs containing five or more rings are adsorbed on to suspended particulate matter (Lee and Vu, 2010). The study by Martins et al. (2012) also showed similar results in a bus station marked by diesel emissions, in which the concentrations of DbA and Ind were predominant. The results of the present study is in agreement with data reported previously in the work of Teixeira et al. (2013) that also showed higher levels of HMW PAHs during the winter season. These can be explained by the lower boundary layer due to low temperatures, thereby restricting the mixing of pollutants in the atmosphere (Li et al., 2006). Other possible reason is that low temperatures made favorable conditions for the condensation/adsorption of these PAHs, especially HMW PAHs, on suspended particles present in air (Ravindra et al., 2006). However, in summer there is less emission originating from mobile sources. Another cause is the intensity of solar radiation in summer, which favors photolysis, chemical degradation processes (reactions with O_3, OH, NO_2) and volatility (Saarnio et al., 2008).

Fig. 3 shows the monthly mean concentrations of ΣPAHs and ambient temperature in Sapucaia do Sul and Canoas in the study period. It is observed that the concentrations of ΣPAHs were higher in the winter months (for the two seasons), while ambient temperatures were lower. This corroborates the seasonality of the concentrations of PAHs and their relation to ambient temperature. At lower temperatures (in winter) there is increased sorption of PAHs in the atmospheric particles, as a result of reduced vapor pressure and/or shifting in the gas/particle distribution induced by ambient temperature variation (Ravindra et al., 2008). In summer, low concentrations may be due to the temperature depended distribution of the more volatile species, and/or to the greater photolytic and thermal decomposition of the most active PAH (Křůmal et al., 2013).

Table 2
Comparison of concentrations of $PM_{1.0}$ and ∑PAHs, in winter and summer, in this study and different areas reported around the world.

	$PM_{1.0}$ (μg m^{-3})	∑16PAHs (ng m^3)	Sampler	Location/source type	Reference
Canoas (This study)	8.60 (summer) 11.62 (winter)	1.32 (summer) 2.02 (winter)	PM162M	Roadside/traffic	This study
Sapucaia do Sul (This study)	13.47 (summer) 17.50 (winter)	1.57 (summer) 3.05 (winter)	PM162M	Urban Road/traffic	This study
Zabrze (Poland)	38.84 (winter)	46.35 (winter)	Impactor Dekati PM10	Urban road/traffic	Klejnowski et al., 2010
Brno (Czech Republic)	19.9 (winter 2009) 33.4 (winter 2010) 13.2 (summer 2009) 12.9 (summer 2010)	22.2 (winter 2009) 39.8 (winter 2010) 5.01 (summer 2009) 1.68 (summer 2010)	High-volume sampler DHA-80 Digitel	Urban road/traffic	Křůmal et al., 2013
Šlapanice (Czech Republic)	19.2 (winter 2009) 35.1 (winter 2010) 13.2 (summer 2009) 11.6 (summer 2010)	21.0 (winter 2009) 38.7 (winter 2010) 5.41 (summer 2009) 1.52 (summer 2010)	High-volume sampler DHA-80 Digitel	Urban/traffic	Křůmal et al., 2013
Lahore (Pakistan)	52 (winter 2007)	–	GRIMM Aerosol Spectrometer	Urban road/traffic	Colbeck et al., 2011
Birmingham (U.K.)	12.0 (May 2004–May 2005)	–	Partisol-Plus Model 2025 Sequential Air Sampler	Urban roadside	Yin and Harrison, 2008
Hong Kong (China)	52.9 (winter) 34.8 (Summer)	–	URG3000ABC Sampler	Roadside/traffic	Cheng et al., 2011

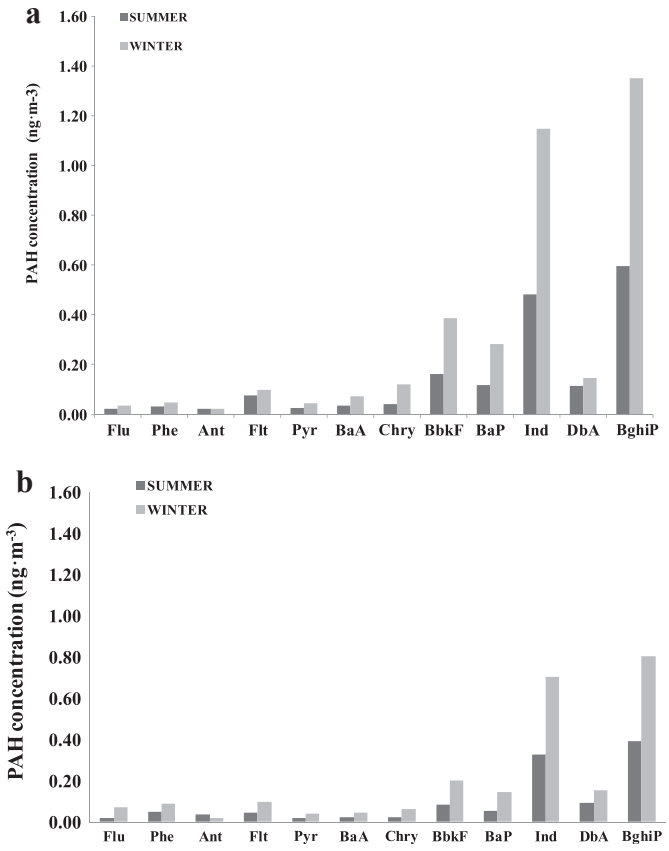

Fig. 2. a,b. Mean concentration of each PAH in winter and summer in Sapucaia do Sul (a) and Canoas (b).

3.2. $PM_{1.0}$ and polycyclic aromatic hydrocarbons correlations with meteorological parameters and other pollutants

Table 3a–c shows the Pearson's correlation matrix between ∑PAHs, $PM_{1.0}$ and other pollutants: PM_{10}, NO, NO_2 and O_3, with meteorological parameters. $PM_{1.0}$ shows a significant negative correlation with wind speed for the two sites: Sapucaia do Sul and Canoas (Table 3a). Elevated wind speed favors the dispersion of atmospheric particulate matter, being the wind turbulence along with a large mixing height causes a dilution and better dispersion of atmospheric particles (Massey et al., 2012). By the wind action the fine and ultrafine particles can be transported long distances. This was verified by Agudelo-Castañeda et al. (2013) conducted in the same study area and by other authors (Cheng et al., 2011; Krumal et al., 2013). $PM_{1.0}$ also showed positive correlation with relative humidity (Table 3a), that may be attributed, possibly, to the influence of clean free tropospheric air masses (Elminir, 2005). Furthermore, it can be seen in Table 3a negative correlation of $PM_{1.0}$ with ambient temperature and solar radiation. The dependence (inverse correlation) of temperature and solar radiation with $PM_{1.0}$ may be due to its association with stagnation and cold fronts (Tai et al., 2010). In winter, these moments are characterized by lower wind speed, greater relative humidity and less solar radiation. Moreover, high temperatures in the summer, the elevated solar radiation and low humidity produce dry particles, thus contributing less to increase in their mass concentrations (Massey et al., 2012). As explained above, carbonaceous are major components in ultrafine particles as carbonaceous soot particles are strong absorbers of solar radiation causing heating of the particles (Gaffney et al., 2009). Was also obtained positive correlation of $PM_{1.0}$ with NO, indicating, probably, that these compounds have similar emission sources.

Concentrations of ΣPAHs showed positive correlation with relative humidity, however, negative with solar radiation and ambient temperature. Also, ΣPAHs showed correlation with NO, however negative with O_3 (Table 3a). In Table 3b,c can be observed the Pearson 's correlation matrix between individual PAHs and meteorological parameters and other pollutants : PM_{10}, NO, NO_2 and O_3 for Sapucaia do Sul and Canoas sites. It can be observed that the PAHs isomers also showed a similar pattern with the ΣPAHs for the two study sites (positive correlation with relative humidity and negative with solar radiation and temperature). The negative correlation with solar radiation evidence the loss process by photolysis of PAHs associated with atmospheric particles. The PAHs degradation by photolysis depends on the intensity of light, temperature and solar radiation and the nature of the particle surface, including the presence and composition of an organic layer in the aerosol (Arey, 1998). In the formation of carbonaceous particles as a byproduct of the combustion, PAHs are considered the main molecular intermediates for soot formation and growth. Carbonaceous are major components in ultrafine particles, constituting, for example, ~45.7% of $PM_{1.0}$ in roadside environments, where vehicular emissions are a major source, too (Lee et al., 2006). The soot

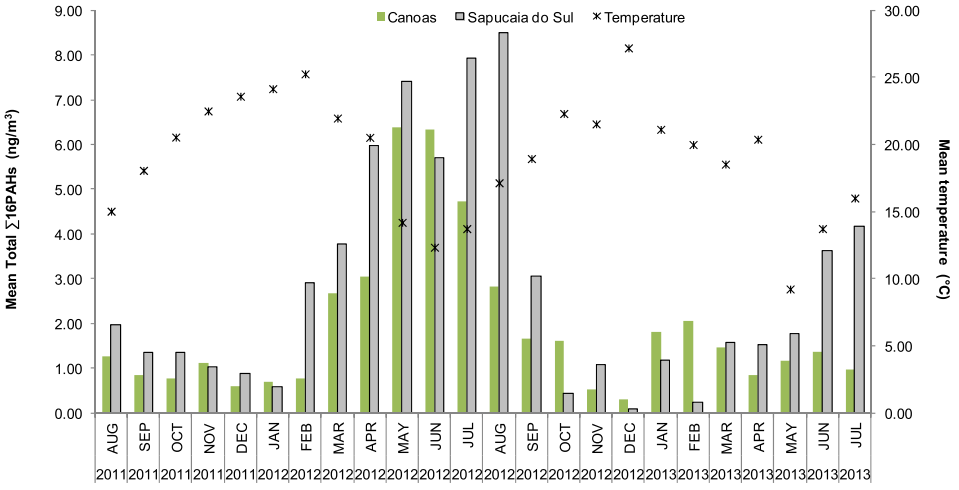

Fig. 3. Monthly mean concentrations of ∑PAHs and Ambient Temperature in Sapucaia do Sul and Canoas in the study period.

Table 3a
Pearson's correlation matrix between ∑PAHs, $PM_{1.0}$ and meteorological parameters and other pollutants: PM_{10}, NO, NO_2 and O_3.

	Wind speed (m/s)	Relative humidity (%)	Radiation (w m^{-2})	NO (μg m^{-3})	NO_2 (μg m^{-3})	O_3 (μg m^{-3})	Ambient temperature (°C)
Sapucaia do Sul – PAHs	−0.256**	0.233*	−0.294**	0.239*	−0.124	−0.338**	−0.203*
Sapucaia do Sul – PM_1	−0.246*	0.198*	−0.226*	0.338**	0.020	−0.245*	−0.133
Canoas – PAHs	−0.099	0.243*	−0.228*	0.262*	−0.001		−0.208*
Canoas – PM_1	−0.352**	0.249*	−0.213*	0.286**	0.095		−0.200*

PM_{10} and O_3data were available only for Sapucaia do Sul.
* Significant at the 0.05 level (2-tail).
** Significant at the 0.01 level (2-tail).

nuclei grow through several chemical reactions, reaching diameters larger than 10 nm, at which point they begin coagulating and consequently, their rapid growth due to surface reactions (Seinfeld and Pandis, 2006). The correlation of PAHs with solar radiation, probably, was not higher because the carbonaceous material apparently protect the PAH from photolysis. The PAH degradation by O_3 may also occur under this condition, such that the PAHs is protected, not being on the surface and available for reaction. Accordingly, a negative correlation of O_3 with ΣPAHs was obtained (Table 3).

PAHs negative correlation with temperature indicates that at low temperatures the adsorption of PAH increases (Ravindra et al., 2006; Masiol et al., 2013). However, Ant showed a different pattern, showed no correlation with radiation for Sapucaia do Sul and Canoas. However, this isomer showed a positive correlation with the wind speed at Canoas site (the prevailing direction is E–SE, while in fall and winter, besides E–SE winds, winds from W and NW also occur). This can be attributed to the transport of Ant in the aged particles originating from emissions of the coal-fired power plants located near the study area (about 60 km), and can easily be degraded during their transport (Yang et al., 2010). This may also explain the lack of correlation of this pollutant with NO, O_3 and ambient temperature.

The positive correlation of relative humidity with the concentration of ΣPAHs could be due to the depositional effect on the particulate matter of PAHs in the gas phase as a consequence of environmental humidity (Mastral et al., 2003). The works of Yang et al. (2013) and Mastral et al. (2003) have explained that this meteorological parameter influences the concentration of PAHs in the environment, possibly, because the gas/particle partition of PAHs depends, partially, on the relative humidity (Mastral et al., 2003; Ravindra et al., 2008). .

The positive correlation of ΣPAHs and the concentration of each isomer with NO indicate, probably, that these compounds have similar emission sources. This reveals that the concentrations of PAHs associated with $PM_{1.0}$ can be oxidized by NO (Ringuet et al., 2012; Teixeira et al., 2011) or originate from the same source or mixed sources occurring at the same time. The DbA showed a different pattern, having no correlation with pollutant NO.

3.3. Analysis of PAHs emission sources using diagnostic ratios

In the present work, the following diagnostic ratios were selected: Flu/(Flu + Pyr), [Flt/(Flt + Pyr)], [Ind/(Ind + BghiP)], [BaA/(BaA + Chry)], [Phe/(Phe + Ant)], [BaP/BghiP], [BaP/(BaP + Chry)], [Flu/(Flu + Pyr)]. These ratios should be evaluated with caution, due to the fact that PAHs are emitted by a variety of sources, and their profiles can change by its reactivity (Ravindra et al., 2008). The ratio can be altered due to the reactivity of some PAH species with other atmospheric species, such as ozone and/or oxides of nitrogen. Emission profiles of PAHs can be affected by fuel chemical composition and test cycle (Westerholm and Li, 1994; Mi et al., 2000). In addition, atmospheric PAH profiles can be affected by meteorological variables such as UV light and temperature; furthermore half-lives of these compounds in the atmosphere vary (De Martinis et al., 2002; WHO, 1998). Despite these facts, some authors consider the ratios between some of these compounds as "fingerprints" of emission sources (Khalili et al., 1995; Li and Kamens, 1993).

Table 4 presents a comparison of mean diagnostic ratios of PAH in $PM_{1.0}$ of Sapucaia do Sul and Canoas. Previous studies have estimated that, in urban areas, the major emission sources of PAHs are originated from vehicular traffic (Gunawardena et al., 2012; Lee et al., 1995; Lim et al., 1999).

The ratio [Flt/(Flt + Pyr)], was 0.71 and 0.75 for Sapucaia do Sul and Canoas, respectively, values within the range reported by other studies (0.6–0.7) indicating emissions from vehicular sources with diesel engines (Sicre et al., 1987; Ravindra et al., 2008). The proximity of the sampling to the BR-116 highway, characterized by having an intense vehicular traffic, especially of heavy-duty vehicles using diesel (Teixeira et al., 2012), characterize the influence of these emission sources. Pyr adsorbes on diesel particles reacts faster with NO_2, but with OH radicals the reaction rates are the same (Esteve et al., 2004, 2006). According to some studies, among which we cite Esteve et al. (2004, 2006), Perraudin et al. (2007) and Bedjanian et al. (2010), Pyr is more reactive than Flu.

Tobiszewski and Namieśnik (2012) reported that the diagnostic ratios do not change with particle size and Wang et al. (2006) show that diagnostic ratios are virtually the same in samples of $PM_{2.5–10}$ and $PM_{2.5}$ [Flt/(Flt + Pyr)], BaP/(BaP + Chry) and [Phe/(Phe + Ant)] ratios studied at the same sites, were calculated for coarse fraction (2.5 and 10) (Teixeira et al., 2012) showing lower PAH diagnostic ratios than fine particles. Isto pode-se dizer que estes diagnostic ratios do change with particle size. BaP is easily decomposed by light and oxidants (Alves et al., 2012). Heterogeneous reactions of BaP adsorbed on diesel particles with nitrogen oxides are more rapid.

According to Ravindra et al. (2008), Pyr/BaP ratios close to unity are characteristic of gasoline and influence around 10 are typical of diesel influence. The mean Pyr/BaP ratio was 0.43 in Sapucaia South and 0.56 in Canoas, respectively (Table 4). These ratios can be compared to those reported in the literature for the contribution of fuel combustion such as gasoline (Ravindra et al., 2008).

[Ind/(Ind + BghiP)] ratio was 0.45 in Sapucaia do Sul and 0.44 in Canoas indicating that the PAHs produced were from the emission of diesel vehicles. The literature reported values of 0.35–0.70, 0.56 and 0.62 in [Ind/(Ind + BghiP)] for diesel-engines, coal and wood burning, respectively (Grimmer et al., 1983; Rogge et al., 1993; Kavouras et al., 2001; Ravindra et al., 2006). However, some authors (Ravindra et al., 2006) reported the value of 0.56 as coal combustion. Nevertheless, Fig. 4a also shows uniform values of the ratios Ind/(Ind + BghiP) indicating the diesel emissions as a source and the influence of coal power plants, as mentioned earlier. Ind and BghiP photolytically degrade at comparable rates (Yang et al., 2010), thus their ratios preserve the original compositional information during atmospheric transport. The HMW PAH diagnostic

Table 3b
Pearson's correlation matrix between individual PAHs and meteorological parameters and other pollutants: PM_{10}, NO, NO_2 and O_3 for Sapucaia do Sul site.

	Flu	Phe	Ant	Flt	Pyr	BaA	Chry	BbkF	BaP	Ind	DbA	BghiP	WS	RH	RAD	NO (μg m^{-3})	NO_2 (μg m^{-3})	O_3·(μg m^{-3})	TEMP
Flu	1	0.502**	0.174	0.504**	0.569**	0.537**	0.606**	0.560**	0.581**	0.467**	0.407**	0.501**	−0.379**	0.304**	−0.315**	0.199*	−0.044	−0.544**	−0.144
Phe		1	0.139	0.746**	0.729**	0.553**	0.677**	0.668**	0.474**	0.588**	0.465**	0.680**	−0.085	0.310**	−0.288**	0.304*	−0.129	−0.054	−0.338**
Ant			1	0.374**	0.308**	0.345**	0.354**	0.352**	0.399**	0.357**	0.421**	0.355**	−0.214*	−0.221*	−0.017	−0.199	−0.351**	−0.020	0.037
Flt				1	0.798**	0.677**	0.787**	0.774**	0.726**	0.866**	0.829**	0.889**	−0.193*	0.306**	−0.235*	0.222*	−0.185	−0.250*	−0.238*
Pyr					1	0.870**	0.915**	0.867**	0.857**	0.691**	0.680**	0.732**	−0.187*	0.376**	−0.262**	0.262*	−0.109	−0.217	−0.291**
BaA						1	0.883**	0.810**	0.811**	0.576**	0.717**	0.643**	−0.223*	0.470**	−0.340**	0.337**	−0.097	−0.184	−0.398**
Chry							1	0.900**	0.899**	0.761**	0.733**	0.791**	−0.265**	0.461**	−0.382**	0.343**	−0.029	−0.297**	−0.378**
BbkF								1	0.899**	0.775**	0.771**	0.816**	−0.303**	0.342**	−0.299**	0.313**	−0.119	−0.326**	−0.314**
BaP									1	0.732**	0.674**	0.779**	−0.222*	0.371**	−0.329**	0.308**	−0.095	−0.309**	−0.287**
Ind										1	0.820**	0.949**	−0.248**	0.242**	−0.261**	0.229*	−0.104	−0.231*	−0.249**
DbA											1	0.824**	−0.253*	0.345**	−0.253*	0.220	−0.133	−0.311*	−0.238*
BghiP												1	−0.257**	0.294**	−0.294**	0.273**	−0.128	−0.262*	−0.301**
WS													1	−0.079	0.235*	−0.131	−0.197	0.449**	0.148
RH														1	−0.452**	0.238*	0.197	−0.043	−0.292**
RAD															1	−0.397**	−0.281**	0.093	0.530**
NO (μg m^{-3})																1	0.637**	−0.076	−0.505**
NO_2·(μg m^{-3})																	1	−0.171	−0.258*
O_3·(μg m^{-3})																		1	−0.074
TEMP																			1

* Significant at the 0.05 level (2-tail), ** Significant at the 0.01 level (2-tail). WS: Wind speed (m s^{-1}); RH: Relative Humidity (%); RAD: Radiation (w m^{-2}); TEMP: Ambient temperature (°C).

Table 3c
Pearson's correlation matrix between individual PAHs and meteorological parameters and other pollutants: PM_{10}, NO, NO_2 and O_3 for Canoas site.

	Flu	Phe	Ant	Flt	Pyr	BaA	Chry	BbkF	BaP	Ind	DbA	BghiP	WS	RH	RAD	NO (μg m^{-3})	NO_2 (μg m^{-3})	TEMP
Flu	1	0.840**	−0.038	0.101	0.555**	0.274*	0.550**	0.567**	0.548**	0.405**	0.448**	0.415**	−0.205	0.265*	−0.259*	0.287*	0.108	−0.258*
Phe		1	0.329**	0.070	0.734**	0.603**	0.719**	0.690**	0.662**	0.450**	0.319**	0.478**	−0.156	0.233*	−0.242*	0.326**	0.032	−0.212*
Ant			1	0.050	0.254**	0.493**	0.175	0.211*	0.070	0.072	−0.031	0.092	0.198*	−0.094	0.088	−0.125	−0.241*	0.060
Flt				1	0.208*	0.220*	0.210*	0.237*	0.228*	0.308**	0.371**	0.298**	0.038	0.318**	−0.363**	0.248*	0.165	−0.321**
Pyr					1	0.765**	0.730**	0.683**	0.626**	0.390**	0.296**	0.443**	−0.005	0.434**	−0.275**	0.360**	−0.053	−0.222*
BaA						1	0.814**	0.818**	0.763**	0.573**	0.402**	0.624**	0.095	0.451**	−0.198*	0.253*	−0.138	−0.281**
Chry							1	0.951**	0.948**	0.780**	0.628**	0.815**	−0.099	0.400**	−0.287**	0.359**	0.030	−0.313**
BbkF								1	0.967**	0.833**	0.670**	0.861**	−0.063	0.346**	−0.265**	0.357**	0.021	−0.385**
BaP									1	0.849**	0.704**	0.872**	−0.131	0.379**	−0.294**	0.325**	0.063	−0.354**
Ind										1	0.875**	0.990**	−0.113	0.259**	−0.252**	0.253*	0.146	−0.342**
DbA											1	0.856**	−0.145	0.120	−0.240*	0.182	0.148	−0.230*
BghiP												1	−0.099	0.235*	−0.261**	0.268*	0.117	−0.347**
WS													1	−0.248**	0.155	−0.031	−0.192	−0.075
RH														1	−0.626**	0.174	0.140	−0.322**
RAD															1	−0.414**	−0.319**	0.476**
NO·(μg m^{-3})																1	0.618**	−0.551**
NO_2·(μg m^{-3})																	1	−0.379**
TEMP																		1

* Significant at the 0.05 level (2-tail), ** Significant at the 0.01 level (2-tail). WS: Wind speed (m s^{-1}); RH: Relative Humidity (%); RAD: Radiation (w m^{-2}); TEMP: Ambient temperature (°C).

Table 4
Comparison of mean diagnostic ratios of PAH in $PM_{1.0}$ obtained for the MAPA and the main emission sources.

Ratios	Sapucaia do Sul	Canoas	Value	Sources	References
[Flt/(Flt + Pyr)]	0.71	0.75	<0.4	Petrogenic	De La Torre-Roche et al., 2009
			0.4–0.5	Liquid fossil fuel combustion	
			>**0.5**	Coal/biomass combustion	
[Ind/(Ind + BghiP)]	0.45	0.44	**0.35–0.70**	Diesel-engines	Rogge et al. (1993), Grimmer et al. (1983),
			0.56	Coal	Kavouras et al. (2001), Ravindra et al. (2006)
			0.62	Wood burning	
[BaA/(BaA + Chry)]	0.53	0.44	0.48	Coal/coke combustion	Sicre et al. (1987)
			0.46	Wood combustion	Schauer et al. (2001) Fine et al. (2001)
			0.33–0.38	Gasoline	Li and Kamens (1993), Rogge et al. (1993)
			0.38–0.65	Diesel	Kavouras et al. (2001), Sicre et al. (1987), Simcik et al. (1999)
[Phe/(Phe + Ant)]	0.61	0.64	>**0.7**	Lubricant oils and fossil fuels	Alves et al. (2001)
[BaP/BghiP]	0.83	0.16	**0.86**	Diesel	Manoli et al. (2004)
			<0.6	Gasoline	Pandey et al. (1999)
[BaP/(BaP + Chry)]	0.69	0.71	0.5	Diesel	Guo et al. (2003)
			0.73	Gasoline	Khalili et al. (1995)
[Flu/(Flu + Pyr)]	0.28	0.32	>0.5	Diesel	Fang et al. (2004), Tsapakis et al. (2002),
			<**0.5**	Gasoline	Ravindra et al. (2006), Mandalakis et al. (2002)
[Pyr/BaP]	0.43	0.56	~10	Diesel engine	Ravindra et al. (2008)
			~**1**	Gasoline engine	
[BghiP/Ind]	0.99	1.16	**1.1**	Diesel	Schauer et al. (1999, 2001,2002)
			3.5	Gasoline	
			0.8	wood	
[BaA/BaP]	0.61	0.62	**0.5**	Gasoline exhaust	Li and Kamens (1993); Khalili et al. (1995)
			1.0	Diesel exhaust	
			1.0	Wood Combustion	

ratio, Ind/(Ind + BghiP), is reported as being less influenced by reactivity than LMW PAH diagnostic ratios (Zhang et al., 2005), as these PAH are relatively stable (Alam et al., 2013), thus the diagnostic ratio will not be influenced too. In fact, most of the HMW PAH remains in fine particles (Fang et al., 2004; Wu et al., 2013).

The mean ratio [BaA/(BaA + Chry)] was 0.53 and 0.44 for Sapucaia do Sul and Canoas, respectively, being that these values are within the limits of the studies of Sicre et al. (1987), Simcik et al. (1999) and Kavouras et al. (2001), revealing strong influence of diesel vehicles. For Canoas, the mean ratio [BaA/(BaA + Chry)] is closer to the value 0.46 for wood combustion (Fine et al., 2001; Schauer et al., 2001). Fig. 4a shows the scatter ratio–ratio plot for BaA/(BaA + Chry) and Ind/(Ind + BghiP). The results of the BaA/(BaA + Chry) ratios show that most of the values obtained were in the range of 0.38–0.65, thus indicating diesel emissions (Kavouras et al., 2001; Sicre et al., 1987; Simcik et al., 1999). Though, some values were close to other ratio values various sources, this will be better discussed in the item PMF analysis.

The diagnostic ratio [Phe/(Phe + Ant)] has been used to identify petrogenic hydrocarbons, values >0.7 are typically associated with lubricant oils and fossil fuels (Alves et al., 2001). The mean value was 0.61 and 0.64 for Sapucaia and Canoas, respectively. Although the mean ratios were not >0.7, their values are close (Fig. 4b). Phenanthrene has been evidenced as an important PAH derived from lubricant oils and burning fossil fuels in the MAPA, as observed in other cities in Latin America (Sienra et al., 2005). PAHs are most likely to accumulate in lubricating oil during combustion process in engine over time, although that the dominant source of PAHs in the emissions is expected to be from the fuel (Kleeman et al., 2008; Russel, 2013). However, Phe can also be originating from petrogenic sources like unburned petroleum. This part will be detailed in the following item: PMF analysis. Must be used with caution this ratio, by the fact that its value can be altered by the degradation of Ant during transportation due to their higher reactivity (Yang et al., 2010). Ding et al. (2007) reported that a lower ratio, due to Ant, is reflective of more aged PAHs, reflecting data from the present study.

Similarly, the mean of the [BaP/(BaP + Chry)]ratio, used to estimate the vehicular contribution, was 0.69 and 0.71 for Sapucaia do Sul and Canoas, respectively. These values are close to 0.73 (Fig. 4b) indicating the influence of emissions from gasoline vehicles (Khalili et al., 1995; Guo et al., 2003).

The diagnostic ratio [BaP/BghiP], in this study, was 0.83 for Sapucaia do Sul and 0.16 for Canoas, indicating influence of emission of vehicular sources using diesel and gasoline engines, respectively (Manoli et al., 2004; Pandey et al., 1999).

In the same way, the means of [Flu/(Flu + Pyr)] ratio (Table 4), (0.28–0.32), compared with those reported in the literature (Mandalakis et al., 2002; Tsapakis et al., 2002; Fang et al., 2004; Ravindra et al., 2006) indicated the influence of light and heavy-duty vehicular sources for Sapucaia do Sul and Canoas.

Li and Kamens (1993) and Khalili et al. (1995) publicated that the [BaA/BaP]ratio was 0.5 for gasoline exhaust, 1.0 for diesel exhaust and 1.0 for wood combustion. The mean [BaA/BaP]ratio for both sites were similar: 0.61 in Sapucaia do Sul and 0.62 in Canoas, indicating gasoline exhaust contribution. Also, the [BghiP/Ind] ratio of 0.99 and 1.16 for Sapucaia do Sul and Canoas, respectively, indicated gasoline exhaust contribution (Schauer et al., 2002).

Consequently, the results showed that the principal emission source of PAHs associated with $PM_{1.0}$ in the study area was the engine combustion: of diesel and of gasoline. The emissions of mobile sources must be evaluated with caution, because they are function not only of the type of fuel, but also of the vehicle age, maintenance and capacity of the engine, vehicle model and if the vehicle has been heated. For example, the emissions from vehicles using diesel are significantly higher than vehicles using gasoline. Also, the majority of PAHs in diesel exhaust will result from PAHs in the fuel surviving the combustion process and only ~20% of the emitted PAHs result from pyrosynthesis or combustion of lubricating oils. However, combustion within petrol engines appears to result in a high proportion of the fuel PAHs being destroyed, with $\geq$50% of emitted PAHs being formed during the combustion process (Howsan and Jones, 2010).

3.4 PMF analysis

The determination of number of factors in PMF is an important process and depends on the goodness of fit to the original data and

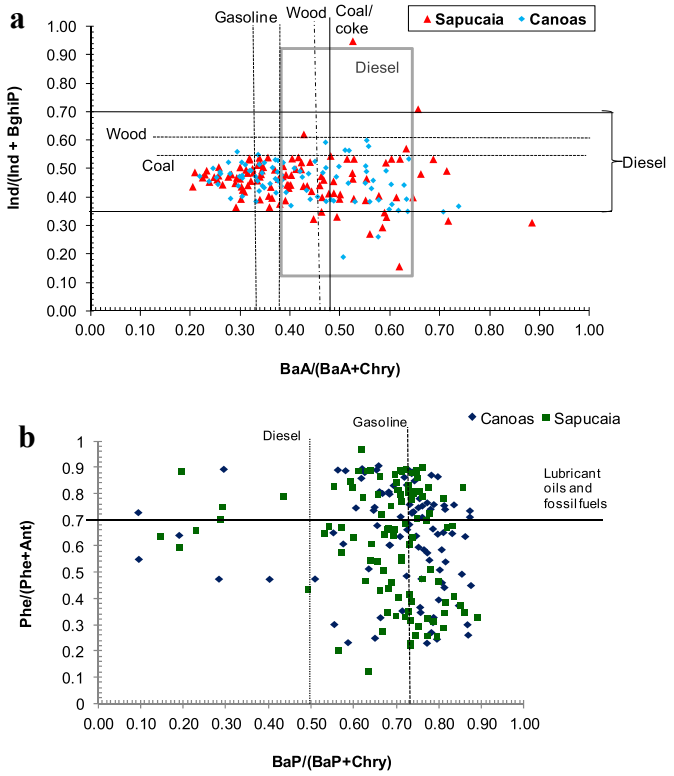

Fig. 4. a,b. Scatter ratio–ratio plot for BaA/(BaA + Chry) and Ind/(Ind + BghiP); Phe/(Phe + Ant) and BaP/(BaP + Chry). For the meaning of the abbreviations see Section 3.2.

physically realistic results. The *Q* value analysis indicates the agreement of the model fit (Comero et al., 2009) and the r^2 value indicates the correlation between measured and estimated concentrations (Wang et al., 2009). These values can help to determine the best number of factors to be chosen for modeling. *Q* theoretical is considered to be a good starting point for solution interpretation (Reff et al., 2007). The theoretical value of *Q* was calculated using Equation (3). 30 runs were made for each sampling site using random seed mode. From the 30 runs the convergent run with the minimum *Q* value was used for the solutions presented in this study. Were calculated the *Q* values for runs using six and five factors and the results showed that either one was much better than the other. Results using six factors were chosen because they had the most meaningful results, that is the profiles can be explained by known source patterns. For Sapucaia do Sul and Canoas, *Q* theoretical values were 531 and 573, respectively. The *Q* values obtained using PMF were 550 for Sapucaia do Sul and 566 for Canoas. Values are very similar, indicating an appropriate uncertainty in the modeling input. The values of the scaled residuals were in the recommended range (−3 to +3) (Comero et al., 2009). The mean r^2 values for all PAHs was 0.95 for Sapucaia do Sul and 0.96 for Canoas, indicating a good fit between the measured and predicted concentrations.

For Canoas, after fixing the number of sources, the PMF solutions for multiple values of *F* peak parameter were explored and analyzed for rotational ambiguity (Paatero et al., 2002). Was plotted the factor contributions from the PMF analysis for each factor against each other and adjusted *F* peak values until the edges in the plots become parallel to the plot axes (Reff et al., 2007). The *F* peak value of −0.1 was chosen as it does not increased the *Q* value dramatically (less than a 100 units). *Q* value was 560 for Canoas. For Sapucaia do Sul, was chosen an *F* peak = 0. The contributions and profiles did not change noticeably. Profiles obtained from the PMF model are in Table 5.

Each profile obtained by PMF in this study was compared with several profiles reported by previous works. The identified sources in this study were vehicular traffic, diesel and gasoline exhaust, coal combustion, wood combustion and incomplete combustion/unburned petroleum.

The profile of factor 1 in Canoas and Sapucaia do Sul showed BghiP and Ind with dominant concentrations. This profile was attributed to gasoline emissions (Schauer et al., 2002; Rogge et al., 1993). Zielinska (2005) previously identified these PAHs as effective markers of gasoline exhaust because they are emitted at higher concentrations than diesel exhaust and are not present in fresh lubricant oil. The contribution of gasoline engines emissions of Sapucaia do Sul was lower (17%) than in Canoas (19%). This emission source is in agreement with the item “4.3 Analysis of PAHs emission sources using diagnostic ratios” and in earlier studies (Teixeira et al., 2011).

The profile of factor 2 of Sapucaia do Sul and profile of factor 4 of Canoas, presented the following PAHs: Ant, Ind and BghiP. These two profiles had a contribution of 10% and 9% for Sapucaia do Sul and Canoas, respectively. These compounds (Ant, BghiP, Ind) originate from coal combustion (Howsan and Jones, 2010). This source was identified in the item “4.3 Analysis of PAHs emission sources using diagnostic ratios” and previous works conducted in the same study area: Teixeira et al. (2012, 2013). Teixeira et al. (2013) reported the contribution of this source of 9% in Sapucaia do Sul, similar to the value obtained in the present study. The coal combustion was not the main source of PAHs in the study area, although it accounted for 9–10% of the total emissions in the studied sites. This is, probably, due to the location of the two Coal Power Plants which are 60 km away from the study area. The burning of coal used in the power plants is Responsible for the luminescence of PAHs not only due to an incomplete combustion, but also due to the degradation of the fuel molecules (Dallarosa et al., 2005b).

The profile of factor 3 explained 25% of the sum of the measures PAHs in Sapucaia do Sul site. This profile had high dominance of HMW PAHs: BbkF, BaP, Ind and BghiP. This dominance was also observed in profile of factor 2 Canoas. This profile accounted for 22% of the sum of the PAHs. This profile was identified as emissions of diesel vehicles. Diesel- powered vehicles emissions have a similar profile to gasoline, but with higher ratios of BbkF (Howsan and Jones, 2010). The LMW PAHs may originate from diesel fuel that escapes combustion and diesel exhaust particulate, which are derived from unburned fuel and from engine lubricating oil (Miguel et al., 1998). The majority of particulate matter in diesel exhaust is composed of fine particles that are primarily formed from the condensation of organic matter on an elemental carbon core, which are generally called soot particles (Portet-Koltalo and Machour, 2013). Distribution of this profile in the two study sites is similar, but in Sapucaia do Sul their contribution was higher. This contribution has been obtained in previous studies (Teixeira et al., 2013) for particulate matter <2.5 μm.

The profile of factor 4 of Sapucaia do Sul had dominance of Flu, Phe and Flt, similar to factor 5 of Canoas site. This profile had dominance of mainly PAHs of LMW, indicating the compounds of incomplete combustion and unburned petroleum (Park et al., 2011; Ho and Lee, 2002). Incomplete combustion/unburned petroleum was found to be the second main source of PAH emissions in the study area, with a contribution of 21% (Sapucaia do Sul) and 23% (Canoas). Several studies have attributed high loadings of Phe to unburned petroleum and its association with LMW PAHs (Jang et al., 2013; Park et al., 2011). The presence of these compounds in this profile might be explained by emission from unburned

Table 5
Factor profiles (Percentage of factor total − %) generated by PMF for Sapucaia do Sul and Canoas site.

PAH	Sapucaia do Sul						Canoas					
	Factor 1	Factor 2	Factor 3	Factor 4	Factor 5	Factor 6	Factor 1	Factor 2	Factor 3	Factor 4	Factor 5	Factor 6
Flu	–	–	0.26	17.6	–	–	0.06	–	0.22	0.29	19.1	0.16
Phe	1.37	4.79	–	41.4	6.17	–	2.08	0.18	2.49	2.16	33.1	13.4
Ant	–	18.6	0.24	–	3.94	–	0.70	0.03	0.59	28.4	2.80	1.99
Flt	3.36	4.78	0.96	10.2	6.92	3.11	4.04	0.58	3.13	6.61	11.6	11.0
Pyr	0.49	0.84	1.12	3.18	8.57	1.36	0.54	1.42	0.40	0.79	2.55	12.9
BaA	–	0.01	1.53	0.40	13.0	5.93	0.12	2.14	0.43	1.87	1.15	14.1
Chry	1.27	–	4.43	2.98	8.45	1.37	0.93	3.19	0.86	–	2.37	7.35
BbkF	3.76	5.26	19.5	–	14.8	14.6	2.51	21.6	3.96	6.59	2.23	4.58
BaP	0.84	4.70	14.6	6.27	6.35	8.94	2.14	14.8	2.53	–	2.23	4.64
Ind	43.3	20.2	23.8	–	11.1	–	40.6	21.7	31.3	8.24	10.1	11.6
DbA	5.68	5.24	–	2.72	–	52.5	3.45	–	26.6	–	4.38	–
BghiP	39.9	35.6	33.5	15.3	20.8	12.2	42.9	34.3	27.5	45.1	8.48	18.3
	Gasoline	Coal combustion	Diesel	Incomplete combustion/ unburned petroleum	Wood combustion	Vehicular[a]	Gasoline	Diesel	Vehicular[a]	Coal combustion	Incomplete combustion/ unburned petroleum	Wood combustion
Contribution	17%	10%	25%	21%	15%	12%	19%	22%	12%	9%	23%	15%

[a] Mixed vehicular combustibles.

diesel oil and gasoline (Braga et al., 2005). However, in the previous study of Teixeira et al. (2012) this source unit was also identified.

The profile of factor 5 of Sapucaia do Sul showed predominance of the following compounds: Pyr, BaA, BbkF, BghiP, BaP and Ind. The profile of factor 6 of Canoas was similar, with dominance of compounds of medium and high molecular weight: Flt, Pyr, BaA, BghiP, Ind and Phe. These two profiles had a contribution of 15% each. These two profiles were identified as of combustion of wood because of the presence, especially, of Flt, Pyr and BaA (Schauer et al., 2001). Wood was found to be the third main source. Teixeira et al. (2013) identified this source for multiple sites within the MAPA. In Table 4, the analysis of the diagnostic ratio BaA/(BaA + Chry) showed the influence of this source, confirming the results obtained. The Rio Grande do Sul (RS) state has large charcoal production, being the 8th bigger producer of charcoal in Brazil. The counties in RS that has the highest charcoal production are located in or near the study area (SEPLAG, 2013). In the state there are about 2000 kilns to produce charcoal from acacia wood, being an alternative source of income for many families within the MAPA (EMATER 2013). Most of these small kilns do not have a system of emissions control or filters. It also should be noted that wood combustion can have other purposes, such as energy production in industries, drying of grains, ceramic drying (brick), among others.

The profile of factor 6 of Sapucaia do Sul accounted for 12% of the sum of the measured PAHs. This profile had dominance of BbkF, DbA and BghiP. The profile of factor 3 of Canoas was similar, thus, additionally, with dominance of Ind. This profile 3 had a contribution of 12% in Canoas. This profile can be assigned to mixed vehicular sources at this location, due to intense vehicular traffic (Khalili et al., 1995; Larsen and Baker, 2003). High values of DbA and Ind were reported in finer particles (<0.25 μm) in studies done in Brazil in environments marked by heavy-duty vehicles using diesel/biodiesel fuel blend (Martins et al., 2012). While in the study in another city at Brazil done by Da Rocha et al. (2009), performed in environments marked by heavy-duty vehicles that use diesel or biodiesel, the higher concentrations were Chry, Pyr, BbF and BghiP. Consequently, these two profiles were identified as from vehicular emissions, for presenting PAHs typical of gasoline- and diesel, giving a mixed profile.

The results indicated a significant influence of vehicular sources, as the main source, with contributions of 54% in Sapucaia do Sul (Gasoline + Diesel + Vehicular) and 53% in Canoas (Gasoline + Diesel + Vehicular). These results can be associated to the proximity of the sampling sites with highways of intense vehicular traffic, the BR -290 highway, and principally the BR-116 highway. A large number of light and heavy-duty vehicles circulating cause a large vehicular emission. Similar results were obtained in previous studies for particles <2.5 μm and <10 μm material in the MAPA (Teixeira et al., 2012, 2013). These results can be related to the data shown in Table 4 showing the diagnostic ratios, which is characterized mainly by diesel and gasoline emissions.

3.5. Toxic equivalent factors

The toxic equivalent factors were calculated to characterize the risk of cancer from PAH exposure to $PM_{1.0}$ samples. BaPeq was calculated using Eq. (6). In Fig. 5 may be observed the BaPeq values for summer and winter in the two sampling sites: Sapucaia do Sul and Canoas. The mean BaPeq values were 0.645 ng m^3 and 0.321 ng m^3 in Sapucaia do Sul, respectively; and 0.419 ng m^3 and 0.203 ng m^3 in Canoas, respectively. May be observed (Fig. 5) clearly that the mean BaPeq toxic equivalency concentrations were found to be 3 times higher in the winter in both sites. These results were reported in previous works, such as Gaga et al. (2012).

The highest obtained value was in Sapucaia do Sul in winter (0.645 ng m^3) and the lowest in summer in Canoas (0.203 ng m^3). The relative contribution of each PAH to the BaPeq levels may be observed in Fig. 5. BaP and DahA dominated the BaPeq levels. The carcinogenicity activity contribution of BaP was in the range of 27.1% (Canoas summer) up to 44.0% (Sapucaia winter); and the contribution of DahA was of 22.7% (Sapucaia winter) up to 45.3% (Canoas summer). The contribution of Ind for the BaPeq levels was of 15.0% (Sapucaia summer) up to 17.8% (Sapucaia winter). The contribution of BaP to BaPeq levels was similar to the work of Yang et al. (2010); Amador-Muñoz et al. (2010). The obtained contribution of BaP and DahA were similar to those obtained by Teixeira et al. (2012), although the contribution of Ind was slightly higher. DahA is moderately active as a carcinogen between BaA and BaP in activity and Ind exhibits lower activity than BaP as a carcinogen (Harvey, 1991).

According to the International Agency for Research on Cancer (IARC, 2010), BaP has been classified as carcinogenic to human, DahA as probably carcinogenic to humans and Ind as possibly carcinogenic to humans; although that, of particular note is that Chry, BbF, BkF, BaP, DahA, and Ant have been found to be carcinogenic in experimental animals after inhalation or intratracheal

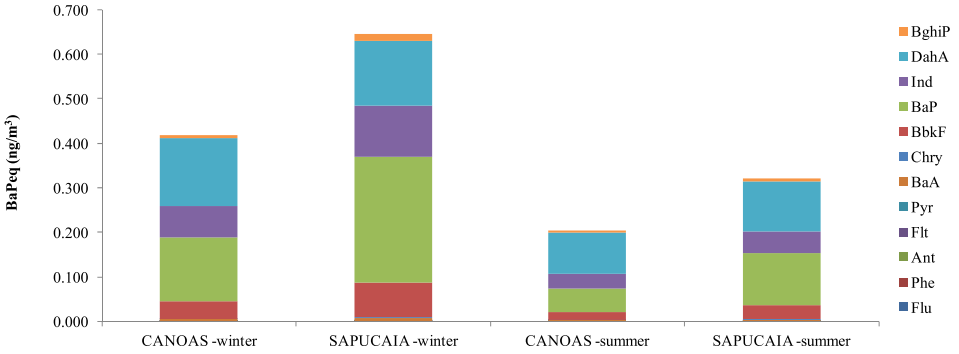

Fig. 5. BaPeq values in winter and summer at Sapucaia do Sul and Canoas.

ingestion, increasing concern about the levels of these carcinogens in ambient air (IARC, 2013). The European parliament and the council of the European Union established ambient air quality guidelines for PAHs (1.0 ng $m^{-3}$of BaP in PM_{10} fraction). This limit and the scientific publication: Air Pollution and Cancer (IARC, 2013) demonstrate the importance that these pollutants require maximum reduction and their study.

4. Conclusions

The mean concentration of total PAHs and $PM_{1.0}$ in Sapucaia do Sul were higher than those of Canoas, confirming the influence by combustion sources, mobile sources and some industrial processes.

Concentrations of PAHs associated with $PM_{1.0}$ were significantly higher in winter than in summer in the study area, particularly for higher molecular weight PAHs, thus showing a seasonal trend.

Negative correlation of $PM_{1.0}$ with wind velocity was obtained due to the fact that wind favors the dispersion of atmospheric particulate matter. In addition, a positive correlation of $PM_{1.0}$ with relative humidity was also obtained, that may be attributed possibly to the influence of clean free tropospheric air masses. The negative correlation of $PM_{1.0}$ with ambient temperature and solar radiation may be due to its association with stagnation and cold fronts. Positive correlation of PAHs with relative humidity and negative with solar radiation, temperature, O_3 and NO demonstrates the PAHs degradation by photolysis and chemical reactions with these pollutants.

Analysis of the diagnostic ratios confirmed that PAHs in $PM_{1.0}$ originate, especially, from diesel and gasoline emissions, also from wood combustion, lubricant oils and fossil fuels. PMF analysis showed the contribution of 6 sources: gasoline, diesel, mixed vehicular combustibles, wood combustion, coal combustion and incomplete combustion/unburned petroleum.

BaP and DahA dominated BaPeq levels in the study area, varying with the season. Since the previously study until the present work there has not been an increase in the contribution in the BaPeq levels of potentially carcinogenic PAHs, except for Ind. According to the IARC classification BaP is Class 1: carcinogenic to humans and DahA Class 2A: probably carcinogenic to humans, and Ind Classe 2B: possibly carcinogenic to humans.

Acknowledgments

To FAPERGS and CNPq for the financial support.

References

Agudelo-Castañeda, D.M., Teixeira, E.C., Rolim, S.B., Pereira, F.N., Wiegand, F., 2013. Measurement of particle number and related pollutant concentrations in an urban area in South Brazil. Atmos. Environ. 70, 254–262.

Agudelo-Castaneda, D.M., Teixeira, E.C., Pereira, F.N., 2014. Time–series analysis of surface ozone and nitrogen oxides concentrations in an urban area at Brazil. Atmos. Pollut. Res. 5, 411–420.

Alam, M.S., Delgado-Saborit, J.M., Stark, C., Harrison, R.M., 2013. Using atmospheric measurements of PAH and quinone compounds at roadside and urban background sites to assess sources and reactivity. Atmos. Environ. 77, 24–35.

Alves, C., Pio, C., Duarte, A., 2001. Composition of extractable organic matter of air particles from rural and urban Portuguese areas. Atmos. Environ. 35, 5485–5496.

Alves, C., Vicente, A., Pio, C., Kiss, G., Hoffer, A., Decesari, S., Prevôt, A.S.H., Minguillón, M.C., Querol, X., Hillamo, R., Spindler, G., Swietlicki, E., 2012. Organic compounds in aerosols from selected European sites – biogenic versus anthropogenic sources. Atmos. Environ. 59, 243–255.

Amador-Muñoz, O., Villalobos-Pietrini, R., Agapito-Nadales, M.C., Munive-Colín, Z., Hernández-Mena, L., Sánchez-Sandoval, M., Gómez-Arroyo, S., Bravo-Cabrera, J.L., Guzmán-Rincón, J., 2010. Solvent extracted organic matter and polycyclic aromatic hydrocarbons distributed in size-segregated airborne particles in a zone of México City: seasonal behavior and human exposure. Atmos. Environ. 44, 122–130.

Arey, J., 1998. Atmospheric reactions of PAHs including formation of nitroarenes. In: Neilson, A.H. (Ed.), The Handbook of Environmental Chemistry, PAHs and Related Compounds, vol. 3. Springer, New York, NY, pp. 347–385. Part 1.

Barra, R., Castillo, C., Torres, J.P.M., 2007. Polycyclic aromatic hydrocarbons in the South American environment. Rev. Environ. Contam. Toxicol. 191, 1–22.

Barrado, A.I., García, S., Castrillejo, Y., Barrado, E., 2013. Exploratory data analysis of PAH, nitro-PAH and hydroxy-PAH concentrations in atmospheric PM10-bound aerosol particles. Correlations with physical and chemical factors. Atmos. Environ. 67, 385–393.

Bathmanabhan, S., Madanayak, S.N.S., 2010. Analysis and interpretation of particulate matter-PM_{10}, $PM_{2.5}$ and PM_1 emissions from the heterogeneous traffic near an urban roadway. Atmos. Pollut. Res. 1, 184–194.

Braga, J., Teixeira, E.C., Fachel, J., 2005. Study of the profile of polycyclic aromatic hydrocarbons in atmospheric particles (PM 10) using multivariate methods. Atmos. Environ. 39, 6587–6596.

Bedjanian, Y., Nguyen, M.L., Le Bras, G., 2010. Kinetics of the reactions of soot surface-bound polycyclic aromatic hydrocarbons with the OH radicals. Atmos. Environ. 44, 1754–1760.

Bi, X., Sheng, G., Peng, P., Chen, Y., Zhang, Z., Fu, J., 2003. Distribution of particulate- and vapor-phase nalkanes and polycyclic aromatic hydrocarbons in urban atmosphere of Guangzhou, China. Atmos. Environ. 37, 289–298.

Bond, T.C., 2004. A technology-based global inventory of black and organic carbon emissions from combustion. J. Geophys. Res. 109, 1–43.

Bourotte, C., Forti, M.C., Taniguchi, S., Bicego, M.C., Lotufo, P.A., 2005. A wintertime study of PAHs in fine and coarse aerosols in Sao Paulo city, Brazil. Atmos. Environ. 39, 3799–3811.

Callén, M.S., López, J.M., Iturmendi, A., Mastral, A.M., 2013. Nature and sources of particle associated polycyclic aromatic hydrocarbons (PAH) in the atmospheric environment of an urban area. Environ. Pollut. 183, 166–174.

Cheng, Y., Zou, S.C., Lee, S.C., Chow, J.C., Ho, K.F., Watson, J.G., Han, Y.M., Zhang, R.J., Zhang, F., Yau, P.S., Huang, Y., Bai, Y., Wu, W.J., 2011. Characteristics and source apportionment of PM_1 emissions at a roadside station. J. Hazard. Mater. 195, 82–91.

Chirico, R., Spezzano, P., Cataldi, D., 2007. Gas-particle partitioning of polycyclic aromatic hydrocarbons during the spring and summer in a suburban site near major traffic arteries. Polycycl. Aromat. Compd. 27, 401–423.

Colbeck, I., Nasir, Z.A., Ahmad, S., Ali, Z., 2011. Exposure to PM_{10}, $PM_{2.5}$, PM_1 and carbon monoxide on roads in Lahore. Aerosol Air Qual. Res. 11, 689–695.

Comero, S., Capitani, L., Gawlik, B.M., 2009. Positive Matrix Factorisation (PMF) — an Introduction to The Chemometric Evaluation of Environmental Monitoring Data Using PMF. Office for Official Publications of the European Communities, Luxembourg, p. 59.

Cristale, J., Silva, F.S., Zocolo, G.J., Marchi, M.R.R., 2012. Influence of sugarcane burning on indoor/outdoor PAH air pollution in Brazil. Environ. Pollut. 169, 210–216.

Dabestani, R., Ivanov, I.N., 1999. A compilation of physical, spectroscopic and photo physical properties of polycyclic aromatic hydrocarbons. Photochem. Photobiol. 70, 10–34.

Da Limu, Y., Ta LiFu, D., Yi Miti, A., Wang, X., Ding, X., 2013. Autumn and wintertime polycyclic aromatic hydrocarbons in $PM_{2.5}$ and $PM_{2.5-10}$ from Urumqi, China. Aerosol Air Qual. Res. 13, 407–414.
Dallarosa, J.B., Mônego, G.J., Teixeira, E.C., Stephens, J.L., Wiegand, F., 2005a. Polycyclic aromatic hydrocarbons in atmospheric particles in the metropolitan area of Porto Alegre, Brazil. Atmos. Environ. 39, 1609–1625.
Dallarosa, J.B., Teixeira, E.C., Pires, M., Fachel, J., 2005b. Study of the profile of polycyclic aromatic hydrocarbons in atmospheric particles (PM10) using multivariate methods. Atmos. Environ. 39, 6587–6596.
Dallarosa, J.B., Teixeira, E.C., Meira, L., Wiegand, F., 2008. Study of the chemical elements and polycyclic aromatic hydrocarbons in atmospheric particles of PM10 and PM2.5 in the urban and rural areas of South Brazil. Atmos. Environ. 89, 76–92.
Da Rocha, G.O., Lopes, W.A., Pereira, P.A.P., Vasconcellos, P.C., Oliveira, F.S., Carvalho, L.S., et al., 2009. Quantification and source identification of atmospheric particulate polycyclic aromatic hydro-carbons and their dry deposition fluxes at three sites in Salvador Basin, Brazil, impacted by mobile and stationary sources. J. Braz. Chem. Soc. 20, 680–692.
De La Torre-Roche, R.J., Lee, W.-Y., Campos-Diaz, S.I., 2009. Soil-borne polycyclic aromatic hydrocarbons in El Paso, Texas: analysis of a potential problem in the United States/Mexico border region. J. Hazard. Mater. 163, 946–958.
De Martinis, B.S., Okamoto, R.A., Kado, N.Y., Gundel, L.A., Carvalho, L.R.F., 2002. Polycyclic aromatic hydrocarbons in a bioassay-fractionated extract of PM10 collected in São Paulo, Brazil. Atmos. Environ. 36, 307–314.
Di Filippo, P., Riccardi, C., Pomata, D., Buiarelli, F., 2010. Concentrations of PAHs, and nitro- and methyl- derivatives associated with a size-segregated urban aerosol. Atmos. Environ. 44, 2742–2749.
Ding, X., Wang, X.M., Xie, Z.Q., Xiang, C.H., Mai, B.X., Sun, L.G., Zheng, M., Sheng, G.Y., Fu, J.M., Poschl, U., 2007. Atmospheric polycyclic aromatic hydrocarbons observed over the North Pacific Ocean and the Arctic area: spatial distribution and source identification. Atmos. Environ. 47, 2061–2072.
Duan, J., Bi, X., Tan, J., Sheng, G., Fu, J., 2007. Seasonal variation on size distribution and concentration of PAHs in Guangzhou city, China. Chemosphere 67, 614–622.
Dybing, E., Schwarze, P.E., Nafstad, P., Victorin, K., Penning, T.M., 2013. Polycyclic aromatic hydrocarbons in ambient air and cancer. In: Straif, K., Cohen, A., Samet, J. (Eds.), Air Pollution and Cancer, IARC Scientific Publications, vol. 161 (Chap. 7).
Elminir, H.K., 2005. Dependence of urban air pollutants on meteorology. Sci. Total Environ. 350, 225–237.
EMATER, 2013. Associação Riograndense de Empreendimentos de Assistência Técnica e Extensão Rural –EMATER/RS. Available in: http://www.emater.tche.br/site/ (accessed in November of 2013).
Esteve, W., Budzinski, H., Villenave, E., 2004. Relative rate constants for the heterogeneous reactions of OH, NO_2 and NO radicals with polycyclic aromatic hydrocarbons adsorbed on carbonaceous particles. Part 1: PAHs adsorbed on 1–2 μm calibrated graphite particles. Atmos. Environ. 38, 6063–6072.
Esteve, W., Budzinski, H., Villenave, E., 2006. Relative rate constants for the heterogeneous reactions of NO_2 and OH radicals with polycyclic aromatic hydrocarbons adsorbed on carbonaceous particles. Part 2: PAHs adsorbed on diesel particulate exhaust SRM 1650a. Atmos. Environ. 40, 201–211.
Fang, G.C., Wu, Y.S., Chen, M.H., Ho, T.T., Huang, S.H., Rau, J.Y., 2004. Polycyclic aromatic hydrocarbons study in Taichung, Taiwan, during 2002–2003. Atmos. Environ. 38, 3385–3391.
Fang, G.C., Wu, Y.S., Chen, J.C., Chang, C.N., Ho, T.T., 2006. Characteristic of polycyclic aromatic hydrocarbon concentrations and source identification for Fine and coarse particulates at Taichung harbor near Taiwan Strait during 2004–2005. Sci. Total Environ. 366, 729–738.
Fernandes, M.B., Brickus, L., Moreira, J.C., Cardoso, J.N., 2002. Atmospheric BTX and polyaromatic hydrocarbons in Rio de Janeiro, Brazil. Atmos. Environ. 47, 417–425.
Fine, P.M., Cass, G.R., Simoneit, B.R., 2001. Chemical characterization of fine particle emissions from fireplace combustion of woods grown in the northeastern United States. Environ. Sci. Technol. 35, 2665–2675.
Gaffney, J.S., Marley, N.A., 2009. The impacts of combustion emissions on air quality and climate – from coal to biofuels and beyond. Atmos. Environ. 43, 23–36.
Gaga, E.O., Ari, A., Döğeroğlu, T., Çakırca, E.E., Machin, N.E., 2012. Atmospheric polycyclic aromatic hydrocarbons in an industrialized city, Kocaeli, Turkey: study of seasonal variations, influence of meteorological parameters and health risk estimation. J. Environ. Monit. 14, 2219–2229.
Grimmer, G., Jacob, J., Naujack, K.W., 1983. Profile of the polycyclic aromatic compounds from crude oils-inventory by GC GC/MS PAH in environmental materials: part 3. Fresenius J. Anal. Chem. 316, 29–36.
Gu, J., Pitz, M., Schnelle-Kreis, J., Diemer, J., Reller, A., Zimmermann, R., Soentgen, J., Stoelzel, M., Wichmann, H.-E., Peters, A., Cyrys, J., 2011. Source apportionment of ambient particles: comparison of positive matrix factorization analysis applied to particle size distribution and chemical composition data. Atmos. Environ. 45, 1849–1857.
Guo, H., Lee, S.C., Ho, K.F., Wang, X.M., Zou, S.C., 2003. Particle-associated polycyclic aromatic hydrocarbons in urban air of Hong Kong. Atmos. Environ. 37, 5307–5317.
Gunawardena, J., Egodawatta, P., Ayoko, G., Goonetilleke, A., 2012. Role of traffic in atmospheric accumulation of heavy metals and polycyclic aromatic hydrocarbons. Atmos. Environ. 54, 502–510.
Harvey, R.G., 1991. In: Coombs, M.M., Ashby, J., Hicks, R.M. (Eds.), Polycyclic Aromatic Hydrocarbons: Chemistry and Carcinogenicity. Cambridge University Press, p. 396.
Ho, K.F., Lee, S.C., 2002. Identification of atmospheric volatile organic compounds (VOCs), polycyclic aromatic hydrocarbons (PAHs) and carbonyl compounds in Hong Kong. Sci. Total Environ. 289, 145–158.
Hopke, P.K., 2003. A Guide to Positive Matrix Factorization. Available in: http://www.epa.gov/ttnamti1/files/ambient/pm25/workshop/laymen.pdf (accessed in November of 2013).
Howsan, M., Jones, C., 2010. Sources of PAHs in the environment. In: Neilson, A.H. (Ed.), PAHs and Related Compounds, The Handbook of Environmental Chemistry, vol. 3. Springer-Verlag Berlin Heidelberg, Germany.
IARC, International Agency for Research on Cancer, 2010. Monographs, Supplement. Available in: http://monographs.iarc.fr/ENG/Classification/ (accessed in December of 2013).
IARC, International Agency for Research on Cancer, 2013. In: Straif, K., Cohen, A., Samet, J. (Eds.), Air Pollution and Cancer, IARC Scientific Publications, vol. 161.
INPE-CPTEC, 2012. Instituto Nacional de Pesquisas Espaciais – Centro de Previsão de Tempo e Estudos Climáticos. Disponível em: http://www.cptec.br/clima (Accesado em maio de 2012).
Jang, E., Alam, M.S., Harrison, R.M., 2013. Source apportionment of polycyclic aromatic hydrocarbons in urban air using positive matrix factorization and spatial distribution analysis. Atmos. Environ. 79, 271–285.
Kavouras, I.G., Koutrakis, P., Tsapakis, M., Lagoudaki, E., Stephanou, E.G., Baer, D.V., et al., 2001. Source apportionment of urban particulate aliphatic and polynuclear aromatic hydrocarbons (PAHs) using multivariate methods. Environ. Sci. Technol. 35, 2288–2294.
Khalili, N.R., Scheff, P.A., Holsen, T.M., 1995. PAH source fingertrips for coke ovens, diesel and gasoline engines, highway tunnels, and wood combustion emissions. Atmos. Environ. 29, 533–542.
Kleeman, M.J., Riddle, S.G., Robert, M.A., Jakober, C.A., 2008. Lubricating oil and fuel contributions to particulate matter emissions from light-duty gasoline and heavy-duty diesel vehicles. Environ. Sci. Technol. 42, 235–242.
Klejnowski, K., Kozielska, B., Krasa, A., Rogula-Koz1owska, W., 2010. Polycyclic aromatic hydrocarbons in PM1, PM2.5, PM10 and TSP in the upper Silesian agglomeration, Poland. Arch. Environ. Prot. 36, 65–72.
Křůmal, K., Mikuška, P., Večeřa, Z., 2013. Polycyclic aromatic hydrocarbons and hopanes in PM1 aerosols in urban areas. Atmos. Environ. 67, 27–37.
Ladji, R., Yassaa, N., Balducci, C., Cecinato, A., Meklati, B.Y., 2009. Distribution of the solvent-extractable organic compounds in fine (PM1) and coarse (PM1–10) particles in urban, industrial and forest atmospheres of Northern Algeria. Sci. Total Environ. 408, 415–424.
Larsen, R.K., Baker, J.E., 2003. Source apportionment of polycyclic aromatic hydrocarbons in the urban atmosphere: a comparison of three methods. Environ. Sci. Technol. 37, 1873–1881.
Lee, W., Wang, Y., Lin, T., Chen, Y., Lina, W., Ku, C., Chengb, J., 1995. PAH characteristics in the ambient air of traffic-source. Sci. Total Environ. 159, 185–200.
Lee, S.C., Cheng, Y., Ho, K.F., Cao, J.J., Louie, P.K.-K., Chow, J.C., 2006. $PM_{1.0}$ and $PM_{2.5}$ characteristics in the roadside environment of Hong Kong. Aerosol Sci. Technol. 40, 157–165.
Lee, B.-K., Vu, V.T., 2010. Sources, distribution and toxicity of polyaromatic hydrocarbons (PAHs) in particulate matter. In: Air Pollution, Vanda Villanyi. InTech, ISBN 978-953-307-143-5. http://dx.doi.org/10.5772/10045. Available from: http://www.intechopen.com/books/air-pollution/sources-distribution-and-toxicity-of-polyaromatic-hydrocarbons-pahs-in-particulate-matter.
Li, C.K., Kamens, R.M., 1993. The use of polycyclic aromatic hydrocarbons as sources signatures in receptor modeling. Atmos. Environ. 27, 523–532.
Li, M., McDow, S., Tollerud, D., Mazureka, M., 2005. Seasonal abundance of organic molecular markers in urban particulate matter from Philadelphia, PA. Atmos. Environ. 40, 2260–2273.
Li, J., Zhang, G., Li, X.D., Qi, S.H., Liu, G.Q., Peng, X.Z., 2006. Source seasonality of polycyclic aromatic hydrocarbons (PAHs) in a subtropical city, Guangzhou, South China. Sci. Total Environ. 355, 145–155.
Lim, L.H., Harrison, R.M., Harrad, S., 1999. The contribution of traffic to atmospheric concentrations of polyaromatic hydrocarbons. Environ. Sci. Technol. 33, 3538–3542.
Ma, Y., Lei, Y.D., Xiao, H., Wania, F., Wang, W., 2010. Critical review and recommended values for the physical–chemical property data of 15 polycyclic aromatic hydrocarbons at 25 °C. J. Chem. Eng. Data 55, 819–825.
Malcolm, H.M., Dobson, S., 2004. The calculation of an environmental assessment level (EAL) for atmospheric PAHs using relative potencies. In: HMIP-commissioned Research. Department of the Environment, London.
Mandalakis, M., Tsapakis, M., Tsoga, A., Stephanou, E.G., 2002. Gas-particle concentrations and distribution of aliphatic hydrocarbons, PAHs, PCBs and PCDD/Fs in the atmosphere of Athens (Greece). Observatory 36, 4023–4035.
Manoli, A., Kouras, K., Samara, C., 2004. Profile analysis of ambient and source emitted particle-bound polycyclic aromatic hydrocarbons from three sites in Northern Greece. Chemosphere 56, 867–878.
Martins, L.D., da Silva Júnior, C.R., Solci, M.C., Pinto, J.P., Souza, D.Z., Vasconcellos, P., Guarieiro, A.L.N., Guarieiro, L.L.N., Sousa, E.T., de Andrade, J.B., 2012. Particle emission from heavy-duty engine fuelled with blended diesel and biodiesel. Environ. Monit. Assess. 184, 2663–2676.
Masiol, M., Formenton, G., Pasqualetto, A., Pavoni, B., 2013. Seasonal trends and spatial variations of PM10-bounded polycyclic aromatic hydrocarbons in Veneto Region, Northeast Italy. Atmos. Environ. 79, 811–821.
Massey, D., Kulshrestha, A., Masih, J., Taneja, A., 2012. Seasonal trends of PM10, PM5.0, PM2.5 & PM1.0 in indoor and outdoor environments of residential homes located in North-Central India. Build. Environ. 47, 223–231.

Mastral, A.M., López, J.M., Callén, M.S., García, T., Murillo, R., Navarro, M.V., 2003. Spatial and temporal PAH concentrations in Zaragoza, Spain. Sci. Total Environ. 307, 111–124.
Mattiuzi, C.D.P., Palagi, A.C., Teixeira, E.C., Wiegand, F., 2012. Poluição Atmosférica do Biodiesel – Estado da Arte. In: Teixera, E.C., Wiegand, F., Tedesco, M. (Eds.), Biodiesel: Impacto Ambiental Agronômico e Atmosférico. Cadernos de Planejamento e Gestão Ambiental N°6. FEPAM, Porto Alegre, pp. 43–67 (Cap. 2).
Mi, H., Lee, W.J., Chen, C.B., Yang, H.H., Wu, S.J., 2000. Effect of fuel aromatic content on PAH emission from a heavy-duty diesel engine. Chemosphere 41, 1783–1790.
Miguel, A.H., Kirchstetter, T.W., Harley, R.A., Hering, S.V., 1998. On-road emissions of particulate polycyclic aromatic hydrocarbons and black carbon from gasoline and diesel vehicles. Environ. Sci. Technol. 32, 450–455.
Morawska, L., Ristovski, Z., Jayaratne, E., Keogh, D., Ling, X., 2008. Ambient nano and ultrafine particles from motor vehicle emissions: characteristics, ambient processing and implications on human exposure. Atmos. Environ. 42, 8113–8138.
Nisbet, C., LaGoy, P., 1992. Toxic equivalency factors (TEFs) for polycyclic aromatic hydrocarbons (PAHs). Regul. Toxicol. Pharmacol. 16, 290–300.
Netto, A.D., Barreto, R.P., Moreira, J.C., Arbilla, G., 2002. Polycyclic aromatic hydrocarbons in total suspended particulate of Niterói, RJ, Brazil: a comparison of summer and Winter samples. Bull. Environ. Contam. Toxicol. N. Y. 69, 173–180.
Okuda, T., Okamoto, K., Tanaka, S., Shen, Z., Han, Y., Huo, Z., 2010. Measurement and source identification of polycyclic aromatic hydrocarbons (PAHs) in the aerosol in Xi'an, China, by using automated column chromatography and applying positive matrix factorization (PMF). Sci. Total Environ. J. 408, 1909–1914.
Paatero, P., 1997. Least squares formulation of robust non-negative factor analysis. Chemom. Intell. Lab. Syst. 37, 23–35.
Paatero, P., Tapper, U., 1994. Positive matrix factorization: a non-negative factor model with optimal utilization of error estimates of data values. Environ. Metrics 5, 11–126.
Paatero, P., Hopke, P.K., Song, X.-H., Ramadan, Z., 2002. Understanding and controlling rotations in factor analytic models. Chemom. Intell. Lab. Syst. 60, 253–264.
Pandey, P.K., Patel, K.S., Lenicek, J., 1999. Polycyclic aromatic hydrocarbons: need for assessment of health risks in India? — study of an urban-industrial location in India. Environ. Monit. Assess. 59, 287–319.
Panther, B.C., Hooper, M.A., Tapper, N.J., 1999. A comparison of air particulate matter and associated polycyclic aromatic hydrocarbons in some tropical and temperate urban environments. Atmos. Environ. 33, 4087–4099.
Park, S.U., Kim, J.G., Jeong, M.J., Song, B.J., 2011. Source identification of atmospheric polycyclic aromatic hydrocarbons in industrial complex using diagnostic ratios and multivariate factor analysis. Arch. Environ. Contam. Toxicol. 60, 576–589.
Pengchai, P., Chantara, S., Sopajaree, K., Wangkarn, S., Tengcharoenkul, U., Rayanakorn, M., 2009. Seasonal variation, risk assessment and source estimation of PM 10 and PM10-bound PAHs in the ambient air of Chiang Mai and Lamphun, Thailand. Environ. Monit. Assess. 154, 197–218.
Perraudin, E., Budzinski, H., Villenave, E., 2007. Kinetic study of the reactions of ozone with polycyclic aromatic hydrocarbons adsorbed on atmospheric model particles. J. Atmos. Chem. 56, 57–82.
PETROBRAS, 2012. Available in: http://www.petrobras.com.br/pt/produtos/para-voce/nas-ruas/ (accessed in May 2012).
Portet-Koltalo, F., Machour, N., 2013. Analytical methodologies for the control of particle-phase polycyclic aromatic compounds from diesel engine exhaust. In: Bari, S. (Ed.), Diesel Engine – Combustion, Emissions and Condition Monitoring. Intech, ISBN 978-953-51-1120-7 (Chap. 4).
Ravindra, K., Bencs, L., Wauters, E., de Hoog, J., Deutsch, F., Roekens, E., Bleux, N., Berghmans, P., Van Grieken, R., 2006. Seasonal and site-specific variation in vapour and aerosol phase PAHs over Flanders (Belgium) and their relation with anthropogenic activities. Atmos. Environ. 40, 771–785.
Ravindra, K., Sokhia, R., Van Griekenet, R., 2008. Atmospheric polycyclic aromatic hydrocarbons: source attribution, emission factors and regulation. Atmos. Environ. 42, 2895–2921.
Reff, A., Eberly, S.I., Bhave, P.V., 2007. Receptor modeling of ambient particulate matter data using positive matrix factorization: review of existing methods. J. Air Waste Manag. Assoc. 57, 146–154.
Ringuet, J., Albinet, A., Leoz-Garziandia, E., Budzinski, H., Villenave, E., 2012. Reactivity of polycyclic aromatic compounds (PAHs, NPAHs and OPAHs) adsorbed on natural aerosol particles exposed to atmospheric oxidants. Atmos. Environ. 61, 15–22.
Rogge, W.F., Hildemann, L.M., Mazurek, M.A., Cass, G.R., Simoneit, B.R.T., 1993. Sources of fine organic aerosol. 2. Noncatalyst and catalyst-equipped automobiles and heavy-duty diesel trucks. Environ. Sci. Technol. 27, 636–651.
Russel, A., 2013. Combustion emissions. In: Straif, K., Cohen, A., Samet, J. (Eds.), Air Pollution and Cancer, IARC Scientific Publications, vol. 161 (Chap 4).
Saarnio, K., Sillanpaa, M., Hillamo, R., Sandell, E., Pennanen, A., Salonen, R., 2008. Polycyclic aromatic hydrocarbons in size-segregated particulate matter from six urban sites in Europe. Atmos. Environ. 42, 9087–9097.
Schauer, J.J., Kleeman, M.J., Cass, G.R., Simoneit, B.R.T., 1999. Measurement of emissions from air pollution sources, 2. C- 1 through C-30 organic compounds from medium duty diesel trucks. Environ. Sci. Technol. 33, 1578–1587.
Schauer, J.J., Kleeman, M.J., Cass, G.R., Simoneit, B.R.T., 2001. Measurement of emissions from air pollution sources: 3. C1–C29 organic compounds from fireplace combustion of wood. Environ. Sci. Technol. 35, 1716–1728.
Schauer, J.J., Kleeman, M.J., Cass, G.R., Simoneit, B.R.T., 2002. Measurement of emissions from air pollution sources, 5. C1–C32 organic compounds from gasoline-powered motor vehicles. Environ. Sci. Technol. 36, 1169–1180.
Seinfeld, J.H., Pandis, S.N., 2006. Atmospheric Chemistry and Physics: Form Air Pollution to Climate Change, second ed. Wiley, New York.
SEPLAG, 2013. Secretaria de Planejamento, Gestão e Participação Cidadã – SEPLAG/RS. Atlas socioeconômico Rio Grande do Sul. http://www.seplag.rs.gov.br/atlas/atlas.asp?menu=608 (accessed November 2013).
Sicre, M.A., Marty, J.C., Saliot, A., Aparício, X., Grimalt, J., Albaigès, J., 1987. Aliphatic and aromatic hydrocarbons in the Mediterranean aerosol. Int. J. Environ. Anal. Chem. 29, 73–94.
Sienra, M., Rosazza, N., Préndez, M., 2005. Polycyclic aromatic hydrocarbons and their molecular diagnostic ratios in urban atmospheric respirable particulate matter. Atmos. Res. 75, 267–281.
Simcik, M.F., Eisenreich, S.J., Lioy, P.J., 1999. Source apportionment and source/sink relationships of PAHs in the coastal atmosphere of Chicago and Lake Michigan. Atmos. Environ. 33, 5071–5079.
Slezakova, K., Pereira, M.C., Reis, M.A., Alvim-Ferraz, M.C., 2007. Influence of traffic emissions on the composition of atmospheric particles of different sizes – part 1: concentrations and elemental characterization. J. Atmos. Chem. 58, 55–68.
Stroher, G.L., Poppi, N.R., Raposo, J.R., De Souza, J.B.G., 2007. Determination of polycyclic aromatic hydrocarbons by gas chromatography–ion trap tandem mass spectrometry and source identifications by methods of diagnostic ratio in the ambient air of Campo Grande, Brazil. Microchem. J. 86, 112–118.
Tai, A.P.K., Mickley, L.J., Jacob, D., 2010. Correlations between fine particulate matter (PM2.5) and meteorological variables in the United States: implications for the sensitivity of PM2.5 to climate change. Atmos. Environ. 44, 3976–3984.
Teixeira, E.C., Feltes, S., Santana, E.R., 2008. Estudo das emissões de fontes móveis na Região Metropolotana de Porto Alegre, Rio Grande do Sul. Quím. Nova 31 (2), 244–248.
Teixeira, E.C., Santana, R.E., Wiegand, F., 2010. 1st Inventory of Air Emissions from Mobile Sources in the State of Rio Grande Do Sul – Base Year: 2009. Fundação Estadual de Proteção Ambiental Henrique Luis Roessler, Porto Alegre (in Portuguese).
Teixeira, E.C., Oliveira, K., Meincke, L., Alam, K., 2011. Study of nitro-polycyclic aromatic hydrocarbons in fine and coarse atmospheric particles. Atmos. Res. 101, 631–639.
Teixeira, E.C., Mattiuzi, C.D.P., Feltes, S., Wiegand, F., Santana, E.R.R., 2012. Estimated atmospheric emissions from biodiesel and characterization of pollutants in the metropolitan area of Porto Alegre-RS. An. Acad. Bras. Ciências 84 (3), 245–261.
Teixeira, E.C., Mattiuzi, C.D.P., Agudelo-Castañeda, D.M., Oliveira, K., Wiegand, F., 2013. Polycyclic aromatic hydrocarbons study in atmospheric fine and coarse particles using diagnostic ratios and receptor model in urban/industrial region. Environ. Monit. Assess. 185, 9587–9602.
Tobiszewski, M., Namieśnik, J., 2012. PAH diagnostic ratios for the identification of pollution emission sources. Environ. Pollut. J. 162, 110–119.
Tsapakis, M., Lagoudaki, E., Stephanou, E.G., Kavouras, I.G., Koutrakis, P., Oyola, P., Von Baer, D., 2002. The composition and sources of HV PM10–2.5 organic aerosol in two urban areas of Chile. Atmos. Environ. 36, 3851–3863.
USEPA U.S. Environmental Protection Agency, 1999. Determination of Polycyclic Aromatic Hydrocarbons (PAHs) in Ambient Air Using Gas Chromatography/Mass Spectrometry (GC/MS). Compendium Method TO-13A, second ed.. In: Compendium of Methods for the Determination of Toxic Organic Compounds in Ambient Air Center for Environmental Research Information. Office of Research and Development. U.S. Environmental Protection Agency, Cincinnati, OH.
USEPA, 1994. Quality Assurance Handbook for Air Pollution Measurement Systems. In: Ambient Air Specific Methods, vol. II. US Environmental Protection Agency; US Government Printing Office, Washington, DC. Section 2,11; EPA/600/R-94/038a.
USEPA, 2008. EPA Positive Matrix Factorization (PMF) 3.0 Fundamentals and User Guide. USEPA Office of Research and Development.
Vasconcellos, P.C., Souza, D.Z., Magalhães, D., Da Rocha, G.O., 2011. Seasonal variation of n-alkanes and polycyclic aromatic hydrocarbon concentrations in PM10 samples collected at urban sites of São Paulo State, Brazil. Water Air Soil Pollut 222, 325–336.
Vestenius, M., Leppänen, S., Anttila, P., Kyllönen, K., Hatakka, J., Hellén, H., Hyvärinen, A.-P., Hakola, H., 2011. Background concentrations and source apportionment of polycyclic aromatic hydrocarbons in south-eastern Finland. Atmos. Environ. 45, 3391–3399.
Wang, G., Huang, L., Niu, H., Dai, Z., 2006. Aliphatic and polycyclic aromatic hydrocarbons of atmospheric aerosols in five locations of Nanjing urban area, China. Atmos. Res. 81, 54–66.
Wang, D., Tian, F., Yang, M., Liu, C., Li, Y.-F., 2009. Application of positive matrix factorization to identify potential sources of PAHs in soil of Dalian, China. Environ. Pollut. 157, 1559–1564.
Westerholm, R., Li, H., 1994. A multivariate statistical analysis of fuel related polycyclic aromatic hydrocarbon (PAH) emissions from heavy duty diesel vehicles. Environ. Sci. Technol. 28, 965–992.
Wingfors, H., Hägglund, L., Magnusson, R., 2011. Characterization of the size-distribution of aerosols and particle-bound content of oxygenated PAHs, PAHs, and n-alkanes in urban environments in Afghanistan. Atmos. Environ. 45, 4360–4369.
WHO, World Health Organization, 1998. Selected Non-heterocyclic Polycyclic Aromatic Hydrocarbons. International Programme on Chemical Safety. Environmental Health Criteria. World Health Organization, Geneva, p. 202.

Wu, Y., Yang, L., Zheng, X., Zhang, S., Song, S., Li, J., Hao, J., 2013. Characterization and source apportionment of particulate PAHs in the roadside environment in Beijing. Sci. Total Environ. 470–471C, 76–83.
Yang, Y., Guo, P., Zhang, Q., Li, D., Zhao, L., Mu, D., 2010. Seasonal variation, sources and gas/particle partitioning of polycyclic aromatic hydrocarbons in Guangzhou, China. Sci. Total Environ. 408, 2492–2500.
Yang, T.T., Lin, S.T., Gung, H.F., Shie, R.H., Wu, J.J., 2013. Effect of relative humidity on polycyclic aromatic hydrocarbon emissions from smoldering incense. Aerosol Air Qual. Res. 13, 662–671.
Yin, J., Harrison, R.M., 2008. Pragmatic mass closure study for PM1, PM2.5 and PM10 at roadside, urban background and rural sites. Atmos. Environ. 42, 980–988.
Zhang, X.L., Tao, S., Liu, W.X., Yang, Y., Zuo, Q., Liu, S.Z., 2005. Source diagnostics of polycyclic aromatic hydrocarbons based on species ratios: a multimedia approach. Environ. Sci. Technol. 39, 9109–9114.
Zhang, Y., Tao, S., 2009. Global atmospheric emission inventory of polycyclic aromatic hydrocarbons (PAHs) for 2004. Atmos. Environ. 43, 812–819.
Zhao, Y., Wang, S., Duan, L., Lei, Y., Cao, P., Hao, J., 2008. Primary air pollutant emissions of coal-fired power plants in China: current status and future prediction. Atmos. Environ. 42, 8442–8452.
Zielinska, B., 2005. Atmospheric transformation of diesel emissions. Exp. Toxicol. Pathol. 57, 31–42.

CAPITULO IV

Time–series analysis of surface ozone and nitrogen oxides concentrations in an urban area at Brazil

AGUDELO-CASTAÑEDA, D. M.; Teixeira, E.C.; Pereira, F.N.

Atmospheric Pollution Research 5, 411-420, 2014.

Atmospheric Pollution Research 5 (2014) 411–420

Atmospheric Pollution Research

www.atmospolres.com

Time–series analysis of surface ozone and nitrogen oxides concentrations in an urban area at Brazil

Dayana Milena Agudelo–Castaneda [1], Elba Calesso Teixeira [1,2], Felipe Norte Pereira [2]

[1] *Postgraduate Program in Remote Sensing and Meteorology, Geosciences Institute, Universidade Federal do Rio Grande do Sul (UFRGS), Brazil*
[2] *Research Department, Fundação Estadual de Proteção Ambiental Henrique Luis Roessler, RS. Av. Borges de Medeiros, 261, 90020–021, Porto Alegre, Brazil*

ABSTRACT

The purpose of the present work was to study the concentration variations in O_3, NO, NO_2, NO_X over a 4–year period (2006–2009), using the Kolmogorov–Zurbenko filter. Data were decomposed into seasonal and trend components. Seasonal component of the time–series analysis (2006–2009) of NO and NO_x in Canoas and Esteio showed values above average during the cold seasons, while O_3 showed an opposite pattern. The trend component was marked by the decrease of NO_2 at Canoas and the increase of NO at Esteio, thus revealing their variation (NO and NO_x) due to local emissions. Furthermore, evaluations of the mean daily concentrations of NO, NO_x, NO_2, O_3, PM_{10} and CO, and correlations of these pollutants with meteorological parameters (ambient temperature, wind velocity, solar radiation and relative humidity) allowed the confirmation of the influence of mobile sources in the study area.

Keywords: *Nitrogen oxides, ozone, traffic air pollution*

Corresponding Author:
Elba Calesso Teixeira
☎ : *+55-51-32889408*
✉ : *gerpro.pesquisa@fepam.rs.gov.br*
elbact.ez@terra.com.br

Article History:
Received: 04 November 2013
Revised: 17 February 2014
Accepted: 18 February 2014

doi: 10.5094/APR.2014.048

1. Introduction

Air pollution caused by photochemical oxidants, especially in urban areas, has risen in later years (Notario et al., 2012), mainly by vehicular fleet increase. Tropospheric ozone (O_3) is formed by a series of complex photochemical reactions between nitrogen oxides (NO_X=NO+NO_2) and volatile organic compounds (VOCs) in the presence of sunlight (Finlayson–Pitts and Pitts, 2000). NO_X is a reactive pollutant and its major effects on O_3 are limited to its proximity to emission sources (Uherek et al., 2010). The O_3 formation by reactions involving the catalytic action of NO_X on the oxidation of CO is also possible (Seinfeld and Pandis, 2006). CO is emitted directly from the fuel combustion and therefore makes some contribution to tropospheric O_3 production in the boundary layer (Jenkin and Clemitshaw, 2000). NO_X emitted by heavy vehicles produce five times the amount of NO_X by mass of burnt fuel compared to gasoline vehicles (Kirchstetter et al., 1998). Also, the addition of biodiesel in diesel can slightly increase NO_X emissions (Coronado et al., 2009).

Due to the chemical coupling of surface O_3 and NO_X, the response to NO_X emissions reductions is remarkably not linear and any resultant reduction in the level of nitrogen dioxide (NO_2) is invariably accompanied by an increase in the atmospheric concentration of O_3 (Mazzeo et al., 2005).

Although elevated O_3 concentrations had been registered in cities, the highest values normally occur at downwind locations, due to the transport of precursors. Depending on weather conditions, O_3 precursors can be transported over long distances and originate O_3 formation in locations far from their sources (Castell–Balaguer et al., 2012). Stedman (2004) studied the influence of the decrease in CO and NO_X concentrations; however O_3 concentrations seem to be steady or even increased in the last few years.

Several studies highlight the importance of meteorological factors in O_3 formation and transport (Millan et al., 2000; Thompson et al., 2001). The studies have shown O_3 concentrations increase with high temperatures and solar radiation intensities (Garcia et al., 2005; Castell et al., 2008; Teixeira et al., 2009; Han et al., 2011; Castell–Balaguer et al., 2012). Other authors, such as Pudasainee et al. (2006), reported that daily variations of ground–level O_3 occur more frequently in the spring and summer than in the winter. Teixeira et al. (2009) reported seasonal variations of surface ozone in the same study area during one year period (in 2006), with maximum O_3 concentration during summer and spring.

The Kolmogorov–Zurbenko (KZ) filter developed by Rao and Zurbenko (1994), used in the present study, has been widely used for treating ozone data, since other statistical methods are poorly developed for situations of O_3 changes due to meteorological variations larger in magnitude than those induced by emissions (Rao et al., 1997). The KZ filter is a good method to separate O_3 time series effectively into their various spectral components (Kang et al., 2013). Some studies, such as Dallarosa et al. (2007), Teixeira et al. (2009), Meira et al. (2009), and Cuchiara and Carvalho (2012), did not have their results filtered to remove the seasonal

component of temporal variability in order to examine the data and detect changes in the emission of O_3 and their precursors.

Thus, the purpose of the present study was to study the variations in O_3, NO, NO_2, NO_X concentrations over a 4–year period (2006–2009). The data were decomposed into their seasonal and trend components by applying the Kolmogorov–Zurbenko filter. Moreover, meteorological parameters (ambient temperature, wind velocity, solar radiation, and relative humidity) were correlated with O_3, NO, NO_2, NO_X, PM_{10} and CO concentrations. Also, the mean daily variation of the concentration of those pollutants was also calculated.

2. Methodology

2.1. Study area

The chosen region for this study was the metropolitan area of Porto Alegre (MAPA). It is located in the eastern part of Rio Grande do Sul state at south Brazil, and has a total area of 84 764 km^2. This area is represented by a stretch of 32 counties (SEPLAG, 2011) and is the most urbanized region of Rio Grande do Sul state. The air quality in the MAPA is under direct influence of industrial activities and, especially, emissions from mobile sources which account for about 40% of emissions in the state (Teixeira et al., 2010). Additional details and explanations of the samplings sites locations are shown in Figure 1.

The study area has a strong influence of light and heavy–duty vehicles, with daily traffic congestions, and also because of the proximity of the BR–116 highway. The different industrial typologies include several stationary sources such as an oil refinery, steel mills that uses natural gas, and coal–fired power plants, as reported in Teixeira et al. (2010; 2012). Sampling sites were Canoas and Esteio in the study area.

Due to its location, winter in the MAPA is strongly influenced by cold air masses migrating from Polar Regions. The seasons are well defined and the rain is evenly distributed all over the year. According to Koppen's international system of climate classification, the climate type of the study area is a humid subtropical climate (Cfa) with well distributed rain all over the year, and an average temperature above 22.0 °C during the warmest month of the year. The prevailing wind direction is SE, followed by NE (EMBRAPA, 2003). The average annual speed of wind is 2.2 m s^{-1} (INMET, 2009). In the cold seasons, there is less dispersion of pollutants due to lower wind speeds, higher incidence of calm winds, and greater variability in wind direction, associated with a lower thickness of the mixing layer (due to migration of polar air masses over the region). In warm seasons, the dispersion is favored by higher wind speeds, lower incidence of calm winds, and increased thickness of the mixing layer (Teixeira et al., 2012). During the day, the wind reaches its lowest speed at dawn and early morning, and highest speeds in the late afternoon, between 5:00–7:00 p.m. This pattern is related to energy availability at the surface (sensible heat) during the day, intensifying local and mesoscale atmospheric circulations. The prevailing wind results from interactions of mesoscale phenomena, especially sea/land breezes (from the Atlantic Ocean and the Patos Lagoon) and valley/mountain breezes (from the nearby Serra Geral Mountains located to the north of the MAPA). Details about the annual average and maximum per day of the meteorological variables ambient temperature, relative humidity, rainfall, number of days with rainfall ≥1 mm, wind speed, and pressure by season: summer (Jan/Feb/Mar), autumn (Apr/May/Jun), winter (Jul/Aug/Sep), and spring (Oct/Nov/Dec) for the sampling period (2006–2009) of the present study can be found in Table 1.

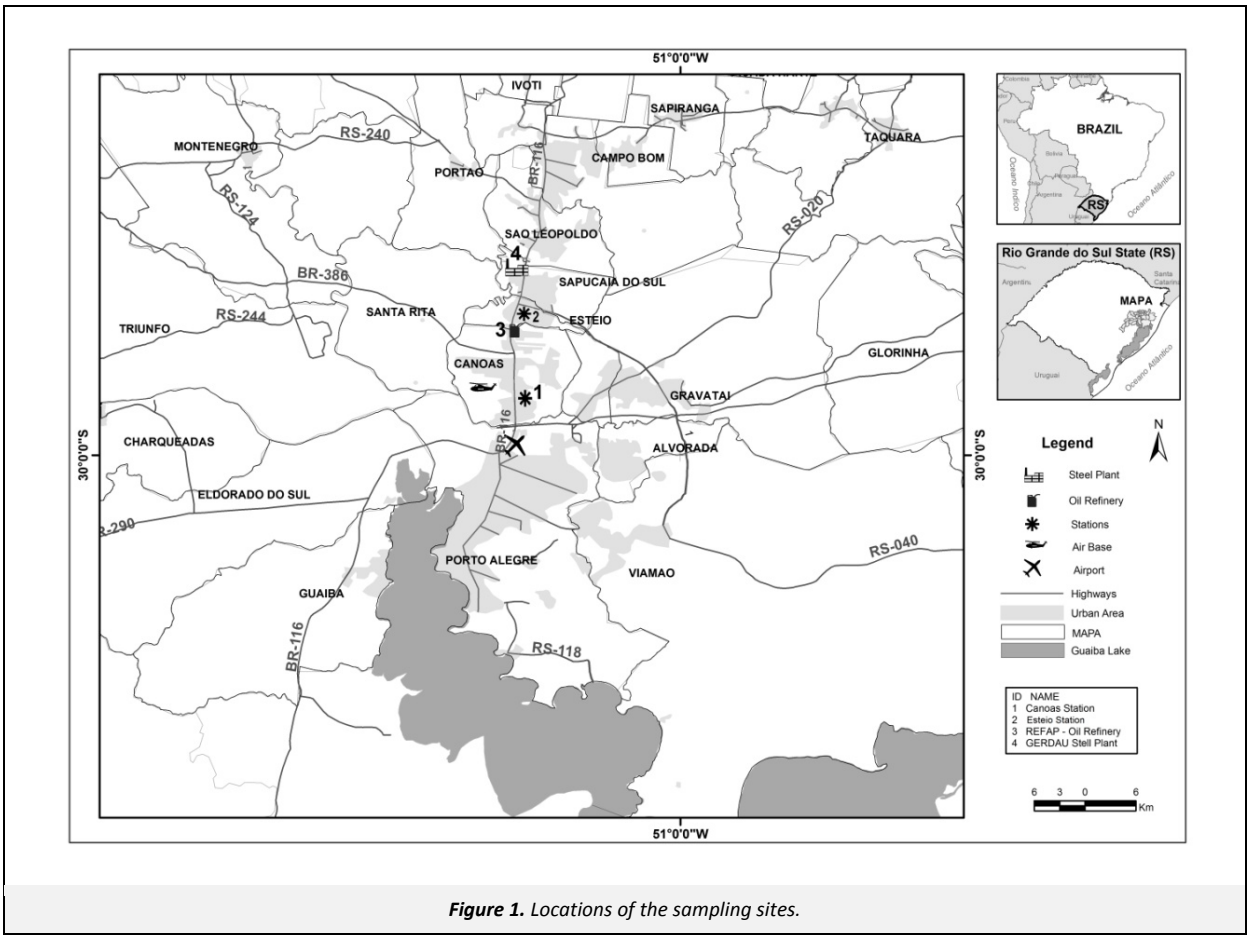

Figure 1. *Locations of the sampling sites.*

Table 1. *Meteorological data for the sampling period (2006-2009)*

Parameter	Unit	Summer	Autumn	Winter	Spring
Ambient temperature	°C	24.2	17.0	15.5	21.6
Maximum daily temperature	°C	30.1	23.3	20.4	26.2
Minimum daily temperature	°C	20.3	14.3	11.4	16.6
Relative Humidity	%	72.7	77.1	76.8	72.5
Maximum daily relative humidity	%	89.1	89.6	90.8	89.3
Minimum daily relative humidity	%	48.2	55.4	55.9	49.8
Precipitation[a]	mm	320	339	444	376
Number days with precipitation[b]	days	28.0	23.0	28.0	26.0
Wind speed	m s^{-1}	1.7	1.3	1.6	1.8
Pressure	hPa	1 007	1 012	1 013	1 008

Source: Instituto Nacional de Meteorologia – INMET
[a] *Precipitation average of the stations in the study period*
[b] *Number of days per season in the study period*

During the period of study (2006–2009), the average rainfall in winter was 444.2 mm $year^{-1}$, 28% higher than in summer (320.4 mm $year^{-1}$). The wind speed was higher in spring and lower in autumn, with the average rate slightly lower than the climatological normals. The atmospheric pressure was higher in autumn and winter, with values slightly below the climatological normals.

Average temperatures (Table 1) showed behavior similar to the climatological normals. Temperatures (average, maximum and minimum) in the summer were about 9–10 °C higher than those in the winter. Average maximum daily temperature in the summer was 30.7 °C and in the winter 20.4 °C, while the average minimum daily temperature in the summer was 20.3 °C and 11.4 °C in the winter. This same range between the daily maximum and minimum temperatures was observed in all seasons. The relative humidity was slightly below the climatological normals, and did not show much variation among the different seasons. However, the variation between the daily averages of maximum and minimum relative humidity was 46% in the summer and 38% in the winter.

2.2. Sampling and calibration

The pollutants NO, NO_2, NO_X ($NO+NO_2$), O_3, and CO were measured continuously during a 4–year period (2006–2009). The equipments used for measurements included a nitrogen oxide analyzer (AC31M–using chemiluminescence method), an ozone analyzer (O341M–LCD/UV Photometry), a carbon monoxide analyzer (CO11M–using infrared absorption), and a PM_{10} analyzer (MP101M–using beta radiation method). All equipments were made by Environnement S.A. Air temperature (°C), relative humidity (%), solar radiation (W m^{-2}), wind direction (°) and wind speed (m s^{-1}) were measured continuously by a weather station, at 15–min intervals, using a thermo hygrometer, a global radiometer, and an anemometer. All the analyzers were located in Canoas and Esteio, the sampling sites of the study area (Figure 1).

In order to have a good quality control of the data, monthly calibrations were performed in these analyzers. For the AC31M and CO11M, calibration gases with uncertainty <3% were used, together with the MGC 101 multicalibrator (Multigas Multi–Point Calibrator). The calibrations of the O341M analyzer were done with an ozone generator present in the MGC. For the MP101M, it was used a reference gauge provided by the manufacturer.

2.3. KZ filter

The KZ filter treatment was applied to the 15–min data to analyze the temporal series for the period 2006–2009. This filter was proposed by Kolmogorov and formally defined by Zurbenko (1986). It can be written as:

$$KZ_{m,p}[X(t)] = \sum_{S=-\frac{p(m-1)}{2}}^{\frac{p(m-1)}{2}} \frac{a_s}{m^p} X(t+S) \quad (1)$$

where, *X(t)* corresponds to the time series, *t* is a position in the time series and a_s corresponds to the coefficients of the polynomial $(1+z+z^2+\ldots+z^{m-1})^p$.

The KZ filter can also be defined as *p*–times iterations of a moving average [Equation (2)] with window length *m*.

$$MA = \sum_{S=-(m-1)/2}^{(m-1)/2} \frac{X(t+S)}{m} \quad (2)$$

The KZ filter is a low–pass filter, removing high frequency variations in the time series. The effective width (*P*) of this filter depends of the number of iterations (*p*) and window size (*m*), estimated as $m\sqrt{P} \leq P$ (Milanchus et al., 1998).

The KZ filter is capable of separating out both trend and short–term variations in the time–series, and the seasonal component, too. The short–term component is attributable to weather and short–term fluctuations in precursor emissions, the seasonal component is a result of changes in the solar angle, and the trend–term results from changes in overall emissions, pollutant transport, climate, policy, and/or economics (Rao and Zurbenko, 1994; Wise and Comrie, 2005). The seasonal component reflects "normal" variations that recur every year to the same extent (OECD, 2007). It is also referred to as the seasonality of a time series.

The KZ filter is based on the Rao and Zurbenko (1994) statement that a time–series of atmospheric pollutants can be represented by:

$$A(t)=e(t)+S(t)+W(t) \quad (3)$$

where, *A(t)*, *e(t)*, *S(t)* and *W(t)* are the original time–series, the trend–term, the seasonal variation, and the short–term component, respectively. The sum of the trend–term and the seasonal variation corresponds to the baseline component.

In this work, we used a *p* value of 5 and an *m* value of 15 days for the baseline (Rao et al., 1997). To obtain the trend component, we used a value of $KZ_{(m,p)}$ equal to $KZ_{(365,3)}$ as used in Wise and Comrie (2005) for tropospheric ozone. By subtracting the value of *e(t)* from baseline, the seasonal component *S(t)* was obtained.

The KZ filter has several advantages because it can be applied directly to datasets that have missing values, without the need for special treatment for gaps. In the present study, the quantity of missing data corresponded to 7.4 % of the database. Several authors such as Sebald et al. (2000), Wise and Comrie (2005), Papanastasiou et al. (2012), Kang et al. (2013) have used this type of filter.

2.4. Statistical analyses

With the 15–min data the mean hourly concentrations for $NO/NO_X/NO_2/O_3$ for each of the four seasons were calculated. Also, the mean daily variations of studied pollutants were calculated. Correlation analyses between hourly mean concentrations of $O_3/NO/NO_X/OX/PM_{10}/CO$ and meteorological parameters were performed. A scatter plot of the variation of daily mean $[NO_2]/[OX]$ as a function of NO_X was used to provide a better overview and interpretation of the relations between NO_X and the pollutants $NO_2/NO_X/O_3$.

3. Results and Discussion

3.1. Temporal–series variability of NO_X and O_3

The variability of atmospheric pollutant concentrations depends on specific emissions and general meteorological conditions. NO_X (NO_2+NO) is a primary contaminant and O_3 is a secondary contaminant that originates in the atmosphere through a set of complex reactions (Seinfeld and Pandis, 2006). Previous authors (Teixeira et al., 2009; Agudelo–Castaneda et al., 2013) studying surface O_3 in the MAPA have found that its concentrations are influenced by NO_X precursors and meteorological conditions (temperature and solar radiation). The present work examined time–series of atmospheric pollutant concentrations (NO, NO_2, NO_X and O_3) in a longer study period (4–years).The Kolmogorov–Zurbenko filter was employed to separate the seasonal component [*S(t)*] of the time–series and also to obtain the trend–term component [*e(t)*].

Figure 2a and 2b shows the trend–term of the time–series (2006–2009) for Canoas and Esteio regarding NO, NO_2, NO_X and O_3 concentrations [*e(t)*]. The trend was marked by two different situations: NO_2 decrease in Canoas and NO increase in Esteio. In Canoas (Figure 2a), NO_X concentrations were dominated by NO_2 concentrations, indicating a significant contribution of NO_2. Additionally, NO_2 and NO_X concentrations in Canoas (Figure 2a) show a decrease from 2007 to the end of the studied period. In Esteio (Figure 2b) was observed a similar behavior for NO_2, although was a minor decrease, possibly, due to the processes modifications of a refinery located in the study area. These modifications, such as equipment improvements and partial replacement of fuel oil by refinery gas, resulted in lower NO_X emissions from this stationary source. Also, in 2007 the frequency of wind speed <1 m s^{-2} was higher (frequency: 52.4%) than in 2006. Thus, lower wind speeds may have increased the influence of local emission sources.

Elevated NO_X and NO concentrations were observed in Esteio (Figure 2b), in all the studied period. Moreover, this site showed higher NO concentrations than Canoas, which can be attributed to their stronger vehicular influence, characterized by heavy–duty fleet, in Esteio. This vehicular influence in the study area, especially of diesel–fueled vehicles, was evidenced in previous studies (Teixeira et al., 2008; Teixeira et al., 2009; Feltes et al., 2010; Teixeira et al., 2011; Teixeira et al., 2012; Agudelo–Castaneda et al., 2013).

The O_3 trend–term of the sampling sites showed a different behavior (Figure 2a and 2b). Figure 2a showed increased levels of O_3 concentration since 2007 in Canoas, probably due to decreased levels of NO and, consequently, a lower O_3 consumption, producing an accumulation of tropospheric O_3. In Esteio (Figure 2b), a different behavior was observed, a decreased O_3 concentration since 2007. As explained above, Esteio had increased NO and NO_X concentrations levels that may cause an O_3 reduction. In a NO_X–limited atmosphere (with high NO_X concentrations) O_3 may depend on the overall level of NO_X (Seinfeld and Pandis, 2006). Also, O_3 ambient concentration is strongly influenced by diurnal fluctuation of NO_2 and the ratio of NO_2 to NO (Sebald et al., 2000).

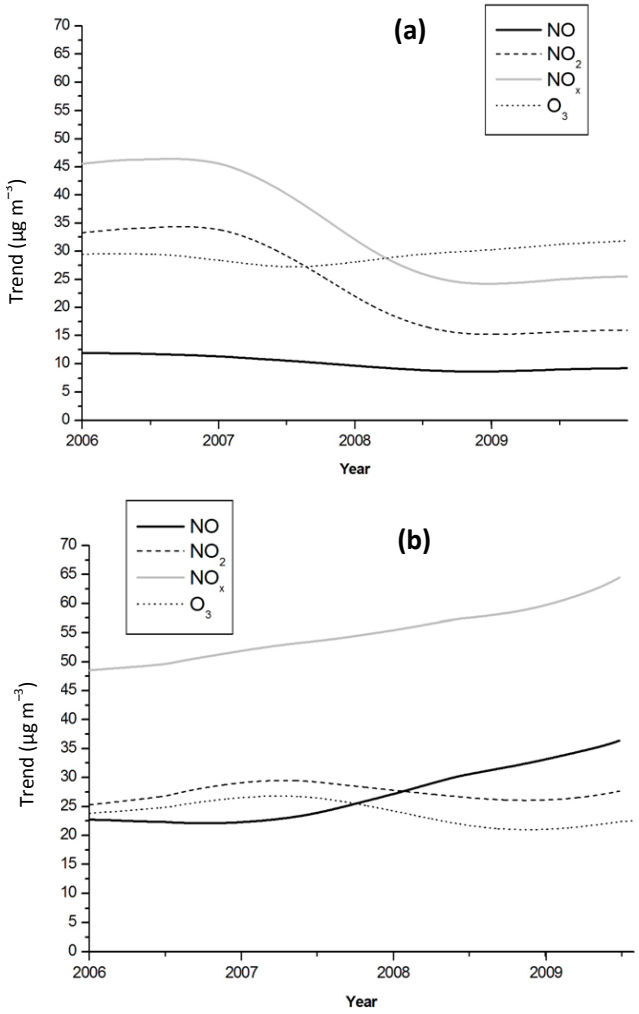

Figure 2. *Trend–term component of time–series (2006–2009) for Canoas* ***(a)*** *and Esteio* ***(b)*** *of NO, NO_2, NO_X and O_3 concentrations.*

Figure 3a and 3b shows the seasonal component of the time–series (2006–2009) of NO, NO_2, NO_X and O_3 concentrations for Canoas and Esteio. Overall, it can be observed that at both sites the values of NO, NO_2 and NO_X were above average from May to October of each year. These months corresponded to the colder seasons of the year: winter and autumn (Figure 3a and 3b). Below average values of these pollutants (NO, NO_2, NO_X) were observed between November and February, which corresponded to the warmer seasons of the year: spring and summer. O_3 (Figure 3a and 3b) showed an opposite behavior, with concentrations below average in the colder months (winter and autumn) and above average in the warmer months (spring and summer).

The seasonal variation of these pollutants may be better assessed in the Figure 4. Figure 4 shows the mean concentration of NO, NO_X, NO_2 and O_3, in winter, spring, summer, and autumn in Canoas and Esteio. In general, levels of nitrogen oxides (NO, NO_2, NO_X) concentrations in the cold seasons (autumn and winter) and of O_3 in the warm seasons (summer and spring) were higher.

Greater O_3 concentrations during spring and summer were due to favorable temperature and abundance of solar radiation, thus promoting photochemical reactions. The lower O_3 concentrations during the colder months may be attributed to the presence of higher concentrations of NO, NO_2 and NO_X and to specific weather conditions such as lower solar radiation, lower mixing layer, and to weak winds (Notario et al., 2012). In these colder days, the photochemical formation of O_3 is inhibited by the lack of intense solar radiation (Sadanaga et al., 2008; Geddes et al., 2009).

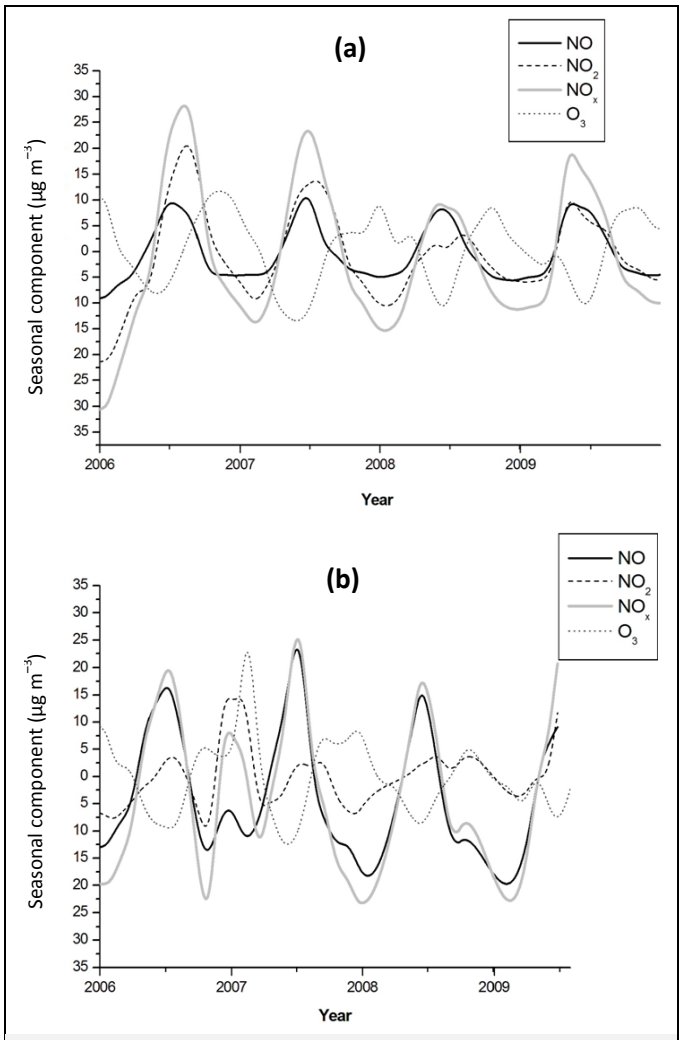

Figure 3. *Seasonal component of time–series (2006–2009) for Canoas* ***(a)*** *and Esteio* ***(b)*** *of NO, NO_2, NO_X and O_3 concentrations.*

3.2. Daily variations

Figure 5 shows the daily variation of the hourly mean concentrations of NO, NO_2, NO_X, OX, CO, and O_3 from 2006 to 2009 for Canoas and Esteio. NO_2 and O_3 can be observed together as OX ($OX=NO_2+O_3$), i.e., the total amount of photochemical oxidants. In fact, OX represents better, as it is less sensitive to emissions and its uncertainties. OX is not influenced by the rapid photo–stationary balance between NO, NO_2, and O_3 (Monteiro et al., 2005). In both sites, OX concentration incremented slowly after sunrise (Figure 5), reached a maximum during the day (Canoas: 74.23 µg m^{-3}; Esteio: 70.64 µg m^{-3}), and decreased until the next morning. OX concentration increase is due to photochemical O_3 formation. Some authors (Han et al., 2011) have reported that OX variation during daytime and nighttime would be expected, if the photochemical processes have an influence on OX levels in polluted areas. The variation of surface O_3, within a day, may be helpful in delineating the processes responsible for O_3 formation at a particular location (Singla et al., 2011).

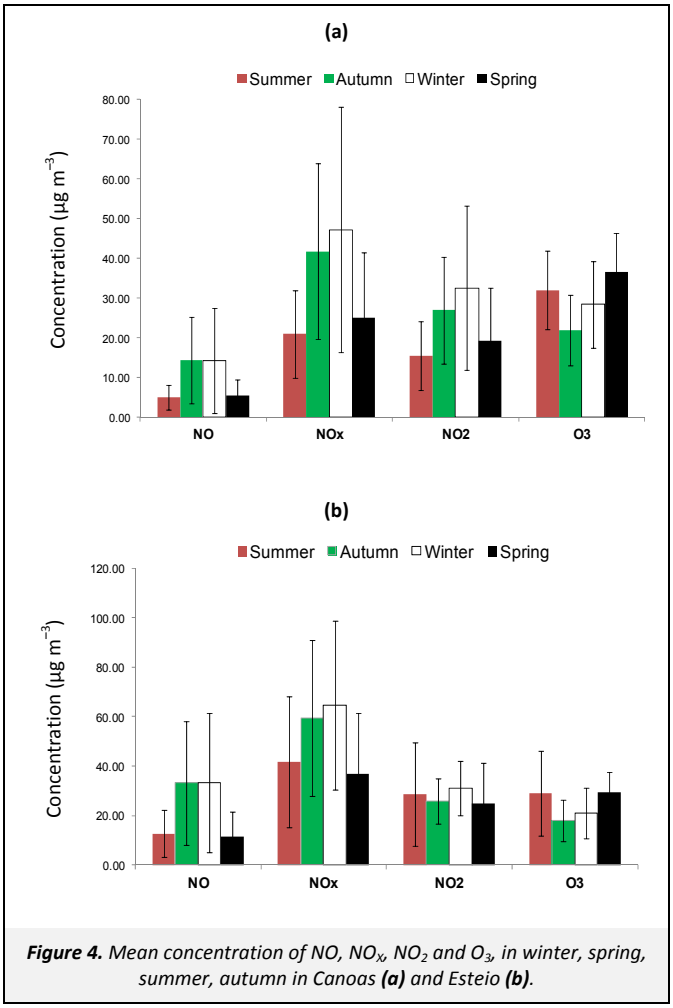

Figure 4. *Mean concentration of NO, NO_X, NO_2 and O_3, in winter, spring, summer, autumn in Canoas* ***(a)*** *and Esteio* ***(b)****.*

It may be seen in Figure 5, that NO as well as CO increase at 6:00 at both sites, along with an increase in emissions from motor vehicles or, possibly, industrial activities, showing their highest concentrations at 8:00. As explained before, the two sites (Canoas and Esteio) of the study area has a strong vehicular influence, especially Esteio. Hence, NO mainly emitted by vehicle exhausts is present in elevated concentrations. NO (see Figure 5) showed morning peak values of 28.51 µg m^{-3} in Canoas and 74.54 µg m^{-3} in Esteio, at 8:00. NO_2 peak concentrations were 32.25 µg m^{-3} and 35.06 µg m^{-3} in Canoas and Esteio, respectively, at 10:00. There is a displacement of about 2 h in the morning between NO and NO_2 peaks (Figure 5). In the morning, NO_2 is produced by oxidation of NO (Jenkin and Clemitshaw, 2000), as NO may be converted in NO_2 in the presence of peroxi radicals (Dallarosa et al., 2007). CO showed peak values of 0.60 ppm at Canoas and 0.74 ppm at Esteio in the morning, and 0.66 ppm (Canoas) and 0.82 ppm (Esteio) in the late afternoon (18:00) during the rush hour. At night, concentrations of NO, NO_2 and CO exhibited a slight increase caused by the rise of vehicular traffic during the rush hour (18:00) and the influence of the stability of the nocturnal boundary layer. At this time, NO_2 reached peaks at 18:00 (36.18 µg m^{-3}) and 20:00 (30.91 µg m^{-3}) for Esteio and Canoas, respectively. These concentrations were similar to the peaks exhibited in the morning. Jenkin and Clemitshaw (2000) reported that at night the OH radical can be ignored since it is produced mainly from the photolysis of stable molecules. Therefore, NO_2 cannot be photolyzed to regenerate NO, or removed by reaction with OH, which will react with O_3 to form NO_3, thereby removing O_3.

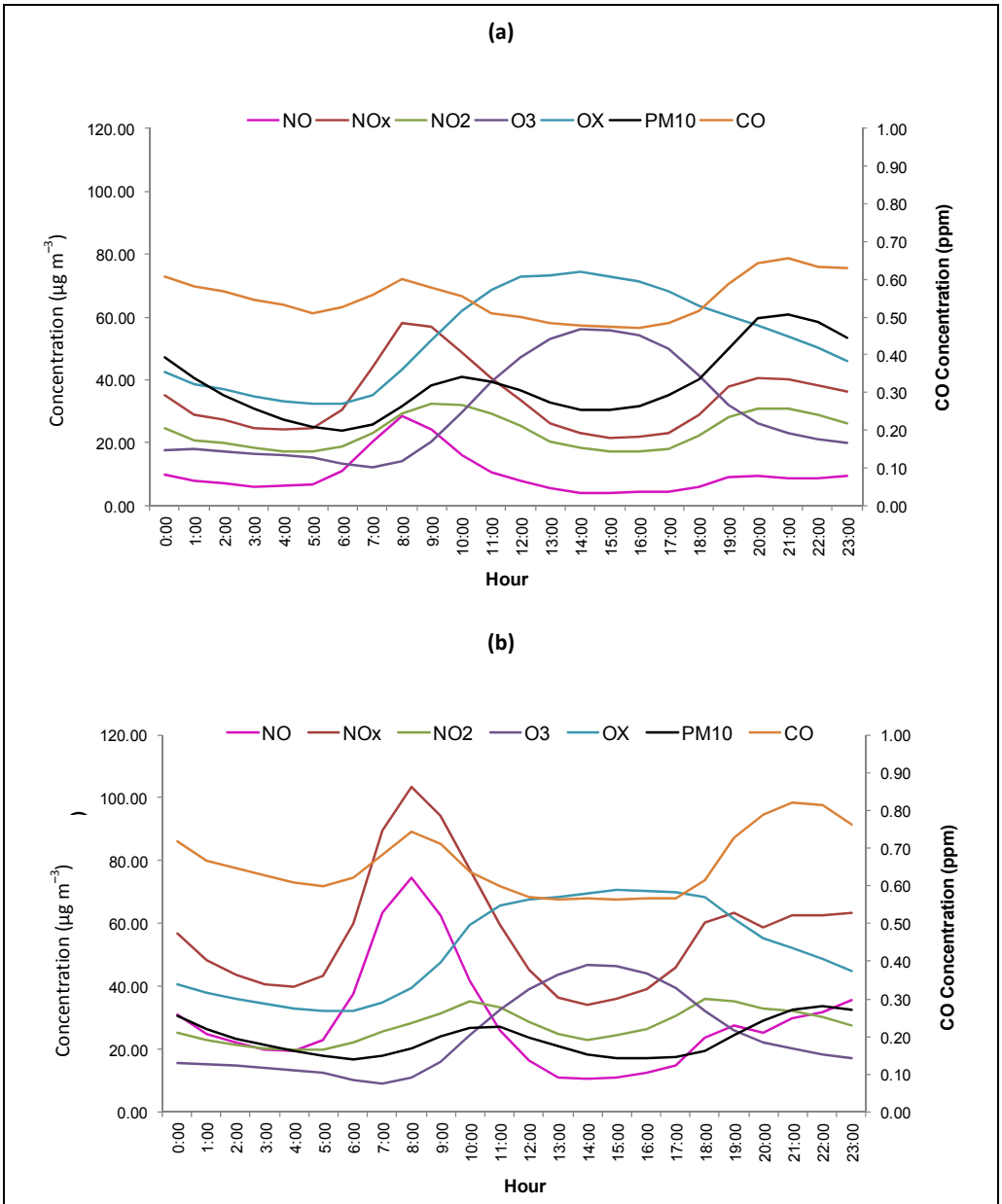

Figure 5. *Mean daily variation of NO, NO_x, NO_2, O_3, OX, PM_{10}, and CO, concentrations for the study period (2006-2009) for Canoas* ***(a)*** *and Esteio* ***(b)****.*

Likewise, Figure 5 exhibits an increase in O_3 concentrations during the day, beginning at 8:00 and reaching its maximum at 14:00 in Canoas (55.96 µg m^{-3}) and Esteio (46.71 µg m^{-3}). NO is converted to NO_2 via reaction with O_3, and during daytime hours NO_2 is converted back to NO as a result of photolysis, which leads to the regeneration of O_3 (Han et al., 2011). Han et al. (2011) reported similar results, were O_3 in urban atmospheres reached peaks during the day, usually at 14:00–15:00, when there is a maximum in the intensity of solar radiation and temperature. This increase is probably marked by photolysis of NO_2, and expansion of the height of the boundary layer during the day, that can result in the mixing of O_3 due to thermal stratification and heat transfer by convection to the surface from air at higher altitudes (Swamy, et al., 2012). After reaching the peak concentration at 14:00, O_3 concentration reduces slowly due to the decrease in photo-chemical activity. The pattern observed in the present study is in agreement with previous works done in the same study area (Agudelo–Castaneda et al., 2013).

Canoas O_3 concentrations (see Figure 5) are slightly higher than in Esteio, probably because concentrations of O_3 precursors (NO, NO_X) in Canoas are lower. As explained above, Canoas has less traffic influence than Esteio. Also, Esteio is located downstream of the prevailing winds of Alberto Pasqualini oil refinery (Teixeira et al., 2009; 2012).

OX concentrations in Canoas and Esteio (Figure 5) were marked by NO_2 concentrations, especially in the early morning hours when concentrations raised mainly due to increase of vehicular traffic. Higher OX concentrations occurred in the afternoon, thus revealing an influence of photochemical processes (Han et al., 2011; Notario et al., 2012). At night, OX decreases due to the absence of solar radiation. This lack of radiation hinders the formation of NO_2 and O_3 by photolytic reactions, as well as the reactions of NO_2 with NO_3, and of NO_2 with O_3 (Jenkin and Clemitshaw, 2000).

The daily CO concentrations (Figure 5) exhibited a similar behavior for the two studied sites, indicating influence of gasoline–fueled vehicles. CO concentration increased between 6:00 and 9:00; also in the late afternoon (18:00) during the rush hour extending into the night. Even after the CO decrease (after 20:00), this and other pollutants maintain high concentrations during the night due to the formation of the nocturnal boundary layer (NBL) near the surface, trapping these pollutants in the lower troposphere. The observed behavior of NO and CO (increase of emissions at 6:00 at both sites) is characteristic of urban areas with the influence of mobile sources (Raga et al., 2001).

The data reported in the present study are consistent with those of several studies (Park et al., 2008; Hagler et al., 2009; Teixeira et al., 2009; Carslaw et al., 2011), which report the influence of vehicle emissions in the concentration increase of some pollutants, mainly nitrogen oxide and CO.

3.3. Association of NO, NO_2, NO_X, PM_{10}, CO, O_3, OX with meteorological parameters

Tables 2 and 3 show the correlation coefficients between hourly pollutant concentrations (NO, NO_2, NO_X, PM_{10}, CO, O_3, OX) and meteorological parameters, for Canoas and Esteio sites. Positive correlations (>0.5) were found between nitrogen oxides (NO, NO_2, NO_X) and CO, evidencing that these pollutants had the same source and confirming the influence of mobile sources. Nitrogen oxides (NO, NO_2, NO_X) presented a significant correlation with O_3 (<0.5), although inverse. These results are similar to those obtained by He and Lu (2012). For being a photochemical pollutant, O_3 also had a significant correlation with solar radiation and temperature, for both studied sites. These relationships of O_3 have also been reported in the studies of Teixeira et al. (2009) and Pudasainee et al. (2006). In addition, the results of the present study showed OX correlation with solar radiation and ambient temperature, indicating the influence of photochemical processes on this pollutant in urban areas (Han et al., 2011).

Table 2. *Pearson correlation coefficients between hourly mean O_3, NO, NO_X, OX, PM_{10} and CO concentrations and meteorological parameters (ambient temperature, wind velocity, solar radiation and relative humidity) of Canoas*

	PM_{10}	OX	NO	NO_X	NO_2	O_3	CO	W. V.[a]	S. R.[b]	A. T.[c]	R. H.[d]
PM_{10}	1	0.120[e]	0.194[e]	0.270[e]	0.269[e]	–0.088[e]	0.241[e]	–0.030[e]	–0.016[f]	0.113[e]	–0.108[e]
OX		1	0.107[e]	0.413[e]	0.574[e]	0.652[e]	0.173[e]	0.187[e]	0.405[e]	0.311[e]	–0.532[e]
NO			1	0.849[e]	0.531[e]	–0.364[e]	0.419[e]	–0.321[e]	–0.081[e]	–0.224[e]	0.155[e]
NO_X				1	0.899[e]	–0.343[e]	0.519[e]	–0.345[e]	–0.090[e]	–0.186[e]	0.111[e]
NO_2					1	–0.247[e]	0.488[e]	–0.278[e]	–0.077[e]	–0.112[e]	0.048[e]
O_3						1	–0.256[e]	0.413[e]	0.558[e]	0.486[e]	–0.682[e]
CO							1	–0.111[e]	–0.103[e]	–0.041[e]	0.064[e]
W. V.[a]								1	0.198[e]	0.190[e]	–0.299[e]
S. R.[b]									1	0.570[e]	–0.627[e]
A. T.[c]										1	–0.481[e]
R. H.[d]											1

[a] *Wind Velocity*
[b] *Solar Radiation*
[c] *Ambient Temperature*
[d] *Relative Humidity*
[e] *Correlation is significant at the 0.01 level (2-tailed)*
[f] *Correlation is significant at the 0.05 level (2-tailed)*

Table 3. *Pearson correlation coefficients between hourly mean O_3, NO, NO_x, OX, PM_{10} and CO concentrations and meteorological parameters (ambient temperature, wind velocity, solar radiation and relative humidity) of Esteio*

	PM_{10}	OX	NO	NO_X	NO_2	O_3	CO	W. V.[a]	S. R.[b]	A. T.[c]	R. H.[d]
PM_{10}	1	0.134[e]	0.388[e]	0.431[e]	0.299[e]	–0.127[e]	0.441[e]	–0.070[e]	–0.064[e]	–0.002	–0.037[e]
OX		1	–0.069[e]	0.235[e]	0.673[e]	0.666[e]	–0.100[e]	0.127[e]	0.373[e]	0.286[e]	–0.520[e]
NO			1	0.913[e]	0.312[e]	–0.408[e]	0.544[e]	–0.332[e]	–0.156[e]	–0.296[e]	0.218[e]
NO_X				1	0.673[e]	–0.362[e]	0.523[e]	–0.356[e]	–0.151[e]	–0.236[e]	0.168[e]
NO_2					1	–0.104[e]	0.225[e]	–0.226[e]	–0.062[e]	0.027[e]	–0.036[e]
O_3						1	–0.253[e]	0.169[e]	0.562[e]	0.474[e]	–0.622[e]
CO							1	–0.150[e]	–0.197[e]	–0.151[e]	0.188[e]
W. V.[a]								1	0.058[e]	0.307[e]	–0.171[e]
S. R.[b]									1	0.473[e]	–0.596[e]
A. T.[c]										1	–0.484[e]
R. H.[d]											1

[a] *Wind Velocity*
[b] *Solar Radiation*
[c] *Ambient Temperature*
[d] *Relative Humidity*
[e] *Correlation is significant at the 0.01 level (2-tailed)*
[f] *Correlation is significant at the 0.05 level (2-tailed)*

Furthermore, the results showed a significant, although <0.5, correlation between CO and O_3. This is due to the fact that in the atmosphere, CO is a major sink of hydroxyl radicals (OH), which are mainly generated by O_3 (Teixeira et al., 2009). Particles (PM_{10}) and NO_X had a significant correlation (coefficient <0.5) indicating that various sources with different emission rates, such as particle resuspension and some stationary sources were the major sources of these pollutants in Canoas and Esteio.

In the present study, wind speed showed a significant correlation with O_3 and an inverse correlation with nitrogen oxides in Esteio and Canoas (Tables 2 and 3). This relationship is explained by the fact that a higher wind speed (except for the very strong winds) enhances the dispersion and mixing of these atmospheric pollutants emitted at closer sources (i.e., at highways and stationary sources), thus optimizing the O_3 formation from precursors. These data show agreement with other studies, e.g. Jones et al. (2010) and Guerra and Miranda (2011).

The correlations of nitrogen oxides (NO, NO_2, NO_X), PM_{10} and CO with relative humidity (Tables 2 and 3) were significant at the 0.01 level. This can be attributed to the influence of the migration of new air masses over the study area (mainly polar air masses), which can bring clean atmospheric air and minimize the cumulative concentrations of these pollutants (background). These results are similar to those reported in other studies (Elminir, 2005; Mavroidis and Ilia, 2012).

Also, Tables 2 and 3 show the obtained negative correlation of O_3 with the relative humidity. This relationship can be explained by the fact that when relative humidity increases, the major photochemical paths for O_3 removal are reinforced (Reddy et al., 2012). However, high values of relative humidity may be associated with atmospheric instability and large cloud cover, which can slow down photochemical processes, with O_3 being depleted by wet deposition (Nishanth et al., 2012). As well by the fact that both (O_3 and relative humidity) have an opposite behavior; relative humidity has its peak at night (with decreasing air temperature), while O_3 shows its minimum value due to the absence of solar radiation, and vice–versa. Agudelo–Castaneda et al. (2013) also reported this behavior. The work of Song et al. (2011) reported similar results, high relative humidity may retard the O_3 production to some extent.

Nitrogen oxides (mainly NO_2) and PM_{10} exhibited a negative and a positive correlation (<0.5) with temperature, respectively. CO also correlated with temperature. This relationship may be explained by the fact that NO_X and CO favor the O_3 production in the presence of sunlight and high temperatures (Jacob and Winner, 2009).

3.4. Relationship between NO_2, NO_X and OX

In some studies, analysis of the $[NO_2]/[OX]$ ratio values have been used to explore the ground–level O_3 concentration variations and the relationship between OX and NO_X data (Clapp and Jenkin, 2001; Han et al., 2011). A photostationary state relationship exists between NO, NO_2 and O_3 (Clapp and Jenkin, 2001; Han et al., 2011). Based on this, it can be possible to infer an expected variation. Figure 6 shows the linear regression analysis with daily mean $[NO_2]/[OX]$ ratio as a function of NO_X for the sampling sites (Canoas and Esteio). Data reveal that for lower values of the $[NO_2]/[OX]$ ratio, there are low values of NO_X, implying that in these instants OX concentrations are predominantly marked by high O_3 concentrations. Also, with increasing NO_X concentrations, a great part of OX is in the form of NO_2. The high values of $[NO_2]/[OX]$ can also be explained by the oxidation process of NO to NO_2 with concentrations of NO_X being marked mainly by the concentration of NO_2.

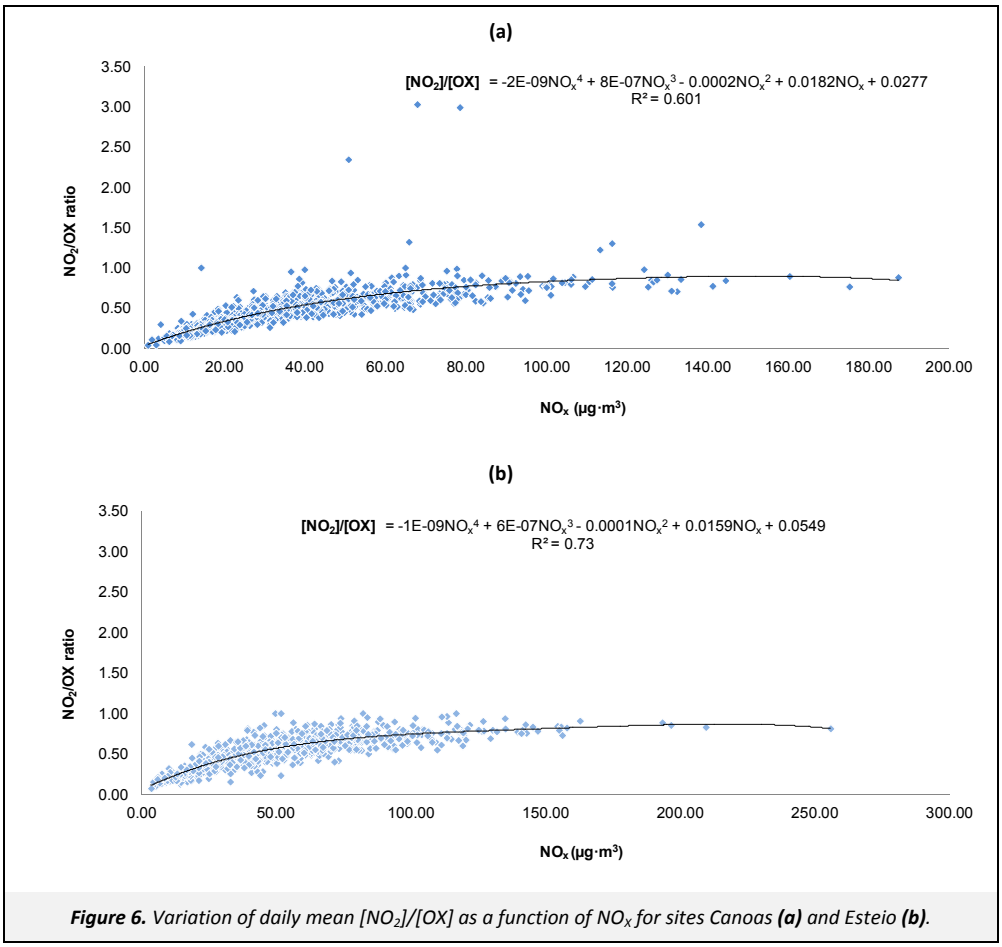

Figure 6. *Variation of daily mean $[NO_2]/[OX]$ as a function of NO_X for sites Canoas* ***(a)*** *and Esteio* ***(b)****.*

Similar equations and regression coefficients values were obtained for both sampling sites, despite the fact that Canoas had higher NO_x concentrations than Esteio. Equations showed intercept values of 0.0277 μg m^{-3} and 0.0549 μg m^{-3} for Canoas and Esteio, respectively. However, further studies should be conducted to understand the precise relationship between NO, NO_2 and O_3 and obtain fitted functions.

4. Conclusions

The Kolmogorov–Zurbenko filter proved to be a useful tool in the temporal analysis of O_3, NO, NO_2 and NO_X concentrations in Canoas and Esteio. By applying this filter, it was possible to decompose the time–series in the short–term, trend–term and seasonal component. The trend–term allowed analyzing the variation in the concentration of these pollutants due to local emissions. In this analysis, NO increased in Esteio due to a stronger vehicular influence (light and heavy–duty fleet, traffic congestion, and slow vehicle speed), being in accordance with works done in the study area. In general, trends for NO_X did not show significant changes in concentrations.

The seasonal component showed concentrations of NO, NO_2 and NO_X above average during the winter, due to adverse meteorological conditions, while O_3 concentrations were above average during the summer, due to increased photochemical activity.

Positive correlations (>0.5) between nitrogen oxides (NO, NO_2, NO_X) and CO indicate that these pollutants come from the same source, evidencing the influence of mobile sources in Esteio and Canoas.

PM_{10} and NO_X showed a significant correlation, although with a coefficient <0.5, suggesting that ressuspended particles and some stationary sources as major sources of these pollutants, at Canoas and Esteio.

In the correlation of NO_2/OX with NO_X it was observed that for low NO_2/OX values, there are low NO_X values, indicating that concentrations are predominantly marked by O_3. With high values of NO_2/OX, NO_X concentrations were marked mainly by NO_2 concentrations, which might be explained by the oxidation process of NO to NO_2.

The filter Kolmogorov–Zurbenko, the statistical technique, allowed the evaluation of the pollutant concentrations variations due to anthropogenic sources that are influencing the study area.

It is suggested that future studies should be conducted in order to understand precisely the relationship between NO, NO_2, O_3 and meteorological variables with associated emission sources.

Acknowledgments

We are grateful to FAPERGS and CNPq for their financial support.

References

Agudelo–Castaneda, D.M., Teixeira, E.C., Rolim, S.B.A., Pereira, F.N., Wiegand, F., 2013. Measurement of particle number and related pollutant concentrations in an urban area in South Brazil. *Atmospheric Environment* 70, 254–262.

Carslaw, D.C., Beevers, S.D., Tate, J.E., Westmoreland, E.J., Williams, M.L., 2011. Recent evidence concerning higher NO_x emissions from passenger cars and light duty vehicles. *Atmospheric Environment* 45, 7053–7063.

Castell, N., Mantilla, E., Millan, M.M., 2008. Analysis of tropospheric ozone concentration on a Western Mediterranean site: Castellon (Spain). *Environmental Monitoring and Assessment* 136, 3–11.

Castell–Balaguer, N., Tellez, L., Mantilla, E., 2012. Daily, seasonal and monthly variations in ozone levels recorded at the Turia River basin in Valencia (Eastern Spain). *Environmental Science and Pollution Research* 19, 3461–3480.

Clapp, L.J., Jenkin, M.E., 2001. Analysis of the relationship between ambient levels of O_3, NO_2 and NO as a function of NO_X in the UK. *Atmospheric Environment* 35, 6391–6405.

Coronado, C.R., de Carvalho, J.A., Silveira, J.L., 2009. Biodiesel CO_2 emissions: A comparison with the main fuels in the Brazilian market. *Fuel Processing Technology* 90, 204–211.

Cuchiara, G.C., Carvalho, J.C., 2012. Modelling of photochemical pollution in the metropolitan area of Porto Alegre, Rio Grande do Sul. in biodiesel impact environmental agronomic and atmospheric. Planning book and environmental management, 6, edited by Teixera, E.C., Wiegand, F., Tedesco, M., FEPAM, 87, Porto Alegre, 97–122 (in Portuguese).

Dallarosa, J.B., Teixeira, E.C., Alves, R.C.M., 2007. Application of numerical models in the formation of ozone and its precursors in areas of influence of coal–fired power station – Brazil. *Water Air and Soil Pollution* 178, 385–399.

Elminir, H.K., 2005. Dependence of urban air pollutants on meteorology. *Science of the Total Environment* 350, 225–237.

EMBRAPA (Brazilian Agricultural Research Corporation), 2003. Climate of Rio Grande do Sul, Section of Geography, edited by EMBRAPA, Secretary of Agriculture, Porto Alegre (in Portuguese).

Feltes, S., Teixeira, E. C., Wiegand, F., 2010. Inventory of air emissions from mobile s sources in the Metropolitan Area of Porto Alegre – FLEET DIESEL / BIODIESEL), Proceedings of XVIII Brazilian Congress of Chemical Engineering, September, 19–22, 2010, Foz do Iguaçu, Brazil, pp. 1647-1653 (in Portuguese).

Finlayson–Pitts, B.J., Pitts., J.N., Jr., 2000. *Chemistry of the Upper and Lower Atmosphere*: *Theory, Experiments, and Applications*, Academic Press, San Diego, pp. 40-45.

Garcia, M.A., Sanchez, M.L., Perez, I.A., de Torre, B., 2005. Ground level ozone concentrations at a rural location in Northern Spain. *Science of the Total Environment* 348, 135–150.

Geddes, J.A., Murphy, J.G., Wang, D.K., 2009. Long term changes in nitrogen oxides and volatile organic compounds in Toronto and the challenges facing local ozone control. *Atmospheric Environment* 43, 3407–3415.

Guerra, F.P., Miranda, R.M., 2011. Influence of meteorology in the concentration of atmospheric pollutant $PM_{2.5}$ in RJRM and MRSP. Proceedings of II Congress Brazilian Environmental Management, November 6–9, 2011, Parana, Brazil (in Portuguese).

Hagler, G.S.W., Baldauf, R.W., Thoma, E.D., Long, T.R., Snow, R.F., Kinsey, J.S., Oudejans, L., Gullett, B.K., 2009. Ultrafine particles near a major roadway in Raleigh, North Carolina: Downwind attenuation and correlation with traffic–related pollutants. *Atmospheric Environment* 43, 1229–1234.

Han, S.Q., Bian, H., Feng, Y.C., Liu, A.X., Li, X.J., Zeng, F., Zhang, X.L., 2011. Analysis of the relationship between O_3, NO and NO_2 in Tianjin, China. *Aerosol and Air Quality Research* 11, 128–139.

He, H.D., Lu, W.Z., 2012. Decomposition of pollution contributors to urban ozone levels concerning regional and local scales. *Building and Environment* 49, 97–103.

INMET (National Institute of Meteorology), 2009. http://www.inmet.gov.br/portal/, accessed in May 2009.

Jacob, D.J., Winner, D.A., 2009. Effect of climate change on air quality. *Atmospheric Environment* 43, 51–63.

Jenkin, M.E., Clemitshaw, K.C., 2000. Ozone and other secondary photochemical pollutants: Chemical processes governing their formation in the planetary boundary layer. *Atmospheric Environment* 34, 2499–2527.

Jones, A.M., Harrison, R.M., Baker, J., 2010. The wind speed dependence of the concentrations of airborne particulate matter and NO_x. *Atmospheric Environment* 44, 1682–1690.

Kang, D.W., Hogrefe, C., Foley, K.L., Napelenok, S.L., Mathur, R., Rao, S.T., 2013. Application of the Kolmogorov–Zurbenko filter and the decoupled direct 3D method for the dynamic evaluation of a regional air quality model. *Atmospheric Environment* 80, 58–69.

Kirchstetter, W.T., Miguel, H.A., Harley, A.R., 1998. On–road comparison of exhaust emissions from gasoline and diesel engines. *Proceedings of 8th CRC On–road Vehicle Emissions Workshop*, April 20–22, 1998, San Diego, CA., pp. 53–70.

Mavroidis, I., Ilia, M., 2012. Trends of NO_x, NO_2 and O_3 concentrations at three different types of air quality monitoring stations in Athens, Greece. *Atmospheric Environment* 63, 135–147.

Mazzeo, N.A., Venegas, L.E., Choren, H., 2005. Analysis of NO, NO_2, O_3 and NO_x concentrations measured at a green area of Buenos Aires City during wintertime. *Atmospheric Environment* 39, 3055–3068.

Meira, L., Ducati, J.R., Teixeira, E.C., 2009. Elevation on estimating formation of surface ozone using Models–3. Revista Brasileira de Meteorologia 24, 390–398 (in Portuguese).

Milanchus, M.L., Rao, S.T., Zurbenko, I.G., 1998. Evaluating the effectiveness of ozone management efforts in the presence of meteorological variability. *Journal of the Air & Waste Management Association* 48, 201–215.

Millan, M.M., Mantilla, E., Salvador, R., Carratala, A., Sanz, M.J., Alonso, L., Gangoiti, G., Navazo, M., 2000. Ozone cycles in the western Mediterranean basin: Interpretation of monitoring data in complex coastal terrain. *Journal of Applied Meteorology* 39, 487–508.

Monteiro, A., Vautard, R., Borrego, C., Miranda, A.I., 2005. Long–term simulations of photo oxidant pollution over Portugal using the CHIMERE model. *Atmospheric Environment* 39, 3089–3101.

Nishanth, T., Kumar, M.K.S., Valsaraj, K.T., 2012. Variations in surface ozone and NO_x at Kannur: A tropical, coastal site in India. *Journal of Atmospheric Chemistry* 69, 101–126.

Notario, A., Bravo, I., Adame, J.A., Diaz–de–Mera, Y., Aranda, A., Rodriguez, A., Rodriguez, D., 2012. Analysis of NO, NO_2, NO_x, O_3 and oxidant ($OX=O_3+NO_2$) levels measured in a metropolitan area in the southwest of Iberian Peninsula. *Atmospheric Research* 104, 217–226.

OECD (Organisation for Economic Co–operation and Development), 2007. Guidelines for the reporting of different forms of data, *in Data and Metadata Reporting and Presentation Handbook*, OECD, Paris, pp. 59–72.

Papanastasiou, D.K., Melas, D., Bartzanas, T., Kittas, C., 2012. Estimation of ozone trend in central Greece, based on meteorologically adjusted time series. *Environmental Modeling & Assessment* 17, 353–361.

Park, K., Park, J.Y., Kwak, J.H., Cho, G.N., Kim, J.S., 2008. Seasonal and diurnal variations of ultrafine particle concentration in urban Gwangju, Korea: Observation of ultrafine particle events. *Atmospheric Environment* 42, 788–799.

Pudasainee, D., Sapkota, B., Shrestha, M.L., Kaga, A., Kondo, A., Inoue, Y., 2006. Ground level ozone concentrations and its association with NO_x and meteorological parameters in Kathmandu valley, Nepal. *Atmospheric Environment* 40, 8081–8087.

Raga, G.B., Baumgardner, D., Castro, T., Martinez–Arroyo, A., Navarro–Gonzalez, R., 2001. Mexico City air quality: A qualitative review of gas and aerosol measurements (1960–2000). *Atmospheric Environment* 35, 4041–4058.

Rao, S.T., Zurbenko, I.G., 1994. Detecting and tracking changes in ozone air–quality. *Journal of the Air & Waste Management Association* 44, 1089–1092.

Rao, S.T., Zurbenko, I.G., Neagu, R., Porter, P.S., Ku, J.Y., Henry, R.F., 1997. Space and time scales in ambient ozone data. *Bulletin of the American Meteorological Society* 78, 2153–2166.

Reddy, B.S.K., Kumar, K.R., Balakrishnaiah, G., Gopal, K.R., Reddy, R.R., Sivakumar, V., Lingaswamy, A.P., Arafath, S.M., Umadevi, K., Kumari, S.P., Ahammed, Y.N., Lal, S., 2012. Analysis of diurnal and seasonal behavior of surface ozone and its precursors (NO_x) at a semi–arid rural site in Southern India. *Aerosol and Air Quality Research* 12, 1081–1094.

Sadanaga, Y., Shibata, S., Hamana, M., Takenaka, N., Bandow, H., 2008. Weekday/weekend difference of ozone and its precursors in urban areas of Japan, focusing on nitrogen oxides and hydrocarbons. *Atmospheric Environment* 42, 4708–4723.

Sebald, L., Treffeisen, R., Reimer, E., Hies, T., 2000. Spectral analysis of air pollutants. Part 2: Ozone time series. *Atmospheric Environment* 34, 3503–3509.

Seinfeld, J.H., Pandis, S.N., 2006. *Atmospheric Chemistry and Physics*: *From Air Pollution to Climate Change*, 2nd edition, John Wiley & Sons, New Jersey, U.S., pp. 1203.

SEPLAG (Secretary of Planning, Management and Citizen Participation), 2011. Charcoal, http://www.seplag.rs.gov.br/atlas/atlas.asp?menu=608, accessed in August 2011.

Singla, V., Satsangi, A., Pachauri, T., Lakhani, A., Kumari, K.M., 2011. Ozone formation and destruction at a sub–urban site in North Central region of India. *Atmospheric Research* 101, 373–385.

Song, F., Shin, J.Y., Jusino–Atresino, R., Gao, Y., 2011. Relationships among the springtime ground–level NO_x, O_3 and NO_3 in the vicinity of highways in the US East Coast. *Atmospheric Pollution Research* 2, 374–383.

Stedman, D.H., 2004. Photochemical ozone formation, simplified. *Environmental Chemistry* 1, 65–66.

Swamy, Y.V., Venkanna, R., Nikhil, G.N., Chitanya, D.N.S.K., Sinha, P.R., Ramakrishna, M., Rao, A.G., 2012. Impact of nitrogen oxides, volatile organic compounds and black carbon on atmospheric ozone levels at a semi arid urban site in Hyderabad. *Aerosol and Air Quality Research* 12, 662–671.

Teixeira, E.C., Mattiuzi, C. D.P., Feltes, S., Wiegand, F., Santana, E.R.R., 2012. Estimated atmospheric emissions from biodiesel and characterization of pollutants in the metropolitan area of Porto Alegre–RS. *Anais da Academia Brasileira de Ciencias* 84, 245–261.

Teixeira, E.C., Mattiuzi, C.D.P., Wiegand, F., Feltes, S., Norte, F. 2011. Estimated atmospheric emissions from mobile sources and assessment of air quality in an urban area, in *Air Quality Monitoring, Assessment and Management,* edited by Mazzeo, N.A., Intech, Rijeka, Croatia, pp. 149– 172.

Teixeira, E.C., Santana, R.E., Wiegand, F., 2010. 1st Inventory of air emissions from mobile sources in the state of Rio Grande do Sul – Base Year: 2009. Fundação Estadual de Proteção Ambiental Henrique Luis Roessler, Porto Alegre (in Portuguese).

Teixeira, E.C., de Santana, E.R., Wiegand, F., Fachel, J., 2009. Measurement of surface ozone and its precursors in an urban area in South Brazil. *Atmospheric Environment* 43, 2213–2220.

Teixeira, E.C., Feltes, S., Santana, E.R.R., 2008. Study of emissions from mobile sources in the metropolitan region of Porto Alegre–RS. *Quimica Nova* 31, 244–248.

Thompson, M.L., Reynolds, J., Cox, L.H., Guttorp, P., Sampson, P.D., 2001. A review of statistical methods for the meteorological adjustment of tropospheric ozone. *Atmospheric Environment* 35, 617–630.

Uherek, E., Halenka, T., Borken–Kleefeld, J., Balkanski, Y., Berntsen, T., Borrego, C., Gauss, M., Hoor, P., Juda–Rezler, K., Lelieveld, J., Melas, D., Rypdal, K., Schmid, S., 2010. Transport impacts on atmosphere and climate: Land transport. *Atmospheric Environment* 44, 4772–4816.

Wise, E.K., Comrie, A.C., 2005. Extending the Kolmogorov–Zurbenko filter: Application to ozone, particulate matter, and meteorological trends. *Journal of the Air & Waste Management Association* 55, 1208–1216.

Zurbenko, I., 1986. *The Spectral Analysis of Time Series*, North–Holland, New York, pp. 248.

CAPITULO V

Infrared spectra of emissivity, transmittance and reflectance of PAHs and comparison with samples of atmospheric particulates (< 1µm)

AGUDELO-CASTAÑEDA, D. M.; Teixeira, E.C.; Schneider, I.; Rolim, S.; Balzaretti, N.

A ser submetido na revista *Journal of Aerosol Science*

INFRARED SPECTRA OF EMISSIVITY, TRANSMITTANCE AND REFLECTANCE OF PAHs AND COMPARISON WITH SAMPLES OF ATMOSPHERIC PARTICULATES (< 1µm)

Dayana M. Agudelo-Castañeda[1], Elba Calesso Teixeira[1,2], Ismael Schneider[1], Silvia Rolim[1], Naira Balzaretti[3], Gabriel Silva e Silva[4]

[1] Programa de Pós-graduação em Sensoriamento Remoto, Universidade Federal do Rio Grande do Sul (UFRGS), Porto Alegre, RS, Brazil
[2] Fundação Estadual de Proteção Ambiental Henrique Luís Roessler, Porto Alegre, RS, Brazil.
[3] Instituto de Física, Universidade Federal do Rio Grande do Sul (UFRGS), Porto Alegre, RS, Brazil
[4] Engenharia Química, Centro Universitário La Salle.

ABSTRACT

PAHs are a group of various complex organic compounds composed of carbon and hydrogen and two or more condensed benzene rings. In the atmosphere are produced from incomplete combustion or pyrolysis of organic matter. Amongst the PAH sources are coal and wood burning, oil and gas burning, vehicles engines and open burning. PAHs are of great concern to human health mainly because of their known carcinogenic and mutagenic properties. Consequently, is very important to study atmospheric PAHs, especially associated with ultrafine particles. This study aimed to identify the spectral features of PAHs in samples of particulate matter <1µm ($PM_{1.0}$) using infrared spectrometry. Spectral measurements of emissivity and transmittance were obtained by infrared spectroscopy using FTIR D&P and BOMEM MB-series FTIR-Hartmann & Braun Michelson spectrometers, respectively. The identification of the spectra molecular vibrations was assigned by comparison with previous works.

The solid PAHs standards results allowed to effectively identify PAHs in atmospheric particulate matter. The results of the $PM_{1.0}$ samples compared with solid standards and other studies showed that in the 680-900 cm^{-1} spectral range appeared the greatest number of bands due to CC out-of-plane angular deformations and CH out-of-plane angular deformations. Bands of medium intensity in the 2900-3050 cm^{-1} region were also observed, although with lower intensity due to CH stretching, typical of aromatic compounds. Bands in the 900-2000 cm^{-1} spectral region were observed although with lower intensity. The transmittance spectra results were consistent with PAHs previous

studies. This study confirms that these PAHs can be distinguished by their infrared spectral fingerprints.

1. INTRODUCTION

Particulate matter is of great interest because is one of the pollutants that may have negative human health impacts. Atmospheric aerosols contribute to adverse health and environmental effects, environmental visibility degradation and radiative forcing (Jacobson and Hansson, 2000). In order to understand and mitigate the atmospheric aerosol impacts is important to determine its physical and chemical properties (Coury and Dillner, 2009).

In the present study samples of particulate matter <1µm ($PM_{1.0}$) were collected, which are more hazardous because they can enter the respiratory tract (Slezakova et al., 2007). Also, because they have a larger specific area they can absorb greater concentrations of toxic and/or carcinogenic compounds, which justifies the importance of this study.

Polycyclic aromatic hydrocarbons (PAHs) are a group of several complex organic compounds consisting of carbon and hydrogen and two or more condensed benzene rings (Ravindra et al., 2008). PAHs are of great concern to the public health mainly due to their known carcinogenic and mutagenic properties (Panther et al., 1999). In addition, PAHs recognized as carcinogenic are primarily associated with particulate matter and their greatest concentrations are present in the respirable fraction, typically smaller than 5µm (Di Filippo et al., 2010; Sienra et al., 2005). PAHs are generated from the incomplete combustion or pyrolysis of organic matter (Li *et al*., 2005). Coal, wood and oil combustion, and vehicle engines are the major contribution of PAH sources in the atmosphere. In urban environments, various studies have reported that mobile emissions are the primary source of pollution by fine and ultrafine particles (Harrison et al., 1999; Shi and Harrison, 1999; Shi et al., 1999) and that heavy traffic and vehicles, especially those running on diesel, are the main sources of PAHs (Tsapakins et al., 2002; Fang et al., 2004; Guo, 2003; Manoli et al., 2004; Ravindra et al., 2006; Ströher et al., 2007).

Many studies have been conducted for analysis of PAHs using gas chromatography associated with mass spectrometry (GC/MS) (Dallarosa et al., 2005b, 2005a; Teixeira et al., 2012), although this method has many disadvantages. GC/MS requires a relatively large amount of aerosol mass, extraction, complex derivatization procedures for detecting

compounds of varying polarity, and it is not possible to detect large molecules (Yu et al., 1998). In contrast, spectroscopy has some advantages. For individual aerosol particles, spectroscopy can perform chemical fingerprinting (Allen and Palen, 1989). Among other advantages of spectroscopy is its ability to detect compounds in small amounts without extraction or derivatization (nondestructive method); instrumentation can be used in the sampling site, thus eliminating losses or transformations during transportation, cooling and storage (Allen et al., 1994; Marshall et al., 1994; Coury and Dillner, 2008; Navarta et al., 2008), and perform measurements in virtually real time. Also, in spectroscopy, small samples of diverse sizes can be used, and there is no need for sample preparation. With this technique, several samples can be selected to perform the GC/MS quantitative analysis later, which is beneficial because it reduces costs.

The FTIR technique can be used to identify a compound or investigate the chemical composition of a sample through its vibrational spectrum, which is considered as one of its most characteristic physical-chemical properties, particularly in organic compounds. The vibrational modes depend on the type of the internal structure of the constituents, the size of the ionic radius, bonding forces and ionic impurities contained in the matter (Meneses, 2001). The total energy contained in the material consists of the components associated to electronic, vibrational, rotational and translational energy. The infrared spectrum covers only the region of energy corresponding to the vibrational and rotational modes, bringing intrinsic information on the chemical and structural composition of the material.

The present paper focused on the analysis of infrared emissivity and transmittance spectra of PAHs solid standards and $PM_{1.0}$ samples. The objective was to identify PAHs in the emissivity and transmittance spectra of $PM_{1.0}$ samples collected on filters without prior treatment.

2. MATERIALS AND METHODS

2.1 Instruments

To obtain Fourier transform infrared (FTIR) emissivity spectra was used the portable field spectrometer model 102F of Design and Prototypes. Analyses were carried out in the *Centro Estadual de Pesquisa em Sensoriamento Remoto e Meteorologia* (CEPSRM) (State Research Center for Remote Sensing and Meteorology) of the Federal University of Rio Grande do Sul (UFRGS). FTIR consists of an optical/electronic module, the

Michelson interferometer and infrared detectors. The spectrometer has two detectors, an InSb (Indio-antimony) and a MCT (Mercury-cadmium-tellurium) detector covering 3330-2000 cm^{-1} and 2000-700 cm^{-1} spectral ranges, respectively, cooled by liquid nitrogen (Salisbury, 1998). Also, has a set of blackbodies that can be set to different temperatures in between 5°C and 60°C during the instrument calibration. The spectral range analyzed was from 1660 to 700 cm^{-1}, with a spectral resolution of 4 cm^{-1} and spectral accuracy of + / - 1 cm^{-1}. 1660-3330 cm^{-1} range was not analyzed due to low signal to noise ratio of the equipment in this range (Korb et al., 1996). Also, within this range (1660 - 3330 cm^{-1}) transmittance is low due to the presence of absorption bands of methane, CO_2 and water vapor (Korb et al., 1996). Data were obtained from an average of 100 scans, i.e., 100 co-added interferograms. Measurements were performed at a distance less than one meter (50 cm) to minimize atmospheric attenuation (Korb et al., 1996). In addition, all emissivity measurements were performed in conditions of clear sky without clouds and relative humidity ranging from low to moderate (<60%). A foreoptic of 2.54 cm in diameter at a distance less than 50 cm was used to guarantee that the field of view (FOV) was smaller than the sample, which had a diameter of 47 mm.

The transmittance spectra were obtained by a BOMEM MB-series FTIR-Hartmann & Braun Michelson spectrometer equipped with DTGS detector. The analyzes were performed at the Institute of Physics of the Universidade Federal do Rio Grande do Sul (Federal University of Rio Grande do Sul).The transmittance spectra were measured with a resolution of 4 cm^{-1}, and 50 scans were taken to obtain an appropriate signal to noise ratio. The spectral range measured was from 400 to 4000 cm^{-1}. The PM_1 transmittance spectra were collected from each sample and are presented in arbitrary units (a.u.). The spectra were calculated using a blank filter, without sample, as background.

2.3 Calibration and operation of the FTIR spectral radiometer

Emission and responsiveness of the instrument were calibrated with blackbody with controlled temperature (Salisbury, 1998). Calibration consisted of measuring the radiation of two blackbodies at two known temperatures, and the own emission of the instrument is deducted. In addition, calibration of downwelling radiance is also performed. Downwelling radiance of the hemisphere above the target is measured by a reflector located at the target, a gold plate with emissivity of $\varepsilon = 0.040$ in the spectral

range. More details on the radiometric calibration of the instrument can be found in the studies by Hook and Kahle, (1996) e Korb et al., (1996).

Measured radiance actually consists of the sum of various radiances entering the equipment sensor, and for the conditions used in the present study the equation (1) that explains the relation between the radiances can be read as (Salvaggio and Miller, 2001):

$$L_s(\lambda) = \varepsilon_s(\lambda) B(\lambda, T_S) + [1 - \varepsilon_S(\lambda)] L_{DWR}(\lambda) \quad (1)$$

where:

$L_S(\lambda)$ is the total spectral radiance entering the sensor; B (λ,T_S) is the radiance of a blackbody at the sample temperature (T_S); (1 - ε_s) is the sample reflectance; and L_{DWR} is the downwelling radiance.

The sample emissivity can be determined using the equation (2), where the radiance measured must be divided by the Planck function of blackbody radiance at the sample temperature (T_S), which is unknown.

$$\varepsilon_s(\lambda) = \frac{L_s(\lambda) - L_{DWR}(\lambda)}{B(\lambda, T_s) - L_{DWR}(\lambda)} \quad (2)$$

Where:

$\varepsilon_s(\lambda)$: emissivity of the sample surface as a function of the wavelength
$L_s(\lambda)$: calibrated radiance of the sample
$L_{DWR}(\lambda)$: calibrated radiance of the incident radiance
$B(\lambda,T_s)$: Planck function at the sample temperature

Temperature of the sample was defined according to the procedure described by Johnson et al., (1998) and Ribeiro da Luz and Crowley, (2007). Firstly, the temperature measured by an infrared digital thermometer Minipa MT-350 with accuracy of ±2°C was selected. Figure 1 shows an example of emissivity spectra obtained as a function of the diverse temperatures chosen. The spectral radiometer calculates the spectra in μm, and using the Excel program were converted to frequency (cm^{-1}) in order to compare the results with other studies. Figure 1, water bands in 8.18, 8.24 and 12.58 μm show the residual characteristics of the downwelling radiance (Ribeiro da Luz, 2005). If the temperature

chosen is higher than the actual temperature of the sample (overestimated temperature), the residual characteristics of the downwelling radiance will point downwards. If the temperature chosen is lower than the sample, the residual characteristics will point upwards (underestimated temperature), similarly to the downwelling radiance (Horton et al., 1998). Through a trial-and-error process, it was possible to obtain the best emissivity curve, i.e., in which the residual characteristics of the downwelling radiance were minimized. May be seen that for the spectrum obtained for a temperature of 32°C, the residual characteristics of downwelling radiance do not exist, indicating that this is the appropriate temperature. The configuration geometry of the emissivity measurements was as follows: distance of <50cm between the sensor and the sample; sample size of 47 mm diameter; optical angle of 90°.

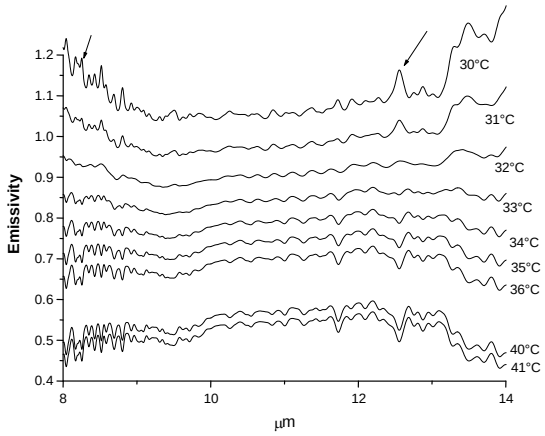

Figure 6. Emissivity spectra obtained for a sample temperature range of 30°C to 41°C

2.4 Preparation of the PAHs solid standards

Transmittance spectra: the solid standards were prepared in solid KBr pellets to obtain transmittance spectra.

Emissivity spectra: the standards were placed with no preparation in 50-mm diameter dishes. Sigma-Aldrich PAHs solid standards with 99% purity were used. Spectra of the following standards were obtained: fluoranthene, pyrene, benzo [*a*]pyrene and benzo[*a*]anthracene.

2.5 Sampling of atmospheric particulate matter

PM_1 sampling was performed by a sequential automatic particle sampler model PM162M from Environnement S.A. using a volumetric flow rate of 1.0 $m^3 \cdot h^{-1}$. PM_1samples were collected on PTFE (polytetrafluorethylene) filters with 47 mm diameter, Zefluor™ membrane, specifically designed for organic sampling (Peltonen and Kuljukka, 1995). The equipment for collection of particulate matter <1µm (PM_1) was installed at the following geographic coordinates (UTM) 29°49'06"S / 51°09'34"W (Sapucaia do Sul); and 29°55'50"S / 51°10'56"W (Canoas). Sampling was carried out at a constant flow rate of $1m^3 \cdot h^{-1}$ for 72h and 12h for the determination of emissivity (FTIR) and transmittance spectra, respectively. These sampling times were found to be appropriate for a good resolution of bands corresponding to organic species. Studies show that PTFE filters are more adapted to FTIR tests: have lower absorption bands (overlapping peaks) in infrared analyses than nucleopore or quartz filters (Ghauch et al., 2006).

3. RESULTS

This section includes the results of experimental infrared spectra using the spectrometers described in the previous section. First, the emissivity spectra (FTIR) were analyzed, and then the transmittance spectra. In each case the spectra of PAHs solid standards were analyzed, viz. fluorantene, pyrene, benzo [*a*]pyrene and benzo[*a*]anthracene, and samples of particulate matter ($PM_{1.0}$) collected on PTFE filters.

The molecular vibrations derived from the peaks found in the various spectra were identified according to existing literature (Semmler et al., 1991), (Onchoke and Parks, 2011), (Onchoke et al., 2006) , (Carrasco Flores et al., 2005).

3.1 Spectra of PAHs solid standards

Emissivity

Using FTIR spectral radiometer, experimental emissivity spectra of solid standards (Sigma-Aldrich, 99% purity) of PAHs were obtained: fluoranthene and pyrene.

Identification of the spectra molecular vibrations was achieved by comparison with the spectral database developed by scientific papers previously published [Semmler et al., (1991); Onchoke and Parks, (2011); Onchoke et al., (2006); Carrasco Flores et al., (2005); Hopey et al., (2008); Allen et al., (1994); Polidori et al., (2008); Tsai and Kuo, (2006); Reff et al., (2007); Reff et al., (2005)].

Table 1 shows the designation of the features identified in the experimental emissivity spectra of fluoranthene and pyrene. Was observed that in the emissivity spectra the fluoranthene spectrum (Figure S1 in the supplementary material) had features of higher intensity than the pyrene spectrum (Figure S1 in the supplementary material). The features at 700 cm^{-1} and 1646 cm^{-1} were not included in Table 1 for being the absorption bands of CO_2 and water vapor in the atmosphere, respectively (Jellison and Miller, 2004). Vibrations from CC out-of-plane angular deformation and CH out of plane (Table 1) were identified in the 700-850 cm^{-1} spectral range for both standards. Previous studies (Semmler et al., 1991) have shown that in the 600-900 cm^{-1} spectral range at least one band will occur in the PAHs spectra.

For fluoranthene, intense and moderate bands were identified at 830 cm^{-1} and 734 cm^{-1}, defined as being CC out-of-plane angular deformation and CH out of plane (Hudgins and Sandford, 1998b; Semmler et al., 1991). Regarding pyrene, at 849 cm^{-1} and 734 cm^{-1}, were also defined as CC out-of-plane angular deformation and CH out of plane (Hudgins and Sandford, 1998a; Semmler et al., 1991). The 1000-1300 cm^{-1} spectral range contains various peaks of low intensity from CH in-plane aromatic angular deformations (Table 1), except for 1100 cm^{-1}, where the feature relating to CC stretch and CH in-plane angular deformation can be observed (Kubicki, 2001a). In the range from 1350 to 1570 cm^{-1} features of high intensity were observed in the fluoranthene spectrum, however of low intensity in the pyrene spectrum. In the fluoranthene spectrum (Table 1), the features are mostly due to the presence of five rings of cyclopentadienyl (Hudgins and Sandford, 1998a). For pyrene (Table 1) features were observed mainly in the range 1313 to 1323 cm^{-1}, resulting from the CH in-plane angular deformation. The features in the range 1358 to 1488 cm^{-1} appear as CC stretch and CH in-plane angular deformation only in the fluoranthene spectra.

Table 3. Designation of features identified in the experimental emissivity spectra of fluoranthene and pyrene in the 700-1660 cm^{-1} spectral range and in the transmittance spectra of Fluoranthene, Pyrene, Benzo[a]Pyrene and Benzo[a]Anthracene in the 400-4000 cm^{-1} spectral range. Unit: cm^{-1}.

Fluoranthene		**Pyrene**		**Benzo[a] Pyrene**	**Benzo[a] Anthracene**	**Vibrational assignments**
Emissivity	Transmittance	Emissivity	Transmittance	Transmittance	Transmittance	
	426				422	γ (CC) + γ(CH)
				455		γ (CC) + γ(CH)
					471	δ(CC) + δ(CH)
	482					δ(CC) + δ(CH)
			496			δ(CC)
					511	γ(CH)
				534		γ(CH)
			540			γ(CC) + γ(CH)
	617					τ(CCCC) + ν(CH)
				635		γ(CC) + γ(CH)
					648	γ(CH)
				689	689	γ (CC)
		710	708			γ (CC) + γ(CH)
		718				γ (CC) + γ(CH)
734		734				γ (CC) + γ(CH)
	746		748		748	γ(CH)
				762		γ(CH)
775	775	775				γ (CC) + γ(CH)
					783	γ(CH)
	826	815		822	812	γ(CH)
830			839	835		γ(CH)
		849				γ(CH)
874				874		γ(CH)
					885	γ(CH)
911	910		912			γ(CH)
	939					γ(CH)
				945		γ(CH)
					953	γ(CH)
			962			γ(CH)
	970					γ(CH)
					1009	δ(CH)
1022						ν(CC) + δ(CH)
				1034	1038	δ(CH)
1043						δ(CH)
		1065				δ(CH)
1100		1102	1095		1097	*ν*(CC) + δ(CH)

				1121		*v*(CC) + δ(CH)
1140	1134		1136			δ(CH)
1156	1159			1163		δ(CH)
				1176		δ(CH)
1180	1182		1184			δ(CH)
	1215					*v*(CC) + δ(CH)
		1244	1240	1244	1238	*v*(CC) + δ(CH)
1268				1269		*v*(CC) + δ(CH)
1293	1290					δ(CH)
		1313	1312	1312		*v*(CC)+δ(CH)
		1323				δCH
1358						*v*(CC) + δ(CH)
				1408		*v*(CC)
					1414	*v*(CC) + δ(CH)
1420	1425					v(CC) + δ(CH)
1434			1433			v(CC) + δ(CH)
	1439					δ(CH)
1456	1452			1458		*v*(CC) + δ(CH)
1471						*v*(CC) + δ(CH)
1488	1485					*v*(CC) + δ(CH)
					1499	*v*(CC) + δ(CH)
		1532				v(CC) + δ(CH)
		1552				v(CC) + δ(CH)
			1593	1595		*v*(CC)
1624						v(CC) + δ(CH)
		1644				v(CC) + δ(CH)
1646						v(CC)
	3037/3049		3028/3043	3030/3074	3030/3047	$v(CH)_{(aromatic)}$

v = Stretch; δ = In plane; γ = Out of plane

Transmittance

Experimental transmittance spectra of solid standards (Sigma-Aldrich, 99% purity) of the PAHs fluoranthene, pyrene, benzo [*a*]pyreno, benzo[*a*]anthracene were obtained using the BOMEM MB-series FTIR-Hartmann & Braun Michelson spectrometer. Figure S2 of the supplementary material shows the transmittance spectra of solid standards of fluoranthene, pyrene, benzo[*a*]pyrene, benzo[*a*]anthracene, respectively, recorded on KBr pellets. The molecular vibrations of transmittance spectra were identified by comparison with previous studies: Semmler et al., (1991); Onchoke and Parks, (2011); Onchoke et al., (2006); Carrasco Flores et al., (2005). Table 1 shows the designation of the features identified in the transmittance spectra of fluoranthene, pyrene, benzo[*a*]pyrene and benzo[*a*]anthracene. The feature at ≈2300 cm^{-1} was not included for

being the CO_2 absorption band (Jellison and Miller, 2004). Similarly to the emissivity spectra, was observed in the PAHs transmittance spectra bands strong bands in the 600-900 cm^{-1} range due to CC out-of-plane angular deformations and CH out-of-plane angular deformations, and of medium and low intensity in 1000-1500 cm^{-1} spectral range. Bands in the 900-2000 cm^{-1} spectral range were observed, however with lower intensity, expect for the CO_2 band at ≈2300 cm^{-1}. In the 3000-3100 cm^{-1} spectral range, bands were also observed, typical of aromatic compounds, due to CH stretch.

3.2 Spectra of samples of atmospheric particulate matter (PM_1)

Emissivity: Figure 2a,b shows the emissivity spectra of samples of PM_1 collected in Canoas and Sapucaia do Sul (RS), respectively. In the emissivity spectra (Figure 2) features in the range of 730-850 cm^{-1} resulting from CC out-of-plane angular deformation and CH out-of-plane can be observed. Features in the range of 1350-1500 cm^{-1} resulting from CC stretch vibrations and CH in-plane angular deformation can also be observed. In all emissivity spectra of PM_1 samples (Figure 2) different peaks occur in the 1620-1650 cm^{-1} spectral range. In this region, diverse compounds absorb, including OH present in water, alcohols and carboxylic acids, and the carbonyl stretch (C = O) more conjugated than aldehydes, ketones and acids (i.e., amides) (Reff et al., 2005). For example, the vibrational mode v_2 of liquid water occurs at 1640 cm^{-1}. Thus, such bands overlap hinders the identification of organic compounds. In the emissivity spectra, the peak at ~1100 cm^{-1} corresponds to the carbon-fluorine bond (C-F), so features at this frequency may overlap and cannot be identified (Ghauch et al., 2006) unambiguously. Concerning the PAHs identification, peak is observed at ≈830 cm^{-1}, indicating a CH out-of-plane angular deformation, possibly associated with an aromatic group (Wang et al., 2007). Other peaks can also be observed in the range of 600-900 cm^{-1}, spectral region where vibrations of CC and CH out-of-plane angular deformation can be observed, among which are the compounds studied in section "3.1 – Spectra of PAHs solid standards" (Semmler et al., 1991). Other authors showed that the 700-900 cm^{-1} spectral range is the most characteristic/distinctive region for identification of PAHs molecules (Langhoff, 1996) and that in PAHs spectra at least one band is found in the 680-900 cm^{-1} spectral range (Semmler et al., 1991).. Moreover, other authors defined the 770-900 cm^{-1} spectral range as typical of PAHs, region that corresponds to the CH out-of-plane angular deformation (Hudgins et al., 1994; Langhoff, 1996; Szczepanski and Vala, 1993). Consequently, the

bands observed in the emissivity spectra (Figure 2) at ≈732 cm^{-1}, ≈767 cm^{-1}, ≈774 cm^{-1}, ≈815 cm^{-1} ,≈830 cm^{-1}, ≈850 cm^{-1} are possibly related to PAHs molecular vibrations. The band at ≈732 cm^{-1} may be due to 4 neighboring CH units; the bands at ≈767 cm^{-1}/ ≈774 cm^{-1} appear due to 3 neighboring CH units, and at ≈815 cm^{-1} /≈830 cm^{-1}/ ≈850 cm^{-1} to 2 neighboring CH units (Semmler et al., 1991). In the 1000-1500 cm^{-1} spectral range bands were also observed due to the vibrations of CC stretch and CH in-plane angular deformation. The PAHs spectra also presented at least one band in the 3000-3100 cm^{-1} spectral range due to CH aromatic stretch.

Transmittance: Figure 3a,b,c shows the transmittance spectra of the same samples. It can be seen that one of the spectra of the samples collected in Canoas (Figure 3b) showed less pronounced peaks than in the other spectra (Figure 3a and 3c) probably because in this sample the concentration of the particulate matter collected and, consequently, of organic compounds and PAHs, was lower than in the other samples. The spectra showed different peaks in the 600-900 cm^{-1} spectral range, corresponding to the vibrations of the aromatic rings, which were also identified in the spectra of PAHs standards. Some peaks also occurred in the 1000-1500 cm^{-1} spectral range, corresponding to the C=C of aromatics, in addition to the CH out-of-plane angular deformation. Nevertheless, in the transmittance spectra, the peaks in the 1250-1300 cm^{-1} range correspond to the carbon-fluorine (C-F) bond. In this region, a high intensity peak was observed due to the influence of the filter (PTFE), so features of compounds at this frequency cannot be identified unambiguously. However, as analyzed in section "3.1 Spectra of PAHs solid standards" the aromatic organic compounds have low intensity peaks in the 3000-3100 cm^{-1} range, resulting from the vibrations from the C-H of aromatics. Consequently, the bands observed in the samples showed low intensity in this spectral region Most of the peaks intensity found in the transmittance spectra was not high probably because of the low concentrations (some nanograms per cubic meter) of the organic compounds, especially PAHs (Allen et al., 1994; Teixeira et al., 2013). For example, the bands in the 3000-3100 cm^{-1} spectral range were observed only in Figures 3a and 3c, and not in Figure 3b.

Figure 3a shows the transmittance spectrum of the particulate matter in the sample collected in Sapucaia do Sul. In the 600-900 cm^{-1} spectral range, the transmittance spectrum (Figure 3a) showed a peak at 634 cm^{-1}, identified in the spectrum of Benzo[*a*]pyrene (Table 1), although at this frequency molecular vibrations from sulfite

ions (SO_3^{2-}) present in the particulate matter can be observed (Tsai and Kuo, 2006). Peaks were observed at 715, 783 and 856 cm^{-1} , corresponding to 5, 3 and 2 CH neighboring units (connected) in the PAHs, respectively (Semmler et al., 1991). In the 1000-1500 cm^{-1} spectral range, the transmittance spectrum presented peaks at 1049, 1157 cm^{-1}, 1255 cm^{-1}, and 1467 cm^{-1}. At 1049 cm^{-1} and 783 cm^{-1} frequencies, overlap may occur due to SiO_4^{-4} ion, which also generates frequencies in this region, typical of silicate ions (Tsai and Kuo, 2006). Some of these bands were identified in the fluoranthene spectrum and benzo[*a*]pyrene spectrum (Table 1), due to CH out-of-plane angular deformations or CC stretch. A peak was also identified at 3041 cm^{-1} due to aromatic CH stretch, observed in the spectra of diverse PAHs, including pyrene. Peaks at 2920 cm^{-1} and 1722 cm^{-1} suggest the presence of aliphatic and carbonyl, respectively.

Figure 3b shows the transmittance spectrum of the particulate matter contained in the sample collected in Canoas on May 27, 2013. The spectrum shows peaks at 688 cm^{-1}, 736 cm^{-1} and 854 cm^{-1} due to CH out-of-plane angular deformations of 5, 4 and 2 CH neighboring units. Nonetheless, at 688 cm^{-1} molecular vibrations arising from sulfite ions (SO_3^{2-}) may occur (Tsai and Kuo, 2006). Bands were also identified at 1153, 1239, 1338 cm^{-1} due to CH in-plane angular deformations, and at 1454, 1522 cm^{-1} due to CC stretch and CH in-plane angular deformations. As explained above, bands in the 3000-3100 cm^{-1} spectral range were not found. Vibrations from carbonyl and aliphatic were observed in bands 1731 and 2929 cm^{-1}.

Figure 3c shows the transmittance spectrum of the particulate matter in the sample collected in Canoas. The transmittance spectrum (Figure 3c) shows peaks at 694 cm^{-1}, 752 cm^{-1}, 819 cm^{-1}. In this case, the bands were observed in the benzo[*a*]pyrene, benzo[*a*]anthracene, fluoranthene and pyrene standards (Table 1). Also, at 694 cm^{-1} molecular vibrations from sulfite ions (SO_3^{2-}) may occur (Tsai and Kuo, 2006). In the 1000-1500 cm^{-1} spectral range, the transmittance spectrum presented peaks at 1377 cm^{-1} and 1504 cm^{-1}. A peak in the 3000-3100 cm^{-1} spectral range, at 3088 cm^{-1}, was observed. This spectral region presents molecular vibrations arising from CC in-plane angular deformations and CH out-of-plane aromatic.

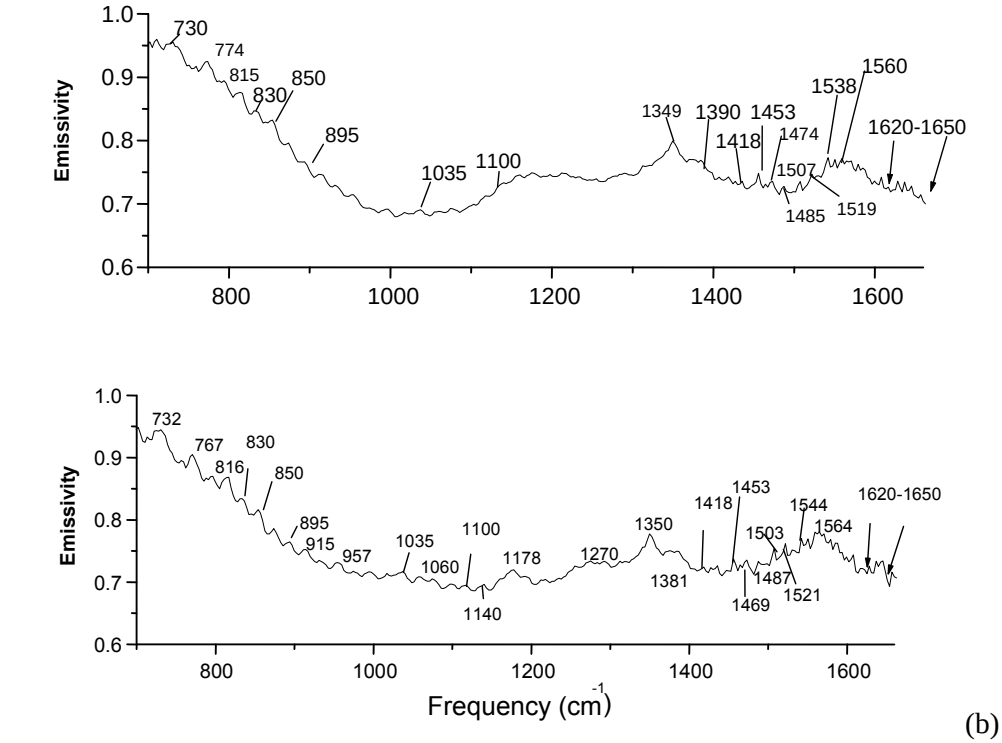

Figure 7a,b. Spectra of emissivity of PM_1 sample collected in Canoas (a), May 2-5, 2012, and in Sapucaia do Sul (b), Jan 22-25, 2012

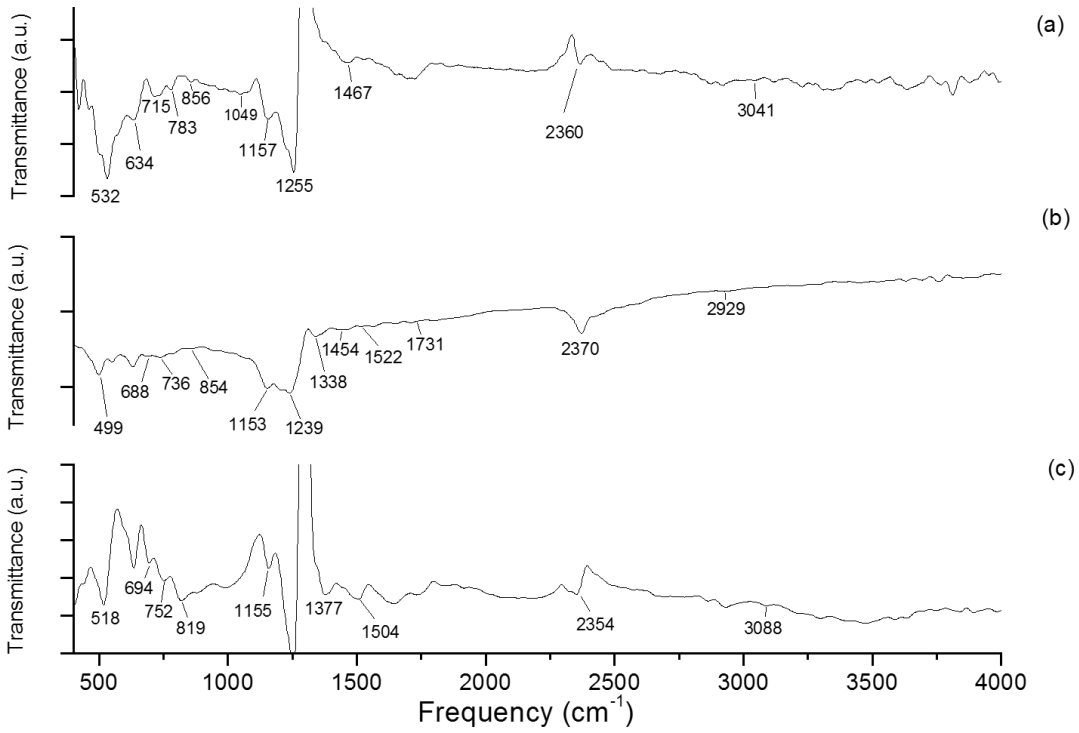

Figure 8. Spectra of transmittance of PM_1 samples collected in (a) Sapucaia do Sul, May 11, 2013, (b) Canoas, May 27, 2013 and (c) Canoas, May 4, 2013

4. DISCUSSION

Can be seen that the emissivity/transmittance spectra of the PAH solid standards showed clear bands when compared to the emissivity/transmittance spectra of PM_1 samples, probably because the intensity and width of the bands depend on composition and density (Kubicki, 2001). In addition, broad bands in the PM_1 sample spectrum was observed as a result of the interaction between PAH and the surface (Dabestani and Ivanov, 1999), because particulate matter is collected in an heterogeneous media (e.g., adsorbed on a filter). In addition, the forms and intensities depend on relative masses and bonding forces (Hamilton, 2010).

When comparing the emissivity/transmittance spectra of filters with particulate matter obtained by different spectrometers, it could be seen that the peaks/bands intensity is higher in the transmittance spectra at low frequencies, e.g., < 1000 cm^{-1}. Diverse peaks were observed in the spectral region with molecular vibrations typical of PAHs, i.e., in the 600-900 cm^{-1} spectral range, which were more pronounced in the transmittance spectra than in the emissivity spectra. On the other hand, in the emissivity spectra more peaks were identified in this spectral range. Even though the peaks in the emissivity spectra were not pronounced, the spectra showed various peaks in the 1000-1500 cm^{-1} spectral range, and in the transmittance spectra only some peaks were found. However, the advantage of the transmittance spectra is related to a larger spectral range (400 – 4000 cm^{-1}), especially in the 3000-3100 cm^{-1} region where frequencies of CH stretch m(C–H), in which some frequencies that are essential to the identification of PAHs also occur.

Briefly, samples of atmospheric particulate matter can be characterized by diverse methods using spectroscopy, either in laboratory or *in situ*. The FTIR spectrometer (used to obtain emissivity spectra) is advantageous because can be taken to the field, thus reducing errors caused by transportation or cooling of the samples, while measurements of transmittance spectra using conventional FTIR spectrometer must be performed in laboratory, which increases such errors. Nevertheless, transmittance technique has some advantages, such as: (i) a larger spectral range; (ii) no interferences in the measures taken *in situ* due to the gases present in the atmosphere. Thus, this study contributes to an extension of knowledge on both methods and their differences in the identification of PAHs in particulate matter. The choice for an appropriate technique depends on the goals

of measurement; each of the methods discussed in this paper offers unique experimental resources and requires further studies that would analyze the effects on the quantification of compounds in the samples.

5. CONCLUSIONS

FTIR and transmittance measurements in the infrared region are useful techniques for the analysis of samples of particulate matter in a simple manner.

The standards spectra allowed to contribute more effectively to the identification of PAHs in atmospheric particulate matter.

The greatest number of bands of high intensity of PAHs occurred in the 680-900 cm^{-1} spectral range due to CC-out-of-plane angular deformations and CH out-of-plane angular deformations.

This study confirms that such PAHs may be differentiated by their infrared spectral fingerprints.

REFERENCES

Allen, D. T. , Palen, E.: Recent advances in aerosol analysis by infrared spectroscopy, Journal of Aerosol Science, 20(4), 1989.

Allen, D. T., Palen, E. J., Haimov, M. I., Hering, S. V, Young, J. R.: Aerosol Science and Technology Fourier Transform Infrared Spectroscopy of Aerosol Collected in a Low Pressure Impactor (LPI / FTIR): Method Development and Field Calibration, Aerosol Science and Technology, (4), 37–41, 1994.

Carrasco Flores, E., Campos Vallette, M. M., Clavijo, R. E. C., Leyton, P., Díaz F., Koch, R.: SERS spectrum and DFT calculations of 6-nitrochrysene on silver islands, Vibrational Spectroscopy, 37(2), 153–160, 2005.

Coury, C. e Dillner, A. M.: A method to quantify organic functional groups and inorganic compounds in ambient aerosols using attenuated total reflectance FTIR spectroscopy and multivariate chemometric techniques, Atmospheric Environment, 42(23), 5923–5932, 2008.

Coury, C. e Dillner, A. M.: ATR-FTIR characterization of organic functional groups and inorganic ions in ambient aerosols at a rural site, Atmospheric Environment, 43(4), 940–948, 2009.

Dabestani, R. and Ivanov, N. I.: A compilation of Physival, Spectroscopic and Photophysical Properties of Polycyclic Aromatic Hydrocarbons, Photochemistry and Photobiology, 70(1), 10–34, 1999.

Dallarosa, J. B., Teixeira, E. C., Pires, M. and Fachel, J.: Study of the profile of polycyclic aromatic hydrocarbons in atmospheric particles (PM10) using multivariate methods, Atmospheric Environment, 39(35), 6587–6596, 2005a.

Dallarosa, J., Monego, J., Teixeira, E., Stefens, J. and Wiegand, F.: Polycyclic aromatic hydrocarbons in atmospheric particles in the metropolitan area of Porto Alegre, Brazil, Atmospheric Environment, 39, 1609–1625, 2005b.

Fang, G.-C., Chang, C.-N., Wu, Y.-S., Fu, P. P.-C., Yang, I.-L. and Chen, M.-H.: Characterization, identification of ambient air and road dust polycyclic aromatic hydrocarbons in central Taiwan, Taichung., The Science of the total environment, 327(1-3), 135–46, 2004.

Di Filippo, P., Riccardi, C., Pomata, D. and Buiarelli, F.: Concentrations of PAHs, and nitro- and methyl- derivatives associated with a size-segregated urban aerosol, Atmospheric Environment, 44(23), 2742–2749, 2010.

Ghauch, A., Deveau, P.-A., Jacob, V. e Baussand, P.: Use of FTIR spectroscopy coupled with ATR for the determination of atmospheric compounds., Talanta, 68(4), 1294–302, 2006.

Guo, H.: Particle-associated polycyclic aromatic hydrocarbons in urban air of Hong Kong, Atmospheric Environment, 37(38), 5307–5317, 2003.

Hamilton, V. E.: Chemie der Erde Thermal infrared (vibrational) spectroscopy of Mg – Fe olivines : A review and applications to determining the composition of planetary surfaces, Chemie der Erde - Geochemistry, 70(1), 7–33, 2010.

Harrison, R. M., Jones, M. and Collins, G.: Measurements of the physical properties of particles in the urban atmosphere, Atmospheric Environment, 33(2), 309–321, 1999.

Hook, S. J. e Kahle, A. B.: The Micro Fourier Transform Intefferometer (μFTIR) A New Field Spectrometer for Acquisition of Infrared Data of Natural Surfaces, Remote Sensing Environent 56, 172–181, 1996.

Hopey, J., Fuller, K., Krishnaswamy, V., Bowdle, D., Newchurch, M. J.: Fourier transform infrared spectroscopy of size-segregated aerosol deposits on foil substrates., Applied optics, 47(13), 2266–74, 2008.

Horton, K. A., Johnson, J. R. , Lucey, P. G.: Infrared Measurements of Pristine and Disturbed Soils 2 . Environmental Effects and Field Data Reduction, Remote Sensing of Environment, 4257, 1998.

Hudgins, D. M., Sandford, S. , Allamandola, L. J.: Infrared spectroscopy of polycyclic aromatic hydrocarbon cations. 1. Matrix-isolated naphthalene and perdeuterated naphthalene. The Journal of physical chemistry, 98(16), 4243–53 , 1994.

Hudgins, D. M. and Sandford, S. A.: Infrared Spectroscopy of Matrix Isolated Polycyclic Aromatic Hydrocarbons . 1 . PAHs Containing Two to Four Rings, The Journal of Physical Chemistry A, 5639(98), 329–343, 1998a.

Hudgins, D. M. and Sandford, S. A.: Infrared Spectroscopy of Matrix Isolated Polycyclic Aromatic Hydrocarbons . 3 . Fluoranthene and the Benzofluoranthenes, The Journal of Physical Chemistry A, 5639(98), 353–360, 1998b.

Jacobson, M. C. e Hansson, H.: Organic Atmospheric Aerosol, Review and State of Science, Reviews of Geophysics, 38(2), 267–294, 2000.

Jellison, G. P. , Miller, D. P.: Plume structure and dynamics from thermocouple and spectrometer measurements, SPIE Proceedings, 5425, 232–243, 2004.

Johnson, J. R., Lucey, P. G., Horton, K. A. and Winter, E. M.: Infrared Measurements of Pristine and Disturbed Soils 1 . Spectral Contrast Differences between Field and Laboratory Data, Remote Sensing of Environment, 46, 34–46, 1998.

Korb, a R., Dybwad, P., Wadsworth, W. and Salisbury, J. W.: Portable Fourier transform infrared spectroradiometer for field measurements of radiance and emissivity., Applied optics, 35(10), 1679–92, 1996.

Kubicki, J. D.: Interpretation of Vibrational Spectra Using Molecular Orbital Theory Calculations, Reviews in Mineralogy and Geochemistry, 42(1), 459–483, 2001a.

Kubicki, J. D.: Interpretation of Vibrational Spectra Using Molecular Orbital Theory Calculations, Reviews in Mineralogy and Geochemistry, 42(1), 459–483, 2001b.

Langhoff, S. R.: ChemInform Abstract: Theoretical Infrared Spectra for Polycyclic Aromatic Hydrocarbon Neutrals, Cations, and Anions., ChemInform, 27(25), 1996.

Li, M., McDow, S., Tollerud, Mazureka, M. Seasonal abundance of organic molecular markers in urban particulate matter from Philadelphia, PA. Atmospheric Environment, 40 (13) 2260-2273, 2005.

Manoli, A., Kouras, K., Samara. Profile Analysis of Ambient and Source Emitted Particle-bound Polycyclic Aromatic Hydrocarbons from Three Sites in Northern Greece, Chemosphere 56, 867-878, 2004.

Marshall, T. L., Chaffin, C. T., Hammaker, R. M., Fateley, W. G. An introduction to open-path FT-IR. Atmospheric monitoring. Environmental Science & Technology 28, 224A-232A,1994.

Meneses, P. R. Fundamentos de Radiometria Óptica Espectral. In: Meneses, P. R.; Netto, J. S. M. (Orgs.) Sensoriamento Remoto: Reflectância dos alvos naturais. Brasília, DF: UnB; Planaltina: Embrapa Cerrados. 26p. 2001.

Navarta, M. D. F., Ojeda, C. B., Rojas, F. S.: Aplicación de la Espectroscopia del Infrarrojo Medio en Química Analítica de Procesos. Boletín de la Sociedad Química de México 2 (3) 93–103. 2008

Onchoke, K. K., Hadad, C. M. and Dutta, P. K.: Structure and vibrational spectra of mononitrated benzo[a]pyrenes., The journal of physical chemistry, 110(1), 76–84, 2006.

Onchoke, K. K. and Parks, M.: Experimental and theoretical study of vibrational spectra of 3-nitrofluoranthene, Journal of Molecular Structure, 999(1-3), 22–28, 2011.

Panther, B. C., Hooper, M. A. , Tapper, N. J.: A comparison of air particulate matter and associated polycyclic aromatic hydrocarbons in some tropical and temperate urban environments, Atmospheric Environment, 33, 4087-4099, 1999.

Peltonen, K. , Kuljukka, T.: Air sampling and analysis of polycyclic aromatic hydrocarbons, Journal of Chromatography A, 710(1), 93–108, 1995.

Polidori, A., Turpin, B. J., Davidson, C. I., Rodenburg, L. , Maimone, F.: Organic PM 2.5 : Fractionation by Polarity, FTIR Spectroscopy, and OM/OC Ratio for the Pittsburgh Aerosol, Aerosol Science and Technology, 42(3), 233–246, 2008.

Ravindra, K., Bencs, L., Wauters, E., De Hoog, J., Deutsch, F., Roekens, E., Bleux, N., Berghmans, P. and Van Grieken, R.: Seasonal and site-specific variation in vapour and aerosol phase PAHs over Flanders (Belgium) and their relation with anthropogenic activities, Atmospheric Environment, 40(4), 771–785, 2006.

Ravindra, K., Sokhi, R. and Vangrieken, R.: Atmospheric polycyclic aromatic hydrocarbons: Source attribution, emission factors and regulation, Atmospheric Environment, 42(13), 2895–2921, 2008.

Reff, a, Turpin, B. J., Porcja, R. J., Giovennetti, R., Cui, W., Weisel, C. P., Zhang, J., Kwon, J., Alimokhtari, S., Morandi, M., Stock, T., Maberti, S., Colome, S., Winer, a, Shendell, D., Jones, J. and Farrar, C.: Functional group characterization of indoor, outdoor, and personal PM: results from RIOPA., Indoor air, 15(1), 53–61, 2005.

Reff, A., Turpin, B. J., Offenberg, J. H., Weisel, C. P., Zhang, J., Morandi, M., Stock, T., Colome, S. and Winer, A.: A functional group characterization of organic PM2.5

exposure: Results from the RIOPA study, Atmospheric Environment, 41(22), 4585–4598, 2007.

Ribeiro da Luz, B. 2005. Propriedades espectrais das plantas no infravermelho termal (2,5-14 μm): da química ao dossel. – São Paulo. Ph.D. dissertation. São Paulo University.

Ribeiro da Luz, B. and Crowley, J. K.: Spectral reflectance and emissivity features of broad leaf plants: Prospects for remote sensing in the thermal infrared (8.0–14.0 μm), Remote Sensing of Environment, 109(4), 393–405, 2007.

Del Rosario Sienra, M., Rosazza, N. G. and Préndez, M.: Polycyclic aromatic hydrocarbons and their molecular diagnostic ratios in urban atmospheric respirable particulate matter, Atmospheric Research, 75(4), 267–281, 2005.

Salisbury, J. W. .: Spectral measurements field guide, Published by the Defense Technology Information Center as Report No. ADA362372, Earth Satellite Corporation, 1998.

Salvaggio, C. and Miller, C. J.: Comparison of field and laboratory collected midwave and longwave infrared emissivity spectra / data reduction techniques, Proceedings of the SPIE, Image Exploitation and Target Recognition, Algorithms for Multispectral, Hyperspectral, and Ultraspectral Imagery VII, 4381, 2001.

Semmler, J., Yang, P. W. and Crawford, G. E.: Gas chromatography/Fourier transform infrared studies of gas-phase polynuclear aromatic hydrocarbons, Vibrational Spectroscopy, 2(4), 189–203, 1991.

Shi, J. P. and Harrison, R. M.: Investigation of Ultrafine Particle Formation during Diesel Exhaust Dilution, Environmental Science & Technology, 33(21), 3730–3736, 1999.

Shi, J. P., Khan, a. a. and Harrison, R. M.: Measurements of ultrafine particle concentration and size distribution in the urban atmosphere, Science of The Total Environment, 235(1-3), 51–64, 1999.

Slezakova, K., Pereira, M. C., Reis, M. a. and Alvim-Ferraz, M. C.: Influence of traffic emissions on the composition of atmospheric particles of different sizes – Part 1: concentrations and elemental characterization, Journal of Atmospheric Chemistry, 58(1), 55–68, 2007.

Socrates, G.: Infrared and Raman Characteristic Group Frequencies. 3th Ed. John Wiley & Sons, Ltd. England. 2004.

Ströher, G. L., Poppi, N. R., Raposo, J. L. and Gomes de Souza, J. B.: Determination of polycyclic aromatic hydrocarbons by gas chromatography — ion trap tandem mass spectrometry and source identifications by methods of diagnostic ratio in the ambient air of Campo Grande, Brazil, Microchemical Journal, 86(1), 112–118, 2007.

Szczepanski, J. , Vala, M.: Infrared Frequencies and Intensities for Astrophysically Important Polycyclic Aromatic Hydrocarbon Cation, The Astrophysical Journal, 414,646-655, 1993.

Teixeira, E. C. Mattiuzi C.D., Agudelo-Castañeda D.M., Garcia K. O., Wiegand F.: Polycyclic aromatic hydrocarbons study in atmospheric fine and coarse particles using diagnostic ratios and receptor model in urban/industrial region, Environmental monitoring and assessment, 185 (11), 9587-9602, 2013.

Teixeira, E. C., Agudelo-Castañeda, D. M., Fachel, J. M. G., Leal, K. A., Garcia, K. D. O. ,Wiegand, F.: Source identification and seasonal variation of polycyclic aromatic hydrocarbons associated with atmospheric fine and coarse particles in the Metropolitan Area of Porto Alegre, RS, Brazil, Atmospheric Research, 118, 390–403, 2012.

Tsai, Y., Kuo, S.: Development of diffuse reflectance infrared Fourier transform spectroscopy for the rapid characterization of aerosols, Atmospheric Environment, 40(10), 1781–1793, 2006.

Tsapakis, M., Lagoudaki, E., Stephanou, E.G., Kavouras, I.G., Koutrakis, P., Oyola, P., Von Baer, D., 2002. The composition and sources of HV PM102.5 organic aerosolin two urban areas of Chile. Atmospheric Environment 36, 3851–3863.

Wang, Y., Szczepanski, J. and Vala, M.: Vibrational spectroscopy of neutral complexes of Fe and polycyclic aromatic hydrocarbons, Chemical Physics, 342(1-3), 107–118, 2007.

Yu, J., Flagan, R. C., Seinfeld, J. H. (1998). Identification of products containing –COOH, -OH, AND –C=O in atmospheric oxidation of hydrocarbons. Environmental Science & Technology, 32(16), 2357–2370

SUPPLEMENTARY MATERIAL

Title: Infrared spectra of emissivity, transmittance and reflectance of PAHs and comparison with samples of atmospheric particles (< 1µm)

Dayana M. Agudelo-Castañeda[1], Elba Calesso Teixeira[1,2], Ismael Schneider[1], Naira Balzaretti[3], Gabriel Silva e Silva[4]

[1] Programa de Pós-graduação em Sensoriamento Remoto, Universidade Federal do Rio Grande do Sul (UFRGS), Porto Alegre, RS, Brazil
[2] Fundação Estadual de Proteção Ambiental Henrique Luís Roessler, Porto Alegre, RS, Brazil.
[3] Instituto de Física, Universidade Federal do Rio Grande do Sul (UFRGS), Porto Alegre, RS, Brazil
[4] Engenharia Química, Centro Universitário La Salle.

LIST OF FIGURES

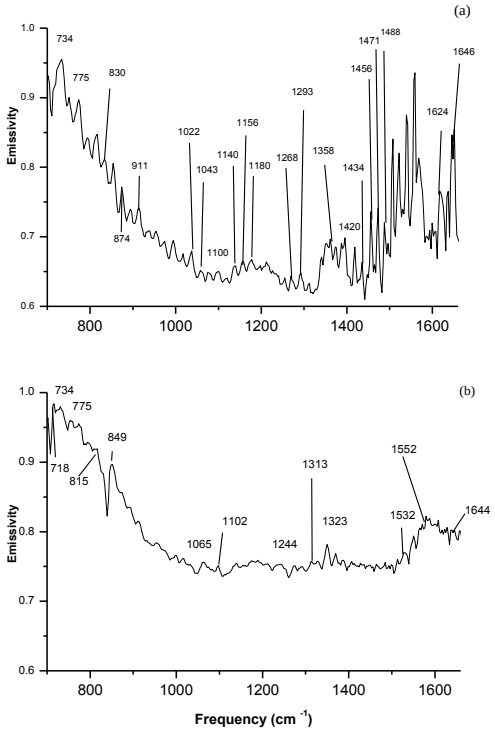

Figure S9a,b,. Emissivity spectrum of Fluoranthene (a) and Pyrene (b) recorded in 47-mm dishes

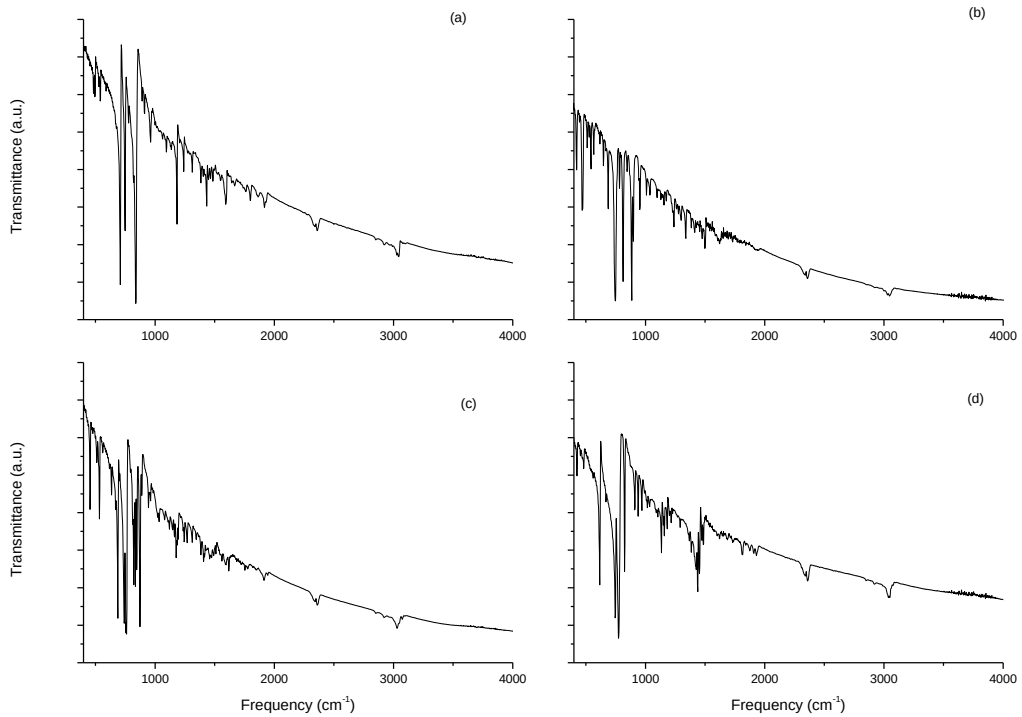

Figure S10 a,b,c,d. Transmittance spectra of Pyrene (a), Benzo[*a*]anthracene (b) Benzo[*a*]pyrene (c), Fluoranthene (d) recorded on KBr pellets

CAPITULO VI

Evaluation of particle number-mass concentration distribution and gaseous pollutants in urban area

AGUDELO-CASTAÑEDA, D. M.; Teixeira, E.C.; Schneider, I.; Pereira, F.N.; Silva, L.F.S.

A ser submetido na Revista *Atmospheric Chemistry and Physics*

Evaluation of particle number-mass concentration distribution and gaseous pollutants in urban area

Dayana M. Agudelo-Castañeda[1], Elba C. Teixeira[1,21], Ismael L. Schneider[1], Felipe N. Pereira[2], Luis F.O. Silva[3]

[1] Programa de Pós-graduação em Sensoriamento Remoto, Universidade Federal do Rio Grande do Sul (UFRGS), Porto Alegre, RS, Brazil

[2] Fundação Estadual de Proteção Ambiental Henrique Luís Roessler, Porto Alegre, RS, Brazil.

[3] Laboratory of Environmental Researches and Nanotechnology Development, Centro Universitário La Salle, Mestrado em Avaliação de Impactos Ambientais em Mineração, Canoas, RS, Brazil

Abstract

Particle number concentration (PN) is of greater significance because PN may indicate better than particle mass (PM) the vehicle emission influence, characteristic of the urban region. However, PM have been mainly investigated and air quality standards are stated for PM concentrations. Consequently, the objective was to evaluate the PN and PM concentration variability in their size ranges and their relationship with O_3, NO, NO_2, and NO_x in order to have a more accurate assessment of atmospheric particles sources in the study area: the Metropolitan Area of Porto Alegre, Brazil. PN and PM were measured using the CPM module with the MP101M analyzer. NO_x (NO, NO_2) concentrations were measured with AC32M, while O_3 with O342M of ENVIRONNEMENT S.A. Sampling period was two years: 2012 and 2013. Principal Component Analysis (PCA) was applied to the set of variables using SPSS®. Results showed PN concentrations were higher for fine fractions (PR1 and PR2.5), while PM were higher for the coarser fractions ($PM_{2.5}$ and PM_{10}). Highest gases (NO_2, O_3) and PN concentrations were observed during the day, whereas highest NO, NO_x and PM concentrations were at night. Besides, higher PN, PM and gases (NO, NO_2, NO_x) were observed in winter, showing seasonal influences. PN and PM presented peaks between 9h and 10h explained by rush hours of mobile sources emissions that increased fine and ultrafine particles. This influence was confirmed by the week variability, where PN and PM, NO, NO_2, NO_x concentrations were higher on weekdays than weekends. Moreover, was obtained correlation between nitrogen oxides and PN concentration, especially of fine particles (PR1 and PR2.5), thus confirming the influence of vehicle exhaust emissions.

Keywords: Air quality, particle number, particle matter, nitrogen oxides, ozone.

1. Introduction

Deterioration of urban air quality due to airborne particulate matter (PM) is receiving more attention. Among the main sources of PM are intense emissions from motor–

[1] Corresponding author. Av. Borges de Medeiros, 261, Porto Alegre - RS - Brazil ,90020-021. Tel: + 55 51 32889408. E-mail address: gerpro.pesquisa@fepam.rs.gov.br (E. C. Teixeira).

vehicles traffic and industrial activities. In recent years, understanding atmospheric particles has been an increasing concern because of their potential to cause adverse health effects, visibility and global climate change (Chen et al., 2010; Colette et al., 2008). The pollution caused by atmospheric particles is not only related to its concentrations, but also to particle size distribution. Information about the mass concentration of suspended particulates can be a good indicator for pollution alert, nevertheless the size distribution and nature of these particles are also important parameters for the determination of their potential impact on human health (Renard et al., 2010). The particle size depends on the multiplicity of sources and processes which lead to their formation, and therefore, on the material from which the particles were formed (Morawska et al., 2008a). Particles may have several sources: products of combustion or formation from chemical reactions in the atmosphere. May be concluded that airborne PM is a complex mixture of many different chemical species (Herrmann et al., 2006) and different physical properties (Pastuszka et al., 2003) originating from a variety of sources. Particle with different aerodynamic diameter have different lifetimes in the atmosphere and those with size <1 μm (PM_1) can travel for days over distances of several hundred kilometers from the source (Splinder et al., 2010). Emissions from gasoline and diesel fuelled vehicles remain the dominant source in polluted urban environments of atmospheric particle number (PN) concentration (Morawska et al., 2008b). Mainly heavy duty vehicles, which contribute more to PN and PM_1 emissions (Koegh et al., 2009). PM_1 measurements provide information about combustion-generated processes, while PM_{10} measurements provide information about mechanical process that produces coarse particles (Morawska et al., 2008b).

Although automotive vehicles are the main source of fine particles in urban areas, the number and size distribution of particles can change rapidly due to the influence of transformation processes, such as coagulation and condensation, and to turbulence, which improves mixing and dilution (Kumar et al., 2011). Moreover, vehicle emissions are a major source of nitrogen oxides emissions, especially in the form of NO (Gaffney & Marley, 2009), causing an almost direct emission in the boundary layer. Diesel engines produce five times the amount of NO_x by mass of burnt fuel compared to gasoline vehicles. Furthermore, the addition of biodiesel to diesel can slightly increase NO_x emissions (Coronado et al., 2009). Recent research shows that the proportion of NO_x in the form of NO_2 from diesel vehicles has increased markedly over the past few years, with important effects on ambient concentrations of NO_2 (Carslaw, 2005; Anttila and

Tuovinen, 2010; Alvarez et al., 2008). These increases have been due to the types of after treatment used on diesel vehicles which result in the increased oxidation of NO to NO_2. These pollutants and atmospheric particles are capable of causing adverse effects on human health (WHO, 2006).

Though not having significant natural or anthropogenic emission sources (PORG, 1997**)**, secondary pollutants such as NO_2 and tropospheric O_3 may be formed by different reactions of primary pollutants in the air (Finlayson-Pitts & Pitts, 2000). According to Jenkin & Clemitshaw (2000), the main conversion reactions between NO and NO_2 are reactions (1), (2), (3), and (4):

$$2\,NO + O_2 \rightarrow 2\,NO_2 \quad (1)$$

However, under most tropospheric conditions, reaction (1) is not significant, and the major way by which NO is converted to NO_2 is by reaction (2) with O_3:

$$NO + O_3 \rightarrow NO_2 + O_2 \quad (2)$$

Under the influence of solar radiation during the day, NO_2 undergoes photolysis and reconverts to NO by reactions (3) and (4) and produce O_3:

$$NO_2 + h\nu(\lambda < 420\,\text{nm}) \rightarrow NO + O(^3P) \quad (3)$$

$$O(^3P) + O_2(+M) \rightarrow O_3 + M \quad (4)$$

where M is a third compound (typically N_2 or O_2), which absorbs the vibrational energy in excess and thereby stabilizes the O_3 molecule formed, *hν* is the energy of one photon (λ <424 nm), and O (^{3}P) is active monatomic oxygen (Han et al., 2011). Photolysis of NO_2 is an important source of O_3 generation (Zielinska, 2005). NO_x has a short chemical lifetime and its major effects on O_3 are limited to its proximity to emission sources (Uherek et al., 2010). In urban areas, concentrations of O_3 are usually lower than in rural areas due to its reaction with NO (from vehicle emissions) to produce NO_2.

Nowadays, existing ambient air quality standards are restricted to $PM_{2.5}$ and PM_{10}, even though these PM fractions, especially PM_{10} are generated by mechanical processes. PN provide valid data of particular importance in epidemiological studies for the evaluation of health effects from PM in ambient air (Tittarelli et al., 2008). Actual regulations are unable to effectively control submicrometer particles emitted from combustion sources such as motor vehicles that have a much stronger impact on human health and a longer

residence time (Aurangojeb, 2011). Submicrometer particles are difficult to measure using the traditional "mass concentration" concept, because these particles have low mass. PN concentration need to be controlled for several reasons such as the ability of fine fraction particles to penetrate into the lungs, affect cellular function and cause harmful effects on human health (Slezakova et al., 2007). Consequently, PN can be an important air quality indicator.

There are few studies on the atmospheric chemistry in the area of study and Brazil, specifically analyzing PN concentrations in PR1 (0.3-1.0 μm), PR2.5 (2.5-1.0 μm), and PR10 (10-2.5 μm) size ranges, which are now being measured for the first time in this specific site. This work is part of an attempt to investigate the PN and PM concentration variability in their size ranges and their relationship with gaseous pollutants (O_3, NO, NO_2, and NO_x) and weather conditions. This is important because the study of particle size distribution allows a more accurate assessment of the atmospheric particles sources in the area of study, as well as of NO, NO_2, and O_3. We also examined the variation of OX (NO_2 + O_3) and the rate of NO_2 photolysis, besides the differences in weekend and weekday concentrations.

2. Methodology

2.1. Study Area

The sampling site selected for this study was Sapucaia do Sul, located in the Metropolitan Area of Porto Alegre (MAPA). The study area is in the central-eastern part of the Brazilian state of Rio Grande do Sul. According to the Brazilian Institute of Geography and Statistics, this area covers an area of 9652.54 km^2, representing 3.76% of the state, and has a population of 4.12 millions (IBGE, 2013), i.e. 37.21% of the total population of Rio Grande do Sul. The MAPA is the most urbanized area of the Rio Grande do Sul state and is characterized by different industries including several stationary sources: oil refineries, steel mills that do not use coke, and coal-fired power plants, wood burning (Teixeira et al., 2011). Among the 31 counties of the MAPA, Sapucaia do Sul is the major contributor of atmospheric emissions due to their large diesel and gasoline vehicular fleet (Teixeira et al., 2008). The sampling site (Sapucaia do Sul) was located near the BR-116 and BR-290 highways, which are characterized by strong traffic and was chosen for being located in the county with the highest vehicular influence. Sapucaia do Sul has a stronger

vehicular influence characterized by light and heavy-duty fleet, traffic congestion, and slow vehicle speed. This site, too, has low industrial influence (oil refinery, coal fired power plant, steel mills which do not use coke) upstream from the prevailing winds

2.2. Equipments:Particles, nitrogen oxides, ozone

PN concentration in PR1 (0.3-1µm), PR2.5 (1-2.5 µm) and PR10 (2.5-10 µm) size ranges were measured using the continuous particulate monitor (CPM). The particle analyzer CPM is an optical analyzer, which uses a laser beam to measure the scattering intensity caused by atmospheric particles present in the air sample by applying the Mie scattering theory (ENVIRONNEMENT, 2010). The MP101M, based on the beta attenuation principle, was used to measure PM_{10}. Also, PM_1 and $PM_{2.5}$ were measured using the CPM module with the MP101M analyzer. However, the PM_1 concentration values may be used as indicative because the equipment is only certified for PM_{10} and $PM_{2.5}$ values. More details on the equipment are reported in Renard *et al*. (2010) and Agudelo-Castañeda et al. (2013).

NO_x (NO, NO_2) concentrations were measured with oxide analyzer (AC31M – using chemiluminescence's method), while O_3 concentration was determined by ozone analyzer (O342M – absorption of UV light), of ENVIRONNEMENT S.A. Meteorological variables: air temperature (ºC), relative humidity (%), wind direction (°), wind speed ($m \cdot s^{-1}$), and solar radiation ($W \cdot m^{-2}$) were measured continuously, at an average of 15-min intervals, using thermo hygrometer, anemometer and global radiometer, respectively, simultaneously with measurements of atmospheric pollutants concentrations.

2.3. Sampling frequency, study period and statistics

During two years: 2012 and 2013 were measured the PN concentrations in fractions PR1, PR2.5, and PR10. NO_x (NO_2 +NO) and O_3 concentrations were measured, too, during this sampling period. Measurements were made every 15 min, continuously. The database was drawn up from the raw data recorded every 15 min, and then the hourly and daily means were calculated. Data were analyzed by using SPSS software. Correlation between pollutants and meteorological parameters was done using hourly mean values by SPSS® *for windows V. 23* statistics software. The Principal Component Analysis (PCA) was

applied to the set of variables to a better interpretation and evaluation of the interrelationships of the studied data set (Jain et al., 2000; Lara et al., 2001). Also, Spearman correlation was applied using the software used SPSS® for Windows v. 23.

3. Results and Discussion

Figure 1a,b,c shows mean day and night concentrations for winter and summer of PN concentration in size ranges: PR1, PR2.5, PR10 and PM concentration: PM_{10}, $PM_{2.5}$, PM_1). Also, gases mean concentrations: NO, NO_x, NO_2 and O_3. PN concentrations (Figure 1a) were higher for fine fraction (PR1 and PR2.5) while for airborne particles mass concentration, higher values corresponded to PM_{10} followed by fine particles: $PM_{2.5}$ and PM_1. The greater PR1 concentration can be explained by the fact that number concentration generally increase as radius decrease, thus the lower radius limit is of great importance in specifying total number concentration. Similarly to this study, PR1 has been evidenced by several authors (reported for urban environment) as the fraction that showed the highest PN concentrations (Zhu, et al., 2004; Morawska et al., 2008a) because ultrafine and fine particles represents over 80% in PN but their mass concentration is insignificant compared with larger particles (Kittelson, 1998). Also, the presence of fine particles in urban environments (PR1), usually originate from vehicular sources (Chen et al., 2010), typical of this study area.

The largest mass concentrations corresponded to coarser particles: PM_{10} (Figure 1b), followed by fine particles ($PM_{2.5}$ and PM_1). Particle mass distribution generally increases as radius increases, so the total mass concentration is strongly influenced by the upper radius limit, in the coarse particle regime (Seinfeld and Pandis, 2006).

Figure 1a,b show higher airborne particle concentrations that predominated in winter, especially PM and in a lesser extent PN. These results can be explained by poor atmospheric mixing and low temperatures causing higher particles concentration in winter (Young et al., 2012) and because the boundary layer is narrower, this situation enhances particle growth (Gómez-Moreno et al., 2011). In addition, these months are characterized by atmospheric inversion particle concentration increase (Kuhn et al., 2005). Also, in summer, PN and PM concentration may be lower, probably, because of the decreased traffic intensity, higher temperatures that decrease the potential formation

of new particles, and more efficient dilution due to more intense turbulent mixing (Johansson et al., 2007).

The PN seasonal variation has been reported in others studies (Wehner and Wiedensohler, 2003; Hussein et al., 2004). These studies have revealed PN seasonal variation in lesser extent, which is consistent with the present work. The seasonal difference for PN concentration can be explained because gaseous compounds that can condense onto the particles are more diluted in summer than in winter, thus the particle growth rate is lower in summer and the atmospheric lifetime is longer (Gómez-Moreno, 2011). In winter, particle and gaseous compounds concentrations are higher and the boundary layer is narrower, enhancing particle growth by condensation and, consequently allowing higher concentrations of particles with bigger diameters.

Figure 1 also shows differences between day and night mean PN (PR1, PR2.5, PR10) and PM concentration (PM_{10}, $PM_{2.5}$ and PM_1). Were observed higher mean PN concentrations (Figure 1a) during the day, especially in the fine fraction, while mean PM concentrations (Figure 1b) were higher at night, especially in the coarser fraction. At night, due to the great spectrum range studied (between 2.5 and 10 microns) and because PM concentration may have been favored by the agglomeration of finer particles. In addition, high humidity at night resulted mass and radius increase, thus favoring the concentration of particles with larger mass (Warneck and Williams, 2012). Was observed, too, that at night (Fig. 1a,b) the decreased PN when PM concentrations were higher was likely because under higher pollution conditions, coagulation between particles and the condensation of semi-volatile species onto particles may prevail (Pey et al., 2013).

Conversely, in daytime hours, in the presence of higher solar radiation and lower PN concentrations, the nucleation processes are favored instead of the coagulation-condensation processes (Pey et al., 2013) and photochemically induced particle formation (Kumar et al., 2013).

Table 1 shows the mean mass concentrations of PM_1, $PM_{2.5}$ and PM_{10} in the present study and other parts of the world. The various studies about PM concentrations in the atmosphere becomes difficult to compare, since they are not the same in regard with sampler type and location that may produce different results. PM_{10} concentrations are slightly higher than those obtained in São Paulo, England (Birmingham), Austria (Vienna, Linz Graz), Scotland (Glasgow) and Finland (Vallila) at urban sites and are lower than in

Delhi, Agra and Lahore. $PM_{2.5}$ and $PM_{1.0}$ concentrations showed significant differences with Delhi, Agra and Lahore, with relatively higher concentrations of PM in comparison to the present study and others sites presented in Table 1.

Figure 1c show mean pollutants concentrations: NO,NO_2,NO_x,O_3. Results presented higher NO and NO_x concentrations at night, moreover NO_2 and O_3 concentrations were higher at day. Also, mean NO, NO_2, NO_x concentrations were higher in winter. However, mean O_3 concentration had, practically, no difference between winter and summer concentrations. This will be explained in the next item which shows diurnal variation of particles and gases.

3.1. Diurnal variation

Figure 2, shows daily variation of mean PN concentration for ranges PR1, PR2.5 and PR10 and PM concentration of PM_{10}, $PM_{2.5}$ and PM_1 for all the studied period. For both, PN (PR1/PR2.5/PR10) and mass concentrations (PM_{10}/$PM_{2.5}$/PM_1) two peaks were evident during 24 hours. PN and PM concentration presented a first peak in the morning between 8:00-9:00 and a second stronger peak in the evening between 18:00-19:00 (Figure 2). Morning peaks may be attributed to the beginning of the traffic flow and to an undeveloped boundary mixed layer, so that all emissions are accumulated (Wang et al., 2010). PN increased in the early hours of the day (Fig. 2), between 7:00- 8:00, due to emissions from anthropogenic sources that may supply a large fraction of the key precursor substances for nucleation. Precursor substances may enhance the gas-phase production of particles (nucleation) by photodissociation or by reaction with hydroxyl radical or ozone that are produced in the atmosphere by photochemical processes (Curtius, 2006). At night were observed higher peaks (22:00), implying an influence of the stability of the mixing layer height. However, after 22:00 was observed a reduction in PN. The decreased PN concentration was caused by coagulation between particles and the condensation of semi-volatile species onto particles (Pey et al., 2013). This peak (Figure 2) can be explained by their association with high traffic flow and atmospheric stability (influence of the development of a nocturnal thermal inversion layer, lower temperature, lower turbulence and, consequently, poor dispersion conditions) (Bigi and Ghermandi, 2011). For mass particle concentrations (PM_{10}, $PM_{2.5}$, PM_1) were observed a similar pattern, with two peaks, too, (Fig. 2), however with a time delay in relation with

PN peaks. These delay may be explained by mass concentration increase, especially PM_{10}. For example, in the early hours reduced PN concentration in the atmosphere favors new particles formation and their growth to larger sizes (Kulmala et al., 2000), while high PN concentrations promote vapors condensation on the existing particles and disfavor new particle formation (Kerminen et al., 2001). Morawska et al. (2008b) reported that PM_1 measurements provide better information in relation to $PM_{2.5}$ about contributions from combustion-generated processes, consequently aids to distinct between combustion and mechanically generated particles. In addition, the study area is characterized by fine and coarse particles, and PM_{10} provides, too, information on particles generated by mechanical processes such as resuspended particles by vehicular traffic, mechanical wear, tear of the tires, though not emitted from motor vehicles (Morawska et al., 2008b), this probably caused the delay between PN and PM peaks.

Figure 3a,b shows the mean daily variation for hourly gases concentration (NO_x, NO_2, NO, O_3) for winter and summer at the study site: Sapucaia do Sul. As explained before, the mean NO, NO_2, NO_x concentrations were higher in winter. However, mean O_3 concentration showed no difference, as reported above (Figure 1c) between winter and summer concentrations. Nevertheless, in the study area, is still unclear the reason why O_3 concentrations were low in both seasons when compared to other works done in urban areas, although some areas may show low surface ozone concentrations, too (Teixeira et al. 2009; Derwent et al., 2008; Li et al., 2005; Oltmans and Leyv II, 1994). Probably, the low O_3 concentrations compared to other studies can be attributed to the sampling site location, near the emission sources as the BR-116 freeway and an oil refinery that contribute to NO abundance, especially in the early morning. The study area has influence form heavy traffic and high NO levels, as reported and verified by several authors (Agudelo-Castañeda et al., 2013; Garcia et al., 2014; Teixeira et al., 2008; Teixeira et al., 2012; Teixeira et al., 2013, Teixeira et al., 2014). Though, free radicals and organic gases needed to convert NO to NO_2 are still been produced in sufficient concentration by photolysis reactions in order to start the NO_2 formation cycle. Moreover, when NO_2 is produced, O_3 builds up. Nonetheless, reactions involving organic gases and free radical are relatively slow and high ozone concentration may be observed downwind of the sampling site. Other authors reported that accumulation of NO_2 contributes to O_3 formation; however, O_3 may be "scavenged" where there is an abundance of NO, resulting in lower O_3 concentrations in heavy traffic areas (Abdul–Wahab et al., 2005;

Ainslie and Steyn, 2007; Geddes et al., 2009; Roberts–Semple et al., 2012; Sadanaga et al., 2008). Moreover, more researches had to be done in order to understand this pattern.

NO_x and NO_2 peaks (Figure 3a,b) occurred in the morning (8:00) and evening (19:00 to 20:00), and O_3 peak occurred near 14:00. In the morning, NO, NO_2 and NO_x peaks corresponded to the rush hours and can be linked to traffic fleet emissions originating from highways (BR-116) located near the sampling station and that presents intense traffic during weekdays. The peak formation of NO_2 is delayed 1-2 hours with the morning NO peak. NO is more reactive than NO_2 and usually this delay can be observed in polluted areas with higher NO concentration, as seen in this and other studies (Han et al., 2011). At night, NO, NO_2, NO_x showed a second peak probably due to NO emission from vehicular sources after the rush hour (Wang et al., 2010).

Though, some differences are observed in the daily variation of the mean concentration of NO, NO_2 and NO_x in winter and summer. NO and NO_x morning winter peak concentrations (Figure 3a) are higher than summer morning peaks. Possibly, because there is less emission of these pollutants: NO and NO_x, that are originating from mobile sources and because of the boundary layer mixing increasing height in summer. Similar results have been reported in previous studies in the study area and elsewhere (Agudelo-Castañeda et al., 2013; Teixeira et al., 2008; Teixeira et al., 2014).

In Figure 3 can be seen that O_3 peaks occurred around 15:00 for both summer and winter. O_3 (Eq. 3 and 4) is formed through photochemical reactions in the lower atmosphere and requires not only the presence of precursors but also of solar radiation, i.e. increased sunlight and high temperatures. Thus, in the evening hours is observed lower O_3 formation due to lack of sunlight presence.

3.2. Weekday/weekend variations

Table 2 shows the mean PN (PR1, PR2.5, PR10) and mass concentration (PM_1, $PM_{2.5}$, PM_{10}) of atmospheric particles and the studied gases (NO, NO_2, NO_x, O_3) during weekdays (Monday–Friday) and weekends, (Saturday-Sunday). The number (PR1, PR2.5, PR10) and mass concentrations (PM_1, $PM_{2.5}$, PM_{10}) of particles during weekdays were higher than weekends (Table 2). PN on weekdays, principally PR1, were higher especially in rush hours, as reported previously (Figure 2). In mass distributions, PM_{10} and $PM_{2.5}$ dominated on weekdays results. Similar results were observed in studies

reported by Agudelo-Castañeda et al., (2013) for this region. These studies showed that higher PN concentrations were observed on weekdays and lower concentrations on Sundays, except for the PR2.5 size range. The higher weekday/weekend ratio, shown in Table 2 was obtained for PR1 (ratio=1.21) and PR2.5 (ratio=1.17) fractions, respectively. These particles, may be in the accumulation mode range (diameter ≤ 1 μm) (Morawska et al., 1998) that originate from vehicles that typically emit particles in this fraction (20-60 nm gasoline; 20-130 nm diesel). These results reveal that higher PR1 and PR2.5 concentrations are, probably, due to primary emissions from motor vehicles, which are characterized by their smaller diameter (fine particles) (Morawska et al., 2008a).

PM concentrations showed that the coarse size fraction dominated (in ≈ 28% of $PM_{2.5}/PM_1$) both on weekdays as on weekends (Table 2). These suggests the presence in the study area of coarse particles (PM_{10}) that are produced by mechanical process, resuspension of road dust by wind and vehicle induced turbulence (Colbeck et al., 2011). The $PM_{2.5}$ and PM_1 concentration indicate the contribution from automobile exhaust, thus these particles would be better reflected by PN concentration (Colbeck et al., 2011), previously reported.

NO, NO_2, NO_x concentrations were higher on weekdays than weekends, while for O_3 the results were different, a higher concentration during weekends. This can be attributed to the fact that higher ozone levels on weekends is due to NO reduction emitted by vehicles (reaction 2) and/or the conversion of NO into NO_2 without consuming an ozone molecule, thus causing ozone to accumulate (reaction 1). Moreover, Marr and Harley (2002) proposed that less sunlight absorption due to lower fine particles concentrations at weekends resulted in enhanced ozone formation during weekends. On weekdays, NO concentrations that were 1.45 times higher than in weekends, affected O_3 concentrations that were 7% higher than those recorded on weekend days. During weekends, traffic decreases and NO emissions are reduced, consequently O_3 concentrations increase.

Figure 4 shows the correlation plot between NO_x and O_3 for weekdays and weekends. In weekdays, O_3 concentrations were higher for specific concentrations of NO_x (especially high values). On weekends, although the concentrations of NO_x were lower than the concentrations of O_3. This might be an indication that on weekends, the inhibition effect of NO_x on O_3 concentrations was more significant (Sadanaga et al., 2008; Roberts–Semple et al., 2012).

3.3. Correlations

Table 3 show the Pearson correlation matrix among mass (PM_1, $PM_{2.5}$, PM_{10}) ($\mu g \cdot m^{-3}$) and number concentrations (PR1, PR2.5, PR10) (N°/L), gaseous pollutants and meteorological parameters. PN concentrations were positively correlated with PM concentrations, indicating that these results are typical of urban polluted environments in which the number of particles is affected not only by primary emissions, but particle processes (particle growth / coagulation) (Johansonn et al., 2007). $PM_{2.5}$ was correlated very well with the PM_{10}, as observed in other studies (Young et al., 2012).

The higher correlation were verified between NO_x and PR1/PR2.5. This confirms that PN concentration is mainly due to vehicle exhaust particles, especially fines particles. Thus, these correlations confirms an association with primary emissions from local traffic. The PN concentrations were positively correlated with ambient temperature, solar radiation and wind speed (except PR1), but negatively correlated with relative humidity. This indicates the positive influence of transport of coarser particles (PR10, PR2.5) from near sites and of photochemistry under dry conditions on the production of particles, principally the fine fraction. High wind speed may favor the particles transport to other areas. Also, low relative humidity, high temperatures and high radiation may prevent the coagulation removal processes for smaller particles (Bigi e Ghermandi, 2011) and enhance the particle production (Shi et al., 2001; Wu et al., 2008), enhancing the PN concentration growth.

Negative correlation between mass concentration (PM_{10}, $PM_{2.5}$) and temperature was obtained, although with low values. A positive correlation between mass concentration (PM_{10}, $PM_{2.5}$, PM_1) and relative humidity and negative correlation with solar radiation and wind speed was also observed. This supports what previously explained, that high relative humidity and low temperatures values favored condensation-coagulation processes increasing the concentration of particles (less fine), thus influencing the mass concentration of particles and not number concentration. This may indicate buildup of particles in the early evening or nighttime hours (Figure 1b and 2), resulting in a greater concentration of PM at night and higher PN concentration in the day. Also, the dependence (inverse correlation) of temperature and solar radiation with PM may be due to its association with stagnation and cold fronts (Tai et al., 2010). These moments were

characterized by lower wind speed, higher relative humidity and lower solar radiation. Moreover, high temperatures in the summer, the higher solar radiation and low humidity produced dry particles not contributing to the increase of PM concentrations (Massey et al., 2012). O_3 had a different behavior, with negative correlations with the PM concentrations and positive with PN concentrations. This may indicate that the secondary photochemical processes are possibly an important influential factor (Young et al., 2012).

Figure 4 shows weekday and weekend comparison of the correlations between NO_x and O_3. The results reveal that O_3 concentrations on weekends were higher than on weekdays and the conversely NO_x concentrations were lower on weekends than on weekdays, reflecting reduced levels of vehicular emissions on weekends. Lower NO levels on weekend mornings consume less O_3 which accumulates later by photochemical reactions (Pudasainee et al., 2006). These authors also reported that the less absorption of sunlight due to lower fine particles concentrations at weekend resulted in enhanced ozone formation during weekend.

3.4. Statistics

The Principal Component Analysis (PCA) by SPSS® *for windows V. 23* statistics software was applied for the variables rank (rank produces new variables containing ranks). For better distribution of factors, varimax rotation was applied with Kaiser normalization and used to maximize the loading of one predictor variable on one component. Table 4 shows the Matrix of Principal Components of Varimax rotation with the results of four factor loads of the principal components. Only loadings with absolute values greater than 0.5 were selected for principal components. Factors associated with characteristic roots >1.0, explained 79.9% of the total variance.

Factor 1 is characterized by high positive loadings of ozone, temperature, radiation and negative loadings of NO and relative humidity. These data are consistent with those discussed previously that show ozone levels usually associated with high temperatures and high radiation (Dawson et al., 2008; Stathopoulou et al., 2008; Swamy et al., 2012). Ozone level tends to increase because of the stronger solar radiation, which helps NO_2 and O_2 dissociate into O_3, as reported above. As verified in this study O_3 concentration decrease during evening and night and can be associated with the combined effect of chemical loss by NO titration and suppressed boundary layer (Swamy et al., 2012). These

authors reported that there is no possibility for further photochemical oxidation to form O_3 at night due to lack of sunlight (Swamy et al., 2012).

Factor 2 and 3 are characterized by PN and PM concentrations, respectively. This indicates the presence of individual characteristics of particle sources in the different seasons. For example, in the atmosphere particles of different sizes can coexist together, that is fine and coarse particles, these particles can reflected traffic emission and can provide information on particles generated by mechanical process, respectively (Moraska et al., 2008b). The coarse fraction, also, can be generate by resuspension of road dust by wind and vehicle induced turbulence. Size distributions are usually presented using either PM or PN weighting. According to Figures 1 and 2, the majority of the PM distribution (i.e., the particulate mass) is found in the coarser fraction. In number distributions, most particles are found in the fine fraction. In other words, atmospheric particles may be composed of numerous small particles holding very little mass, mixed with relatively few larger particles which contain most of the total mass.

Factor 4 is characterized by high loadings of NO_x, NO_2 and NO. As shown previously, NO is a primary pollutant with high diurnal variation that correspond to traffic variation reported by other works performed in this study area (Teixeira et al., 2012). The photochemical reactions contribute in different levels of O_3, NO_x and concentrations and indicate that NO_x can inhibit O_3 more significantly during the day than at night (Roberts–Semple et al., 2012). The conversion of NO to NO_2 by O_3 (reaction 2) during the night is the primary reaction that increases NO_2 at night, with the reverse occurring during the day to increase O_3 and decrease NO_2 (Mazzeo et al., 2005).

4. Conclusion

This study allowed to show that the most significant source of air pollution in the urban studied area is vehicles emissions. This was verified by higher PN concentrations: PR1 followed by PR2.5.

Higher PR1 concentrations occurred because PN concentrations generally increases as radius decrease and dominate in number size distribution; while PM concentrations showed an inverse pattern in relation to PN, increasing as radius increases and dominated by PM_{10} concentration.

PN concentration was less influenced by seasonal variation than PM concentration. PN concentrations of atmospheric particles and especially PM concentrations in all size fractions were higher in winter than in summer.

At night, the results revealed lower mean PN concentration and higher mean values of PM concentration. This implyes that PM concentration for an urban environment, especially between 2.5 and 10 microns, may have been favored by combustion process, mechanical process and resuspended particles of vehicular traffic. PN measurements allowed us information about the influence of emission vehicles in the study area. The results, too, showed the contribution of high humidity at night that induced a relative increase of mass and particle radius, thus favoring the concentration of particles with larger mass. In daytime hours, in the presence of higher solar radiation, the PN concentrations were favored by combustion processes.

The weekly variation showed a higher number (PR1, PR2.5, PR10) and mass concentrations (PM_1, $PM_{2.5}$, PM_{10}) of particles during weekdays than weekends attributed to high traffic density near the study site. Also, the results showed that the highest O_3 concentrations (on the contrary for NO_x) on weekends, reflected the reduction in vehicular emissions levels.

Simultaneous and continuous measurements of NO, NO_2 and NO_x showed higher mean concentration in winter and surface zone (O_3) revealed no difference between winter and summer.

Daily O_3 variation showed higher concentration during the day hours with maximum temperature and solar radiation.

The significant positive correlation between PN and PM concentrations allowed us to confirm the data previously reported, indicating that the study area is an urban polluted environment in which the PN, especially PR1/PR2.5 are affected not only by primary emissions, but by particle processes (particle growth / coagulation). Correlation between nitrogen oxides and number concentration especially fines particles (PR1.0 and PR2.5) confirms an association with primary emissions from local traffic.

The urban area which has a great vehicular emission influence allowed us to confirm contamination of ultrafine, fine particles and nitrogen oxides. Will be necessary more studies of particles <1 μm to understand the particle size distribution and better assess their anthropogenic origin.

Acknowledgments

We would like to thank FAPERGS and CNPq for their financial support.

References

Abdul-Wahab, S.A., Bakheit, C.S., Al-Alawi, S.M., 2005. Principal component and multiple regression analysis in modelling of ground-level ozone and factors affecting its concentrations. Environmental Modelling and Software 20, 1263-1271.

Ainslie, B., Steyn, D.G., 2007. Spatiotemporal trends in episodic ozone pollution in the lower Fraser Valley, British Columbia, in relation to mesoscale atmospheric circulation patterns and emissions. Journal of Applied Meteorology and Climatology 46, 1631-1644.

Agudelo-Castañeda D.M., Teixeira, E.C., Rolim S.B., Pereira, F.N., Wiegand, F. 2013 Measurement of particle number and related pollutant concentrations in an urban area in South Brazil. Atmospheric Environment 70, 254–262.

Alvarez, R.,Weilenmann, M., Favez, J.-Y., 2008. Evidence of increased mass fraction of NO_2 within real-world NOx emissions of modern light vehicles derived from a reliable online measuring method. Atmospheric Environment 42, 4699-4707

Anttila, P., Tuovinen, J.-P., 2010. Trends of primary and secondary pollutant concentrations in Finland in 1994-2007. Atmospheric Environment 44, 30-41

Aurangojeb, M., 2011. Relationship between PM_{10}, NO_2 and particle number concentration: validity of air quality controls. Procedia Environmental Science 6, 60–69.

Bigi, A., Ghermandi, G., 2011. Particle Number Size Distribution and Weight Concentration of Background Urban Aerosol in a Po Valley Site. Water, Air, Soil Pollution 220, 265–278.

Carslaw, D., 2005. Evidence of an increasing NO/NO emissions ratio from road traffic emissions. Atmospheric Environment 39, 4793–4802.

CETESB, 2014. Relatório de qualidade do ar no Estado de São Paulo, 2013 (in Portuguese—www.cetesb.sp.gov.br) Accessed in 01 July 2014

Charron, A., Harrison, R.M., 2003. Primary particle formation from vehicle emissions during exhaust dilution in the roadside atmosphere. Atmospheric Environment 37, 4109-4119.

Chen, S.-C., Tsai, C.-J., Chou, C.-K., Roam, G.-D., Cheng, S.-S., Wang, Y.-N., 2010. Ultrafine particles at three different sampling locations in Taiwan. Atmospheric Environment 44, 533-540.

Chung, Y-S., 1977: Ground-Level Ozone and Regional Transport of Air Pollutants. Journal of Applied Meteorology 16, 1127–1136

Colbeck, I., Nasir, Z.A., Ahmad, S., Ali, Z., 2011. Exposure to PM_{10} , $PM_{2.5}$, PM_{1} and Carbon Monoxide on Roads in Lahore , Pakistan. Aerosol and Air Quality Research 11, 689–695.

Colette, A., Menut, L., Haeffelin, M., and Morille, Y. 2008. Impact of the transport of aerosols from the free troposphere towards the boundary layer on the air quality in the Paris area. Atmospheric Environment 42, 390–402,

Coronado, C.R., Carvalho Jr., J.A., Silveira, J.L., 2009. Biodiesel CO_2 emissions: a comparison with the main fuels in the Brazilian market. Fuel Process Technology 90, 204-211.

Curtius, J., 2006. Nucleation of atmospheric aerosol particles. C. R. Physique 2006; 7: 1027–1045.

Dawson, J.P., Adams, P.J. and Pandis, S.N. 2008. Sensitivity of Ozone to Summertime Climate in the Eastern USA: A Modeling Case Study. Atmospheric Environment 41: 1494–1511

Debaje, S.B., Kakade, A.D., 2006.Weekend ozone effect over rural and urban site in India. Aerosol and Air Quality Research 6 (3), 322-333.

Derwent, R.G., Stevenson, D.S., Doherty, R.M., Collins, W.J., Sanderson M.G. 2008. How is surface ozone in Europe linked to Asian and North American NOx emissions? Atmospheric Environment 42 (32), 7412–7422

ENVIRONNEMENT, 2010. CPM. Continuous Particulate Measurement, Technical Manual. pp. 1 -44.

Finlayson-Pitts, B.J., Pitts Jr., J.N., 2000. Chemistry of the Upper and Lower Atmo- sphere: Theory, Experiments, and Applications. Academic press, San Diego, CA, USA.

Gaffney, J.S., Marley, N.A., 2009. The impacts of combustion emissions on air quality and climate e from coal to biofuels and beyond. Atmospheric Environment 43, 23-36.

Garcia, K.O., Teixeira, E.C., Agudelo-Castañeda, D.M., Braga, M., Alabarse, P.G, Wiegand, F., Kautzmann, R.M, Silva, L.F.O., 2014; Assessment of nitro-polycyclic aromatic hydrocarbons in PM1 near an area of heavy-duty traffic. Science of the Total Environment 479–480, 57–65

Geddes, S., Zahardis, J., Petricci, G.A., 2009. Chemical transformation of peptide containing fine particles: oxidative processing, accretion reactions and impli- cations to the atmospheric fate of cell-derived materials in organic aerosols. Journal of Atmospheric Chemistry 63, 187-202.

Gómez-Moreno, F.J., Pujadas, M., Plaza, J., Rodríguez-Maroto, J.J., Martínez-Lozano, P., Artíñano, B., 2011. Influence of seasonal factors on the atmospheric particle number concentration and size distribution in Madrid. Atmospheric Environment 45, 3169–3180.

Han, S., Bian, H., Feng, Y., Liu, A., Li, X., Zeng, F., Zhang, X., 2011. Analysis of the Relationship between O_3, NO and NO_2 in Tianjin, China. Aerosol and Air Quality Research 11, 128-139.

Herrmann, H., Brüggemann, E., Frank, U., Gnauk, T., Löschau, G., Müller, K., Plewka, A., Spindler, G., 2006. A source study of PM in Saxony by size-segre- gated characterisation. Journal of Atmospheric Chemistry 55, 103-130.

Hussein, T., Puustinen, A., Aalto, P.P., Makela, J.M., Hameri, K., Kulmala, M., 2004. Urban aerosol number size distributions. Atmospheric Chemistry and Physics 4, 391-411.

IBGE, Instituto Brasileiro de Geografia e Estatística – Ministerio do Planejamento, 2013. Disponível em: http: // www.ibge.gov.br/home/estatistica /populacao/estimativa2013/estimativa_tcu.shtm. Acessado em Abril de 2014.

Jain et al., 2000; Jain, M. Kulshrestha, U.C., Sarkar, A.K., Parashar, D.C., 2000. Influence of crustal aerosols on wet deposition at urban and rural sites in India. Atmospheric Environent 34, 5129-5137.

Jaenicke, R., 1978. Über die Dynamik atmosphärischer Aitkenteilchen. Berichte der Bunsen-Gesellschaft für Physikalische Chemie 82, 1198-1202

Jamriska, M., Morawska, L., and Mergernse, K.: 2008.The effect of temperature and humidity on size segregated traffic exhaust particle emissions, Atmospheric Environment 42, 2369–2382.

Jenkin, M.E., Clemitshaw, K.C., 2000. Ozone and other secondary photochemical pollutants: chemical processes governing their formation in the planetary boundary layer. Atmospheric Environment 34, 2499-2527.

Johansson, C., Norman, M., Gidhagen, L., 2007. Spatial & temporal variations of PM10 and particle number concentrations in urban air. Environmental Monitoring and Assessment 127, 477-487.

Kittelson, D.B. 1998. Engines and nanoparticles: a review. Journal Aerosol Science 29: 575–88.

Keogh, D., Ferreira, L., Morawska, L. 2009. Development of a particle number and particle mass vehicle emissions inventory for an urban fleet. Environmental Modelling & Software 24 (11). 1323-1331.

Kuhn, T., Biswas, S., Sioutas C., 2005. Diurnal and seasonal characteristics ofparticle volatility and chemical composition in the vicinity of a light-duty vehicle freeway. Atmospheric Environment 39, 7154–7166.

Kumar, P., Ketzel, M., Vardoulakis, S., Pirjola, L., Britter, R., 2011. Dynamics and dispersion modelling of nanoparticles from road traffic in the urban atmospheric environment: a review. Journal of Aerosol Science 42, 580-603.

Kumar, P., Pirjola, L., Ketzel, M., Harrison, R.M., 2013. Nanoparticle emissions from 11 non-vehicle exhaust sources – A review. Atmospheric Environment 67, 252–277.

Lara, L.B.L.S., Artaxo, P.,Martinelli,L.A.,Victoria,R.L.,Camargo, P.B., Krusche, A., Ayers, G.P., Ferraz, E.S.B., Ballester, M.V., 2001. Chemical composition of rainwater and anthropogenic influences in the Piracicaba river basin, Southeast Brazil. Atmospheric Environment 35, 4937–4945

Li, Q., D. J. Jacob, R. Park, Y. Wang, C. L. Heald, R. Hudman, R. M. Yantosca, R. V. Martin, and M. Evans. 2005. North American pollution outflow and the trapping of convectively lifted pollution by upper-level anticyclone, Journal of Geophysical Research 110, D10301.

Morawska, L., Thomas, S., Bofinger, N., Wainwright, D., Neale, D., 1998. Comprehensive characterization of aerosols in a subtropical urban atmosphere: particle size distribution and correlation with gaseous pollutants. Atmospheric Environment 32, 2467—2478.

Morawska, L., Ristovski, Z., Jayaratne, E.R., Keogh, D.U., Ling, X., 2008a. Ambient nano and ultrafine particles from motor vehicle emissions: characteristics, ambient processing and implications on human exposure. Atmospheric Environment 42, 8113-8138.

Morawska, L., Keogha, D. Thomas, S., Mengersen, K. 2008b. Modality in ambient particle size distributions and its potential as a basis for developing air quality regulation. Atmospheric Environment 42, 1617–1628.

Olivares, G., Johansson, C., Strom, J., Hansson, H.-C., 2007. The role of ambient temperature for particle number concentrations in a street canyon. Atmospheric Environment 41, 2145-2155.

Oliveira, C., Alves, C., Pio, C.A., 2009. Aerosol particle size distributions at a traffic exposed site and an urban background location in Oporto, Portugal. Quimica Nova 32, 928-933.

Oltmans, S.J., Levy II, H. 1994. Surface ozone measurements from a global network. Atmospheric Environment 28, 9–24.

Pastuszka, J.S., Wawroś, A., Talik, E., Paw, U., 2003. Optical and chemical characteristics of the atmospheric aerosol in four towns in southern Poland. Sciences of the Total Environment 309, 237-251.

Pey, J., Drooge, B.L. Van, Ripoll, A., Moreno, T., Grimalt, J.O., Querol, X., Alastuey, A., 2013. An evaluation of mass, number concentration, chemical composition and types of particles in a cafeteria before and after the passage of an antismoking law. Particuology 11, 527–532.

PORG, 1997. Ozone in the United Kingdom. Fourth Report of the UK Photochemical Oxidants Review Group. Department of the Environment, Transport and the Regions, London.

Qin, Y., Tonnesen, G.S. and Wang, Z. (2004). Weekend/ Weekday Differences of Ozone, NOx, CO, VOCs, PM10 and the Light Scatter during Ozone Season in Southern California. Atmos. Environ. 38: 3069–3087.

Renard, J.-B., Thaury, C., Mineau, J.-L., Gaubicher, B., 2010. Small-angle light scattering by airborne particulates: Environnement S.A . Continuous particulate monitor. Measurement Science and Technology 21, 1-10

Roberts-Semple, D., Song, F., Gao, Y., 2012. Seasonal characteristics of ambient nitrogen oxides and ground-level ozone in metropolitan northeastern New Jersey. Atmospheric Pollution Research 3, 247–257.

Ruuskanen, J., Tuch, T.H., Brink, H.T., Peters, A., Khlystov, A., Mirme, A., Kos, G.P.A., Brunekreef, B., Wichman, H.E., Buzorius, G., Vallius, M., Kreyling, W.G., Pekkanen, J., 2001. Concentrations of ultrafine, fine and PM2.5 particles in three European cities. Atmospheric Environment 35, 3729–3738.

Sadanaga, Y., Shibata, S., Hamana, M., Takenaka, N., Bandow, H., 2008. Weekday/weekend difference of ozone and its precursors in urban areas of Japan, focusing on nitrogen oxides and hydrocarbons. Atmospheric Environment 42, 4708-4723.

Seinfeld, J.H., Pandis, S.N. 2006. Atmospheric Chemistry and Physics: From Air Pollution to Climate Change, 2nd Edition. John Wiley & Sons, New Jersey, U.S., pp. 1203

Shi, J.P., Evans, D.E., Khan, A.A., Harrison, R.M., 2001. Sources and concentration of nanoparticles (<10 nm diameter) in the urban atmosphere. Atmospheric Environment 35, 1193-1202

Slezakova K., Pereira, M.C., Reis, M.A., Alvim-Ferraz, M.C., 2007. Influence of traffic emissions on the composition of atmospheric particles of different sizes – Part 1: concentrations and elemental characterization. Journal of Atmospheric Chemistry 58, 55–68.

Song, F., Young Shin, J., Jusino-Atresino, R., Gao, Y., 2011. Relationships among the springtime ground-level NO_x, O_3 and NO_3 in the vicinity of highways in the US East Coast. Atmospheric Pollution Research 2, 374–383.

Spindler, G., Brüggemann, E., Gnauk, T., Grüner, A., Müller, K., Herrmann, H., 2010. A four-year size-segregated characterization study of particles PM_{10}, $PM_{2.5}$ and PM_1 depending on air mass origin at Melpitz. Atmospheric Environment 44, 164-173.

Stathopoulou, E., Mihalakakou, G., Santamouris, M and Bagiorgas, H.S. (2008). On the Impact of Temperature on Tropospheric Ozone Concentration Levels in Urban Environments. Journal of Earth Systems Science 117: 27–236.

Swamy, Y.V., 2012. Impact of Nitrogen Oxides, Volatile Organic Compounds and Black Carbon on Atmospheric Ozone Levels at a Semi Arid Urban Site in Hyderabad. Aeros. Air Quality Research 3, 662–671.

Teixeira, E.C., Feltes, S., Santana, E.R., 2008. Estudo das emissões de fontes móveis na Região Metropolotana de Porto Alegre, Rio Grande do Sul. Química Nova 31 (2), 244-248

Teixeira EC, Garcia KO, Meincke L, Leal KA. 2011. Study of nitro-polycyclic aromatic hydrocarbons in fine and coarse atmospheric particles. Atmospheric Research 101, 631–9.

Teixeira, E.C., Mattiuzi, C.D.P., Feltes, S., Wiegand, F., Santana, E.R.R., 2012. Estimated atmospheric emissions from biodiesel and characterization of pollutants in the metropolitan area of Porto Alegre-RS. Anais da Academia Brasileira de Ciências 84, 245-261.

Teixeira, E.C., Dalla, C., Mattiuzi, P., Agudelo-Castañeda, D.M., Garcia, K.D.O., 2013. Polycyclic aromatic hydrocarbons study in atmospheric fine and coarse particles using diagnostic ratios and receptor model in urban/industrial region. Environmental Monitoring Assessment 185, 9587–9602.

Tittarelli, A., Borgini, A., Bertoldi, M. De Saeger, E., Ruprecht, A., Stefanoni, R., Tagliabue, G., Contiero, P., Crosignani, P. Estimation of particle mass concentration in ambient air using a particle counter. Atmospheric Environment 42 , 8543–8548

Uherek, E., Halenka, T., Borken-Kleefeld, J., Balkanski, Y., Berntsen, T., Borrego, C., Gauss, M., Hoor, P., Juda-Rezler, K., Lelieveld, J., Melas, D., Rypdal, K., Schmid, S., 2010. Transport impacts on atmosphere and climate: land transport. Atmospheric Environment 44, 4772-4816.

Wang, F., Costabile, F., Li, H., Fang, D., Alligrini, I., 2010. Measurements of ultrafine particle size distribution near Rome. Atmospheric Research 98, 69-77.

Warneck P, Williams J. 2012. The atmospheric aerosol. Atmospheric chemist's companion. Springer; p. 127–87

Wehner, B., Wiedensohler, A., 2003. Long term measurements of submicrometer urban aerosols: statistical analysis for correlations with meteorological conditions and trace gases. Atmospheric Chemistry and Physics 3, 867–879.

WHO. World Health Organization, 2006. Air quality guidelines for particulate matter, ozone, nitrogen dioxide and sulfur dioxide - Global update 2005 -. WHO Regional Publications; Germany. 484 pages

Wu, Z., Hu, M., Lin, P., Liu, S., Wehner, B., Wiedensohler, A., 2008. Particle number size distribution in the urban atmosphere of Beijing, China. Atmospheric Environment 42, 7967–7980

Young, L.-H., Wang, Y.-T., Hsu, H.-C., Lin, C.-H., Liou, Y.-J., Lai, Y.-C., Lin, Y.-H., Chang, W.-L., Chiang, H.-L., Cheng, M.-T., 2012. Spatiotemporal variability of submicrometer particle number size distributions in an air quality management district. Science of the Total Environment 425, 135–45.

Zielinska, B., 2005. Atmospheric transformation of diesel emissions. Experimental and Toxicologic Pathology 57, 31-42.

Zhu, Y., Hinds, W., Kim, S. Sioutas, C. 2002. Concentration and Size Distribution of Ultrafine Particles Near a Major Highway, Journal of the Air & Waste Management Association, 52:9, 1032-1042

Zhu, Y., Hinds, W.C., Shen, S., Sioutas, C., 2004. Seasonal trends of concentration and size distribution of ultrafine particles near major highways in Los Angeles. Aerosol Science and Technology 38 (S1), 5–13.

TABLES

Table 1. Average mass concentrations of PM in the sampling site and other parts of the world (μg·m³)

Site	PM_1 (μg·m^{-3})	$PM_{2.5}$ (μg/m³)	PM_{10} (μg/m³)	Sampler	Location/ source Type	Reference
Sapucaia do Sul	2.30*	13.8	38.7	CPM/ MP101M	Urban Road/traffic	This study
São Paulo		14	33	ß-attenuation	Urban	CETESB, 2014
Vienna AUPHEP-1	14.9	18.6	26.5	TEOM®, ß-attenuation	Urban	Gomiscek *et al.*, 2004
Streithofen AUPHEP-2	12.4	15.0	21.1	TEOM®, ß-attenuation	Rural	Gomiscek *et al.*, 2004
Linz AUPHEP-3	14.7	18.8	29.9	TEOM®, ß-attenuation	Urban	Gomiscek *et al.*, 2004
Graz AUPHEP-4	17.5	21.1	31.0	TEOM®, ß-attenuation	Suburban	Gomiscek *et al.*, 2004
Glasgow	-	15.5	25.5	PARTISOL	Urban background	Jímenez *et al.*, 2012
Delhi	-	129.8	222.0	Thermo Andersen ß-attenuation analyzers	Urban center	Tiwari *et al.*, 2014
Lahore	52	91	489	GRIMM Aerosol Spectrometers	Roadside	Colbeck *et al.*, 2011
Vallila	-	9.6	18.7	Eberline monitors ß-attenuation	Traffic	Laakso *et al.*, 2003
Kallio	-	8.2	15.3		Urban backgr.	
Luukki	-	-	10.2		Rural backgr.	
Hyytiälä	4.3	5.8	6.9		Rural backgr	
Agra	104	123	195	Portable Aerosol Spectrometer	Urban	Massey *et al.*, 2012
Birmingham:						
BROS	12	16	26.5	Partisol Plus Sequential Air Sampler	Urban roadside, Urban background, Rural	Yin and Harrison
BCCS	12.6	15.8	23.9			
CPSS	11.7	14.3	19.4			

***** PM_1 concentration values may be used as indicative because the equipment is only certified for PM_{10} and $PM_{2.5}$ values.

Table 2. Mean particle number (PR1, PR2.5, PR10) and mass concentration (PM_1, $PM_{2.5}$, PM_{10}) of atmospheric particles and the studied gases (NO, NO_2, NO_x, O_3) during weekdays (Monday–Friday) and weekends, (Saturday-Sunday).

	NO (μg·m^{-3})	NO_x (μg·m^{-3})	NO_2 (μg·m^{-3})	O_3 (μg·m^{-3})	PM_{10} (μg·m^{-3})	$PM_{2.5}$ (μg·m^{-3})	PM_1 (μg·m^{-3})	PR1 (N°/L)	PR2.5 (N°/L)	PR10 (N°/L)
Weekday	28.0	46.0	18.5	8.60	44.83	15.36	1.49	4.95	4.21	1.64
Weekend	19.3	34.1	15.1	9.26	40.36	13.38	1.33	4.09	3.60	1.49
Ratio weekday/ weekend	1.45	1.35	1.23	0.93	1.11	1.15	1.12	1.21	1.17	1.10

Table 3 Pearson correlation matrix among mass (PM_1, $PM_{2.5}$, PM_{10}) ($\mu g \cdot m^{-3}$) and number concentrations (PR1, PR2.5, PR10) (N°/L), gaseous pollutants and meteorological parameters**.**

	NO	NO_x	NO_2	O_3	PM_{10}	$PM_{2.5}$	PM_1	PR1	PR2.5	PR10	TEMP	RH	RAD	WS	WD
NO	1	,929**	,105**	-,366**	,440**	,426**	,230**	,269**	,220**	,141**	-,278**	,230**	-,227**	-,316**	-,042**
NO_x		1	,461**	-,367**	,484**	,453**	,260**	,331**	,271**	,173**	-,245**	,151**	-,226**	-,293**	-,068**
NO_2			1	-,096**	,241**	,199**	,151**	,256**	,213**	,135**	,024**	-,158**	-,050**	-,024**	-,083**
O_3				1	-,095**	-,126**	-,118**	,104**	,136**	,135**	,362**	-,611**	,531**	,417**	,062**
PM_{10}					1	,800**	,604**	,363**	,325**	,234**	-,125**	,053**	-,149**	-,183**	-,037**
$PM_{2.5}$						1	,588**	,331**	,293**	,209**	-,090**	,022*	-,101**	-,205**	-.007
PM_1							1	,220**	,172**	,116**	.005	,019*	-,058**	-,115**	-,035**
PR1								1	,838**	,610**	,311**	-,319**	,079**	-.015	,020*
PR2.5									1	,637**	,311**	-,333**	,101**	,024*	,022*
PR10										1	,288**	-,274**	,078**	,064**	,043**
TEMP											1	-,604**	,513**	,302**	-,107**
RH												1	-,649**	-,377**	,030**
RAD													1	,251**	,067**
WS														1	-,170**
WD															1

* Significant at the 0.05 level (2-tail), ** Significant at the 0.01 level (2-tail). WS: Wind speed (m/s); WD: Wind Direction; RH: Relative Humidity (%); RAD: Radiation ($w \cdot m^{-2}$); TEMP: Ambient temperature (°C)

Table 4 Matrix of Principal Components of Varimax rotation

	Component			
	1	2	3	4
Rank of NO	-.523	.205	.210	.668
Rank of NOx	-.351	.209	.304	.821
Rank of NO2	.260	-.015	.197	.753
Rank of O3	.803	-.057	-.160	-.305
Rank of PM10	-.098	.335	.828	.200
Rank of PM2.5	-.150	.184	.889	.215
Rank of PM1	-.116	.147	.902	.188
Rank of PR1	.128	.855	.304	.130
Rank of PR2.5	.159	.879	.262	.111
Rank of PR10	.126	.890	.127	.059
Rank of TEMP	.655	.424	-.088	-.106
Rank of UMIDADE	-.831	-.289	.011	-.077
Rank of RADIAÇÃO	.768	.075	-.101	.062

Extraction Method: Principal Component Analysis.
Rotation Method: Varimax with Kaiser Normalization.
Rotation converged in 7 iterations.

FIGURES

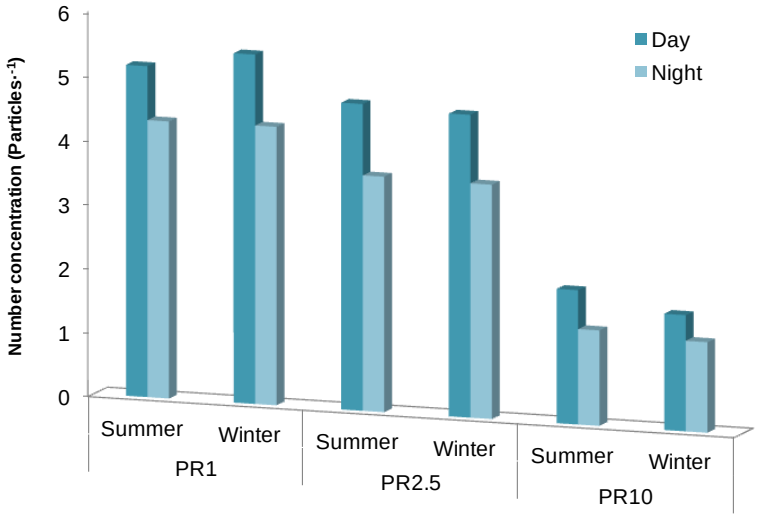
Number concentration (Particles·s-1)
6
5
4
3
2
1
0
Day
Night
Summer
Winter
PR1
Summer
Winter
PR2.5
Summer
Winter
PR10

(a)

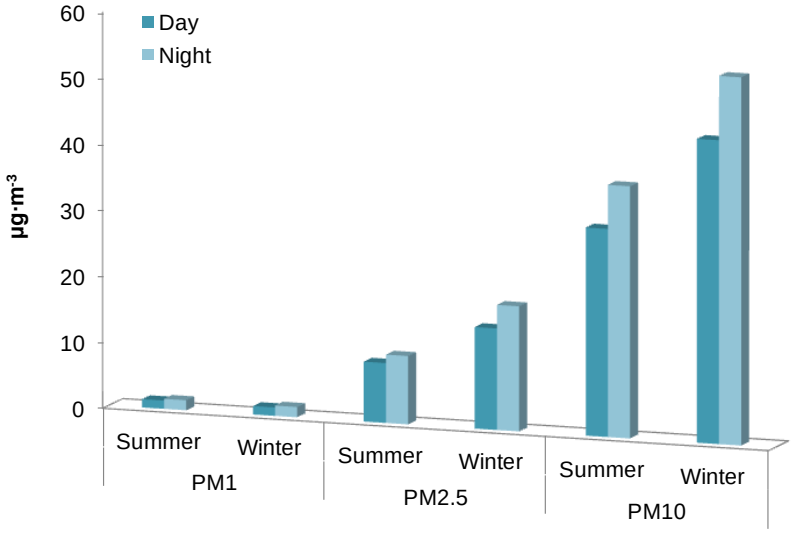
µg·m-3
60
50
40
30
20
10
0
Day
Night
Summer
Winter
PM1
Summer
Winter
PM2.5
Summer
Winter
PM10

(b)

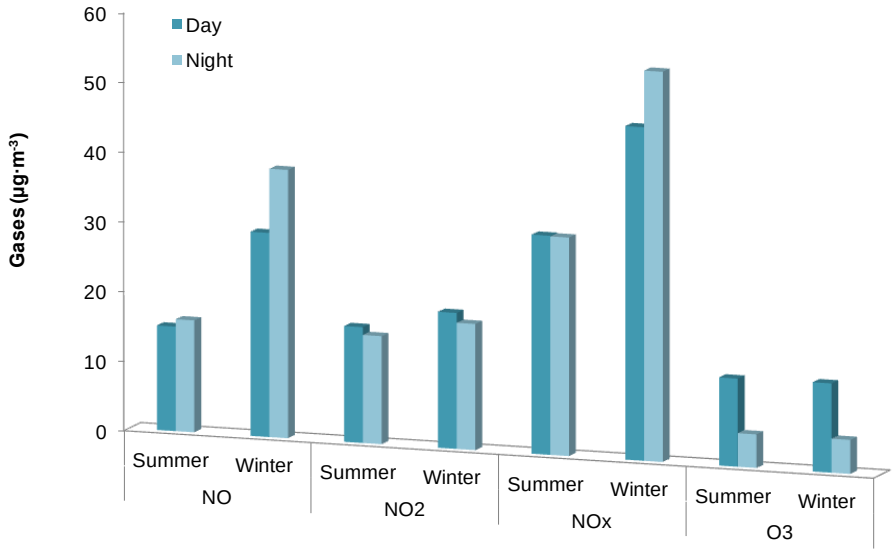

(c)

Figure 1. Mean concentrations of day and night in Summer and Winter for (a) particle number PR1.0/PR2.5/PR10, (b) Particulate matter $PM_1/PM_{2.5}/PM_{10}$ and (c)

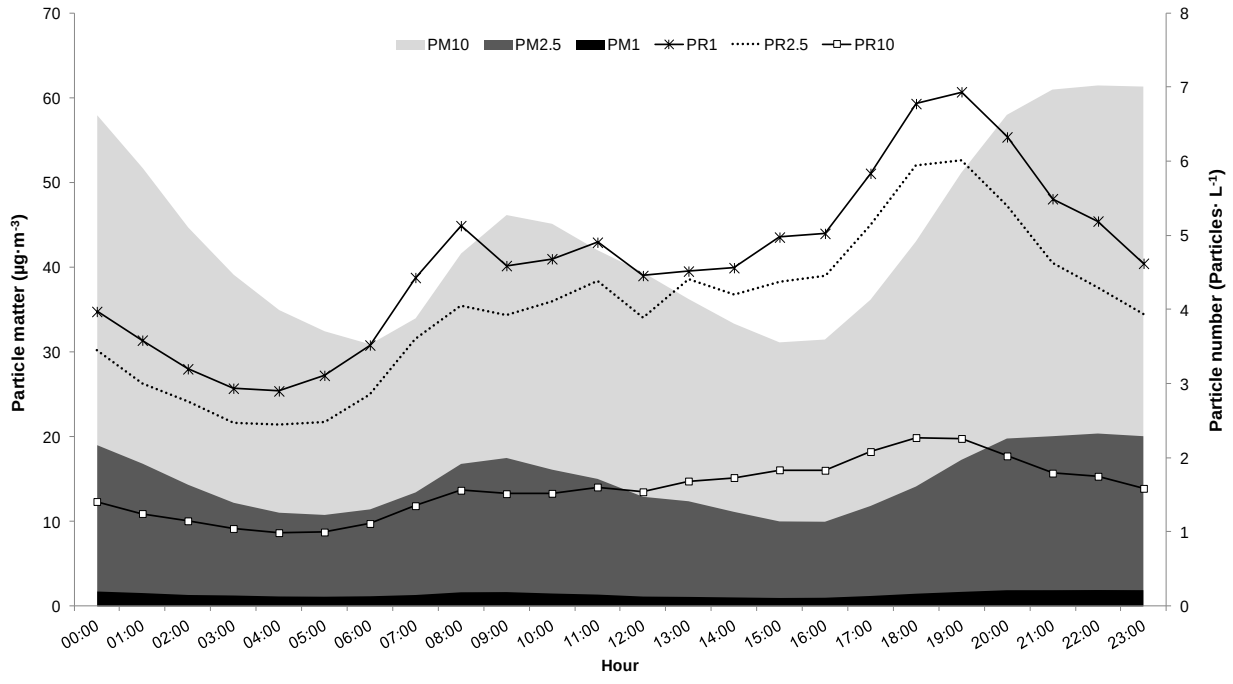

Figure 2. Daily variation of mean (a) particle number concentration for all the studied period at ranges PR1/PR2.5/PR10 and (b) particle matter concentration for $PM_{10}/PM_{2.5}/PM_1$.

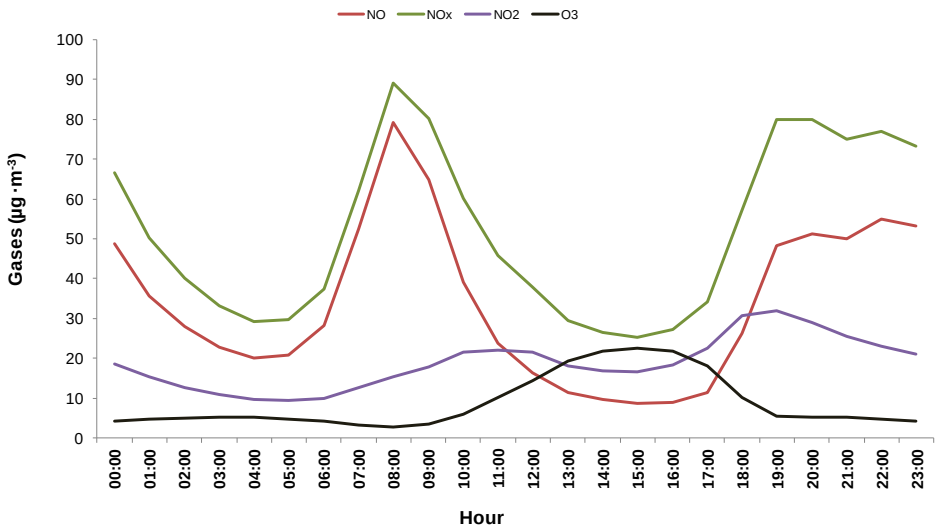

(a)

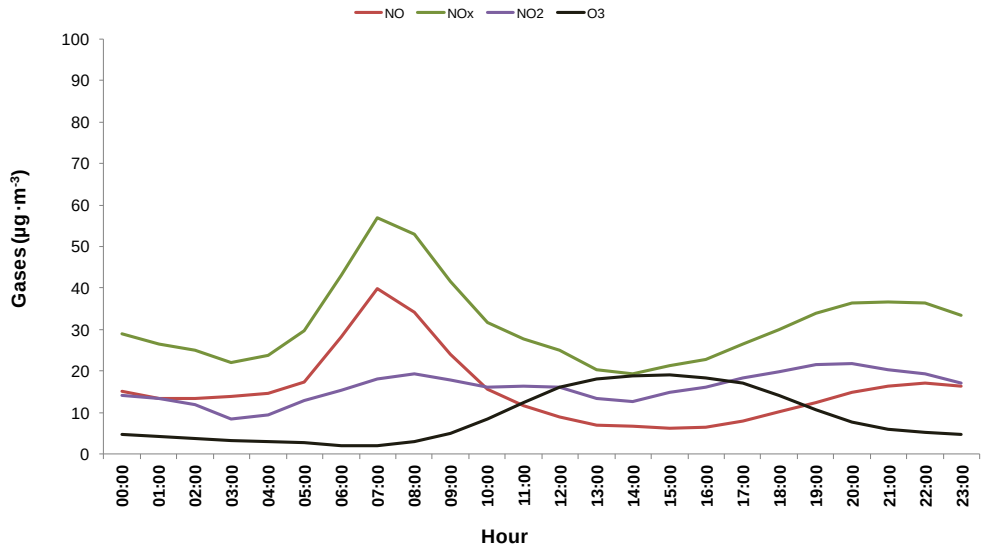

(b)

Figure 3. Mean daily variation of $NO/NO_2/NO_x/O_3$for (a) winter and (b) summer

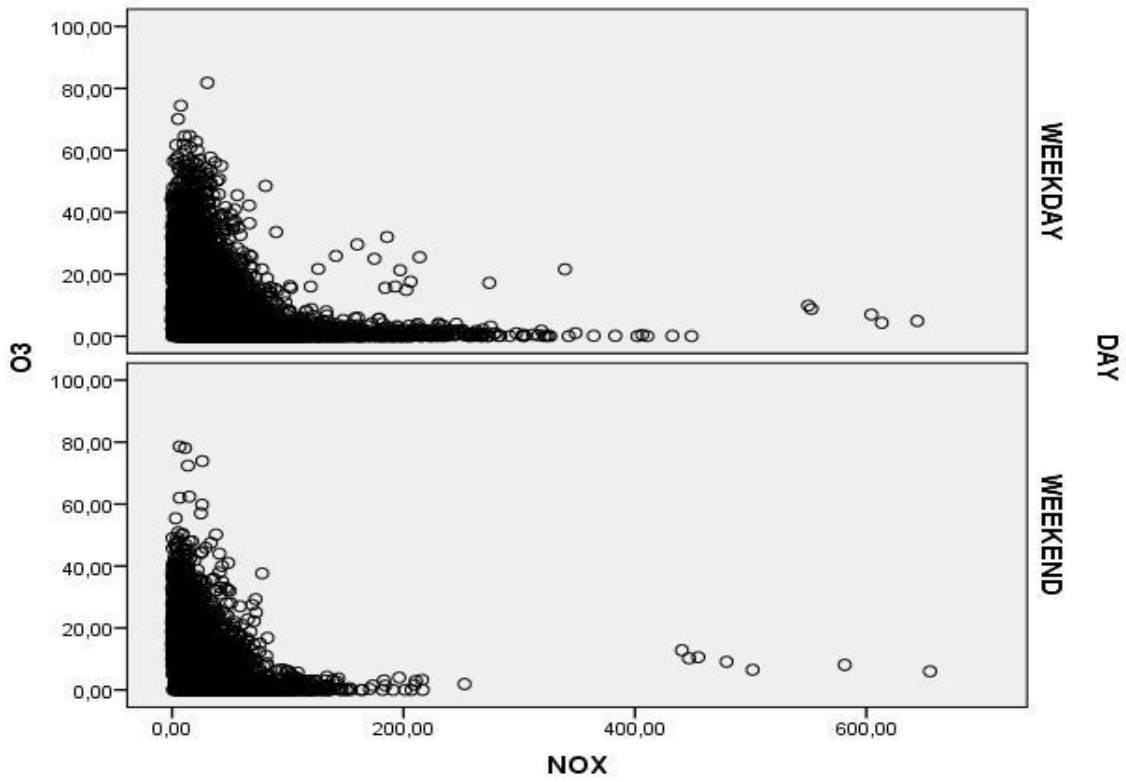

Figure 4. Correlation plot between NO_x and O_3 for weekdays and weekends

CAPITULO VII

CONCLUSÕES E RECOMENDAÇÕES

CONCLUSÕES E RECOMENDAÇÕES

Conclusões

- Com base no trabalho realizado, pode-se dizer:

Pela primeira vez foram analisadas as concentrações médias de HPAs em MP_1 no Brasil, porém poucos estudos existem atualmente no mundo, catalogando o presente trabalho como inédito. Foi confirmado que as concentrações no município de Sapucaia do Sul foram maiores do que as de Canoas, assim como a influência da queima de madeira (contribuição de 15%), combustão de carvão (9-10%), combustão incompleta/petróleo não queimado (21-23%) e especialmente de fontes móveis (contribuição de 53-54%), na área de estudo. Por ser uma área com alto fluxo veicular, foram obtidas maiores concentrações do número de partículas finas por ser originárias das emissões de fontes movéis.

A análise da toxicidade dos HPAs estudados em termos de níveis de BaPeq na área de estudo mostrou que BaP, DahA e Ind dominaram os níveis, variando de acordo com a estação do ano. De acordo com a classificação da IARC, BaP é Classe 1, cancerígeno para os seres humanos; DahA classe 2A, provavelmente cancerígeno aos seres humanos; e Ind Classe 2B, possivelmente cancerígeno para os seres humanos.

Durante o tempo de amostragem (dois anos) na área de estudo, os resultados das concentrações de HPAs associados a MP_1 mostraram uma tendência sazonal, com concentrações maiores no inverno, principalmente para HPAs de maior peso molecular (BghiP, BaP, Ind, BbkF, DbA). As concentrações médias do número (PR1, PR2.5, PR10), massa de partículas (MP_1, $MP_{2,5}$, MP_{10}) e gases (NO, NO_2 e NO_x) também mostraram esta mesma tendência sazonal em Sapucaia do Sul. Contudo, no presente estudo foi utilizado o filtro Kolmogorov-Zurbenko para obter a tendência e o componente sazonal dos seguintes poluentes: NO, NO_2 e NO_x e O_3. Resultados mostraram uma tendência de aumento de NO originário das fontes movéis no município de Esteio. A tendência sazonal foi confirmada pelos resultados, com maiores concentrações no inverno dos óxidos de nitrogênio (NO, NO_2 e NO_x), porém menores de O_3.

No presente trabalho, os resultados conseguiram mostrar o impacto das emissões originárias das fontes movéis nas concentrações de gases (NO, NO_2 e NO_x) e partículas atmosféricas, sendo que nos períodos de alto tráfego de fluxo veicular, as concentrações destes poluentes

aumentaram apresentando picos nos horários de *rush*, principalmente durante os dias de semana.

As maiores concentrações de número de partículas foram obtidas durante o dia, enquanto que as concentrações em massa apresentaram maiores concentrações à noite. Isto, provavelmente, porque à noite a umidade elevada favoreceu o crescimento da massa das partículas e as concentrações elevadas de número de partículas favoreceram a sua coagulação e a condensação de espécies semi-voláteis sobre elas, ocasionando o aumento relativo da massa e do raio das partículas atmosféricas. Durante o dia, o aumento do número pode ser ocasionado, provavelmente, pela radiação solar elevada e a oxidação de hidrocarbonetos aromáticos, que formam aerossóis orgânicos secundários.

Este estudo demonstrou a influência dos parâmetros meteorológicos temperatura, umidade relativa, velocidade do vento e radiação solar sobre a concentração do número de partículas e HPAs. Correlação positiva de HPAs com umidade relativa e negativa com a radiação solar, temperatura, O_3 e NO demonstra a degradação dos HPAs por fotólise e reações químicas com estes poluentes. Correlação positiva entre o número de partículas e a concentração de massa foi obtida, indicando que a área de estudo é um ambiente poluído urbano em que o número de partículas é afetado não só pelas emissões primárias, mas por processos de partículas (crescimento das partículas / coagulação).

Este estudo forneceu resultados para mostrar as vantagens da técnica FTIR (emissividade e transmitância) na região do infravermelho para a análise de amostras de material particulado de uma maneira simples. Os resultados de padrões permitiram contribuir de forma mais embasada na identificação dos HPAs em material particulado atmosférico. O maior número de bandas de fortes intensidades dos HPAs ocorreu na região espectral de 680-900 cm^{-1}, devido às deformações angulares CC fora do plano e deformações angulares CH fora do plano. Este estudo confirma que esses HPAs podem ser diferenciados pelas suas assinaturas espectrais no infravermelho.

Recomendações

Sugere-se que sejam analisadas as concentrações de O_3 na área de estudo, particularmente na localidade de Sapucaia do Sul que apresentou baixas concentrações em ambas estações (inverno e verão), quando comparado a outros trabalhos realizados em áreas urbanas, provavelmente, em virtude de várias razões como: (i) maior velocidade do vento no verão que no inverno; (ii) as reações químicas que consomem O_3 e/ou a falta de radiação solar intensa que inibem a formação fotoquímica de O_3; (iii) O_3 pode ser "eliminado" pelo NO em abundância, resultando em concentrações mais baixas de O_3 em áreas de tráfego intenso. Apesar disso, mais pesquisas precisam ser realizadas para entender este fenômeno.

Com relação às emissões de fontes movéis, sugere-se que este estudo seja utilizado para dar aos diferentes entes públicos bases para propor alternativas de redução e controle das emissões na área de estudo, tomada de decisões politicas e econômicas, etc. Para isto, podem ser empregadas estratégias entre empresas, políticos e o meio acadêmico para melhorar a qualidade do ar urbano e a saúde das pessoas.

Recomenda-se ainda continuar estudando outros poluentes nesta fração de tamanho de partícula (MP_1), por exemplo os metais. Também recomenda-se continuar estudando a técnica FTIR com o objetivo de diminuir os custos do monitoramento.

ANEXO A

Resumos dos trabalhos publicados como co-autor

ANEXOS: Resumos dos trabalhos publicados como co-autor

A.I. GARCIA, K.O. ; TEIXEIRA, E.C. ; AGUDELO-CASTAÑEDA, D.M. ; BRAGA, M. ; ALABARSE, P. G. ; WIEGAND, F. ; KAUTZMANN, R. M. ; OLIVEIRA, L. F. S. . Assessment of nitro-polycyclic aromatic hydrocarbons in PM1 near an area of heavy-duty traffic. Science of the Total Environment, v. 479-480, p. 57-65, 2014.

The objective of this research was to evaluate nitro-polycyclic aromatic hydrocarbons (NPAHs) associated with ultrafine airborne particles (PM_1) in areas affected by vehicles in the metropolitan area of Porto Alegre (MAPA), RS, Brazil. Extraction, isolation/derivatization, and subsequently gas chromatography with electron capture detection (GC/ECD) were the techniques used to extract and determine NPAHs (1-nitronaphthalene, 2-nitrofluorene,3-nitrofluoranthene,1-nitropyrene, and 6-nitrochrysene) associated with PM_1 Airborne particles (PM_1) were collected using PTFE filters in a PM162M automatic sampler. The analytical method was validated by the Standard Reference Material – SRM 1649b – from the National Institute of Standards and Technology (NIST, USA). The results were consistent with the certified values. 3-NFlt and 6-NChr reached highest concentrations of 0.047 $ng \cdot m^{-3}$ and 0.0284 $ng \cdot m^{-3}$, respectively, in Sapucaia do Sul and Canoas. Seasonal variation showed higher NPAH concentrations in cold days. The NPAHs associated with PM_1 were correlated with the pollutants nitrogen oxides and NPAHs with meteorological variables: temperature and wind speed. The results indicated that vehicles with diesel engines were influential. This was confirmed by the study of the ratios NPAHs/PAHs, 1-NPyr/Pyr, and 6-NChr/Chr.

A.II. TEIXEIRA E. C. ; MATTIUZI, C.D.P ; AGUDELO-CASTAÑEDA, D. M. ; GARCIA, K.O. ; WIEGAND, F. Polycyclic aromatic hydrocarbons study in atmospheric fine and coarse particles using diagnostic ratios and receptor model in urban/industrial region. Environmental Monitoring and Assessment (Print), p. 9587-9602, 2013.

Atmospheric fine and coarse particles were collected in Teflon filters in three cities of the region of the Lower Sinos River Basin of Rio Grande do Sul in the year 2010. The filters were Soxhlet extracted, and 14 priority PAHs were analyzed using a gas chromatograph coupled to a mass spectrometer (GC/MS). The principal emission sources of these compounds were assessed by using diagnostic ratios and receptor model: positive matrix factorization (PMF 3.0) of the US Environmental Protection Agency. The results of PAHs concentration for the studied year showed significant levels of high molecular weight (HMW) PAH, Ind, and BghiP, in $PM_{2.5}$ in the winter season, showing the influence of mobile sources. The application of receptor model PMF 3.0 revealed that the main sources of PAHs were vehicle fleet (both diesel and gasoline), followed by coal combustion, wood combustion, and resuspension of dust. The results of the receptor modeling are in agreement with the data obtained by the ratio diagnostic.

A.III. TEIXEIRA E. C. ; AGUDELO-CASTAÑEDA, D. M. ; FACHEL, J.M. ; LEAL, K. A. ; GARCIA, K.O. ; Wiegand, F. Source identification and seasonal variation of polycyclic aromatic hydrocarbons associated with atmospheric fine and coarse particles in the Metropolitan Area of Porto Alegre, RS, Brazil. Atmospheric Research (Print), v. 118, p. 390-403, 2012.

The purpose of the present study was to evaluate the polycyclic aromatic hydrocarbons (PAHs) in fine ($PM_{2.5}$) and coarse particles ($PM_{2.5–10}$) in an urban and industrial area in the Metropolitan Area of Porto Alegre (MAPA), Brazil. Sixteen U.S. Environmental Protection Agency (EPA) priority polycyclic aromatic hydrocarbons (PAHs) were measured. Filters containing ambient

air particulate were extracted with dichloromethane using Soxhlet. Extracts were later analyzed, for determining PAH concentrations, using a gaseous chromatograph coupled with a mass spectrometer (GC-MS). The polycyclic aromatic hydrocarbons (PAHs) were more concentrated in $PM_{2.5}$ with an average of 70% of total PAHs in the MAPA. The target PAH apportionment among the main emission sources was carried out by diagnostic PAH concentration ratios, and principal component analysis (PCA). PAHs with higher molecular weight showed higher percentages in the fine particles in the MAPA. Based on the diagnostic ratios and PCA analysis, it may be concluded that the major contribution of PAHs was from vehicular sources (diesel and gasoline), especially in the $PM_{2.5}$ fraction, as well as coal and wood burning. The winter/summer ratio in the $PM_{2.5}$ and $PM_{2.5–10}$fractions in the MAPA was 3.1 and 1.8, respectively, revealing the seasonal variation of PAHs in the two fractions. The estimated toxicity equivalent factor (TEF), used to assess the contribution of the carcinogenic potency, confirms a significant presence of the moderately active carcinogenic PAHs BaP and DahA in the samples collected in the MAPA.

A.IV. MATTIUZI, C.D.P ; AGUDELO-CASTAÑEDA, D.M. ; TEIXEIRA, E.C. . Determinação das principais fontes emissoras de hidrocarbonetos policíclicos aromáticos na Região Metropolitana de Porto Alegre utilizando o modelo receptor Chemical Mass Balance. FEPAM em Revista (online), v. 6, p. 4-15, 2012.

Os Hidrocarbonetos Policíclicos Aromáticos (HPAs) são compostos químicos conhecidos pelas suas propriedades mutagênicas e carcinogênicas, sendo formados principalmente através de processos de combustão incompleta (Ravindra *et al.*, 2008). Este estudo tem como objetivo determinar as principais fontes emissoras de HPAs através da utilização de um modelo receptor. O modelo escolhido foi o Chemical Mass Balance – CMB 8.2, que é desenvolvido pela Agência de Proteção Ambiental dos Estados Unidos – US EPA. O CMB é um modelo matemático que identifica e quantifica a contribuição das fontes através de procedimentos estatísticos. Os resultados desta modelagem indicaram que as principais fontes de HPAs na Região Metropolitana de Porto Alegre são as fontes móveis (frotas diesel e gasolina), e fontes fixas, como combustão de carvão e de madeira, e fábrica de cimento.

A.V. PAIXÃO, M.A. ; TEIXEIRA E. C. ; AGUDELO-CASTAÑEDA, D. M. ; PEREIRA, F.N. ; MIGLIAVACCA, D.O. . Distribuição do tamanho de partículas atmosféricas na Região Metropolitana. Fepam em Revista (Impresso), v. 5, p. 19-22, 2011.

A maioria das redes de qualidade do ar que utilizam sistemas de amostragem automáticos não alerta em tempo real à população, entretanto, o distribuidor de tamanho determina continuamente e em tempo real a concentração do número de partículas. O objetivo principal do presente trabalho foi estudar a distribuição do tamanho de partículas atmosféricas, nas faixas PR1, PR2,5 e PR10, na Região Metropolitana de Porto Alegre (RS, Brasil), para partículas com diâmetros nas faixas de tamanho <1 µm, 1-2,5 µm e 2,5-10 µm, respectivamente, usando o analisador MP101M com módulo CPM, da Environnement S.A. Os resultados obtidos para a concentração diária do número de partículas por volume (Nbr/L) mostraram que a área de estudo apresenta maior número de partículas finas (1,0-2,5 µm) e ultrafinas (<1,0 µm). Os resultados revelaram concentrações horárias com picos nas primeiras horas do dia, entre 7:00 e 10:00 h, devido ao aumento do fluxo de tráfego. À noite, os dados mostraram concentrações mais elevadas, com um pico às 19:00 h.